CONSOLIDATION BEHAVIOR OF AN

EMBANKMENT ON BOSTON BLUE CLAY

by

JOSEPH FRANCIS WHITTLE, JR.
BS, Rensselaer Polytechnic Institute
(1967)

Submitted in partial fulfillment

of the requirements for the degree of

Master of Science in Civil Engineering

at the

Massachusetts Institute of Technology
June, 1974

Signature of Author. .....
Department of Civil Engineering, May 10, 1974

Certified by...
Thesis Supervisor

Accepted by... ....
Chairman, Departmental Committee on Graduate Students of the Department of Civil Engineering

ABSTRACT

CONSOLIDATION BEHAVIOR OF AN
EMBANKMENT ON BOSTON BLUE CLAY

by

JOSEPH FRANCIS WHITTLE,JR.

Submitted to the Department of Civil Engineering on May 10, 1974 in partial fulfillment of the requirements for the degree of Master of Science in Civil Engineering.

Since August, 1967, data have been collected from a heavily instrumented section of an embankment for the proposed Route I-95 near Boston, Massachusetts. The embankment is 40 feet high, with crest and base widths of 90 and 260 feet respectively, and is underlain by 10 feet of fine sand and 135 feet of CL clay. The field data, and laboratory test results are presented graphically and in tabular form

The finite element program FEECON was used to determine undrained deformations and stresses. When used with hyperbolic stress-strain parameters from $\overline{CK_oUDSS}$ tests on laboratory prepared samples of Boston Blue Clay, FEECON gives good results. The selection of appropriate hyperbolic parameters is discussed. Based on comparisons with field data, the initial excess pore pressures beneath the embankment are best represented by the modified Henkel equation, $\Delta u = \Delta\sigma_{oct} + a\Delta\tau_{oct}$. Henkel's a parameter is related to Skempton's A parameer for the appropriate stress history and stress conditions (plane strain or direct-simple shear).

Pore pressure and settlement data were used to determine the rates of consolidation within the clay. In the top 30 feet of clay where the overconsolidation ratio exceeds 2.5, the consolidation settlement occurs more rapidly than pore pressure dissipation, but the reverse is true in the lower 105 feet. Field compression parameters were computed from the field data. The field RR's are 0.034 to 0.039, and the field CR's are 0.28 to 0.39. These values are 50% and 85% greater than the laboratory values. Based on the field compression parameters, the predicted final consolidation settlement at the top of the clay beneath the embankment centerline is 7.8 feet.

Field coefficients of consolidation were computed by Gray's transformation for a two-layer system considering lateral drainage with an isotropic permeability. The values

which gave the best prediction of settlement versus depth at several times were based on incremental time analysis of pore pressure data. These values are c_{v1} = 0.71 ft^2/day (top 30 feet) and c_{v2} = 0.24 ft^2/day (lower 105 feet) and they exceed laboratory values by a factor of three.

Thesis Supervisor Charles C. Ladd

Title Professor of Civil Engineering

ACKNOWLEDGEMENT

This thesis would not have been possible without the support of my wonderful wife, E'Lyse. She has freely given her love, patience and encouragement, and spent endless hours reducing and tabulating data.

In addition, the financial assistance I have received through the Haley and Aldrich, Inc. Professional Development Program has greatly facilitated the achievement of my educational goal.

Finally, my thanks to Professor Charles C. Ladd, who so skillfully directed all my efforts in the preparation of this thesis.

TABLE OF CONTENTS

LIST OF TABLES

LIST OF FIGURES

1. INTRODUCTION

1.1 BACKGROUND

In August 1967 construction began on an embankment for Interstate highway I-95 across the Revere-Saugus tidal marsh northeast of Boston, Massachusetts. This involved a large embankment, 25 to 40 feet high and 2.4 miles long, constructed over a 40 to 160 feet thick deposit of medium to stiff clay, known as the Boston Blue Clay (BBC).

The embankment design called for staged construction with a surcharge to minimize post-pavement settlements. Because of uncertainties in the amount and rate of settlement, and also end of construction stability, instrumentation was installed at numerous stations along the embankment. One station in particular, Station 246 + 00, known as the M.I.T. - Massachusetts Department of Public Works (MIT-MDPW) Test Section, was heavily instrumented. The instrumentation included settlement platforms, settlement rods, peizometers, slope indicators and total stress cells. Considerable performance data have been collected during the seven years since the start of construction.

1.2 PURPOSE

Various researchers have dealt with different aspects of the embankment performance. However most of the analyses to date have dealt with performance during construction (D'Appolonia, et. al., 1971). In addition, Recker et. al., (1973) and Lambe (1973) have discussed the performance after construction in a general way, but no analyses of the data were made.

One purpose of this report is to present in a readily usable format all data pertaining to the performance of the foundation clay at the test section. This will simplify and encourage further analyses of the field data. In addition, the M.I.T. finite-element progran FEECON was used to make an after-the-fact prediction of undrained performance. This permitted an evaluation of this programs's applicability to plane strain loading in Boston Blue Clay. It also allowed an evaluation of the input parameters used for FEECON. Finally, and of main interest, an analysis of the consolidation behavior beneath the embankment centerline was performed. Compression parameters and the coefficients of consolidation for the in-situ plane strain condition were determined from the field data. Measured and predicted consolidation settlements were also compared.

1.3 SCOPE

Chapter 2 summarizes the initial in-situ conditions at the Test Section. The soil profile, boring data, and test results for samples obtained near the Test Section are included.

Chapter 3 summarizes the construction history of the Test Section, including embankment construction and instrument installation. Field data for the foundation clay, including settlement, inclinometer and piezometer data, are presented in Chapter 4. In addition, problems encountered with data collection are discussed. The application of the FEECON program is presented in Chapter 5. This section includes a discussion of the appropriate stress-strain parameters based on model footing tests, and lab stress-strain-strength data. In Chapter 6, the FEECON predictions are compared with other predictions and measured data. Chapter 7 presents the consolidation analysis beneath the centerline, based on both pore pressure and settlement data. Various methods of back figuring field values for the coefficient of consolidation are discussed and the results compared to field data. Conclusions and recommendations for further study are given in Chapter 8.

2. SUBSURFACE CONDITIONS AND SOIL PROPERTIES

2.1 GENERAL GEOLOGY

The following discussion is based on D.E. Reed's summary of the geology of the Boston area (Reed, 1971). Bedrock at the site is the Cambridge Argillite, which has been subjected to varying degrees of alteration and weathering. Diabase dikes and sills, from less than a foot to hundreds of feet in thickness, are common in the bedrock of the Boston area. The lowest soil unit is usually till, a heterogeneous mixture of soil sizes deposited beneath the ice sheet. The till is frequently covered by outwash sand and gravels, deposited by meltwater from the ice front during retreat of the ice sheet 14,000 to 15,000 years ago.

Depression of the bedrock due to the weight of the glacier, and rising sea level due to melting of the retreating ice sheet, formed the Boston Basin - an innundated trough. Vast quantities of silt and clay size particles settled out of suspension, forming the marine illitic clay called the Boston Blue Clay. In places, the thickness of this deposit exceeds 200 feet.

Sea level lowering associated with a minor readvance of the ice 12,000 years ago (the Lexington Substage) resulted in desication and weathering of the top of the clay.

In addition, meltwater streams often covered the clay surface with outwash sands and gravels. The uppermost layer at the site is peat, which has accumulated since a relative stabilization of the sea level some 2,000 to 3,000 years ago.

2.2 SOIL PROFILE

Figure 2-1 shows boring location and the general site plan. Available boring data are reproduced in Figure 2-2. The assumed soil profile is shown in Figure 2-3. This profile is based not only on boring data, but also on instrument elevations and installation records.

The assumed average profile at Sta. 246 show the natural ground surface (top of the Peat) at elevation (El.) of +5 (U.S.G.S.). The groundwater elevation is +2.5. The surface of the gray shale bedrock (Cambridge Argillite) is at a depth of 168 ft. or El. -163. This is overlain by 8 ft. of silty, clayey sand and gravel which is glacial Till. Standard Penetration Test values (N values) in the Till range from 24 to 171 blows/ft. Above the till, between El. -10 and -145, is 135 feet of gray CL silty Clay (Boston Blue Clay). Lenses and thin layers of silt or very fine silty sand occur within the top 30 ft. of clay, but apparently are discontinuous. The top 10 ft. of clay is a medium-stiff desiccated crust with N = 10, and a bouyant weight of 59 pcf (Guertin, 1967). Below this, the clay is "soft" (N = 2-4) with a lower bouyant weight of

52 pcf (Guertin, 1967). However, field vane values for undrained shear strength (s_u) of 700 - 1200 psf indicate medium to stiff consistency. Immediately above the clay, between El. 0 and -10, is 10 ft. of fine to medium poorly graded sand. N values average about 20 blows/ft. The top layer of very soft Peat and Organic Silt has N values of 0 to 2.

2.3 SOIL PROPERTIES

2.3.1 Index Properties

Figure 2-4 shows the results of Atterberg Limit Tests performed on samples from borings close to Sta. 246. Only data from D22 and D24 (Storch, 1965) and MIT - P11 (Guertin, 1967) are plotted. The average values are: plastic limit, 22%; liquid limit, 44.4%; plasticity index, 22.4%; natural water content, 40.6%. There is consistent increase in natural water content with depth to El. -45, where it becomes roughly constant with depth. There is a similar, but less well defined relation between liquidity index and depth.

2.3.2 Stress History

The stress history, also based on tests from samples from the three nearest borings, is depicted in Figure 2-4. The upper 60 ft. of clay, between El. -10 and -70, is overconsolidated with an overconsolidation ratio (OCR) of about

11 at the top. The data from the MIT - P11 boring agrees very closely with the initial vertical effective stress ($\bar{\sigma}_{vo}$). The commonly-encountered correlation between liquidity index and stress history (LI $\geq$ 100% for OCR = 1) does not occur. However, the boundary between over- and normally consolidated clay of El. -70 is supported by field vane and UC and UUC data.

2.3.3 Compression and Consolidation Data

Figure 2-5 summarizes the compression and consolidation data from Storch (D22, D24) and M.I.T. (MIT - P11) oedometer testing. Values of the recompression ratio (RR = $\frac{Cr}{1+e_o}$) show a great deal of scatter, but the average RR is 0.024. The virgin compression ratio (CR = $\frac{Cc}{1+e_o}$) increases roughly linearly from the top of the clay to El. -70, where it becomes constant with increasing depth. Average CR lab values are 0.15 from El. -10 to -40, 0.19 between El. -40 and -70, and 0.21 below El. -70.

Values for the rate of secondary compression (C_α) at the insitu stress are depicted as plots of C_α ($C_\alpha = \frac{\Delta \varepsilon v}{\Delta \log t}$) versus depth. These values are for MIT - P11 data only. C_α is a stress-dependent parameter, and exhibits expected variation with depth (Ladd, 1971). In the over-consolidated region, C_α increases with increasing depth (as the ratio of initial to maximum past vertical effective stress $\bar{\sigma}_{vo}/\bar{\sigma}_{vm}$ approaches 1) and is roughly constant with depth in the normally consolidated zone

Coefficients of consolidation (C_v) versus depth, at the insitu stress, are also shown. In addition, estimated C_v values at the final effective vertical stresses, $\bar{\sigma}_{vF}$ (from the program FEECON) are shown. These were taken from Guertin's (1967) plots of C_v versus $\bar{\sigma}_{vc}$, on the basis of the ratio $\bar{\sigma}_{vF}/\bar{\sigma}_{vm}$. It is reasonable to assume that the effective C_v versus depth is represented by the average of both sets of C_v values. This approach results in the following average values: C_{v1} (above El. -70 for OCR > 1) = 0.27 ft^2/DAY, C_{v2} (below El. -70, for OCR = 1) = 0.09 ft^2/DAY, C_{v1}/C_{v2} = 3.0.

2.3.4 Undrained Shear Strength

Based on comsolidated-undrained triaxial compression test, $\overline{CIUC}$ (undrained shear after isotropic consolidation) and $\overline{CK_oUC}$ (undrained shear after K_o consolidation), on samples form MIT - P11, the normalized S_u ($S_u/\bar{\sigma}_{vo}$) vs. OCR relation is plotted in Figure 2-6. These tests were performed according to the SHANSEP procedures (Ladd, 1971). They were consolidated to 2-3 times $\bar{\sigma}_{vm}$ and rebounded to $\bar{\sigma}_v$ which gave the appropriate OCR, followed by shear.

Figure 2-7 shows various S_u vs. depth relationships from field and lab data. The strength relationship of Figure 2-6 was used to compute S_u vs. depth at the Test Section (solid line in Figure 2-7). In a similar fashion, S_u for plane strain active and passive (PSA and PSP) and direct simple shear (DSS) conditions are shown as dashed lines. However, these values are based on tests of laboratory prepared samples of resedimented Boston Blue Clay. These techniques and data are extensively covered in Kinner and Ladd (1970) and Ladd and Edgers (1972) among others. Unconfined (UC) and Unconsolidated-Undrained (UUC) test results from all three borings are also presented. Finally, Geonor Field Vane (FV) test results are shown for two tests performed prior to construction at Sta. 244 + 85.

The strength data shown in Figure 2-7 lead to the following observations:

(1) There is a significant difference between S_u with the major compressive stress in the vertical direction (S_uV from $\overline{CK_oU}$PSA data) and the horizontal direction (S_uH from $\overline{CK_oU}$PSP data). This indicates the importance of accounting for strength anisotropy.

(2) U and UU tests give much more scattered results and lower strengths than other test methods.

(3) The FV data are quite consistent below El. -50. Scattered data above this level could be due to sand or silt lenses or varying $\bar{\sigma}_{vm}$ due to varying degrees of desiccation. FV data coincides closely with S_uH from $\overline{CK_oU}$PSP tests in the NC zone.

(4) $\overline{CIUC}$ and $\overline{CK_oUC}$ test data, the most sophisticated data an engineering firm may have, may be slightly conservative or very unsafe, depending upon location. Beneath the centerline where $\bar{\sigma}_{1F}$ is vertical, it may be safe , but away from the centerline, as $\bar{\sigma}_{1F}$ tends toward the horizontal, this type of data is unsafe.

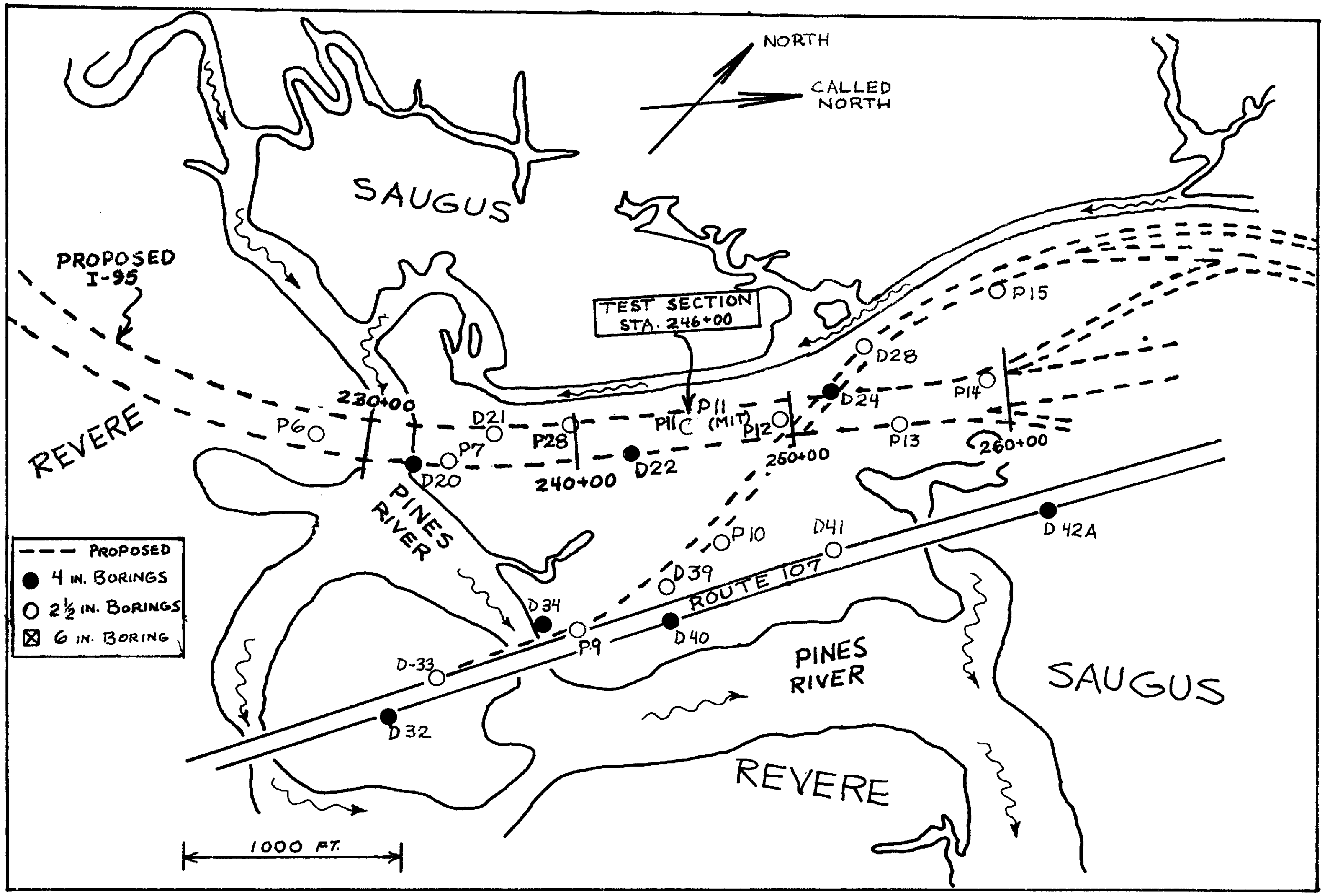

FIGURE 2-1 SITE LOCATION PLAN

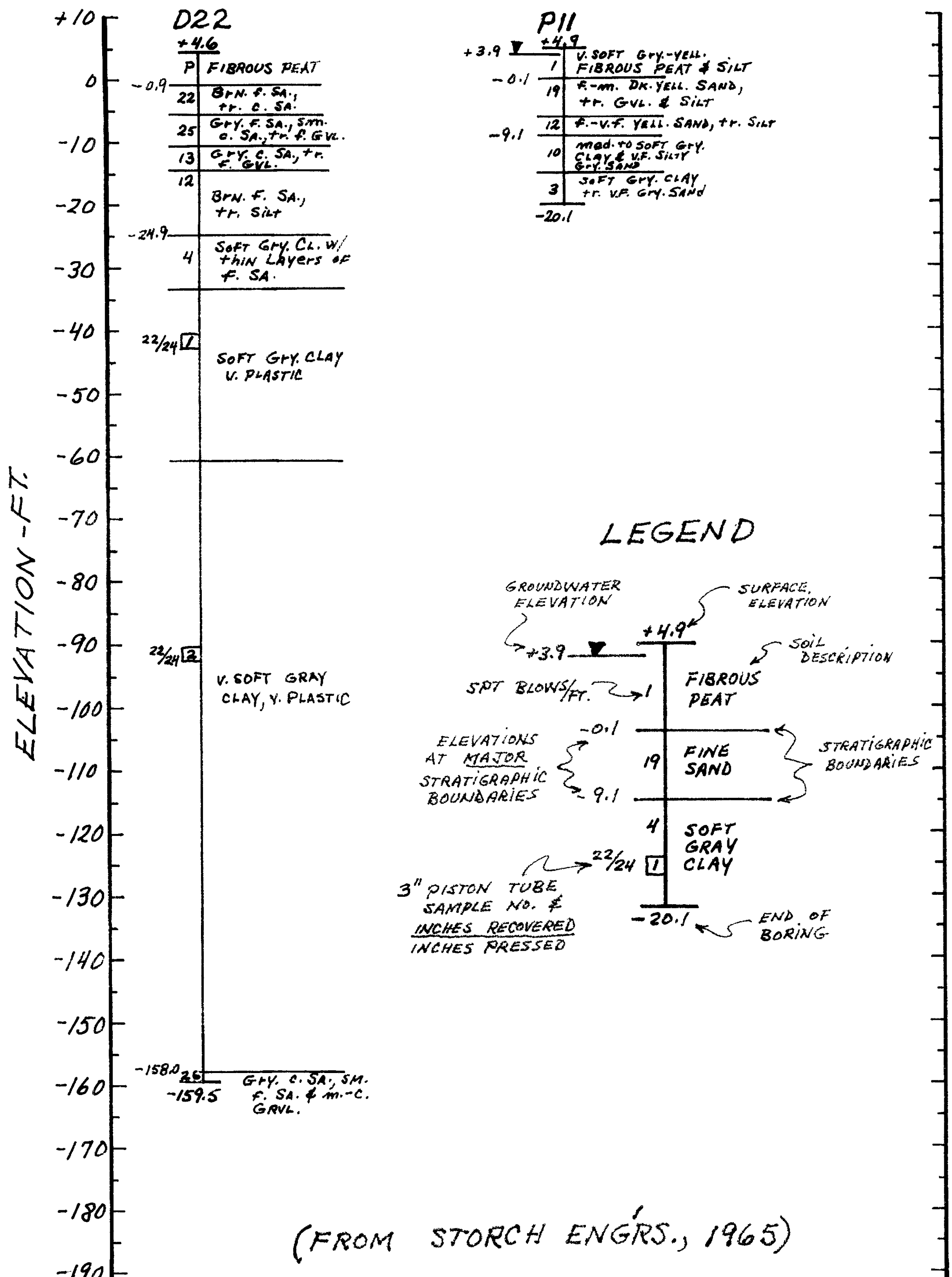

FIGURE 2-2 NEAREST STORCH BORINGS

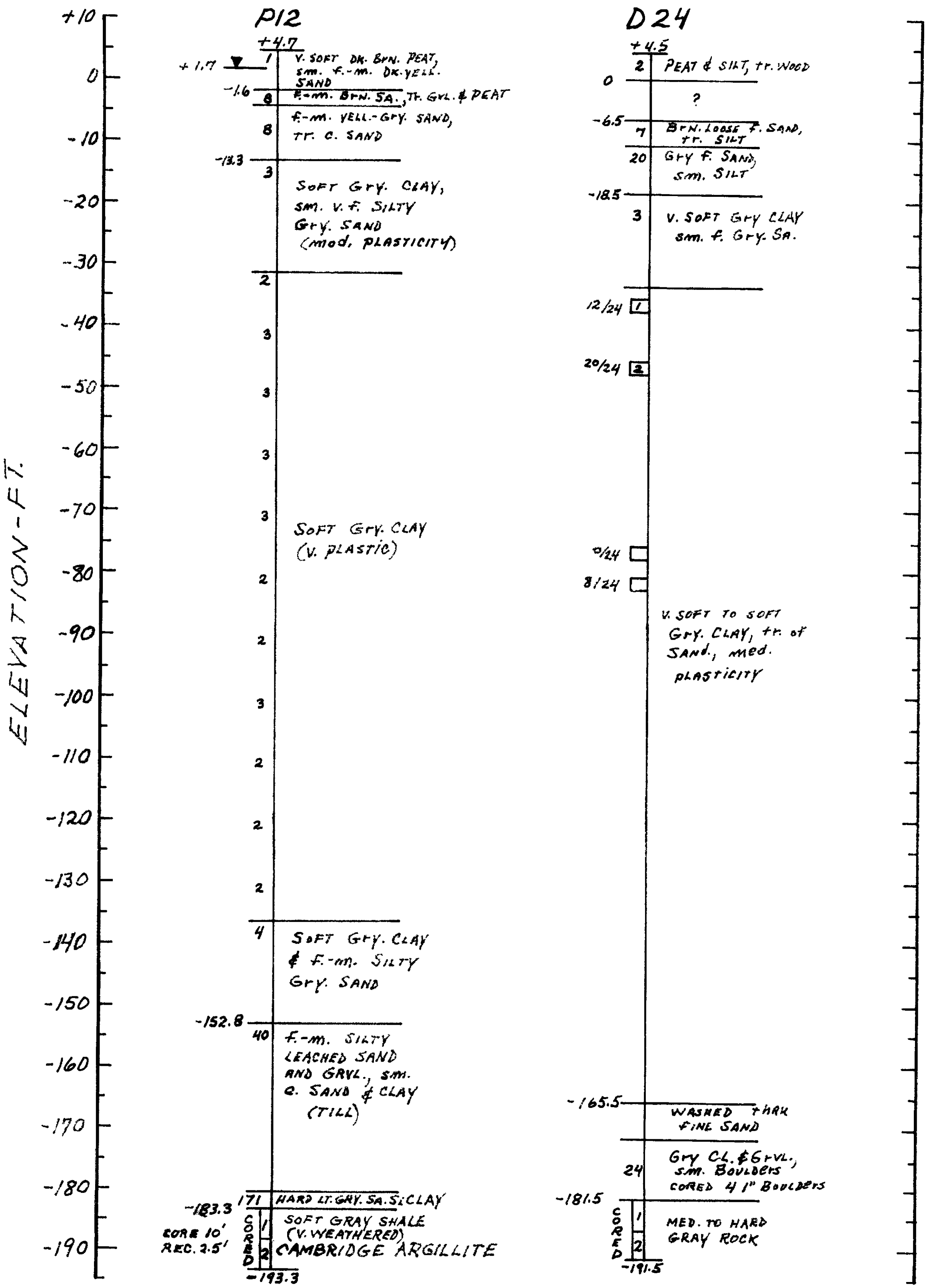

FIGURE 2-2 CONT'D.

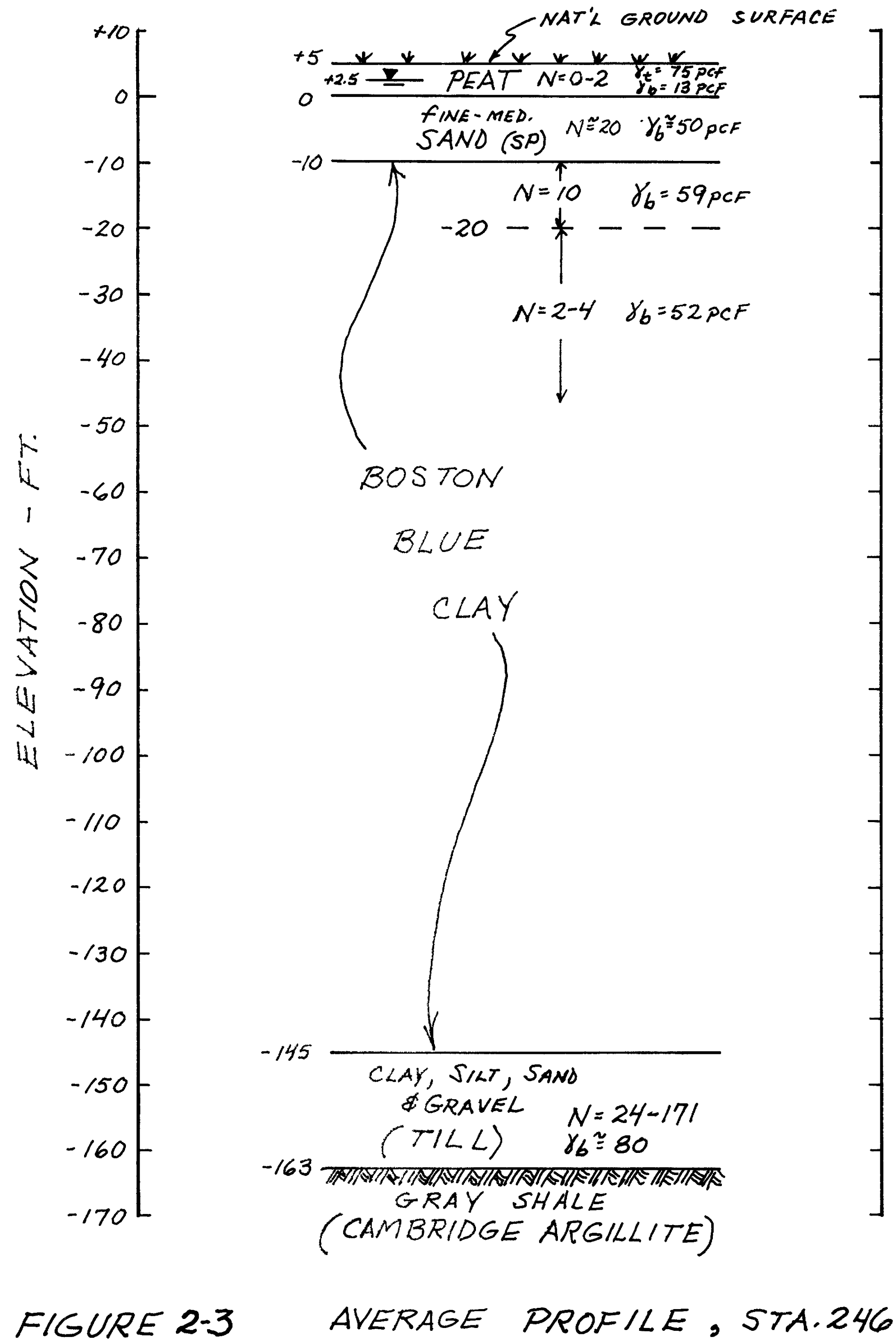

FIGURE 2-3 AVERAGE PROFILE, STA. 246

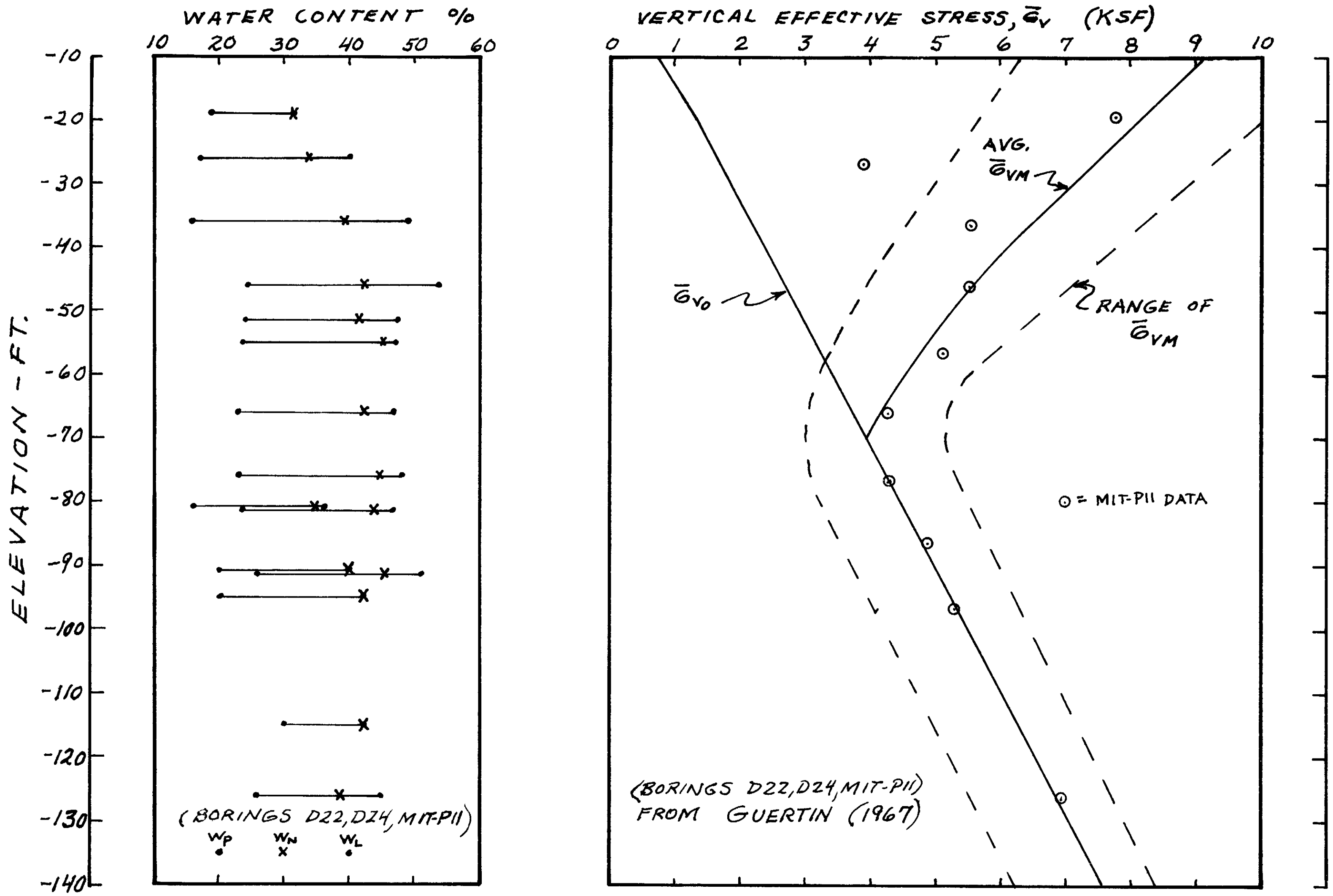

FIGURE 2-4 ATTERBERG LIMITS AND STRESS HISTORY

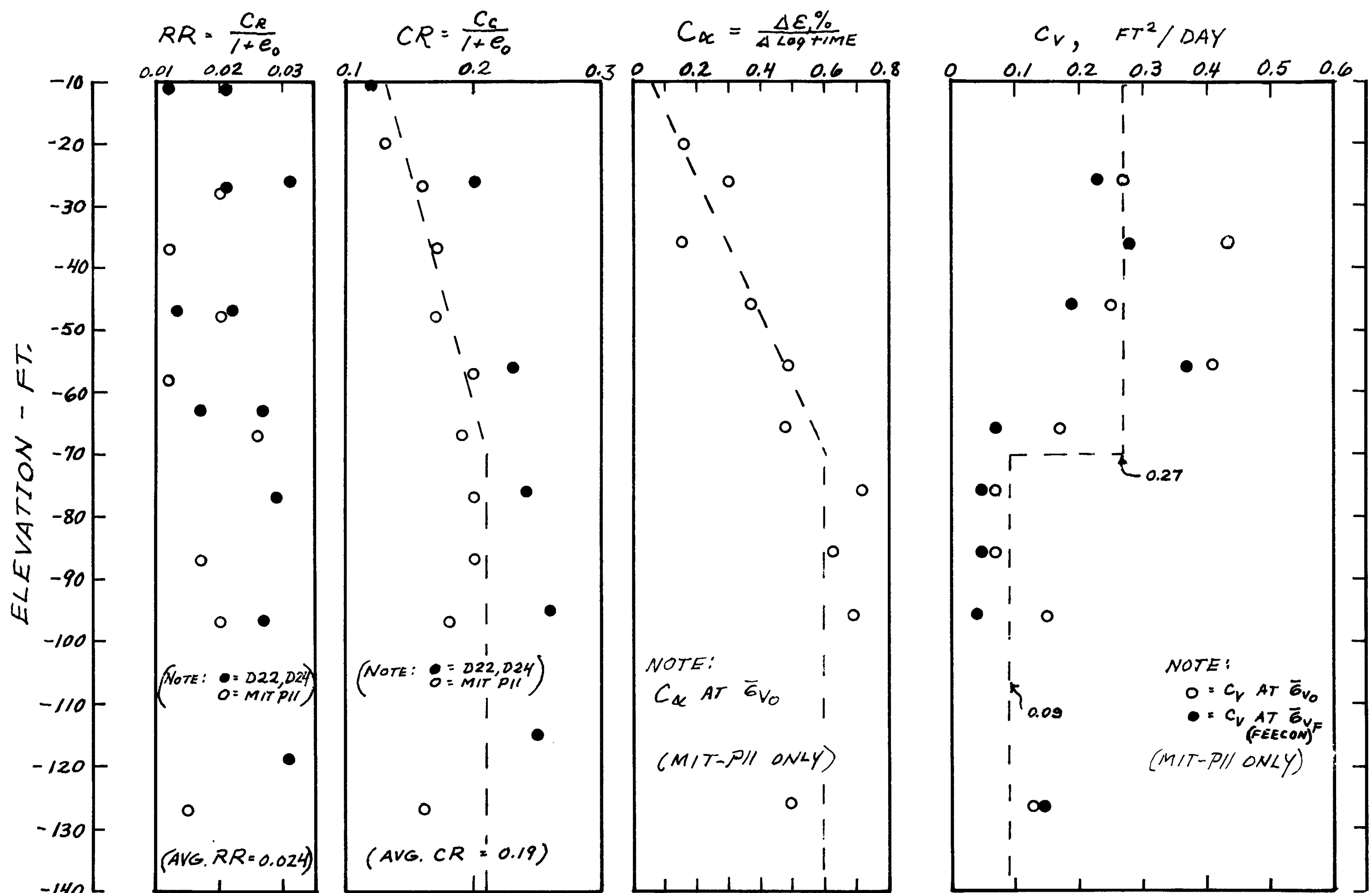

(FROM GUERTIN, 1967)

FIGURE 2-5 COMPRESSION AND CONSOLIDATION DATA, STA. 246

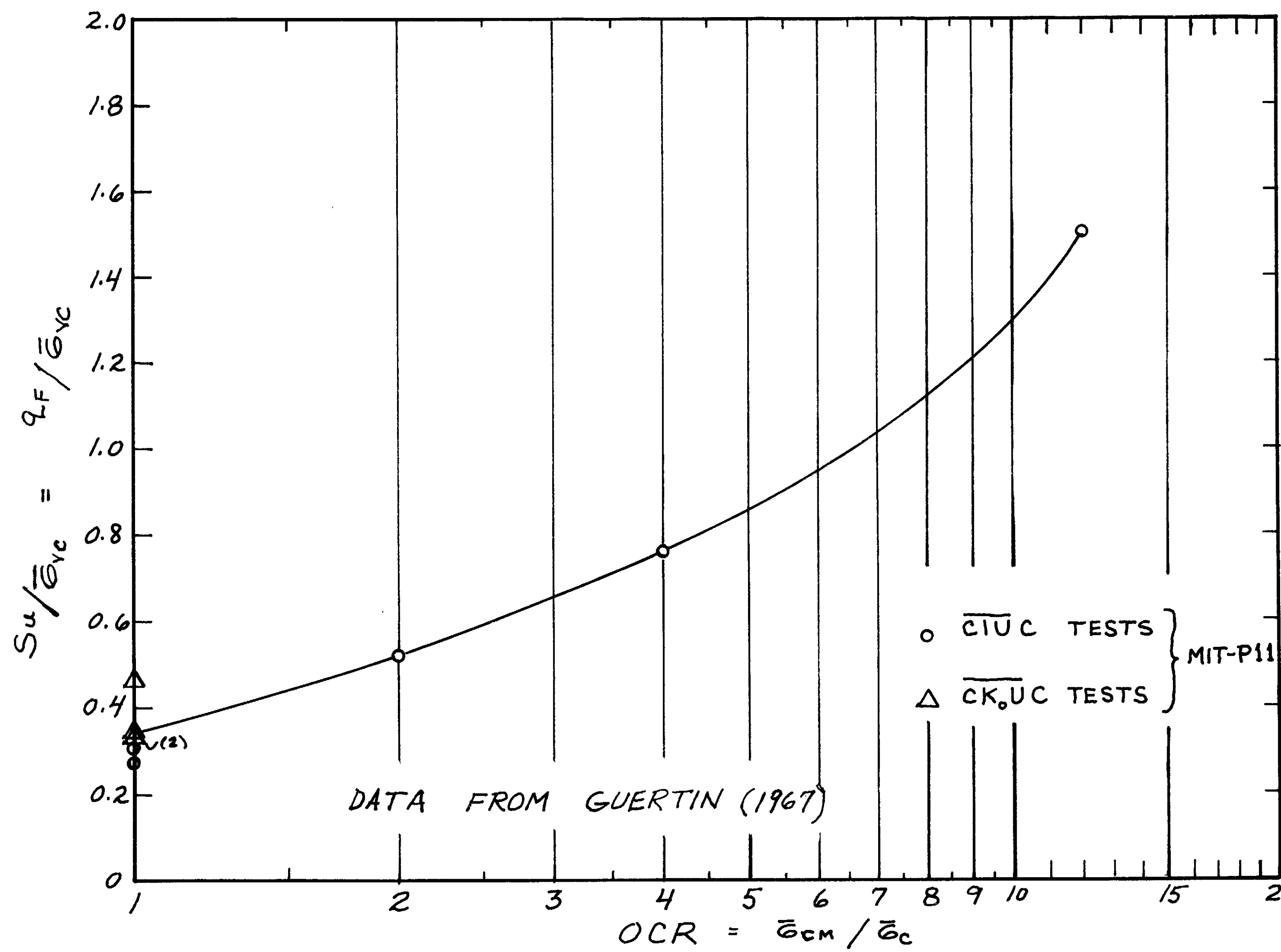

FIGURE 2-6 $S_u/\bar{\sigma}_{vc}$ vs. OCR FROM TRIAXIAL TESTS ON STA. 246 SAMPLES

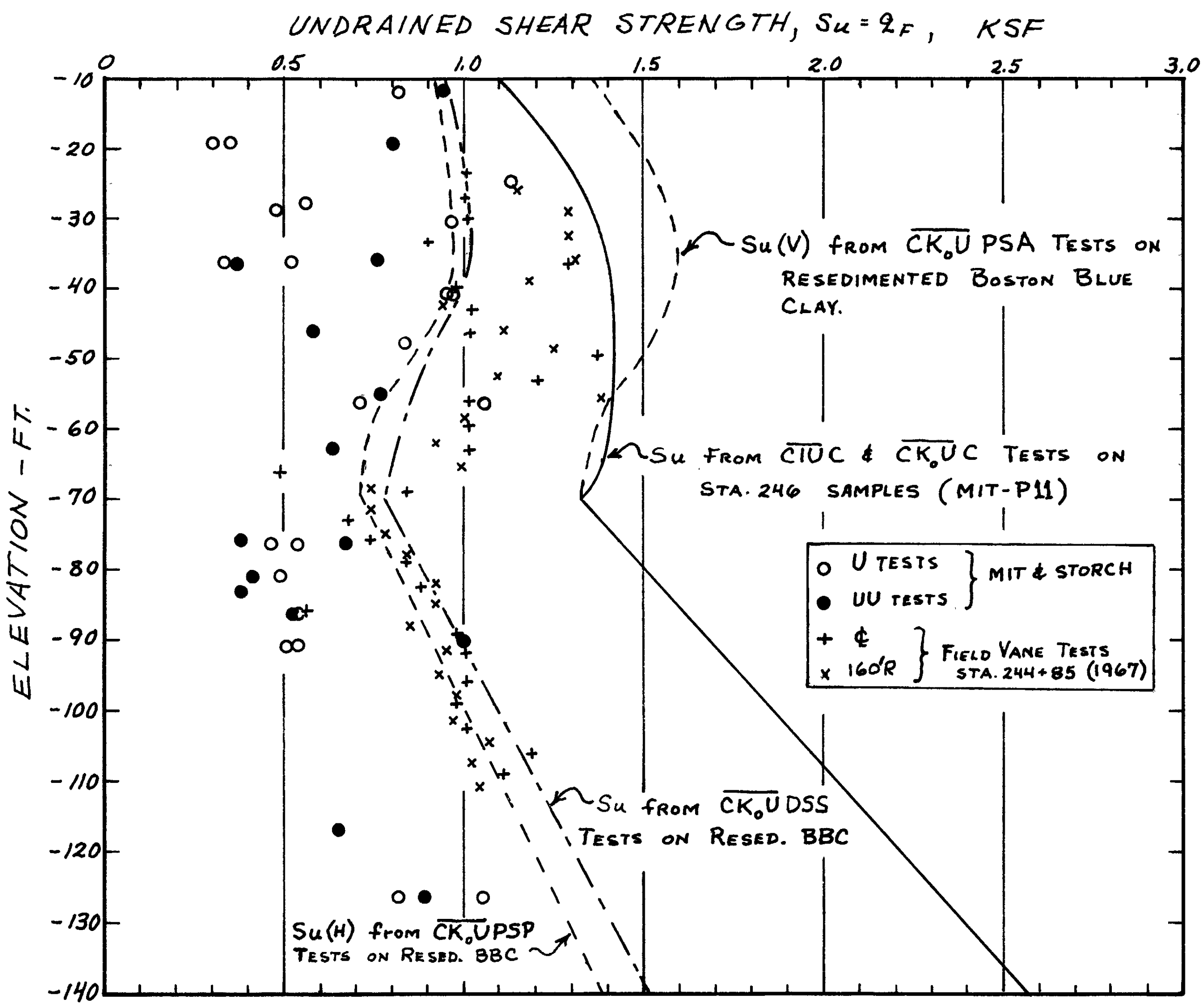

FIGURE 2-7 UNDRAINED SHEAR STRENGTH, STA. 246

3. CONSTRUCTION HISTORY

3.1 GENERAL

Throughout this report, reference is made to time in Construction Days (CD). The date 1 Sept. 1967 was designated as CD 1. It roughly coincides with the completion of the earliest instrument installations. A Date - Construction Day conversion chart is given in Appendix A-1.

3.2 EMBANKMENT CONSTRUCTION

The final design embankment grade for the pavement is El. +18 ft at Sta. 246 (13 ft. above natural grade). To minimize post-contruction settlements, the embankment was preloaded with a surcharge to El. +40 ft. in three stages of filling. (see Figure 3-1).

Stage 1 consisted of excavation of the 5 ft. peat layer followed by replacement with fill (probably end-dumped to El. +5) and continued filling to the Stage 1 El. of +9. The excavation and replacement to original grade ocurred during Dec. 1-7 1967 (CD 92-98). The stage 1 El. of +9 was reached on 1 Jan 1968 (CD 123).

Except for minor construction operations (installation of instruments and access tunnel), no further filling ocurred for almost seven months. Stage 2, which included the placement of about 70% of the final fill height, began on 24 June 1968

(CD 298). This stage continued without interruption until the fill reached El. +36 of 4 Dec. 1968 (CD 461). The final stage, Stage 3, consisted of the placement of the final 4 ft. of fill between 20 April and 12 May 1969 (CD 598-620). Embankment construction is tabulated in Appendix A-2.

The fill material consisted of a well-graded fine to coarse sand with some fine to medium gravel (SW). Results of field unit weight tests on various lifts above El. +22 are given in Figure 3-2 (Wolfskill and Soydemir, 1971). The fill was compacted with rubber-tired rollers above El +5. Based on these data, the average total unit weight is 119 pcf. Since values as low as 102 pcf occur in the compacted fill, a value of 100 pcf was chosen for the dumped fill between El. 0 and +5.

3.3 INSTRUMENTATION

Figures 3-3 and 3-4 show the embankment profiles and instrumentation at Sta. 245 and Sta. 246. Although the details of the instrumentation are covered in Wolfskill and Soydemir (1971), a brief summary is provided here.

There are two groups of instruments. The major group, the "construction instruments", was installed at the Test Section after Stage 1 (El. +9) was completed. A minor group, the "preconstruction instruments", was installed prior to any construction at Sta. 245. These instruments were to provide performance data for the 1st Stage of construction.

Most of the Test Section instruments are accessible from a tunnel beneath the right (East) side of the embankment. This was to provide protection from vandals and weather. The time of initial readings of the instruments are shown in Figure 3-1. Instrumentation is tabulated in Appendix A-1.

At Sta, 245 the settlement instrumentation consisted of six Borros Points, one of which was installed in the till and used as a temporary benchmark. The only other instruments were six M206 single-tube hydraulic piezomenters.

At Sta. 246, all M.I.T.-monitored instrumentation was located between 30'L and 225'R. There were a few MDPW-monitored instruments located further to the left of the centerline. the M.I.T. settlement devices included four settlement platforms at the top of the natural sand. Additionally, deep settlement data were provided by twelve settlement rods in the clay. These consisted of cased 1" o.d. pipes with round 2 1/2" o.d. plates welded 18" above the tips. A permanent cased benchmark was installed in the till.

M.I.T. pore pressure data was provided by 38 piezometers at various offsets and elevations in the clay and till. In addition, 5 porous-point well points were installed in the bottom of the natural sand. Five slope indicators (inclinometers) were also installed beneath the right side of the embankment. Finally, three total-stress cell clusters were installed within the embankment at El. +17.

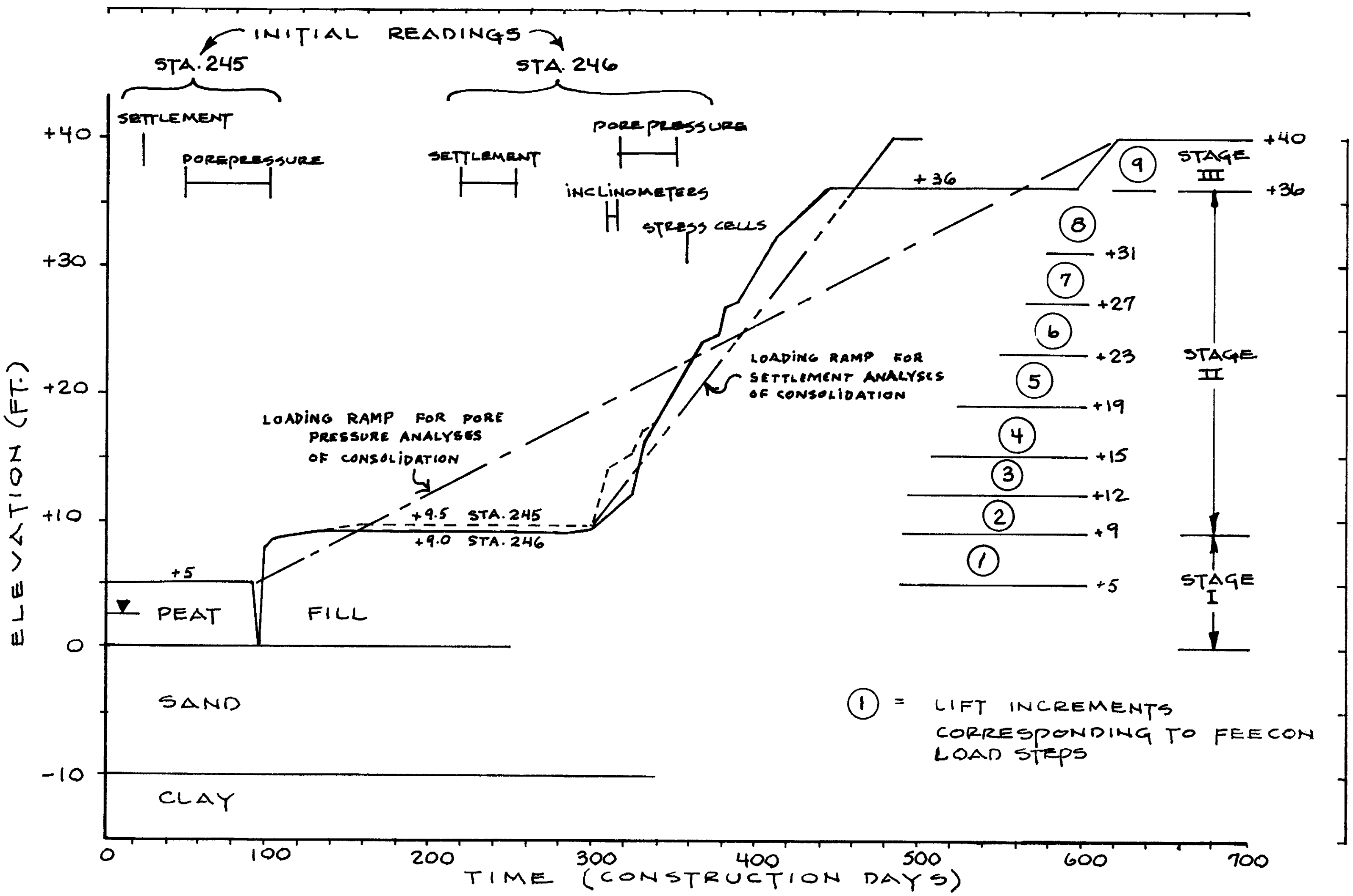

CONSTRUCTION HISTORY

FIGURE 3-1

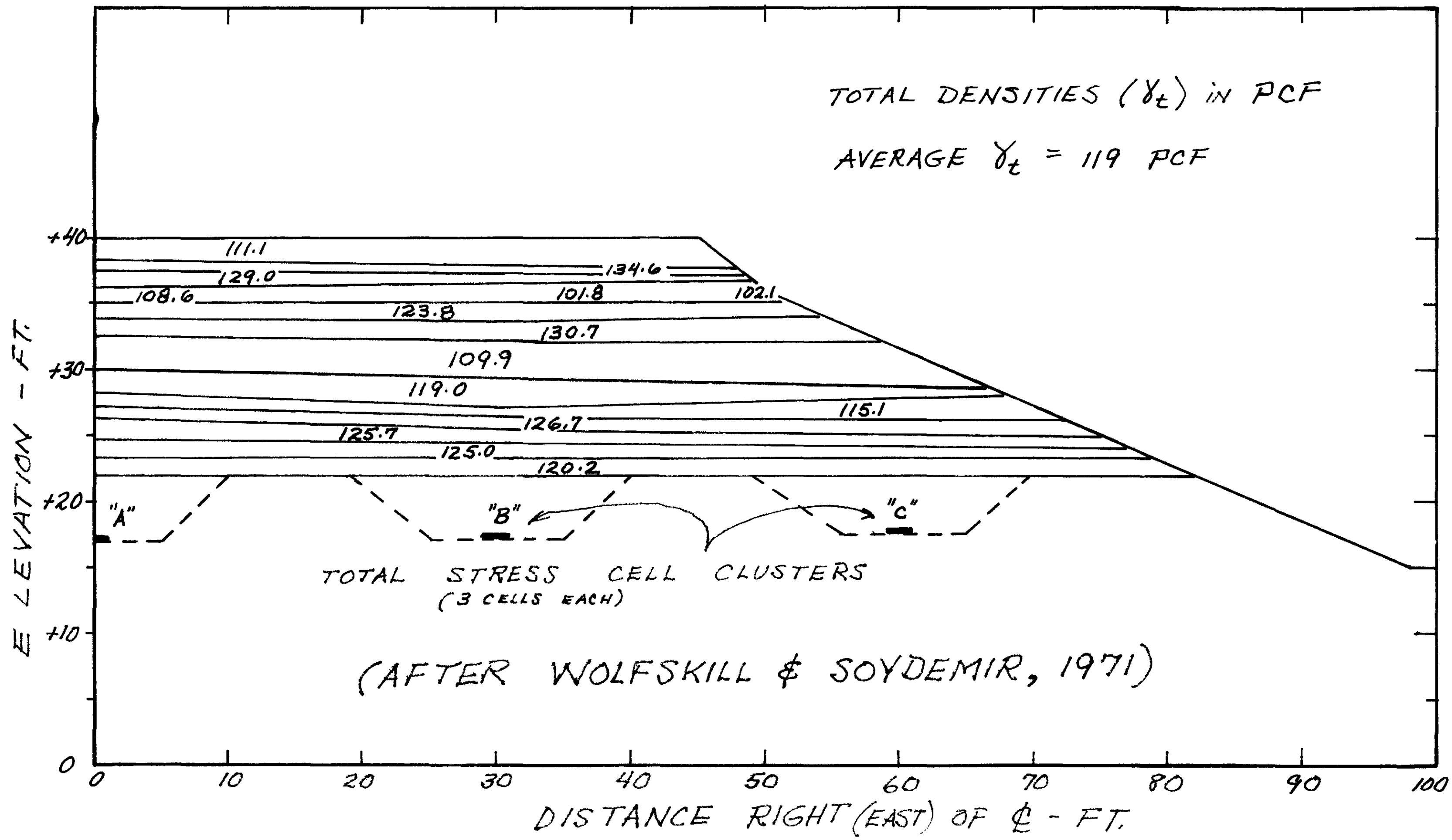

FIGURE 3-2 EMBANKMENT DENSITY

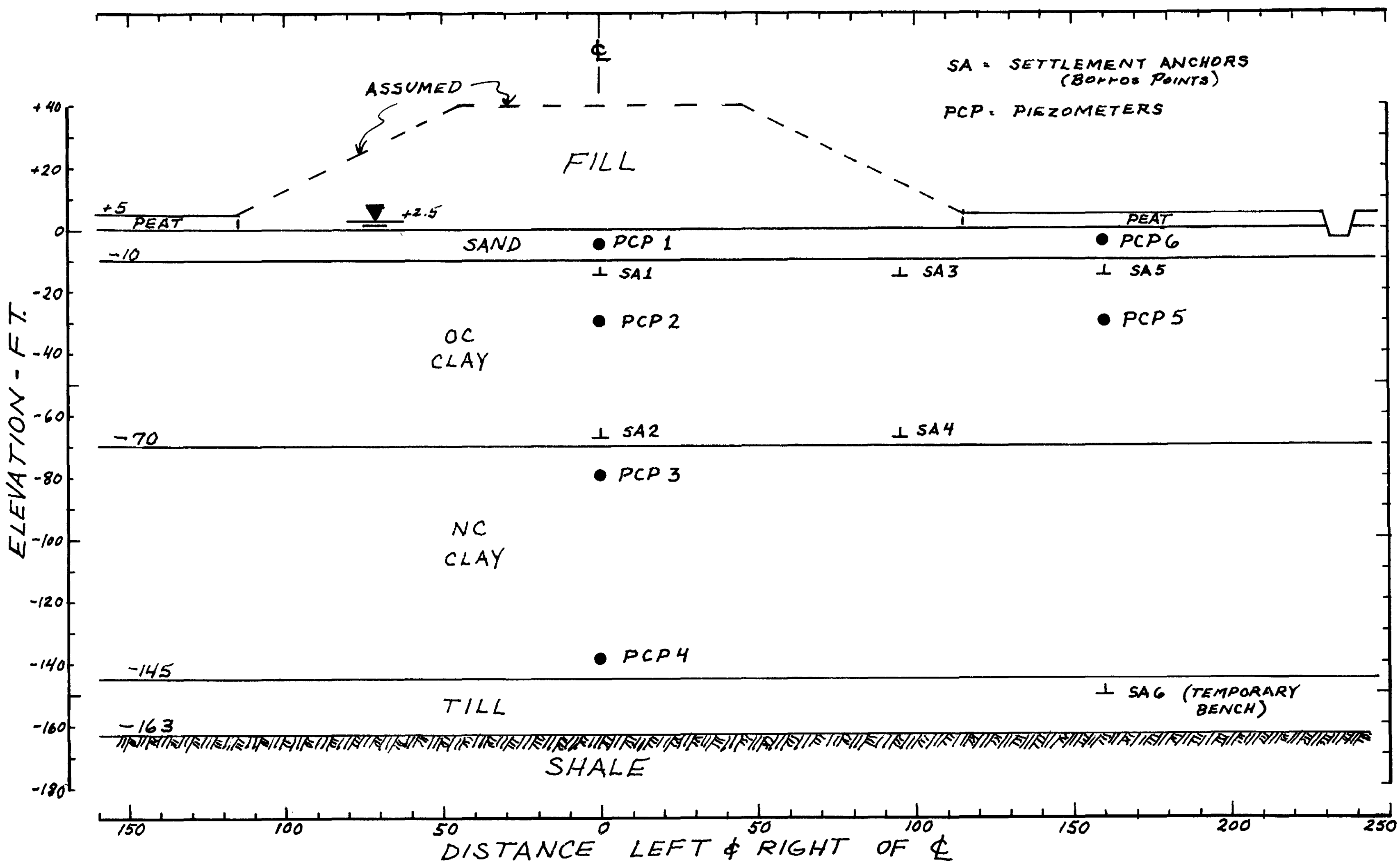

FIGURE 3-3 EMBANKMENT PROFILE AND INSTRUMENTATION, STA. 245

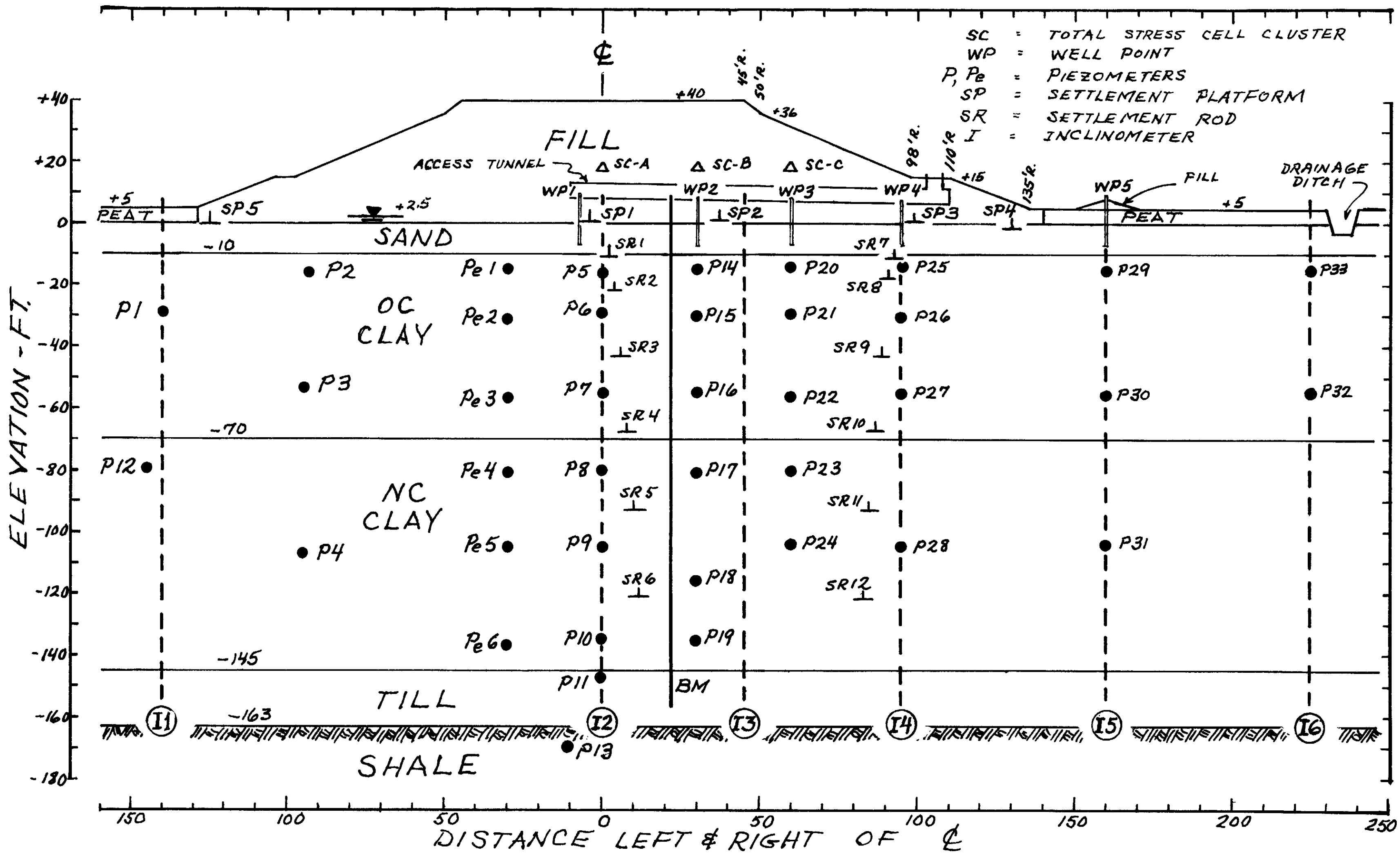

FIGURE 3-4 EMBANKMENT PROFILE AND INSTRUMENTATION, STA. 246

4. EMBANKMENT PERFORMANCE

4.1 GENERAL

Most of the data pertinant to the performance of the foundation clay are presented and utilized in this report. The most important data excluded are the total stress cell measurements for the embankment interior (El. +17). In addition, data from the state monitored instruments were not analyzed.

4.2 SETTLEMENT

Figure 4-1 shows the measured settlement at the top of the sand and the top of the clay beneath the right side of the embankment. Settlements are shown for CD 620 (end of construction) and several times afterward, and are dish-shaped, indicating elastic loading.

Total measured settlements and fill elevation are plotted versus time (log scale) for Sta. 245 and Sta. 246 in Figures 4-2 to 4-4. At Sta 245, readings were not taken during the entire construction period. They appear very erratic because of the small scale. However, the actual variations are not excessive, being only ± 0.02 ft. It is not clear from Sta. 245 data if settlement of the clay due to Stage 1 consolidation was complete prior to Stage 2 filling.

Due to improper installation of some cased settlement rods at Sta. 246, some of the deep settlement data became unusable. The specifications originally called for a minimum vertical distance of 0.5 ft. between the bottom of the casing and the supporting plate on the settlement rod. As actually installed this distance varied greatly - between 0.17 and 1.27 ft. A combination of insufficient clearance and large settlements invalidated the data for four settlement rods: SR4 and SR6 (centerline), and SR10 and SR11 (90' R).

Possible corrected settlements for these rods are shown in Figures 4-2 and 4-3 as dashed lines. Unfortunately, the casing elevations were only monitored twice: upon installation and 8 November 1973 (as an outcome of this study). As a result, the times when casing settlement actually invalidated the data are unkown. Figures 4-2 and 4-3 indicated that this occurred before the following times: SR4, CD1200; SR6, CD1200; SR10, 1300; Srll, CD1100.

An attempt was made to determine the earliest day when casing settlement invalidated the four deep settlement points. It was assumed that the ratio of casing settlement (based on top elevation and assuming no compression) and the settlement of the nearest platforms was a constant between the installation date and 8 Nov. 1973. This allowed an estimate of casing settlement versus time. The earliest invalid day is the day on which the casing settlement exceeded the rod settlement by an amount equal to the initial clearance. The resulting earliest invalid days are: SR4, CD382; SR6, CD860; SR10, CD1470; SR11, CD1037.

Although four rods produced invalid total settlements, seven sets of differential settlement data were invalidated. Casing drag on one rod will result in a reduced apparent differential settlement (or even heave) in the overlying layer, and increased differential settlment in the underlying layer. The measure differential settlements at Sta. 246 are shown in Figures 4-5 and 4-6. The curves plotted represent the measured differential settlements between adjacent settlement rods. For example, SR1-2 is the difference in total measured settlement between SR1 and SR2. Due to casing drag the following remarks can be made about the apparent differential settlements in Figures 4-5 and 4-6:

SR 3-4	too low
SR 4-5	too high
SR 5-6	too low (apparent heave)
SR 6	too high
SR 9-10	too low
SR 10-11	probably too low
SR 11-12	too high

The above errors in measured settlements greatly complicate analysis of the settlement data. All that is certian is that at the centerline, final consolidation settlement has been reached above SR3 (El. -43). Similarly, at 90 ft. right, final consolidation settlement has been reached above SR8

(El. -18) and it is probably close between SR8 and SR9 (El. -43). In Chapter 7, only differential settlement data of known validity is used in consolidation analysis, and the data is plotted in Figures 7-3 and 7-4.

Although the behavior of the natural sand is not an object of this study, one aspect is interesting. The differential settlement between SP3 and SR7, 90'R, indicates that the natural sand dilates after an initial compression. This occurs after the fill height is a maximum above SP3 (El. +16), so that further filling is moving laterally away from SP3.

All settlement data are tabulated in Appendix A-4. The vertical distribution of settlement vs. time is discussed in Chapter 7.

4.3 PORE PRESSURES

Measured excess pore pressures in feet of water are plotted vs. time (log scale) for Sta. 245 and Sta. 246 in Figures 4-7 to 4-14. Since readings were generally made every day, only representative data points (except at Sta. 245) are plotted. The measure excess pressure represents the difference between the measure total head elevation at a piezometer and the "hydrostatic" piezometric elevation at the piezometer.

At Sta. 245, the hydrostatic elevation was assumed equal to the total head elevation indicated by the piezometers in the natural sand. At Sta. 246, the hydrostatic elevation was assumed equal to the water elevation in the nearest well in natural sand. It must be noted that in reality this is not correct. The data for the centerline piezometers indicates that the piezometric water elevations (PWE) in the sand above the clay and the till below are not equal. As a result of an apparent artesian condition, the PWE is increased by five ft. in the till. For simplicity, however, the PWE in the sand was used for all plots. As a result, the till appears to have an excess pore pressure of 5 ft. rather than it's true value of zero (Figure 4-8, P 11)

Readings at Sta. 245 were not made for the entire construction period. All of these piezometers consisted of Geonor M206, single-lead, bronze-point hydraulic piezometers. These appear to be fairly reliable, although they are slightly more erratic (± 2 ft. of head) than the more sophisticated types at Sta. 246. The limited data available for Sta. 245 indicate that at the center of the clay there was essentially no pore pressure dissipation between Stages 1 and 2.

The M.I.T. piezometers at Sta. 246 consisted of two types: Geonor vibrating wire electric piezometers at 30'L, and two-lead, porous-plastic point hydraulic piezometers elsewhere. Although a reliability analysis has been performed by Wolfskill and Soydemir (1971), an up-dated review is advisable. At Sta. 246, the electric piezometers produced consistent data (± 0.5 ft. of head) but only short-term reliability (only 33%, or 2 of 6, were operating at CD 2053). The hydraulic type generally showed the same degree of consistency, but better long-term reliability (52%, or 16 of 31 installed were operating reliably at CD 2053).

For comparison with predicted values (using FEECON), maximum "measured" excess heads were taken as the peak values at the end of Stage 2 filling plus the increase due to Stage 3 filling. It was necessary to estimate excess heads for the inoperative piezometers. For these, an estimated excess head vs. time curve was drawn based on operating piezometers whose locations indicated a similar performance. The results are shown as dashed lines in the Figures.

The maximum "measured" excess heads are tabulated in Table 4-1. In addition, representative piezometer and well data are tabulated in Appendix A-5. The vertical distribution of excess pressure vs. time is discussed in Chapter 7.

4.4 HORIZONTAL DEFLECTION

No inclinometers were installed with the preconstruction instrumentation (Sta. 245), but 6 were installed at Sta. 246. Of these, 5 inclinometers between the centerline and 225'R were read by M.I.T.. The instruments were 3 in. in diameter grooved aluminium casings in 5 ft. sections connected by flexible couplings permitting 6 in. of vertical movement.

Figure 4-15 presents standard plots of horizontal deflection vs. elevation at the end of construction (CD 620) and several times afterward. It was desired to study the horizontal deflections versus time for all depths within the clay. Normal methods of portraying inclinometer data do not permit this where deflections are relatively small (as at the MIT-MDPW Test Section). Therefore, the horizontal deflection at various elevations are plotted vs. time (log scale) in Figures 4-16 to 4-19. Data from the centerline inclinometer (I-2) are not plotted. It indicated a maximum of only 0.8 inches at the end of loading, indicating slightly asymmetrical loading

The inclinometer data are somewhat erratic, but not abnormally so ($\pm$ 0.5 in.) in view of the great depth of clay and relatively small deflections. The most erratic data, between CD600 and CD900 and after CD1700, are probably due to the interchangeable use of several different Wilson torpedoes. Converely, the most consistent data, between CD 1300 and CD 1700, were obtained with the M.I.T. automatic recording instrument "Beaver" (Bromwell et. al., 1971).

The data show that the greatest rate of deflection occurs during filling operations. At the end of the filling there is a slower but constant rate of outward creep (related to log time). Generally, after the end of filling the slopes of the deflection-time curves between El. -10 and El. -70 (OC zone) are approximately parallel. This indicates that there is no creep in this zone, and all outward creep is due to the normally-consolidated clay between El. -70 and El. -145. A study of the differential creep (analogous to the differential settlement) was not undertaken for this report.

The fact that there is no consistently varying break in the deflection-time curve (with location in the clay) suports the assumption that horizontal deflection is not a consolidation-related phenomena. The maximum deflection occurs beneath the embankment slope (I-4, 95'R.) rather than at the toe as one might expect.

The inclinometer data are tabulated in Appendix A-6. Elevations were based on the average of the casing elevations at the first and latest readings.

4.5 INTERNAL EMBANKMENT STRESS

When the fill elevation reached +20 ft., three clusters of stress cells were installed in circular pits excavated to El. +17. The clusters were placed at the centerline, 30 ft. R, and 60 ft. R. Each cluster consisted of three Geonor P-100 vibrating wire total stress cells. The datails of this operation and the results are presented in Wolfskill and Soydemir (1971). Excellent agreement with embankment stresses predicted by Perloff's method (Perloff, et. al., 1970) was achieved with the fill El. at +40. The data agree with total vertical stress based on the weight of the overlying fill for the centerline and 60'R and is 85% of that value at 30'.

℄			30'R.			30'L.			60'R.			95'R.			160'R.			225'R.		
$P_{i_{EZ}}$	EL. FT.	$u_{e_{MAX}}$ FT	$P_{i_{EZ}}$	EL. FT.	$u_{e_{MAX}}$ FT.	$P_{i_{EZ}}$	EL. FT.	$u_{e_{MAX}}$ FT.	$P_{i_{EZ}}$	EL. FT.	$u_{e_{MAX}}$ FT.	$P_{i_{EZ}}$	EL. FT.	$u_{e_{MAX}}$ FT.	$P_{i_{EZ}}$	EL. FT.	$u_{e_{MAX}}$ FT.	$P_{i_{EZ}}$	EL. FT.	$u_{e_{MAX}}$ FT.
P5	-15.9	5.3	P14	-15.0	3.0	Pe 1	-15.0	8.0	P20	-13.8	1.5	P25	-13.6	1.7	P29	-14.5	3.3	P33	-15.0	1.5
P6	-28.6	15.5	P15	-29.7	20.2	Pe 2	-31.2	17.2	P21	-28.8	15.0	P26	-29.9	8.4						
P7	-55.0	47.3	P16	-55.1	47.8	Pe 3	-56.6	47.0	P22	-55.8	42.3	P27	-54.8	26.8	P30	-55.5	18.2	P32	-55.0	5.9
P8	-80.2	54.7	P17	-80.8	51.3	Pe 4	-81.0	52.8	P23	-79.9	49.3									
P9	-105.2	49.8	P18	-115.5	41.0	Pe 5	-105.3	51.5	P24	-104.0	43.7	P28	-104.7	36.8	P31	-104.0	21.3			
P10	-135.0	22.4	P19	-135.0	21.6	Pe 6	-136.6	22.7												
P11	-147.4	12.0																		

TABLE 4-1 MAXIMUM MEASURED EXCESS HEAD, STA. 246

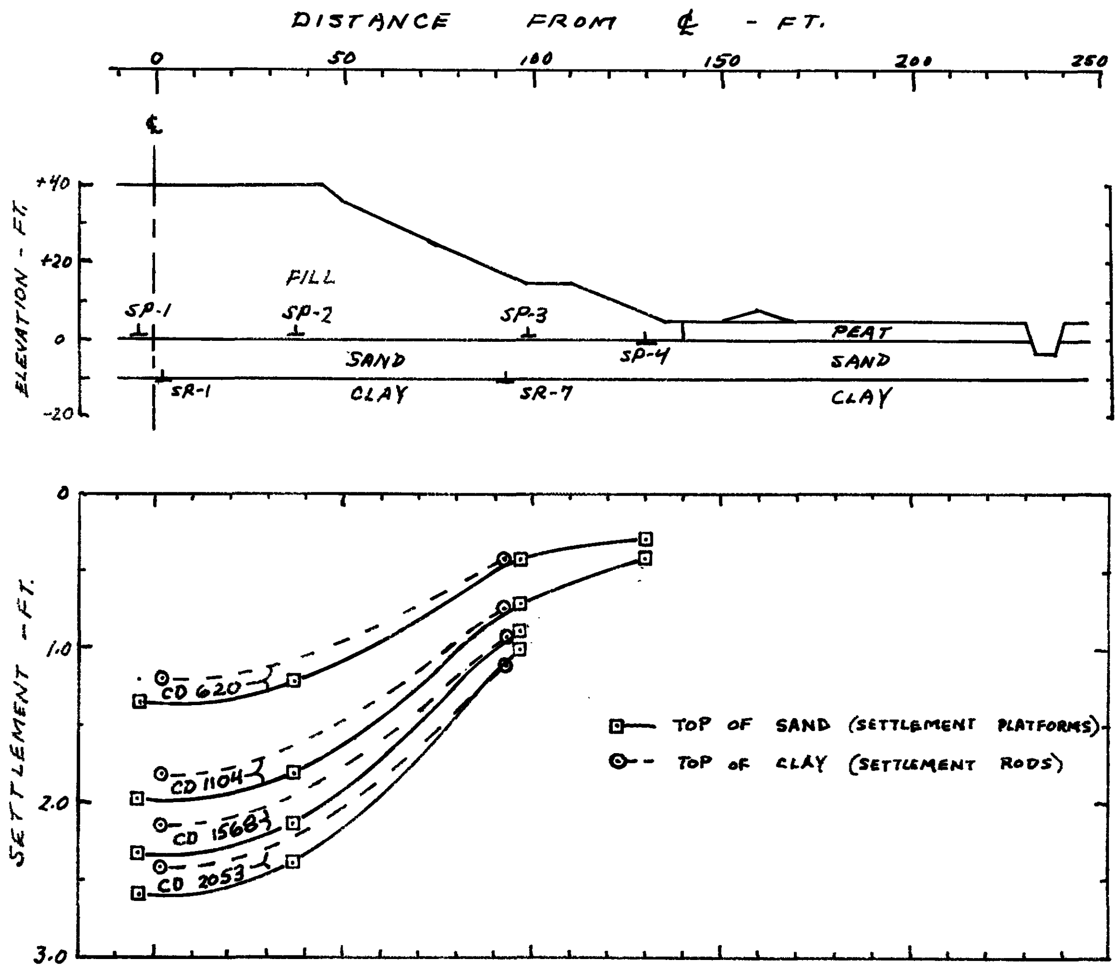

FIGURE 4-1 LATERAL DISTRIBUTION OF MEASURED SETTLEMENT

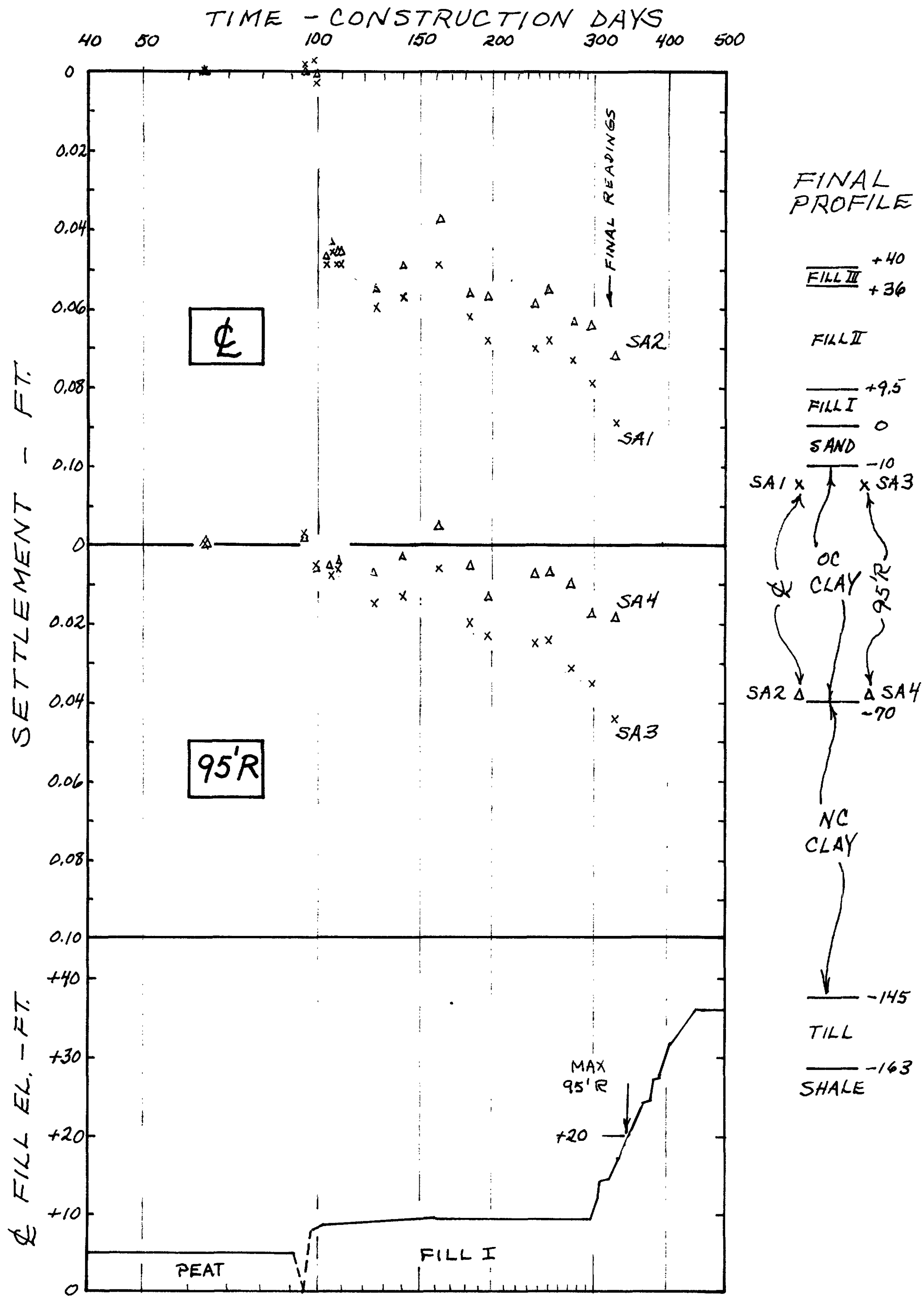

FIGURE 4-2 MEASURED SETTLEMENT, STA. 245, ℄ & 95'R.

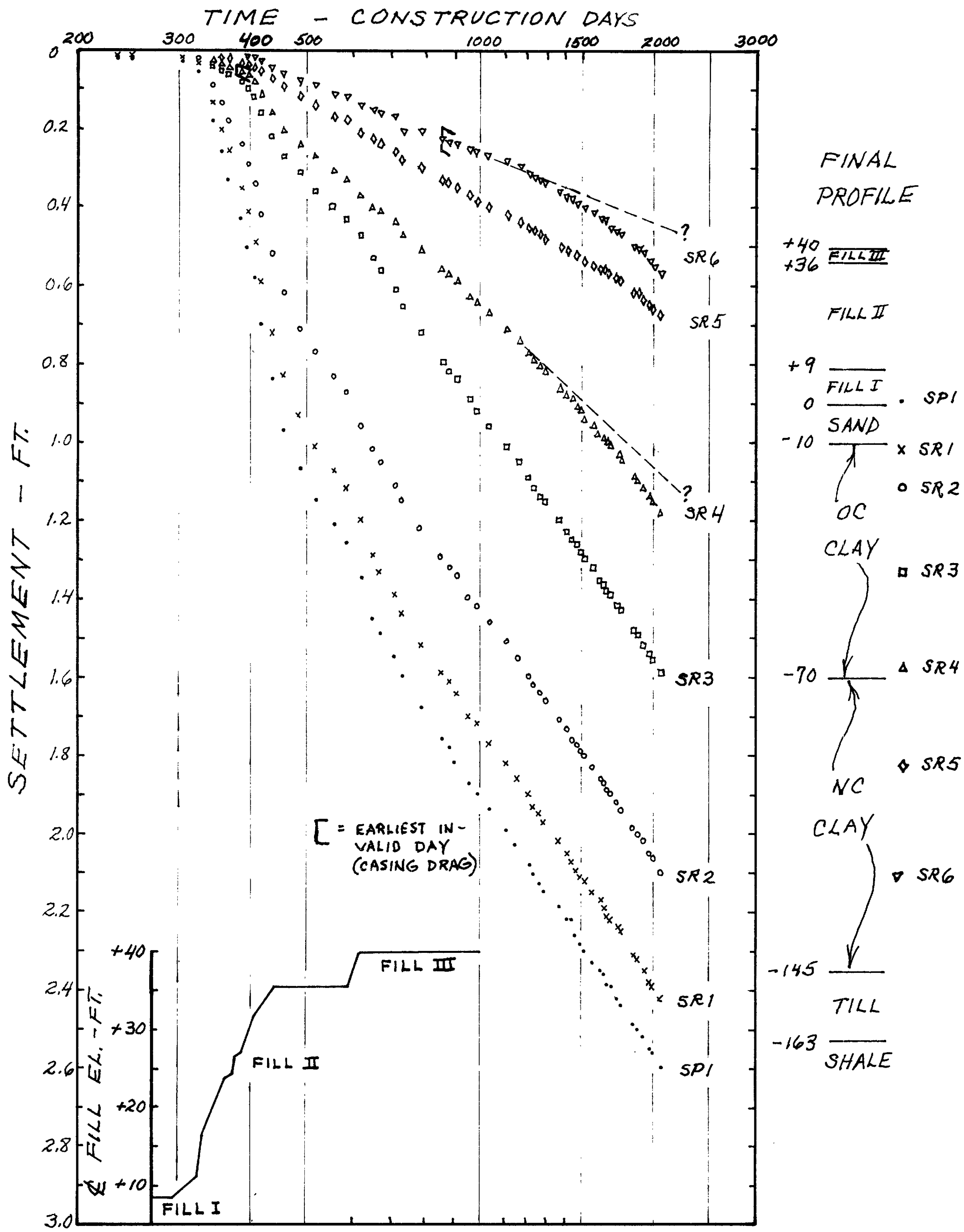

FIGURE 4-3 MEASURED SETTLEMENT, STA. 246, ℄

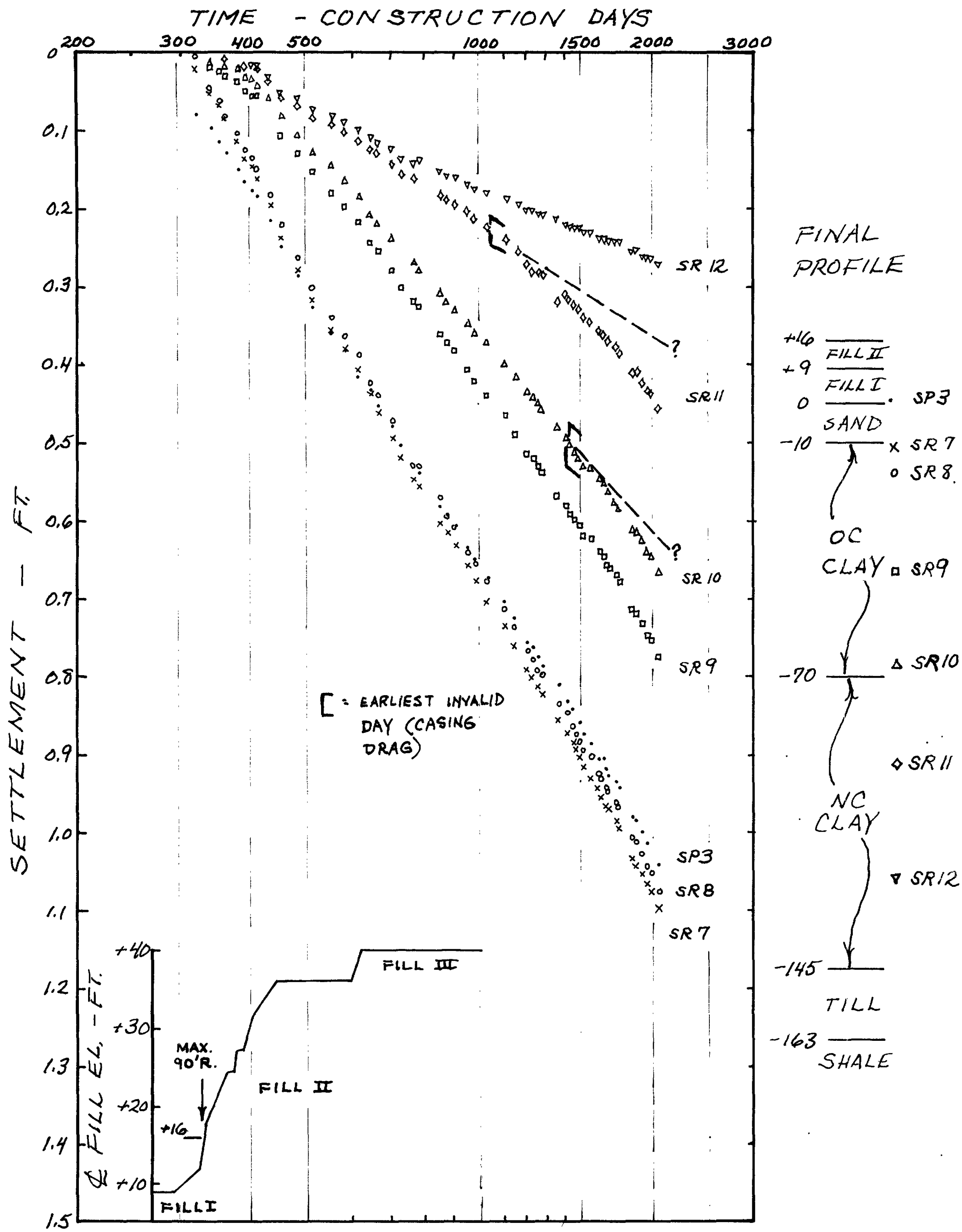

FIGURE 4-4 MEASURED SETTLEMENT, STA. 246, 90'R.

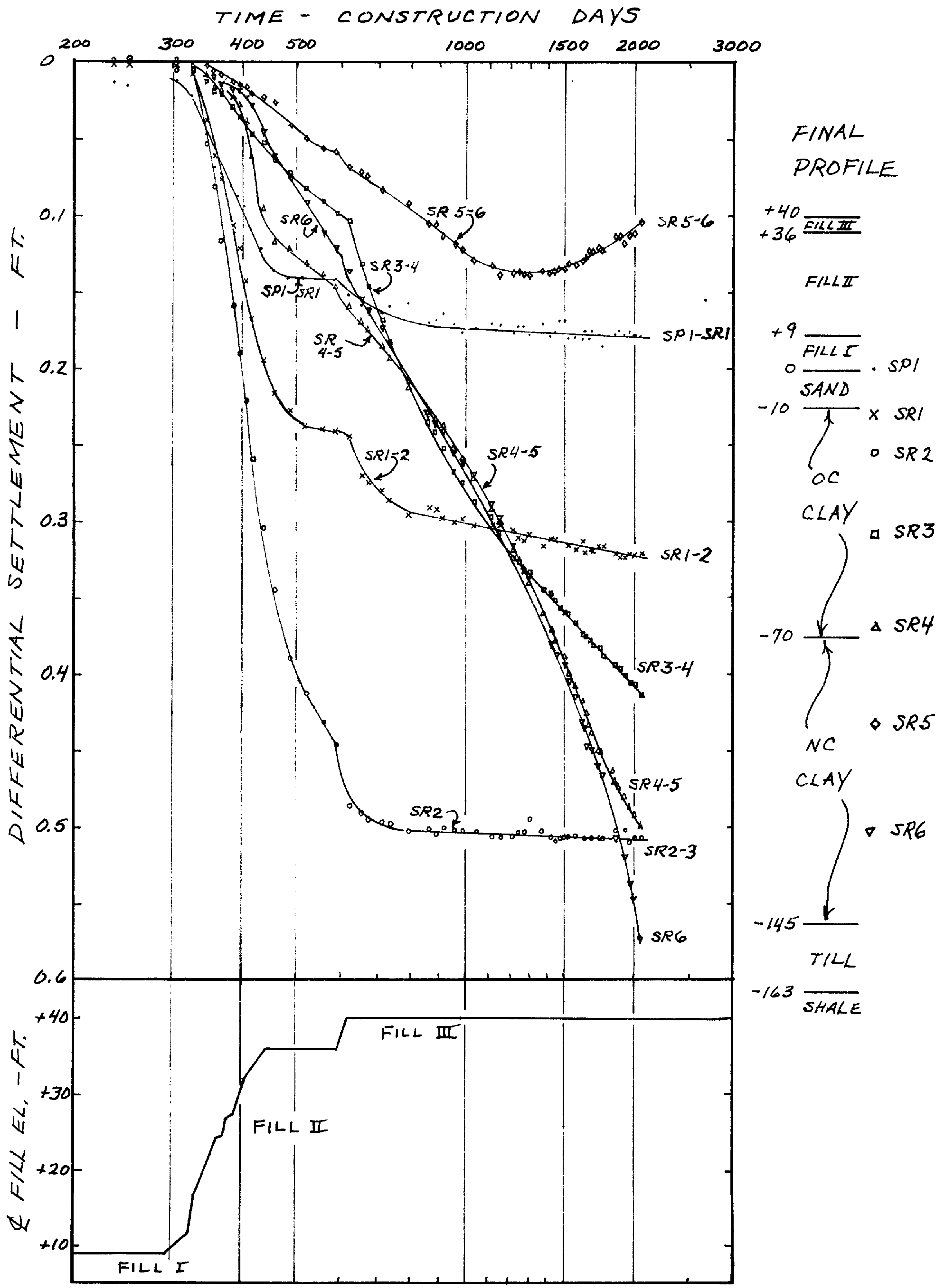

FIGURE 4-5 DIFFERENTIAL SETTLEMENT, STA. 246, ℄

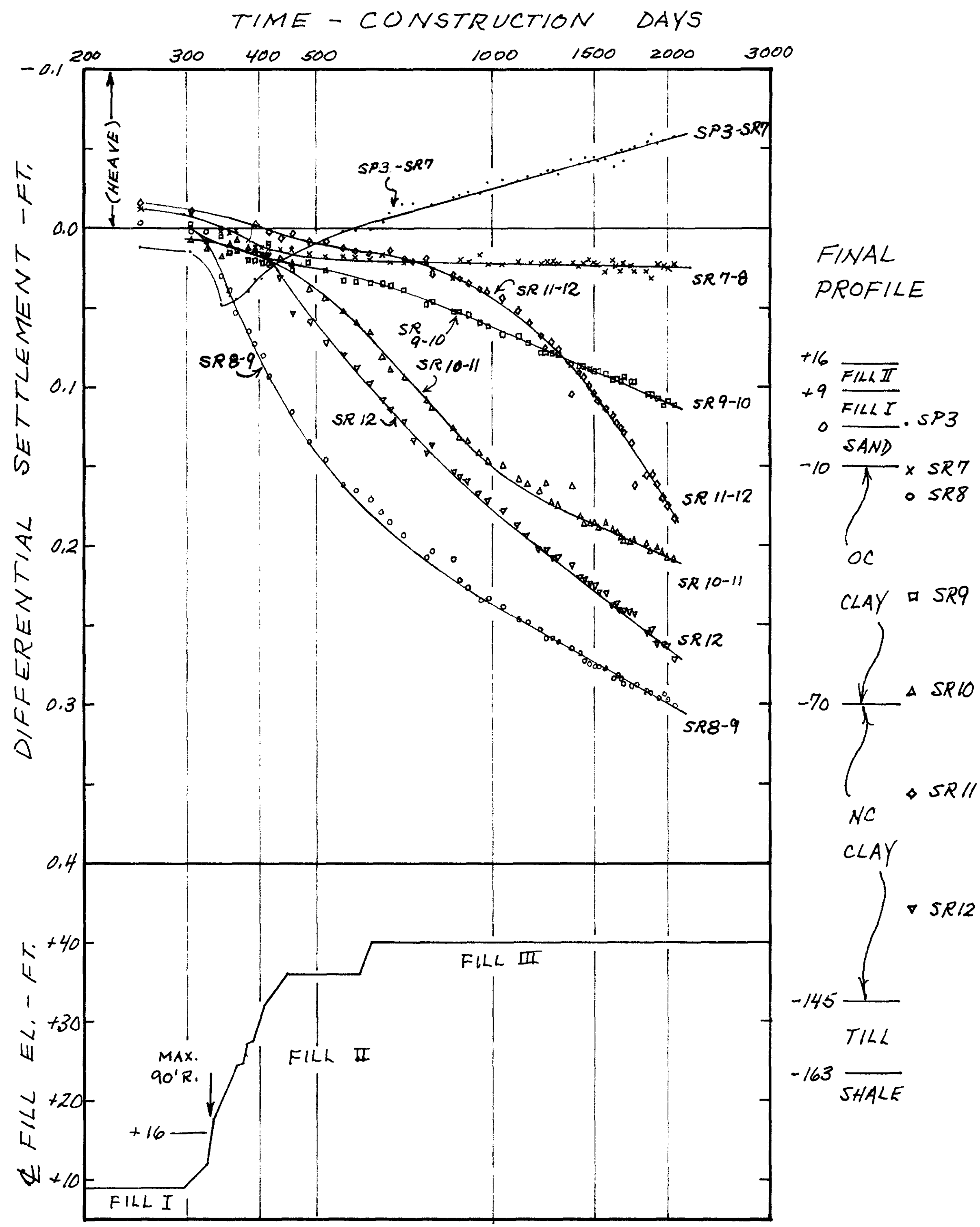

FIGURE 4-6 DIFFERENTIAL SETTLEMENT, STA. 246, 90'R.

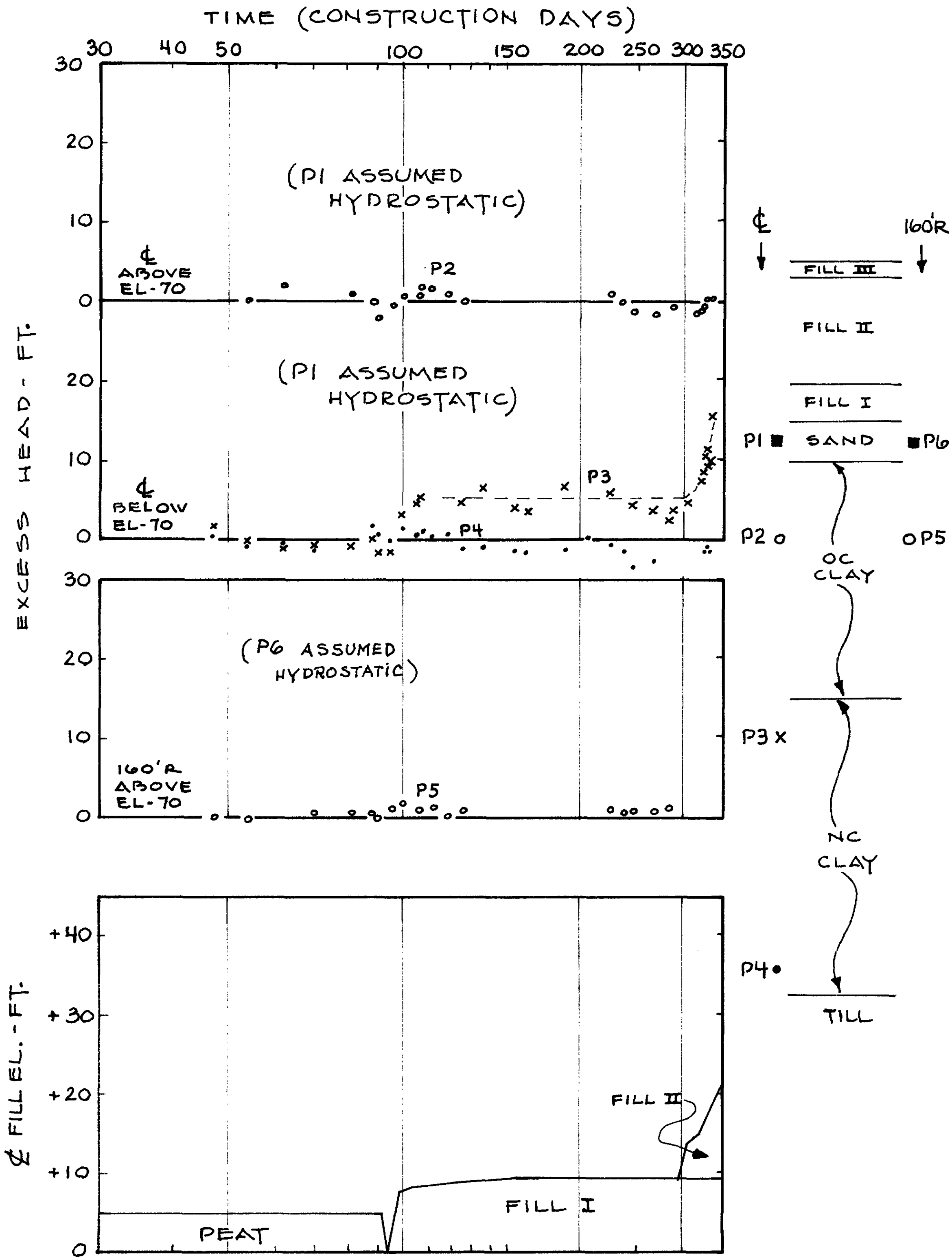

FIGURE 4-7 EXCESS HEAD STA. 245 ℄ & 160'R

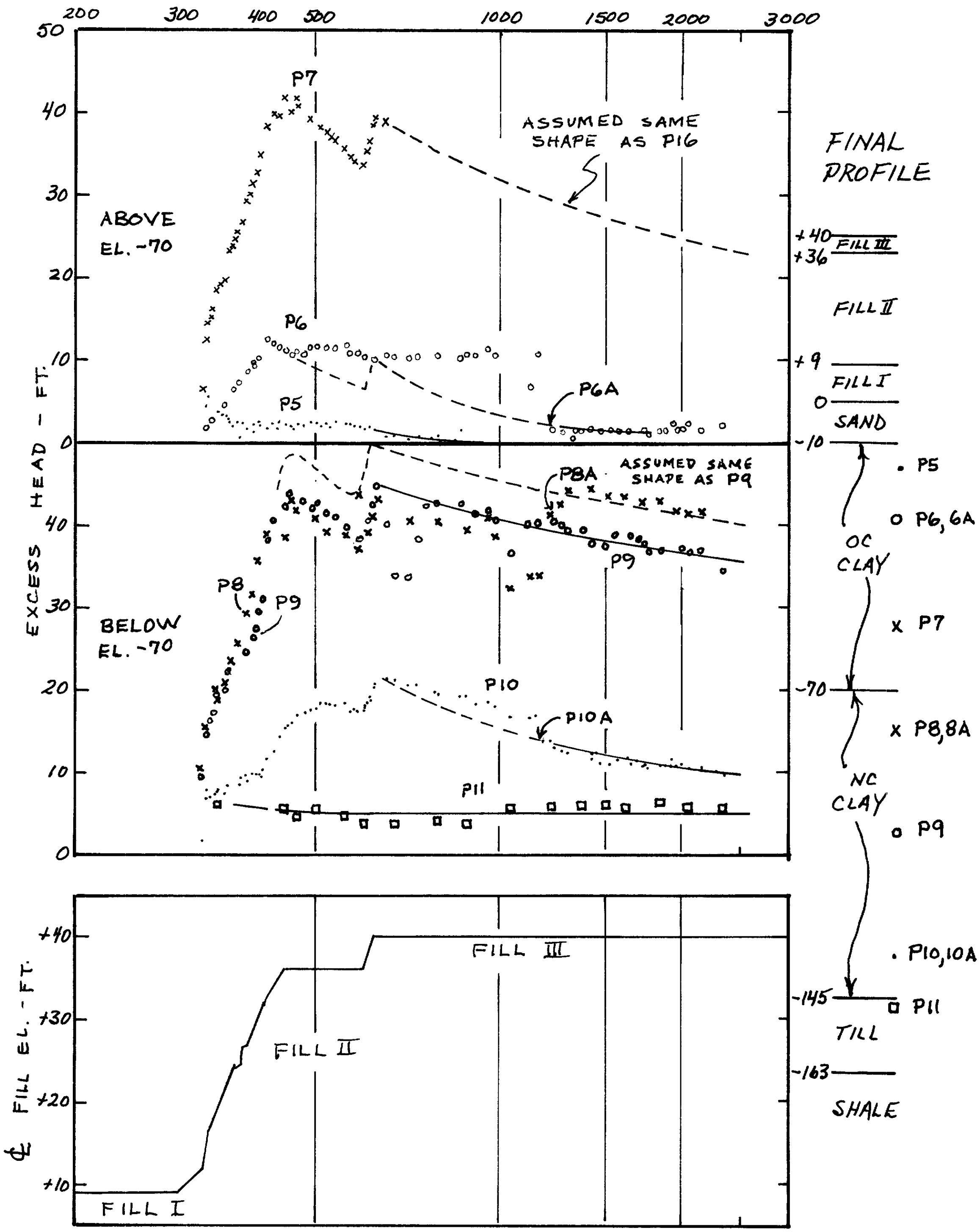

FIGURE 4-8 EXCESS HEAD, STA. 246, ℄

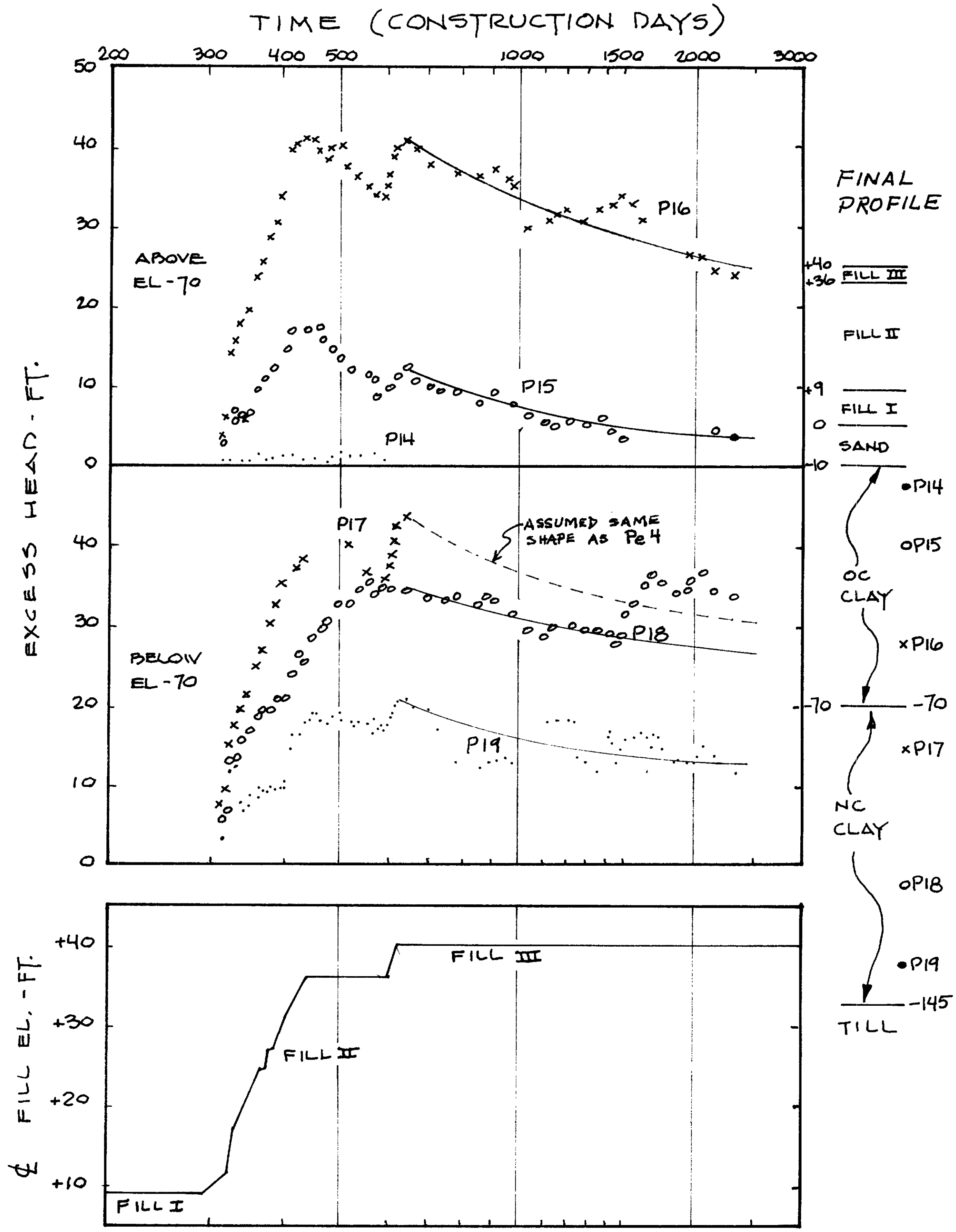

FIGURE 4-9 EXCESS HEAD STA 246 30'R

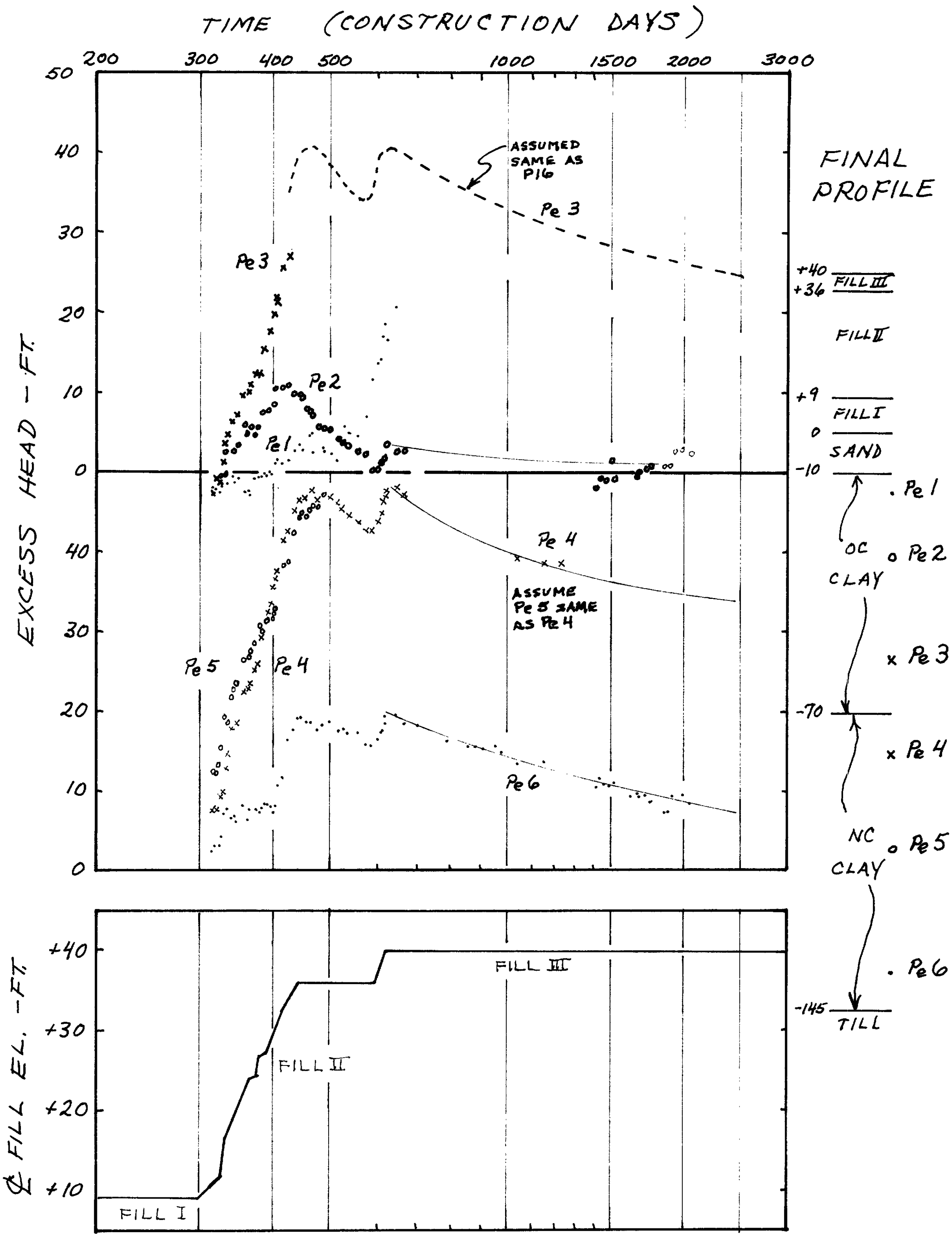

FIGURE 4-10 EXCESS HEAD, STA. 246, 30'L.

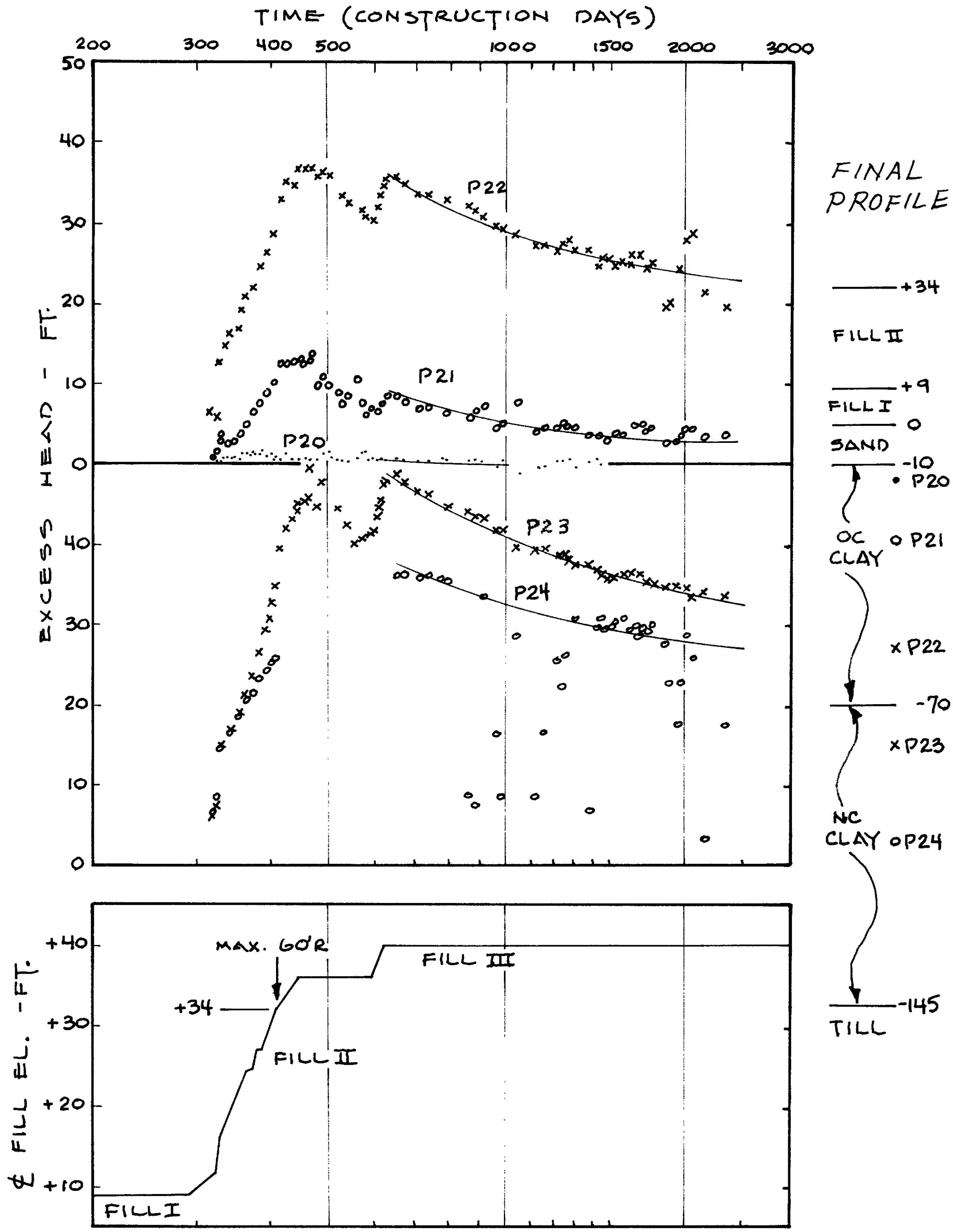

FIGURE 4-11 EXCESS HEAD STA 246 60'R

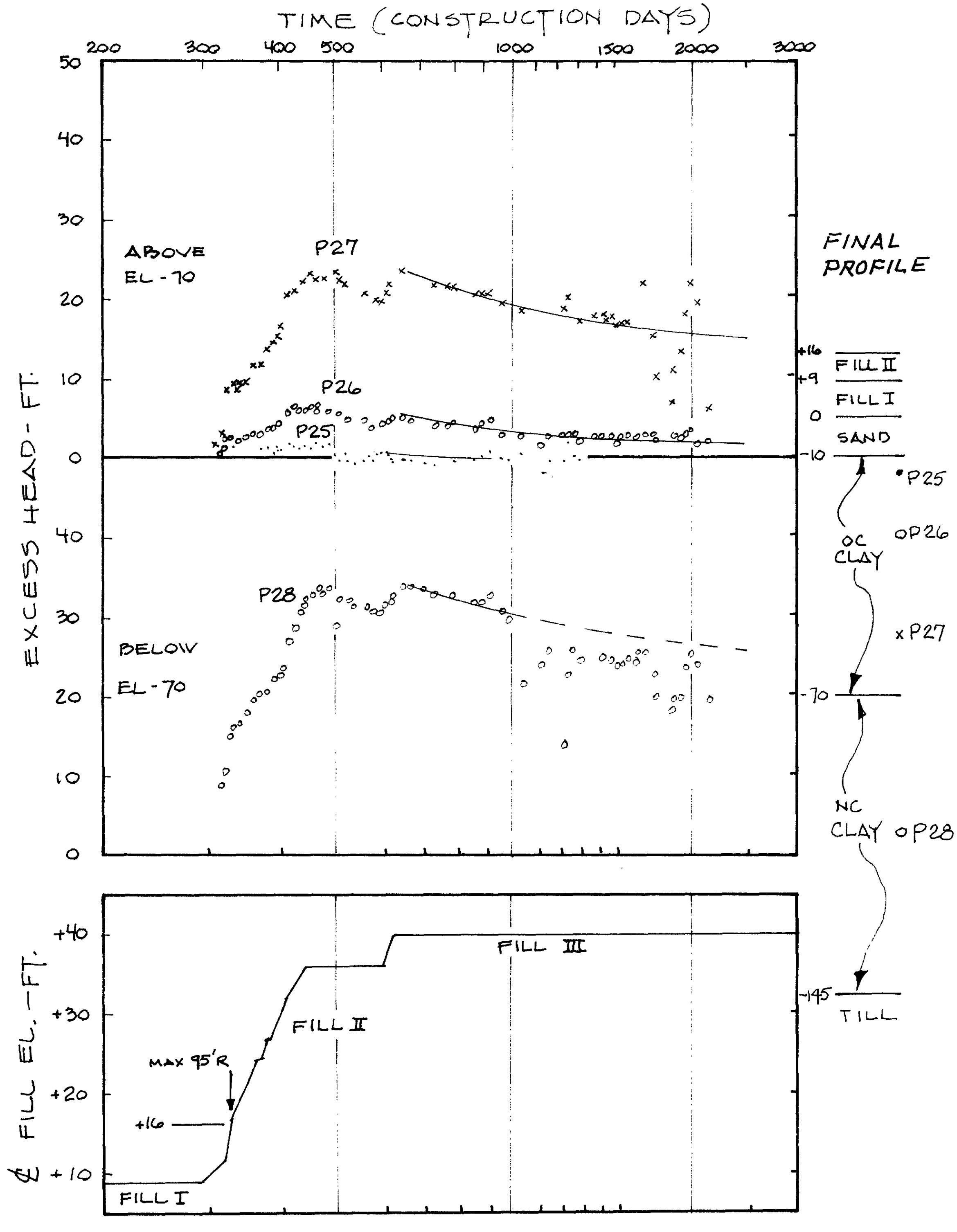

FIGURE 4-12 EXCESS HEAD STA 246 95'R

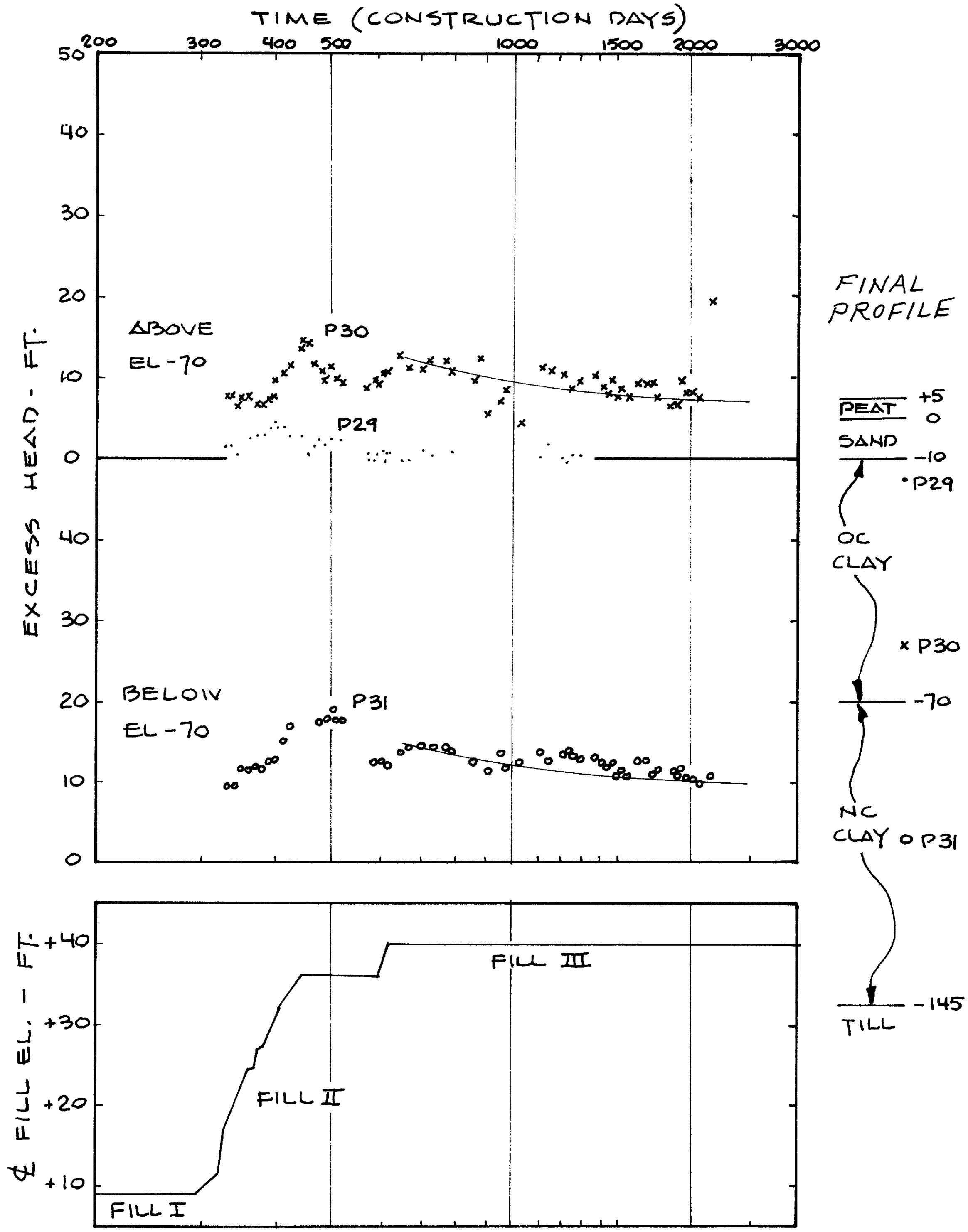

FIGURE 4-13 EXCESS HEAD STA. 246 160'R

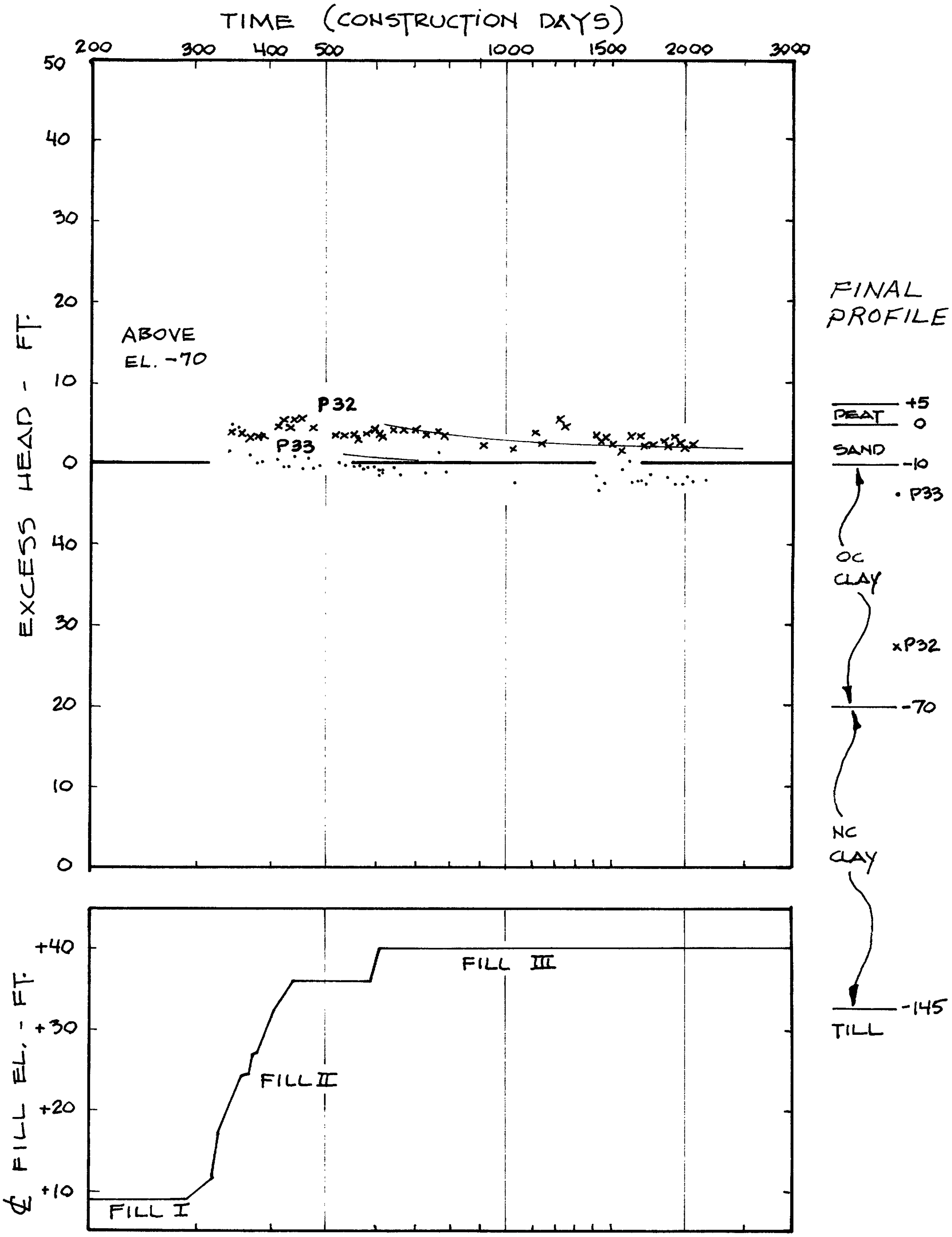

FIGURE 4-14 EXCESS HEAD STA 246 225'R

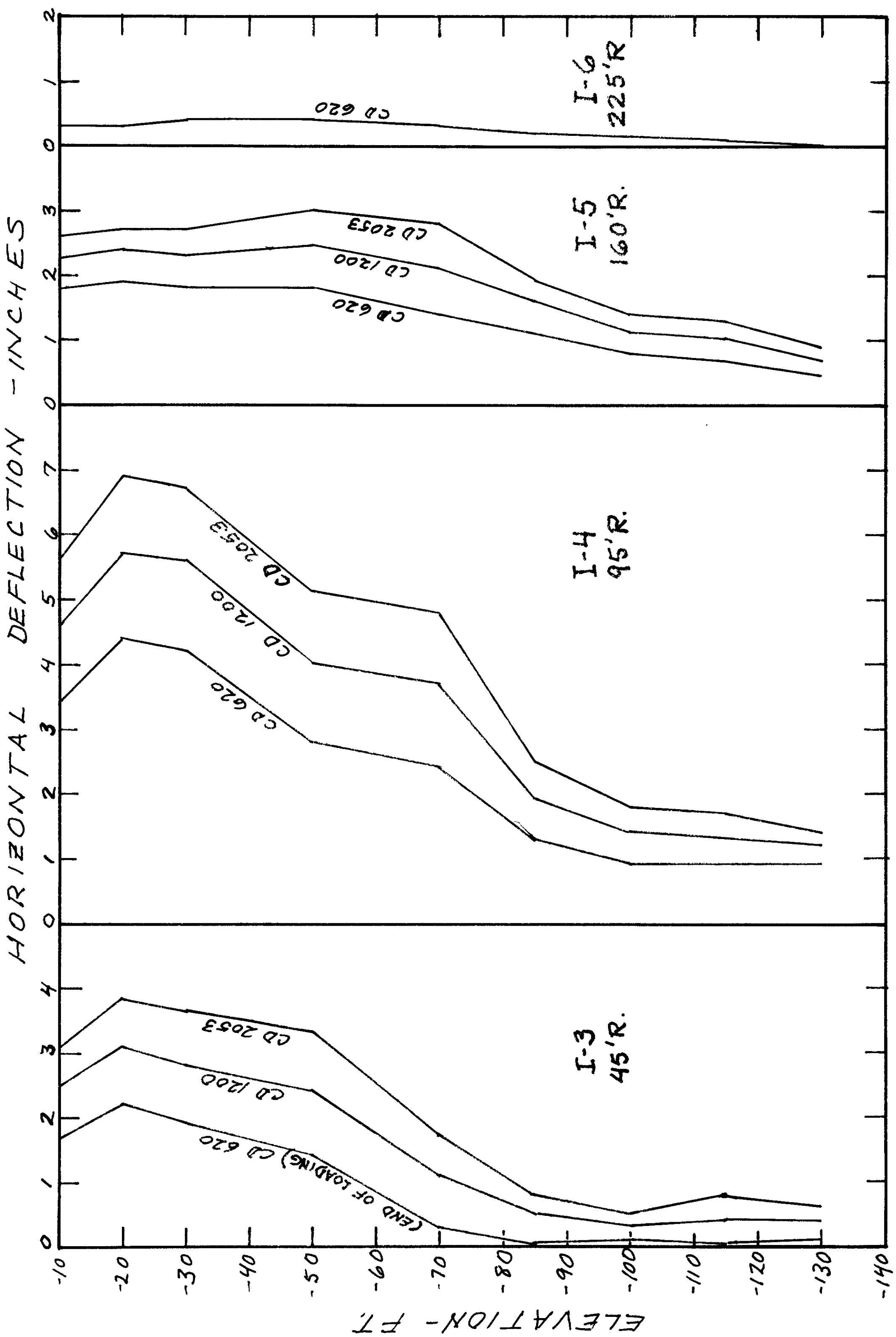

FIGURE 4-15 HORIZONTAL DEFLECTION VS. ELEVATION

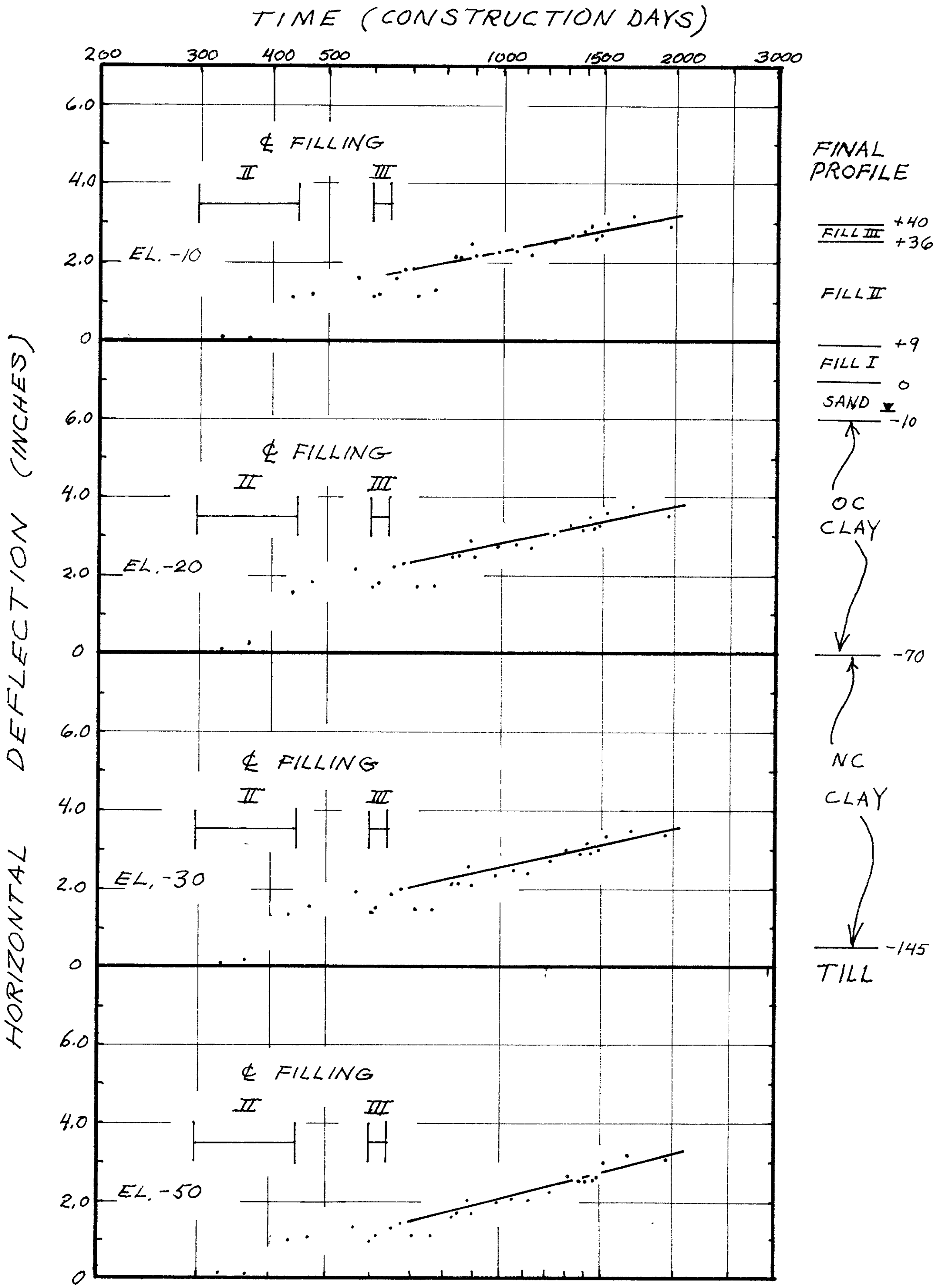

FIGURE 4-16 I-3 MOVEMENT, STA. 246, 45'R

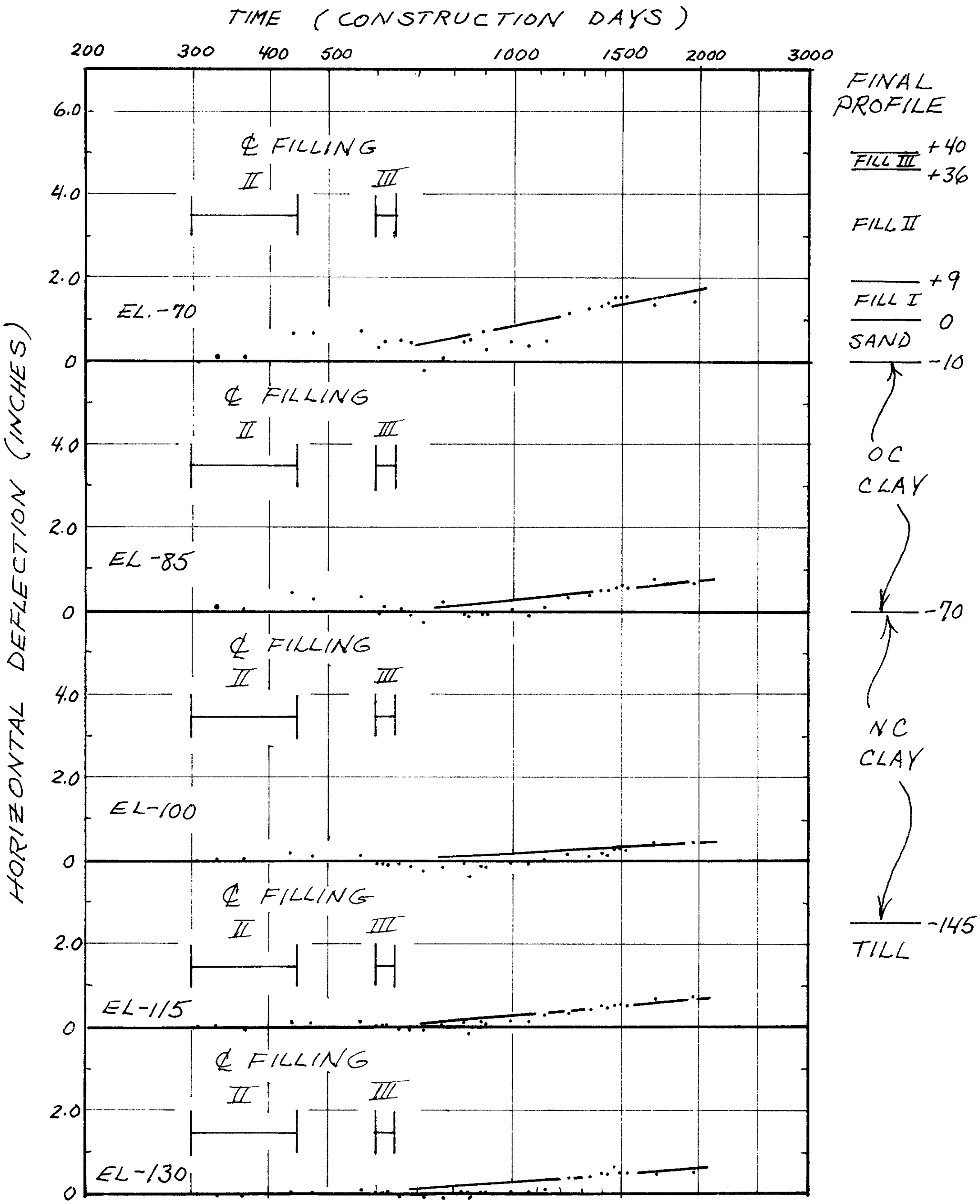

FIGURE 4-16 (I-3) CONT'D.

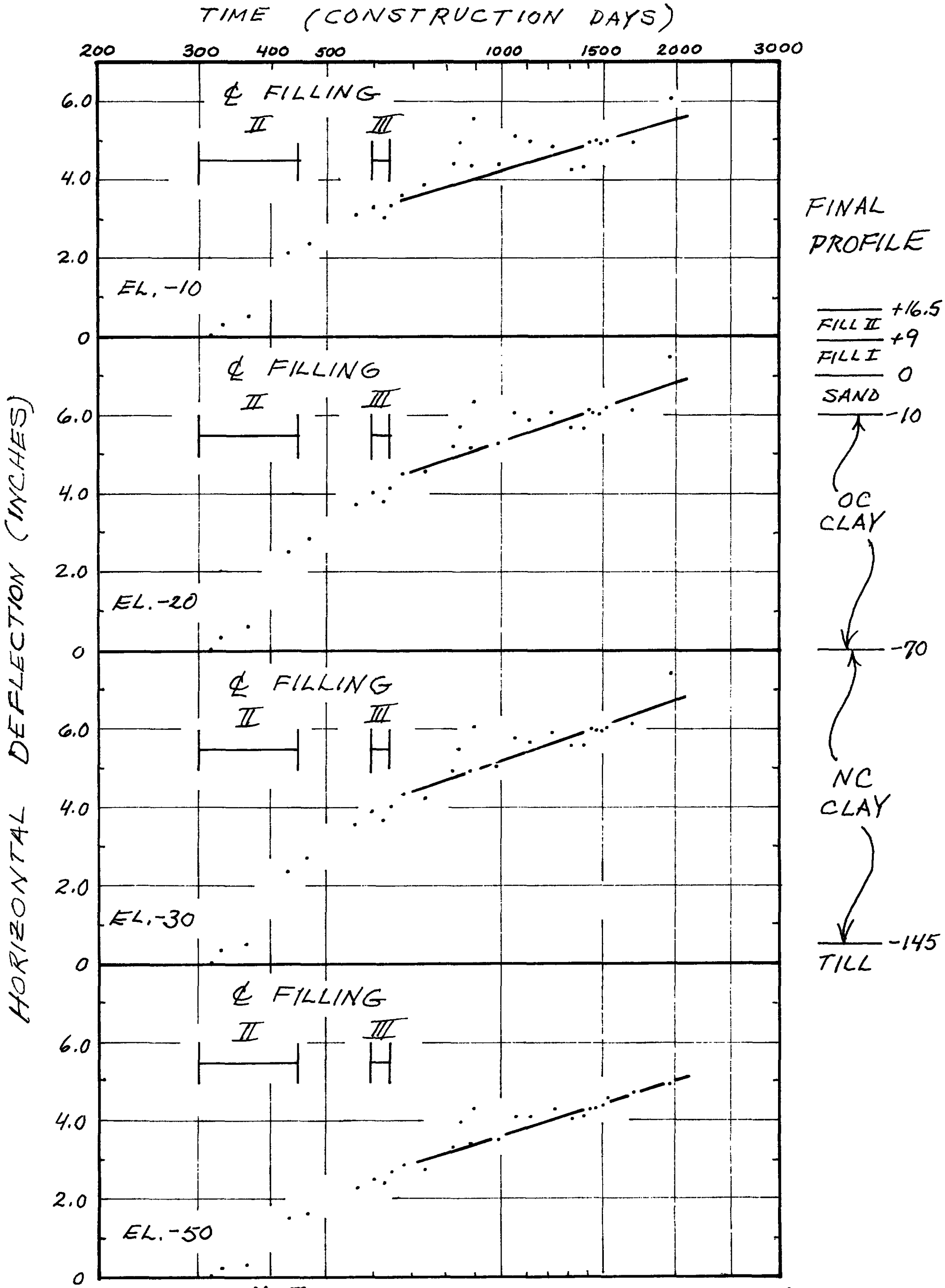

FIGURE 4-17 I-4 MOVEMENT, STA. 246, 95'R.

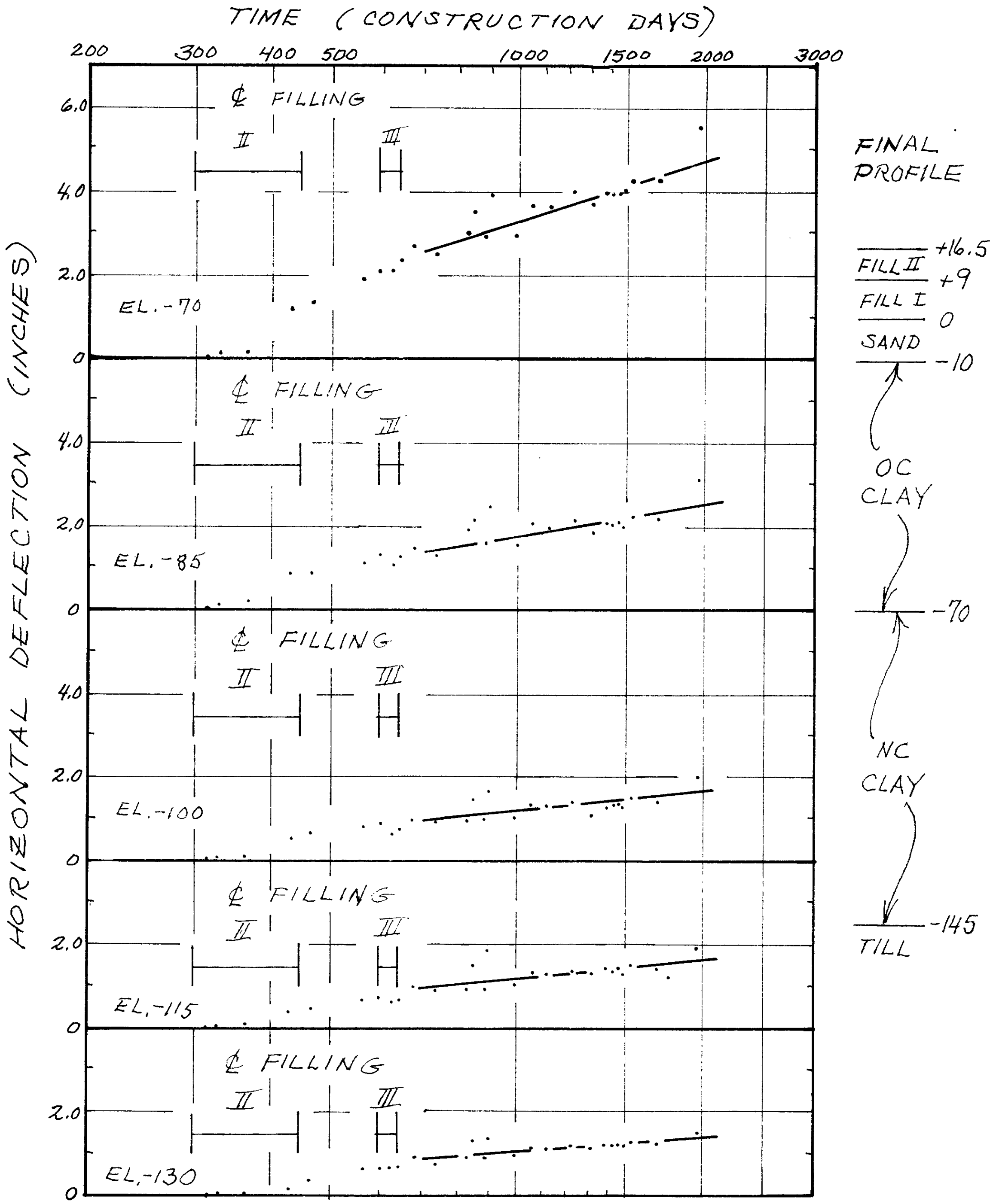

FIGURE 4-17 (I-4) CONT'D.

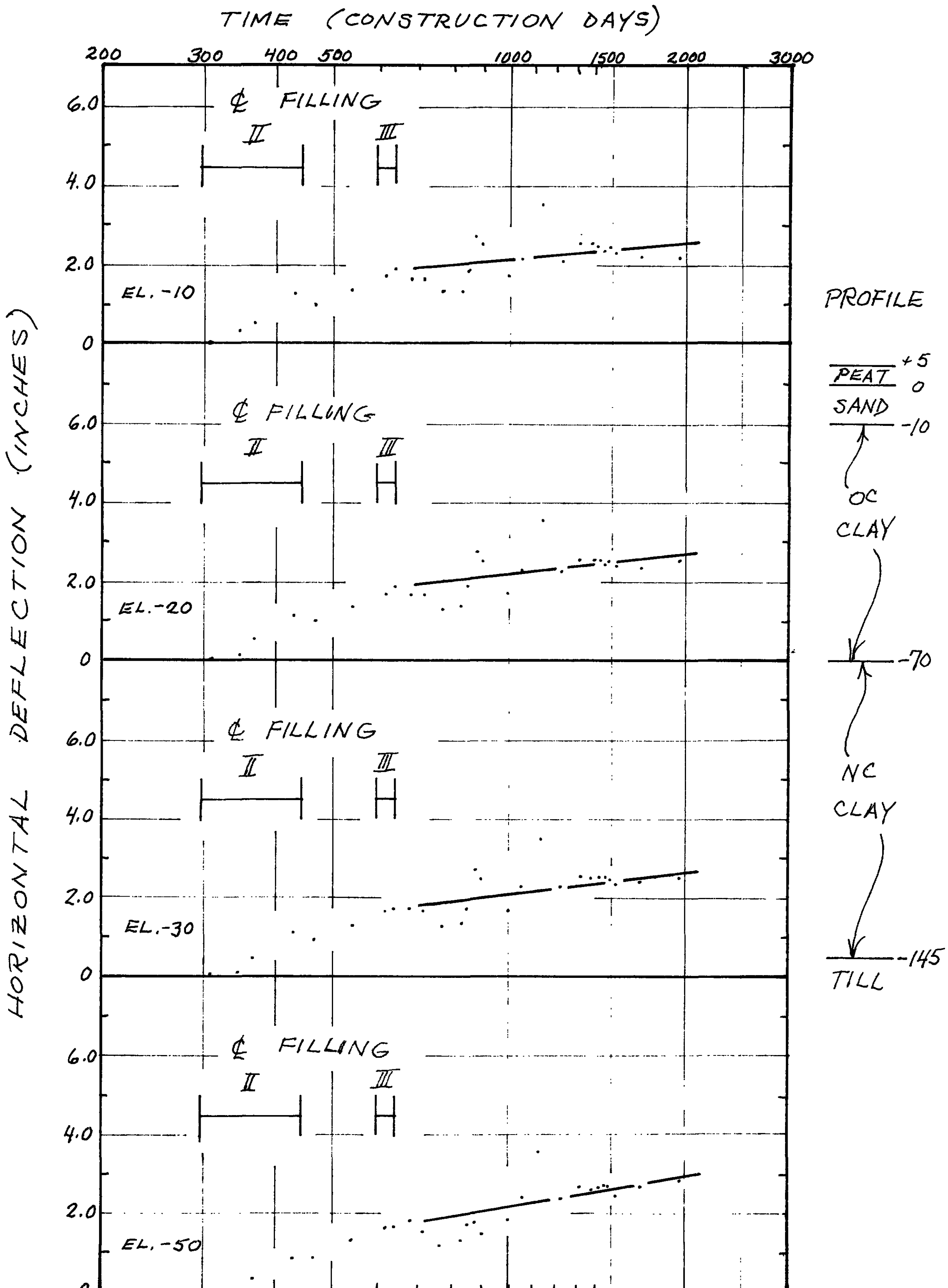

FIGURE 4-18 I-5 MOVEMENT STA. 246, 160'R.

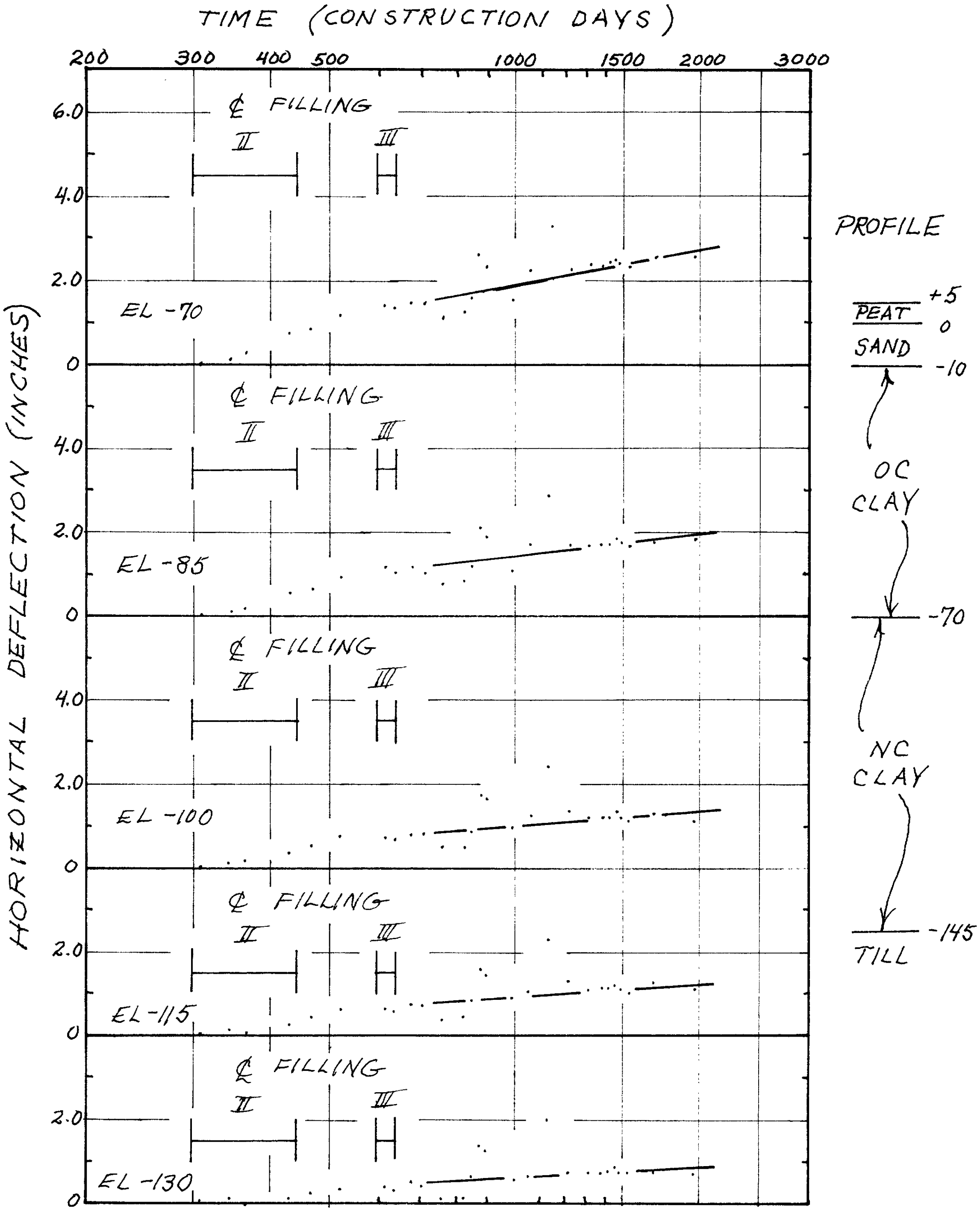

FIGURE 4-18 I-5 CONT'D.

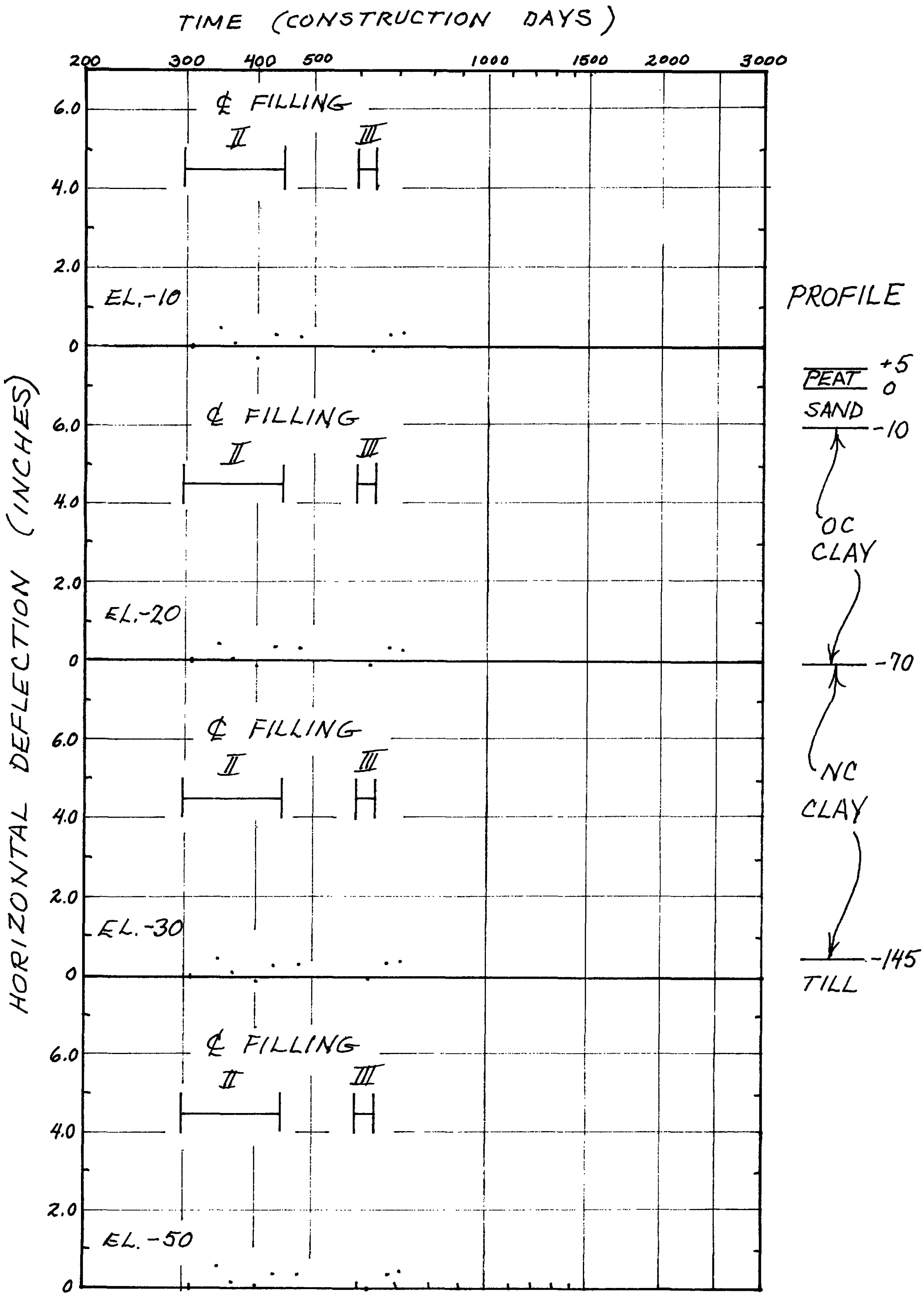

FIGURE 4-19 I-6 MOVEMENT, STA. 246, 225'R.

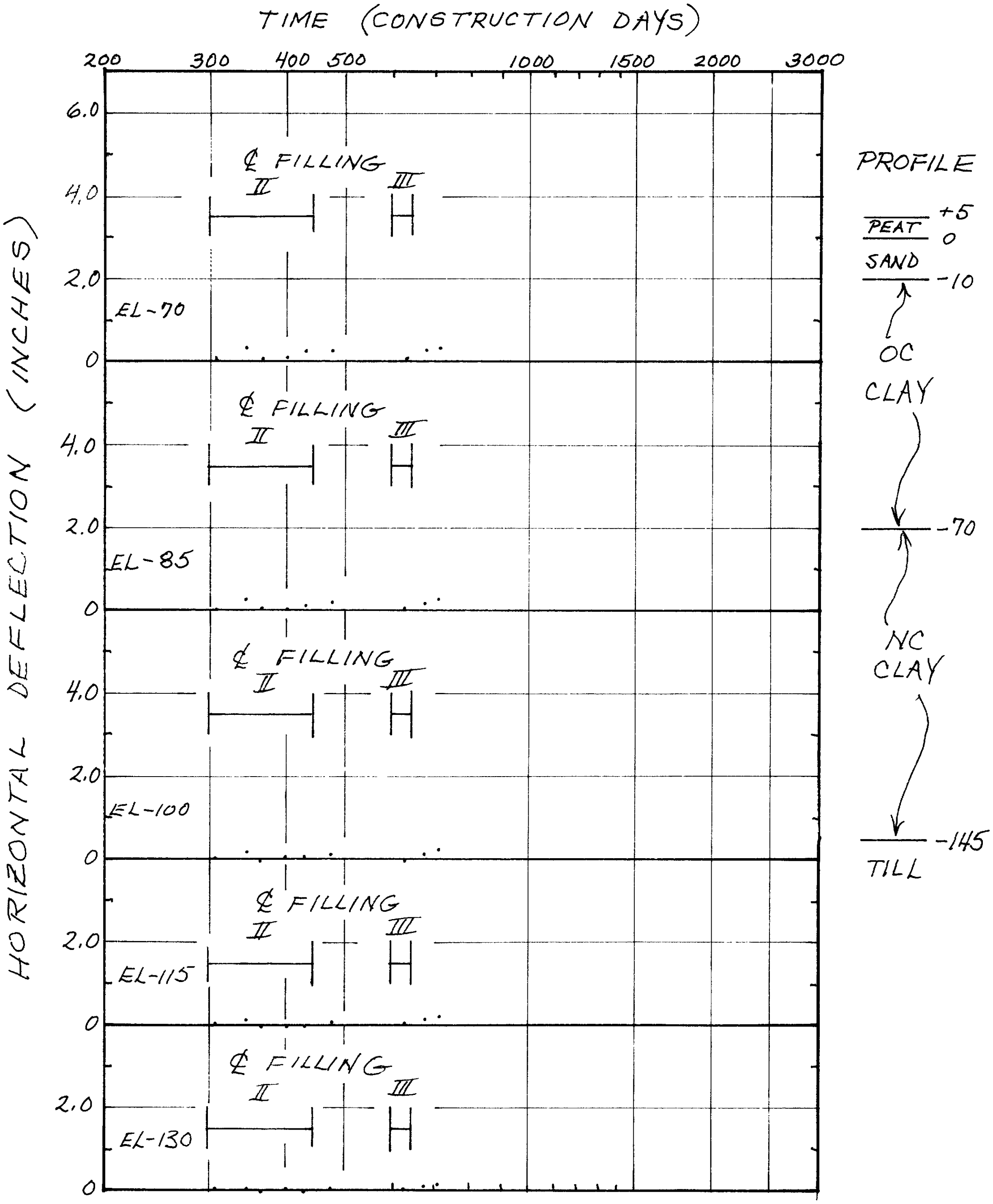

FIGURE 4-19 I-6 CONT'D.

5. PARAMETERS FOR UNDRAINED DEFORMATION AND STRESS FINITE ELEMENT ANALYSIS

5.1 GENERAL

The finite element program FEECON, described in detail elsewhere, (Simon, 1972, Simon et. al., 1972) was used to analyze the undrained behavior of the embankment. This program is exceptionally versatile. It permits the use of several stress-strain relationships including bilinear, hyperbolic, axial stress-strain or shear stress-strain. Anisotropic strengths can be specified for cohesive materials, and initial shear stress can be accounted for.

For analysis of the Test Section, hyperbolic stress-strain relationships were used for both granular and cohesive soils. FEECON uses the incremental method in hyperbolic stress-strain models as shown in Figure 5-1. At the beginning of each load increment, the modulus is set equal to the value of the tangent to the true stress-strain curve corresponding to the existing stress level. It is therefore necessary to use small load increments. Nine increments were used for the Test Section analysis. The finite element mesh is shown in Figure 5-2.

5.2 GRANULAR SOILS

A drained hyperbolic axial stress-strain relation was used for the granular soils (fill and natural sand). This relation is based on work done by Duncan and his associates (at the University of California, Berkeley) with Kondner's original suggestions (Simon, 1972). This stress-strain model is discussed in detail elsewhere (Duncan and Chang, 1970, Simon 1972).

The initial Young's modulus, E_i, is determined empirically and is related to the minor principal stress by Janbu's formula:

$$E_i = \kappa \overline{\rho}a \left(\frac{\overline{\sigma}_3}{\overline{\rho}_n}\right)^n$$

where κ is a dimensionless empirical modulus number, $\overline{\rho}_a$ is the atmospheric pressure in proper units, $\overline{\sigma}_3$ is the minor principal stress and n is a dimensionless empirical exponent.

In addition, the tangent Young's modulus is related to the principal stresses by:

$$E_t = \left[1 - \frac{R_f \ (1 - \sin\overline{\phi})(\overline{\sigma}_1 - \overline{\sigma}_3)}{2 \ \overline{c} \cos \overline{\phi} + 2\overline{\sigma}_3 \sin\overline{\phi}} \right]^2 E_i$$

where $\overline{c}$ and $\overline{\phi}$ are the Mohr-Coulomb strength parameters; R_f is the failure ratio, equal to the ratio between the compressive strength $(\overline{\sigma}_1 - \overline{\sigma}_3)_F$ and asymptotic stress difference for the hyperbolic stress-strain curve; $\overline{\sigma}_1$ and $\overline{\sigma}_3$ are the major and minor principal stresses, respectively.

FEECON also accounts for the stress and strain dependency of the initial and tangent Poisson's rations ($\overline{\nu}_i$andν_t). The initial Poisson's ratio is represented by the equation:

$$\overline{\nu}_i = G - F \log_{10} (\overline{\sigma}_3 / \overline{\rho}_a)$$

where G is the value of $\bar{\nu}_i$ when $\bar{\sigma}_3$ equals $\bar{p}_a$, and F is an empirical constant expressing the dependence of $\bar{\nu}$ on confining stress. The tangent Poisson's ratio is given by:

$$\bar{\nu}_t = \frac{\bar{\nu}_i}{\left[1 - \frac{d(\bar{\sigma}_1 - \bar{\sigma}_3)}{E_t} \right]^2}$$

where d expresses the strain dependency of $\bar{\nu}$, and -d is the slope of the line on a transformed hyperbolic plot of $\varepsilon_r / \varepsilon_a$ vs ε_r (ε_a= axial strain, ε_r= radial strain).

Since the behavior of the embankment material was not an objective of this report, the stress and strain dependency of Poisson's ration was ignored. Parameters F and d were chosen to be zero, so that $\bar{\nu}_t = \bar{\nu}_i = G$ where G is a constant value. The constant Poisson's ratio G was assigned the value of 0.4 for all granular soils. The empirical parameters κ, n, and R_f which determine E_i and E_t were chosen from Mitchell and Gardner's (1971) suggested relationships. These empirical relations are tabulated in Table 5-1.

For all granular soils the cohesion intercept ($\bar{c}$) was assumed to be zero. Friction angles ($\bar{\phi}$) and coefficients of lateral earth pressure at rest (K_o) were estimated, based on soil type and density

Due to a discrepancy between true ground water elevation (+2.5) and that assumed for FEECON (El. 0), the actual unit weights for some soils were adjusted. The procedure is shown in Figure 5-3. The unit weights of the peat natural sand, dumped fill and compacted fill to El. +9 were changed so that the vertical effective stress at the top of the natural sand was equal for both water level conditions. All FEECON parameters used for the granular soils are tabulated in Table 5-2.

5.3 COHESIVE SOILS

5.3.1 General

A hyperbolic shear stress-strain relation with anisotropic strengths was used for the cohesive soils (peat and Boston Blue Clay). FEECON incorporates the fact that the initial shear stress q_o is usually not zero (Simon, 1972). The hyperbolic relation is written as:

$$\Delta q = |q - q_o| = \gamma/[\ 1/G_i + (R_f/\Delta q_f)\gamma]$$

in which $1/G_i$ and $R_f/\Delta q_f$ are analogous to the a and b parameters of Duncan and Chang (1970). G_i is the initial shear modulus; Δq_f is the change in shear stress to cause undrained failure for the appropriate stress condition, whether DSS, PSA or PSP conditions; and R_f is $\Delta q_f/\Delta q$ for $\gamma = \infty$. All cohesive input parameters are tabulated in Table 5-3.

5.3.2 Hyperbolic parameters

D'Appolonia, et. al. (1971), Foott and Ladd (1973) and Simon, et. al. (1972) have shown that the undrained modulus obtained from $\overline{CK_o}UDSS$ tests is a reasonable estimate of the in-situ undrained modulus for many clays. Therefore, this approach was used in analysis for the Test Section. Since $\overline{CK_o}UDSS$ data was not available for the actual undisturbed samples from the Test Section, data from laboratory prepared sample of Boston Blue Clay were used (Ladd and Edgers, 1972).

Figure 5-4 indicates the method used to determine the parameters (G_i, R_f) defining the hyperbolic stress-strain curve. Figures 5-5 to 5-8 present the $\overline{CK_o}UDSS$ data (from Ladd and Edgers, 1972) for resedimented BBC and the derived hyperbolic curves. For the DSS stress system, it is assumed that $\tau h_{max} = \Delta q_f = s_u$.

When the hyperbolic plot of the test data is made, as $\gamma/(\tau h/s_u)\%$ versus $\gamma\%$, R_f is the slope of the line and the intercept (at $\gamma = 0\%$) is s_u/G_i. The normalized initial shear modulus (G_i/σ_{vc}) can then be determined from the normalized undrained shear strength, and G_i computed for each layer as follows:

$$G_i/s_u = 1/\text{intercept}$$

$$G_i/\bar{\sigma}_{vc} = G_i/s_u \times s_u/\bar{\sigma}_{vc}$$

$$G_i = G_i/\bar{\sigma}_{vc} \times \bar{\sigma}_{vc}$$

where $s_u = \tau h_{max}$ for DSS case, and $\bar{\sigma}_{vc}$ = vertical effective consolidation stress.

At all OCR, hyperbolic plots of $\overline{CK_oUDSS}$ data for resedimented BBC curve downward at low values of shear strain. The curvature is very slight or non-existent at OCR = 1, but increases with OCR and creates problems in choosing the best intercept (s_u/G_i). Additionally, the plots curve upward at shear strains greater than the failure shear strain. This is due to the strain-softening nature of the clay, which is apparent at all values of OCR.

The effect of low-strain curvature on hyperbolic parameters is depicted in Figure 5-4, which shows (schematically) both a normalized shear stress-strain curve and the equivalent hyperbolic plot. Various straight-line approximations of the hyperbolic plot are shown, along with their equivalent normalized stress-strain plots, computed from the DSS relation (Simon et. al. 1974)

$$\frac{\tau h}{\bar{\sigma}_{vc}} = \frac{\gamma(\%)}{(100)\frac{\bar{\sigma}_{vc}}{G_i} + \frac{R_f\ \gamma(\%)}{\tau h_{max}/\bar{\sigma}_{vc}}}$$

It is apparent that the straight line which best fits the hyperbolic plot is the equivalent of the curve which most closely approximates the normalized stress-strain data over the full range of strain up to failure. Such "best fit" approximations to the hyperbolic plots appear to be the best method of determining hyperbolic parameters from lab data.

5.3.3 Shear Modulus

Figure 5-9 indicates the normalized initial shear modulus ($G_i/\bar{\sigma}_{vc}$) and R_f values used in the FEECON analysis. Values used for OCR = 1 to 4 were those recommended by Simon et.al. (1974), and were based on comparisons of FEECON analyses with model footing tests (Simon, 1972, Kinner and Ladd, 1970). Values used for OCR = 8 are "best fit" values from hyperbolic plots of $\overline{CK_oU}DSS$ data on the resedimented clay. The values used in this analysis are shown as dashed lines.

Initial re-evaluation of model test footing results indicates that chosen values of G_i and R_f at OCR = 2 and 4 are somewhat too low and too high, respectively. This is in agreement with "best fit" values from $\overline{CK_oU}DSS$ data at those OCR's. Additionally, re-evaluation also shows that for NC clay, there is a reduction in G_i with increased $\bar{\sigma}_{vc}$, rather than a unique G_i at OCR = 1 as implied by Simon, et. al. (1974). This is also in agreement with "best fit" $\overline{CK_oU}DSS$ data. This data for OCR = 1 (Figure 5-9) shows an inverse linear relation between $G_i/\bar{\sigma}_{vc}$ and $\bar{\sigma}_{vc}$ on a log scale. This is generally the same relation porposed by Janbu (1963):

$$G_i = \Gamma \; \rho a \left(\frac{\bar{\sigma}_3}{\rho_a}\right)^n$$

where Γ is the dimensionless empirical shear modulus number.

Conversely, $\overline{CK_oUDSS}$ data indicate no $\bar{\sigma}_{vc}$ dependency of $G_i/\bar{\sigma}_{vc}$ at OCR = 2, 4 and 8.

As a result of these observations, a set of recommended values of $G_i/\bar{\sigma}_{vc}$ and R_f have been determined. These are portrayed as solid lines in Figure 5-9, and account for the effect of $\bar{\sigma}_{vc}$ on $G_i/\bar{\sigma}_{vc}$. There are several curves interpolated between OCR = 1 and 2 for varying $\bar{\sigma}_{vc}$ at the top of the NC clay. Within the NC clay, $G_i/\bar{\sigma}_{vc}$ should vary linearly and inversely as the log of $\bar{\sigma}_{vc}$. The recommended values for OCR = 1 and 2 are based entirely on $\overline{CK_oUDSS}$ data, and should be considered tentative. It is obviously necessary to compare further FEECON predictions using these values with the model footing results.

With FEECON, it is necessary to use a small positive value for the shear modulus after yielding, G_y. This was chosen to be one percent of the initial modulus in all cases.

$$G_y = 0.01G_i$$

5.3.4 Poisson's Ratio

Poisson's ratio must always be less than the theoretical 0.50 for the undrained case. This is due to the fact that the term $1/(1-2\nu)$ becomes infinity in the finite element calculations for $\nu = 0.50$. An initial Poisson's ratio ν_i was chosen as 0.485. With the values chosen for Bulk modulus (K) and G_i, the yielded Poisson's ratio becomes 0.49985.

5.3.5. Bulk Modulus

The bulk modulus K is kept constant at all stress levels. With an initial Poisson's ratio $\nu_i = 0.485$,

$$\frac{K_i}{G_i} = \frac{2}{3}\,\frac{(1+\nu)}{(1-2\nu)} \;;\; \nu = 0.485$$

then, $K_i = K_y = 33G_i$

This relation was used to determine K for all cohesive soils.

5.3.6 Undrained Shear Strength

Figure 5-10 shows the undrained shear strength parameters used in the FEECON analysis. It is necessary to input the undrained strength in the vertical directions s_uV, and the strength ratio Ks ($Ks = s_uH/s_uV$). These parameters are based on $\overline{CK_oU}$PSA (s_uV) and $\overline{CK_oU}$PSP (s_uH) tests on resedimented BBC. Figure 5-11 shows the elliptical anisotropic strength criteria used, based on Davis and Christian (1971). The a/b ratios used are those recommended by Simon, et. al. (1974). They describe the shape of the Davis and Christian strength ellipse (a is the major half axis, b is the minor half axis)

5.3.7 Initial Stress Level and K_o

The initial stress level q_o is expressed as:

$$q_o = 0.5(1 - K_o)\,\bar{\sigma}_{vo}$$

This stress is negative for highly oversonsolidated clays, where $K_o > 1$. The values for K_o were chosen from R.S. Ladd (1965) data for K_o vs. OCR for Boston Blue Clay (Figure 5-12).

5.3.8 Pore Pressure Parameters

FEECON uses Henkel's equation to predict undrained pore pressures:

$$\Delta u = \Delta\sigma_{oct} + a\Delta\tau_{oct}{}^{k}$$

where a and k are Henkel's parameters, and $\Delta\sigma_{oct}$ and $\Delta\tau_{oct}$ are change in octahedral normal and shear stress, respectively. Henkel's parameters, a and k, were both set equal to zero, so that $\Delta u = \Delta\sigma_{oct}$. Other pore pressure and stress relations were then calculated by hand.

5.3.9 Peat Parameters

Since behavior of the peat was not an object of this study, little effort was spent in determination of its parameters. The hyperbolic parameters were taken from $\overline{CK_oU}DSS$ tests performed on the Taylor River (Maine) peats. Other parameters were estimated from generally observed performance of peats in the Boston area.

SOIL GROUP	$\bar{\phi}$, DEGREES		K	n	R_F
	LOW $\bar{\sigma}_3$	HIGH $\bar{\sigma}_3$			
GW	47	35	500	0.3	0.7
GP	46	38	1800	0.3	0.8
SW	50	35	300	0.5	0.7
SP	40	30	1200	0.5	0.8

FROM MITCHELL & GARDNER, 1971

TABLE 5-1 HYPERBOLIC AXIAL STRESS-STRAIN PARAMETERS FOR GRANULAR MATERIALS

MATERIAL AND NO.		EL.	POISSONS RATIO G (ν)	F	d	$\bar{\phi}$	K	n	R_F	$\bar{\gamma}$ PCF	K_o	$\bar{C}$	REMARKS
FILL	1	+40 to +9	0.40	0	0	40°	360	0.5	0.7	119	1.00	0	SW
FILL	2	+9 to +5	0.40	0	0	40°	360	0.5	0.7	150	1.00	0	SW, ADJUSTED $\bar{\gamma}$
FILL (REPLACES PEAT)	3	+5 to 0	0.40	0	0	30°	360	0.5	0.7	44	0.50	0	SW, DUMPED, ADJUSTED $\bar{\gamma}$
NATURAL SAND	5	0 to -10	0.40	0	0	33°	1200	0.5	0.8	50	0.46	0	SP, $N \cong 20$

TABLE 5-2 FEECON PARAMETERS, HYPERBOLIC AXIAL STRESS-STRAIN MATERIALS

MATERIAL	NO.	ELS.	AVG. OCR	$S_u(V)$ PSF	$K_S = \frac{S_u(H)}{S_u(V)}$	a/b	BULK MODULUS $K = 33 \times G_i$ KSF	INITIAL SHEAR MODULUS G_i KSF	YIELDED SHEAR MODULUS $G_Y = 0.01\,G_i$ PSF	R_F	$\bar{\gamma}$ PCF	K_o	INITIAL SHEAR STRESS $q_o = \frac{(1-K_o)}{2}\bar{\sigma}_{v_o}$ PSF
PEAT	4	+5 to 0	1	165	1	1	94.6	2.86	29.0	0.94	44	0.20	+44
BOSTON BLUE CLAY	6	-10 to -20	7.8	1421	0.66	1.00	3282.5	99.47	995	0.91	59	1.25	-126.9
	7	-20 to -30	4.4	1539	0.62	1.08	7410.4	224.51	2245	0.95	52	1.00	0.0
	8	-30 to -40	2.9	1588	0.61	1.14	10,000.7	303.05	3030	0.96	52	0.86	+146.3
	9	-40 to -50	2.0	1540	0.59	1.20	12,058.2	365.40	3654	0.96	52	0.74	+339.3
	10	-50 to -60	1.4	1409	0.56	1.25	14,460.6	438.20	4382	0.96	52	0.61	+610.4
	11	-60 to -70	1.1	1350	0.54	1.29	16,863.0	511.0	5110	0.96	52	0.52	+876.0
	12	-70 to -85	1.0	1462	0.54	1.30	19,866.0	602.0	6020	0.96	52	0.50	+1075.0
	13	-85 to -100	"	1727	"	"	23,469.6	711.20	7112	"	"	"	+1270.0
	14	-100 to -115	"	1992	"	"	27,073.2	820.40	8204	"	"	"	+1465.0
	15	-115 to -130	"	2258	"	"	30,676.8	929.60	9296	"	"	"	+1660.0
	16	-130 to -145	"	2523	"	"	34,280.4	1038.80	10,388	"	"	"	+1855.0

TABLE 5-3 FEECON PARAMETERS, HYPERBOLIC SHEAR STRESS-STRAIN MATERIALS

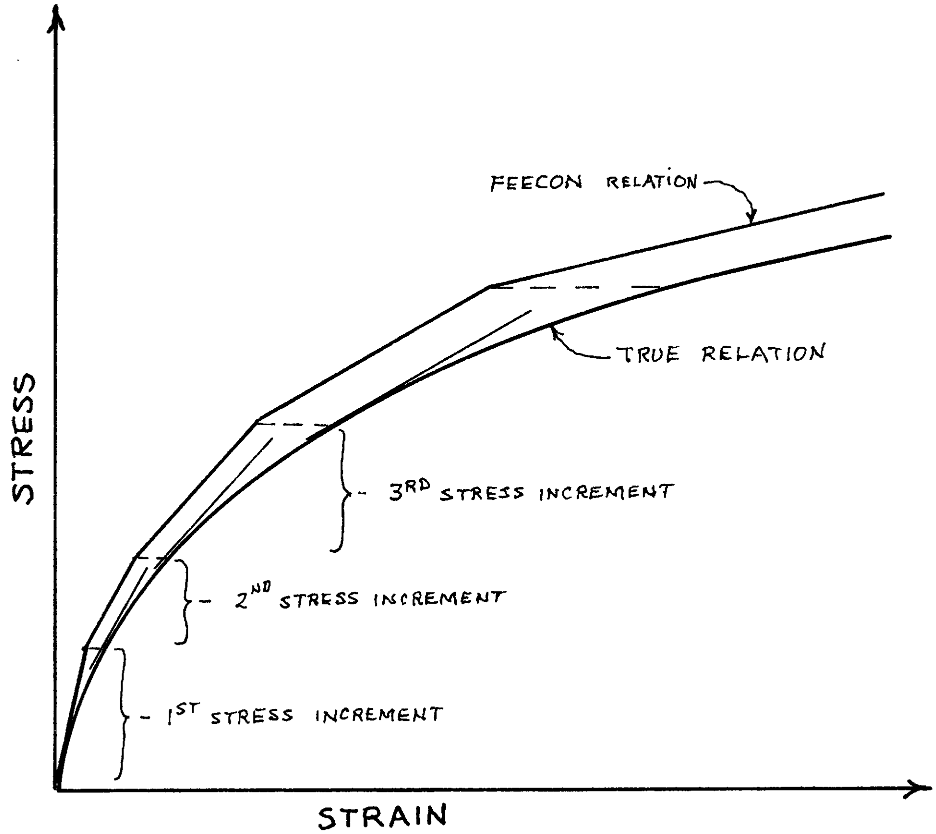

(FROM SIMON, et.al., 1972)

FIGURE 5-1 NON-LINEAR STRESS-STRAIN MODEL BY INCREMENTAL METHOD

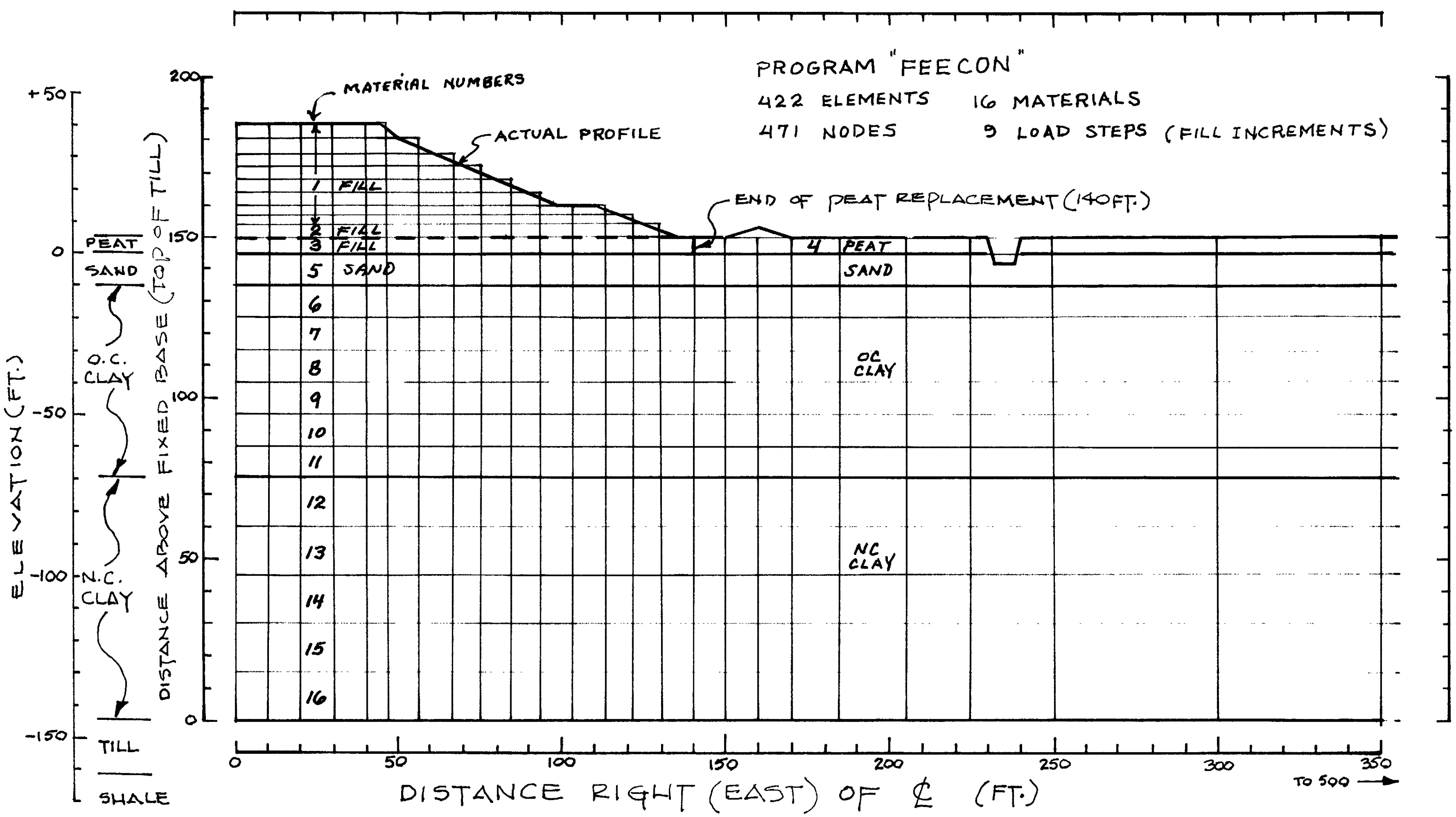

FIGURE 5-2 FINITE ELEMENT MESH

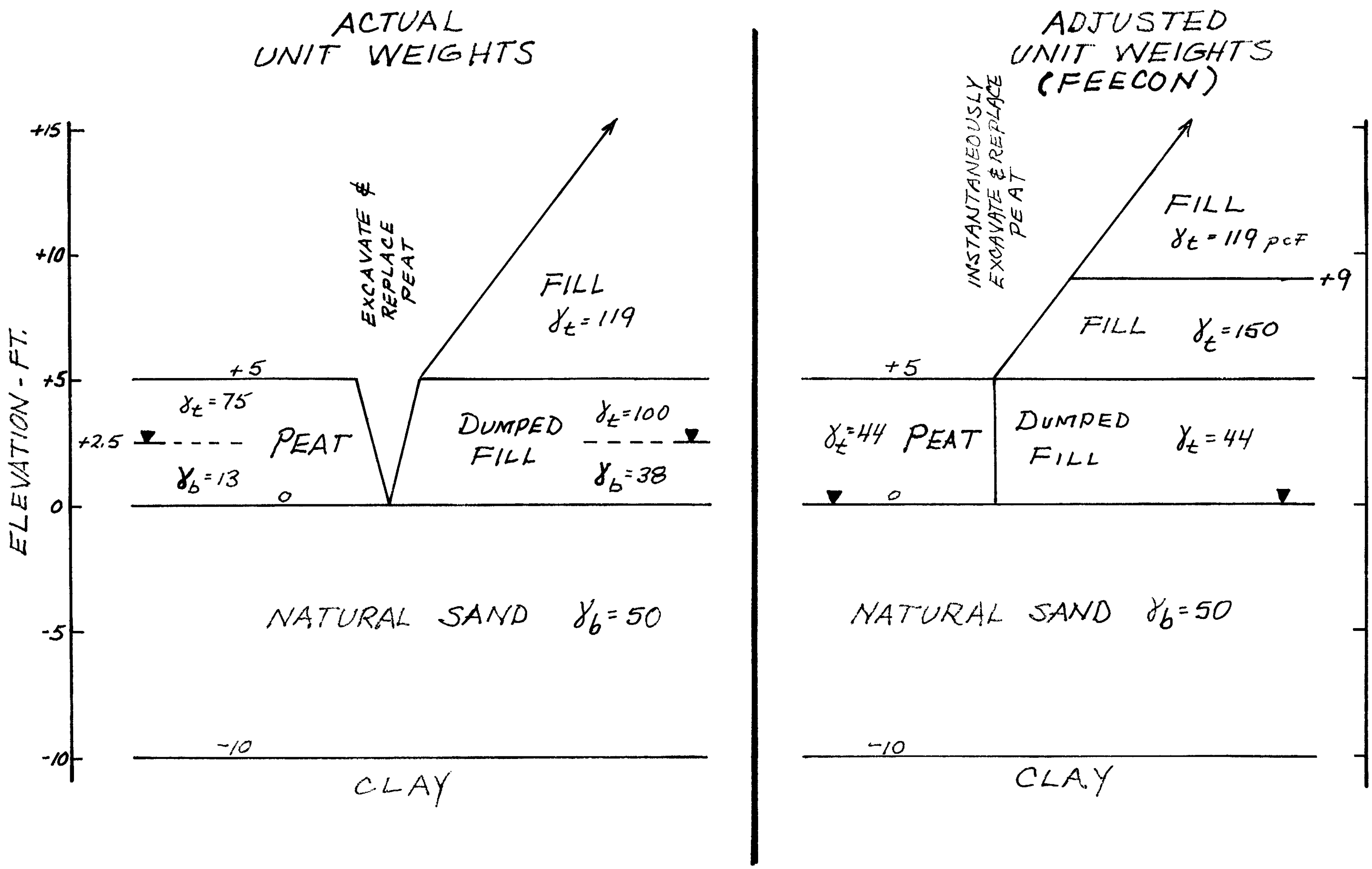

FIGURE 5-3 ADJUSTED FEECON UNIT WEIGHTS

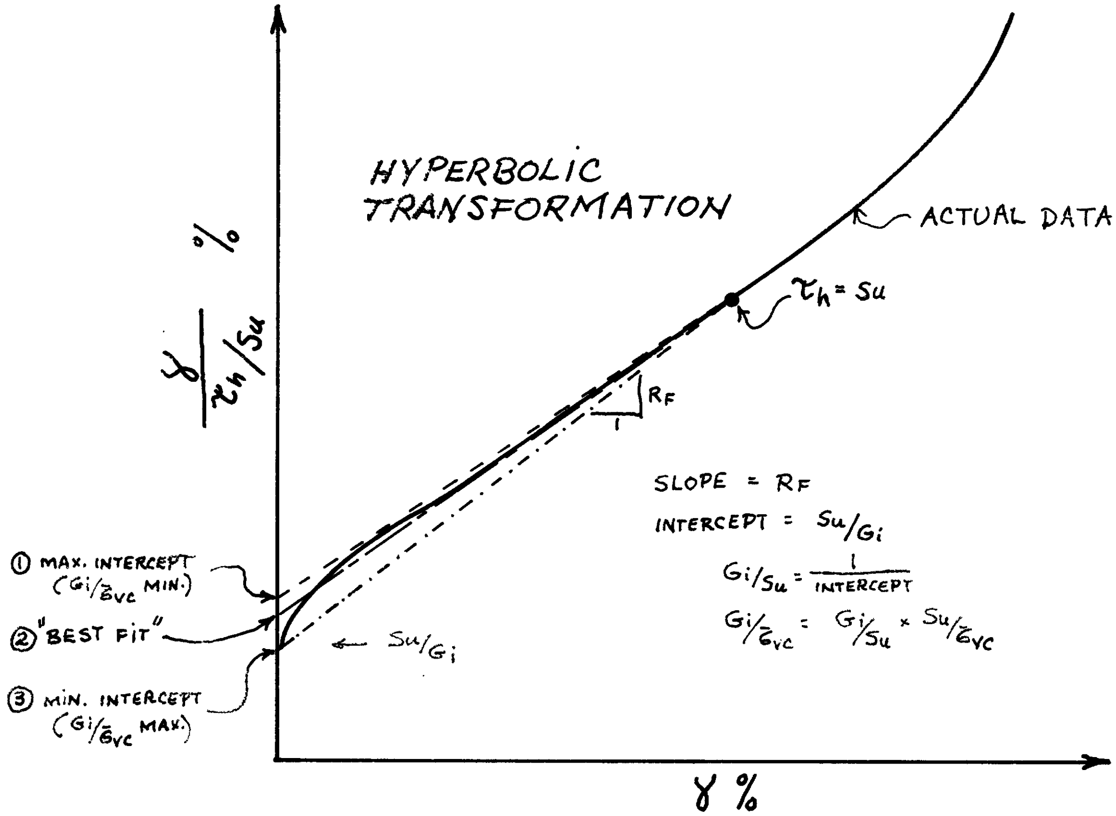

$\tau_h/\bar{\sigma}_{vc}$ BACKFIGURED FROM HYPERBOLIC PARAMETERS:

FOR $\overline{CK_oU}DSS$: $$\tau_h/\bar{\sigma}_{vc} = \frac{\gamma\,(\%)}{(100)\,\frac{\bar{\sigma}_{vc}}{G_I} + \frac{R_F\,\gamma\,(\%)}{S_u/\bar{\sigma}_{vc}}}$$

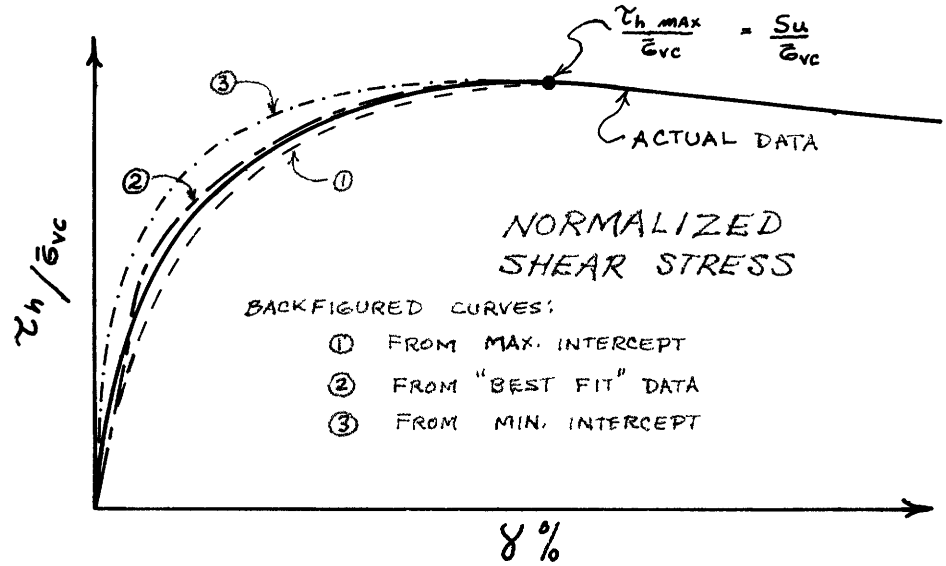

FIGURE 5-4 HYPERBOLIC TRANSFORMATION OF $\overline{CK_oU}DSS$ TEST DATA

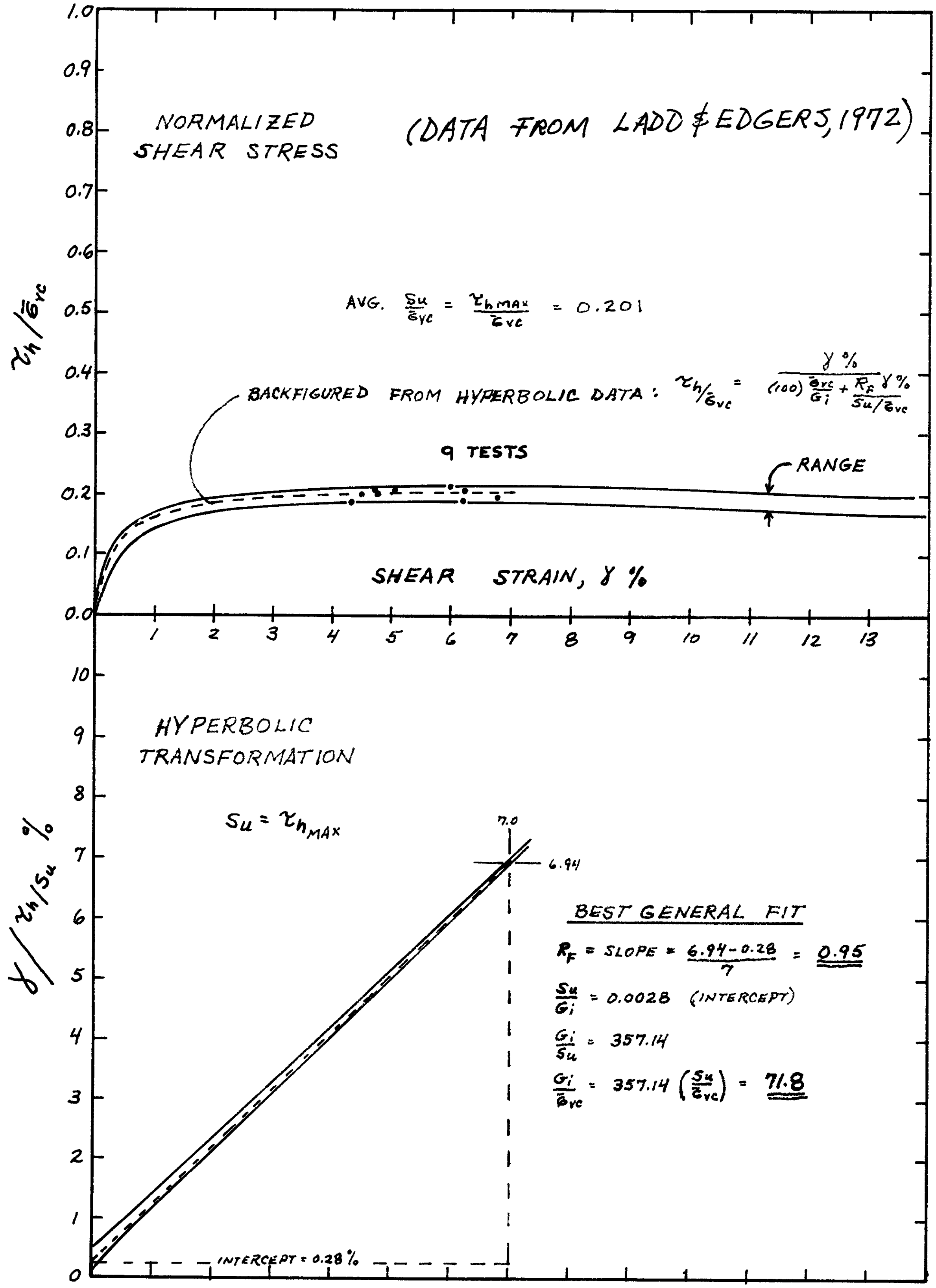

FIGURE 5-5 RESEDIMENTED CLAY, $\overline{CK_0U}$DSS DATA, OCR=1

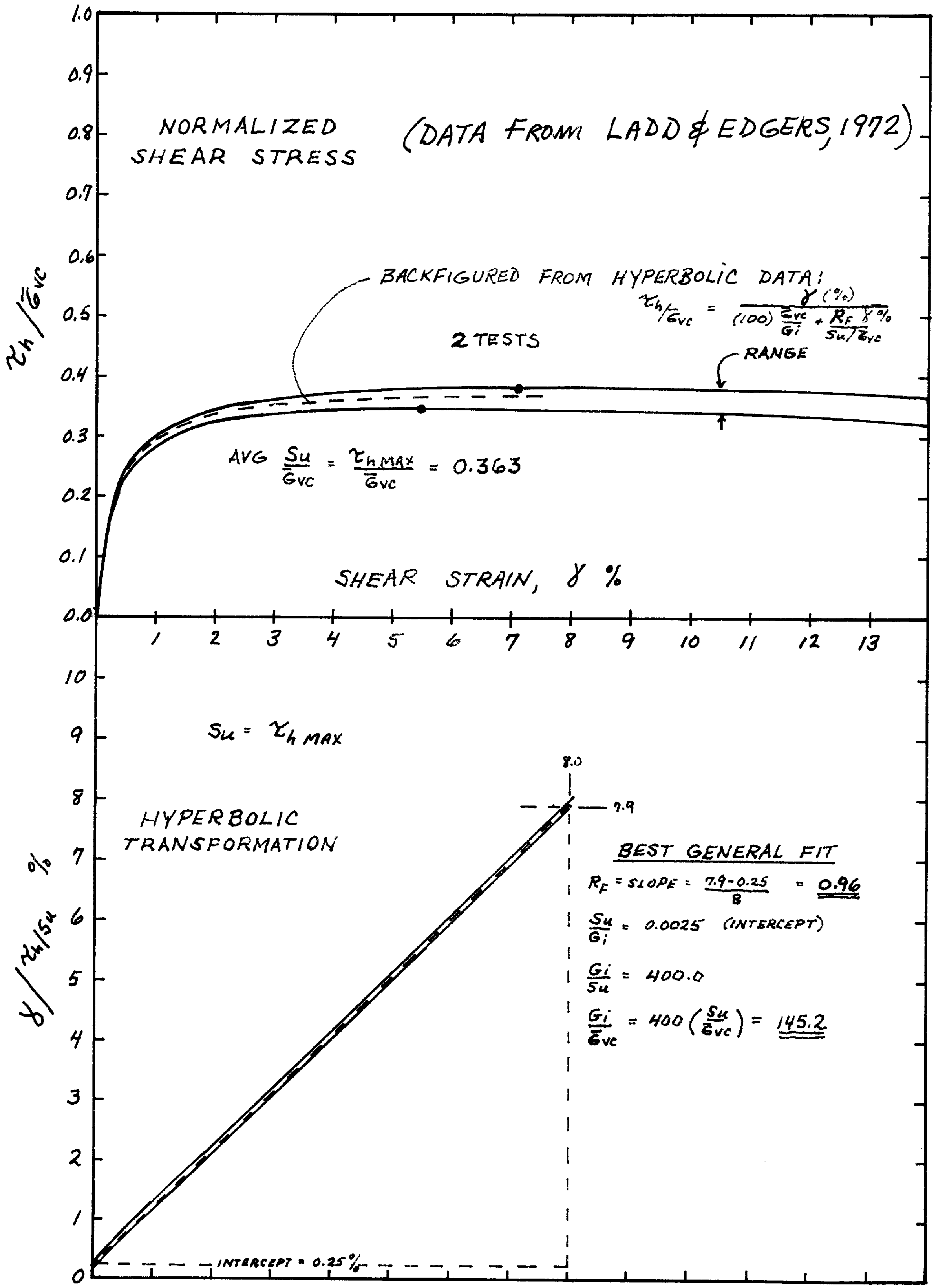

FIGURE 5-6 RESEDIMENTED CLAY, $\overline{CK_0U}DSS$ DATA, OCR=2

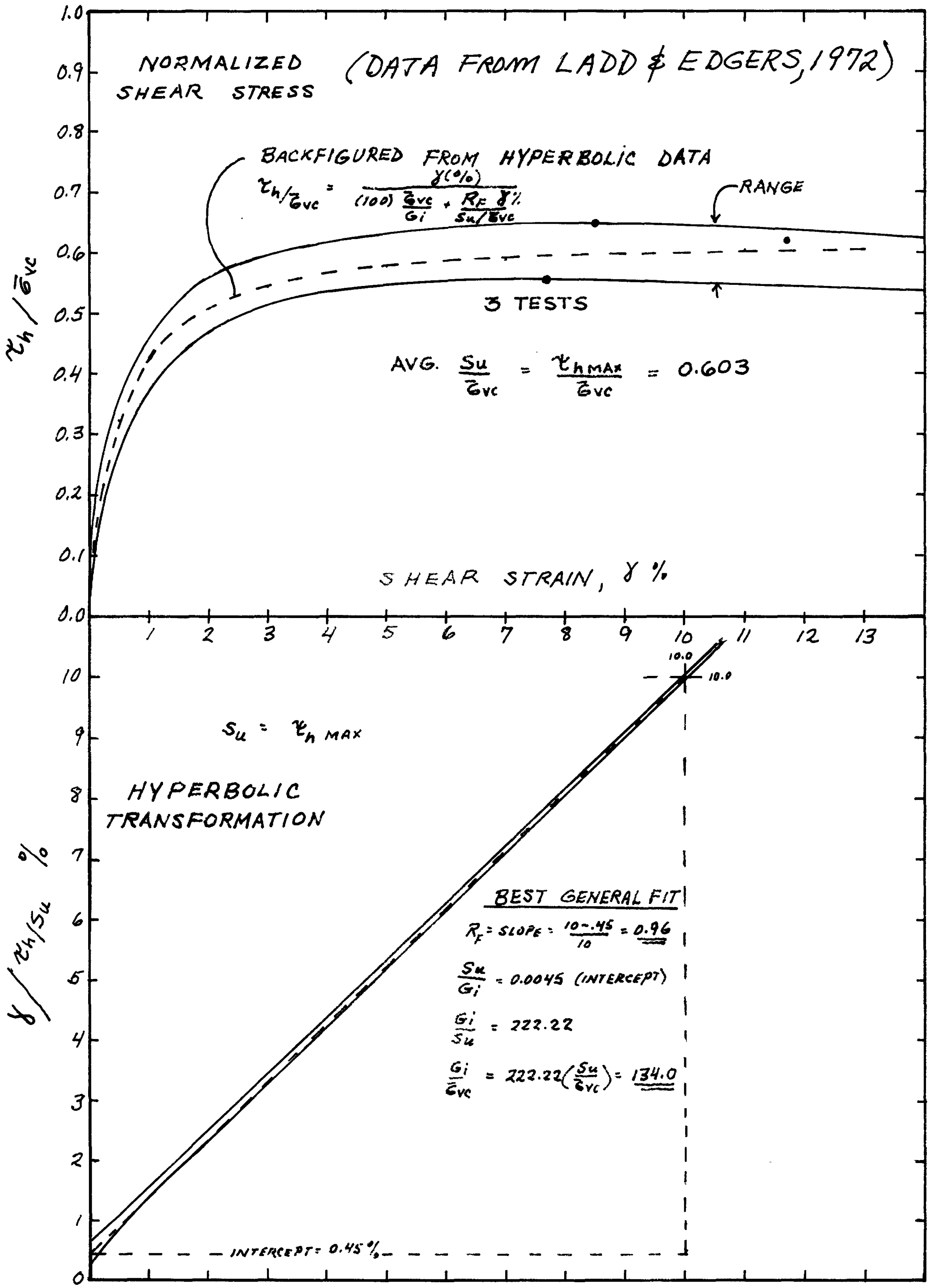

FIGURE 5-7 RESEDIMENTED CLAY, $\overline{CK_oU}$DSS DATA, OCR = 4

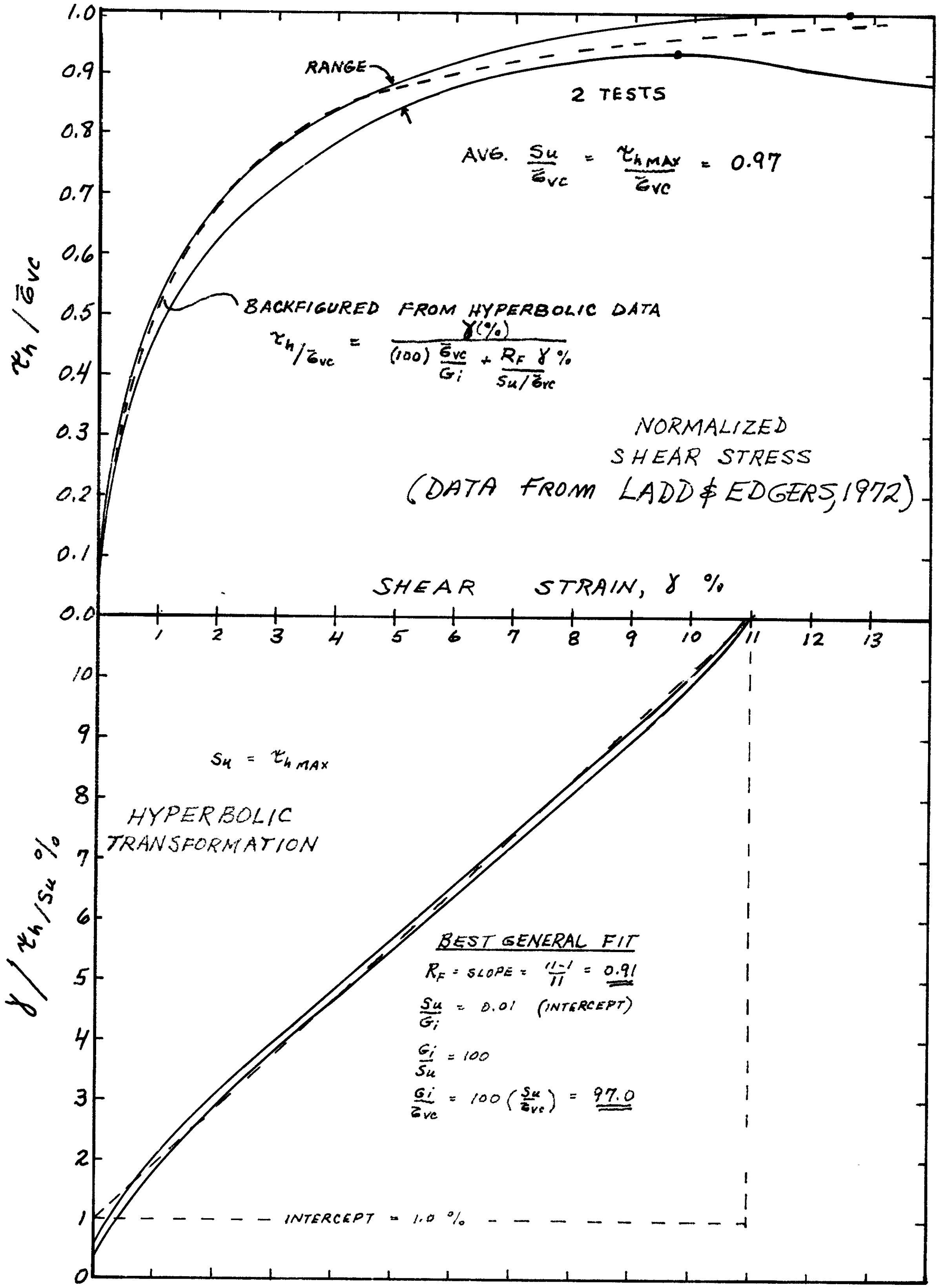

FIGURE 5-8 RESEDIMENTED CLAY, $\overline{CK_oUDSS}$ DATA, OCR = 8

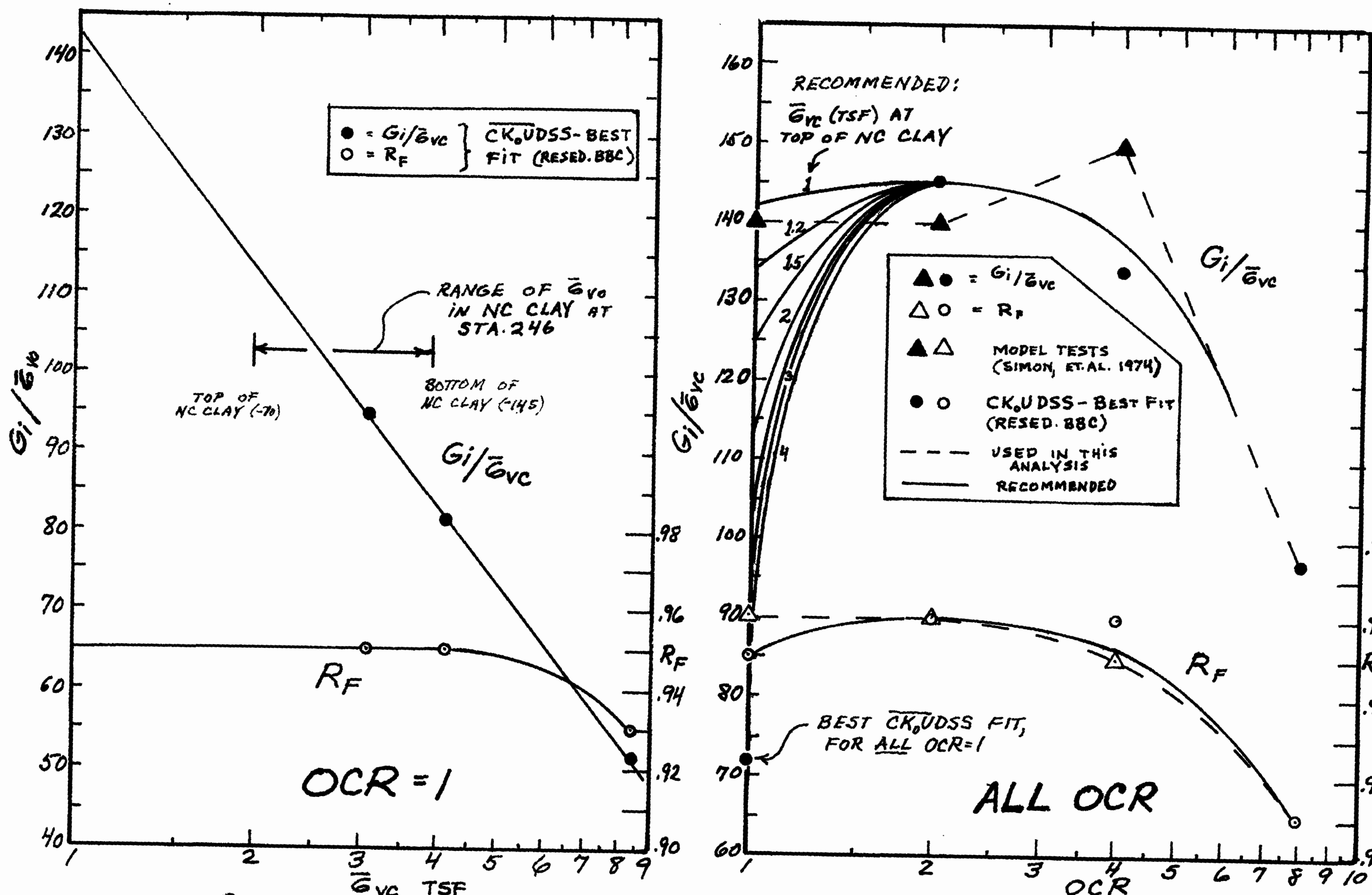

FIGURE 5-9 NORMALIZED SHEAR MODULUS AND R_F FACTOR, RESEDIMENTED CLAY

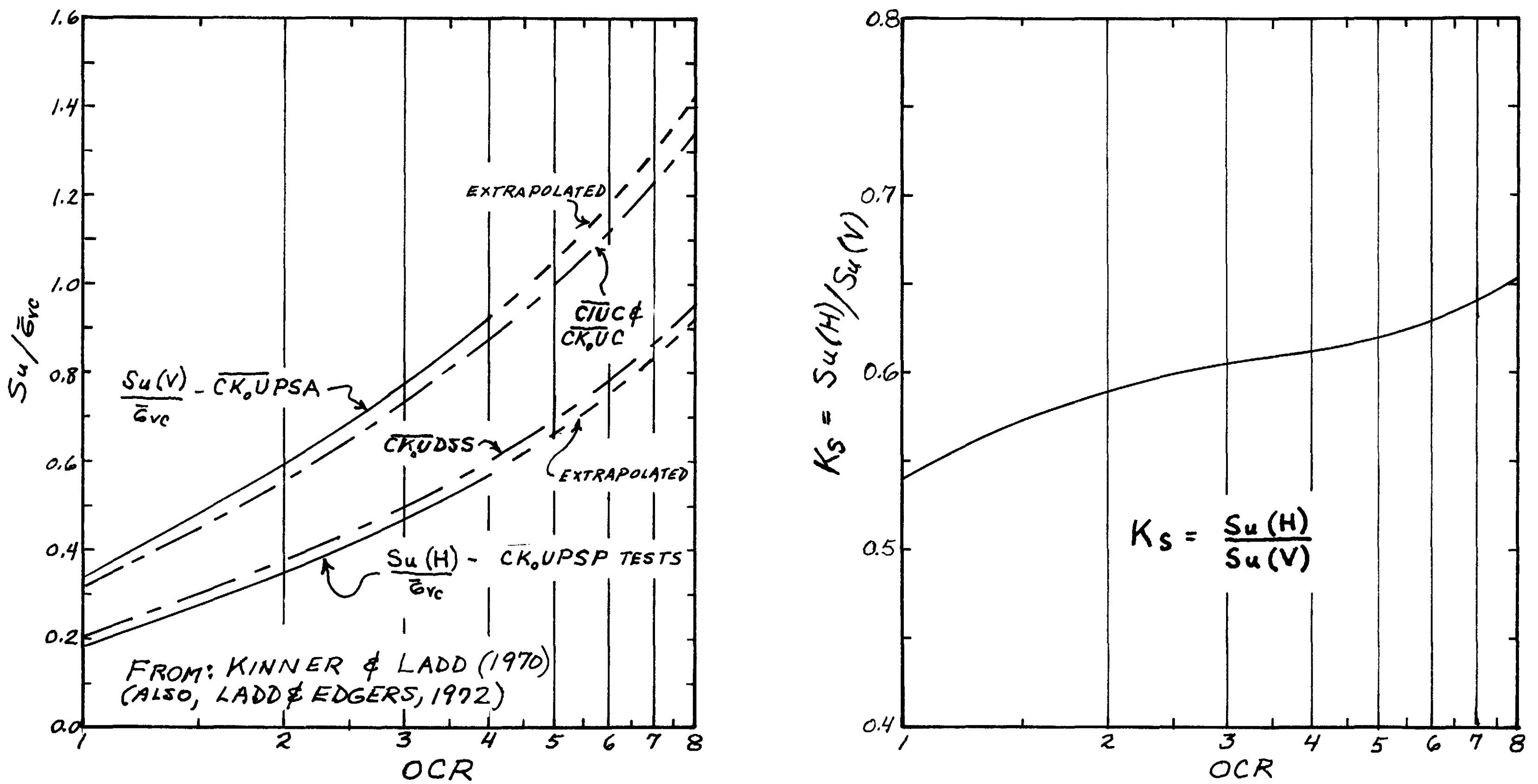

FIGURE 5-10 SHEAR STRENGTH OF RESEDIMENTED BOSTON BLUE CLAY

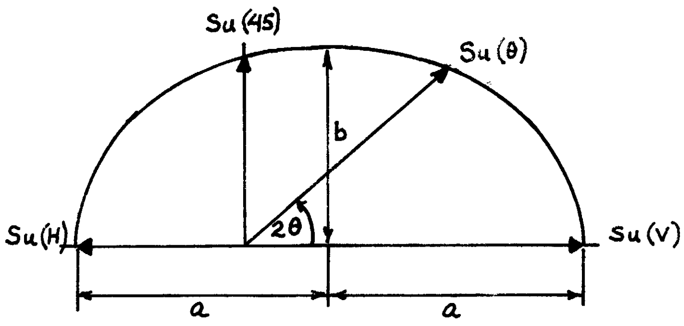

(FROM DAVIS & CHRISTIAN, 1971)

$Su(\theta)$ = UNDRAINED SHEAR STRENGTH WITH MAJOR PRINCIPLE COMPRESSIVE STRESS INCLINED θ FROM VERTICAL

$$\frac{a}{b} = \frac{\sqrt{Su(V) \times Su(H)}}{Su(45)}$$

STRENGTH ANISOTROPY

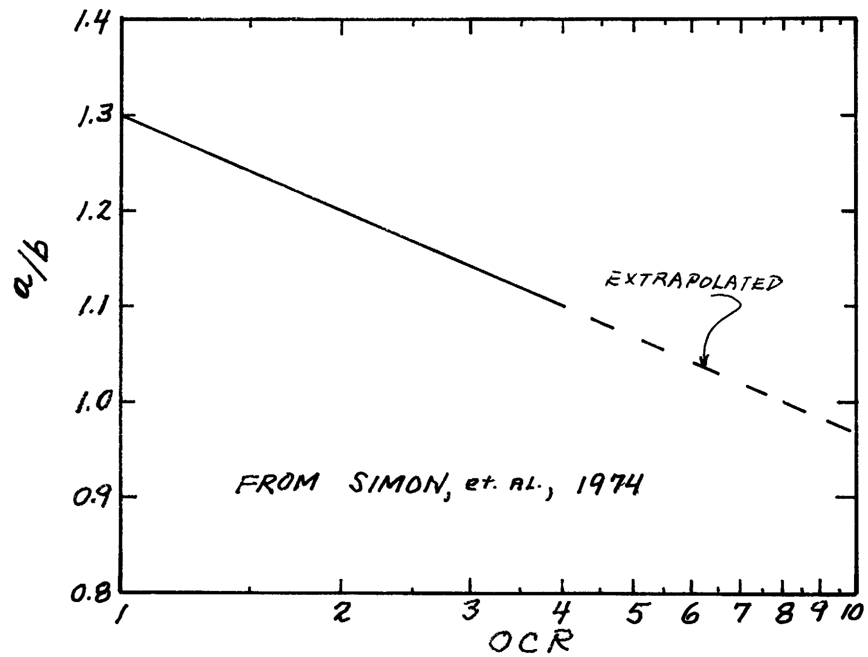

ANISOTROPY OF BOSTON BLUE CLAY

FIGURE 5-11 STRENGTH ANISOTROPY OF BOSTON BLUE CLAY

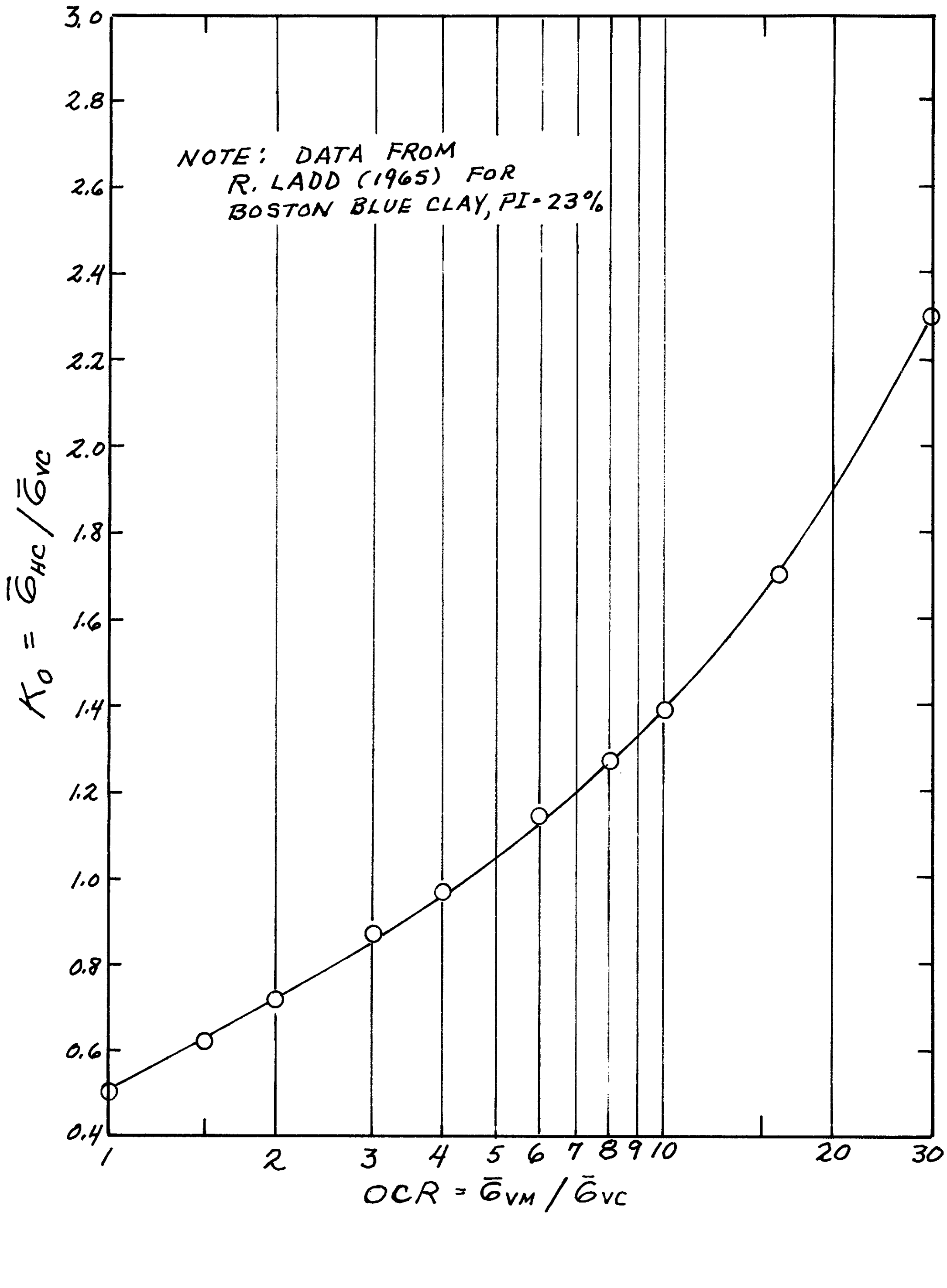

FIGURE 5-12 K_0 FOR BOSTON BLUE CLAY

6. COMPARISON OF PREDICTED AND MEASURED UNDRAINED DEFORMATIONS AND STRESSES

6.1 YIELDING

Figure 6-1 indicates the predicted yielded zones beneath the embankment at Sta. 246. Elements whose yield factor, q/q_{yield}, is greater than 0.95 and 0.90 are also shown. At the full height of the embankment, NC clay and the lowest part of OC clay (where OCR < 1.4) is at or near yield under the entire embankment. This is a greater width of yielding than that indicated by earlier finite element analyses with a bilinear stress-strain relation (D'Appolonia et. al., 1971). However, yielding over the full depth of NC clay agrees with the earlier analyses. This is encouraging, since bilinear analyses have been reported as more effective for predicting the performance of normally consolidated clays (Simon, 1972).

6.2 HORIZONTAL DEFLECTION

Figure 6-2 plots the measured and predicted horizontal deflection at the end of construction (CD 620) for the five inclinometers between the centerline and 225' R. Since moduli were based on $\overline{CK_0UDSS}$ data, it is not surprising that the best agreement occurs in areas where DSS conditions might be expected (I-4 and I-5, 95'R and 160'R). Ladd and Edgers (1972) show that values of $E_u/\bar{\sigma}_{vc}$, for triaxial compression and PSA tests are several times larger than those from DSS tests, for NC clay.

In any event, considering that predicted deflections commonly exceed measured deflections by a factor of three (Poulos, 1970), the close agreement at these location is remarkable. Since the inclinometers were initially read at the beginning of Stage 2 filling, they do not indicate lateral deformations due to Stage 1 filling. Therefore, in order to provide a proper comparison, the indicated predicted deflections are incremental deflections from the beginning of Stage 2 to the end of construction. The predicted deflections at the end of Stage 1 and Stage 3 filling are tabulated in Table 6-1.

6.3 VERTICAL SETTLEMENT

Figures 6-3 and 6-4 compare the settlements measured at the end of construction with predicted undrained settlements for the centerline and 95' R., at Sta. 246 and 245 respectively. For Sta. 245 the comparison is made at the end of load step 3 (CD 329, fill El. +15) since measurements were stopped shortly afterwards.

At Sta. 246, as for the case of horizontal deflections, measured values represent only that settlement due to

Stage 2 and 3 filling. Therefore, the appropriate incremental predicted settlements are shown. In order to reduce the effects of consolidation, the measured values are the totals of incremental settlements measured during filling only (i.e. the settlement between the end of Stage 2 and the beginning of Stage 3 has been removed).

In the typical construction situation, rather small increments of fill are placed relatively slowly. In such a case it is obviously impossible to accurately measure undrained settlements, since consolidation will always occur during construction. This means that only a subjective comparison of predicted and measured settlements can be made. All that can be stated is that the measured settlements should be greater than predicted settlements at the end of construction.

Measured horizontal deflections are much less affected, if at all, by consolidation during loading, as discussed in Chapter 4. Therefore, predicted undrained settlements were corrected based on a comparison of predicted and measured horizontal deflections. The precedure is shown by example in Figure 6-5. At different elevations a correction factor, CF, is computed from the areas to the left of the measured and predicted deflection vs. elevation curves. The predicted initial settlements are then multiplied by CF to produce a corrected prediction. These latter values were considered to be the actual initial settlements.

Original predicted settlements are tabulated in Table 6-2. Table 6-3 presents the computed CF values and the resulting corrected predicted settlements for Sta. 246. For each location, CF was based on the nearest inclinometer. At the centerline, it was necessary to use I-3 (45'R.) data, since horizontal deflection was prevented there for FEECON.

The corrected initial settlements shown in Figure 6-3 suggest that at Sta. 246 there has been significant consolidation settlement at the centerline by the end of construction. In addition, at 95' R., there is a predicted slight initial heave. This is due to filling above El. +16 moving away relative to 95' R. location. The effect is not yet apparent for an earlier time (Figure 6-4) when filling at CD 329 is still above that location. Additionally, heave of the overlying sand layer was measured at 95' R. once fill height exceeded El. +16 (Figure 4-5).

For comparison, initial settlement was calculated for Sta. 246 at the centerline with the method of D'Appolonia et. al. (1971), which might be used in practice. The average s_u was taken as 1.7 ksf from $\overline{CK_oUDSS}$ tests over the full length of the clay. With $E_u = 1200s_u$, b = 85', h = 145', an elastic settlement ρ_e was computed from Davis and Poulos ($\nu = 0.5$) to be 0.056 ft. Then, assuming $q_u = 5.1s_u$, average q = 4.3ksf, $q/q_u = 0.5$, f = 0.5, H/B = 1.0, $\rho_i = 0.073$ ft. (D'Appolonia et. al., 1971). This is less than half the corrected FEECON prediction at the top of the clay (0.20 ft.). D'Appolonia et.al. suggest caution in using their method for non-homogeneous clays.

6.4 FOUNDATION STRESSES

Figure 6-6 shows the predicted final vertical effective stresses (drained - $\bar{\sigma}_{vf}$) beneath the embankment centerline. For comparison, $\bar{\sigma}_{vf}$ distributions for a number of methods are portrayed. As one would expect, the FEECON prediction falls between the two extreme cases of one-dimensional and Boussinesg strip load on a semi-infinite half-space. Additionally, the FEECON prediction is somewhat lower than the Davis & Poulos distribution for a strip on a homogeneous elastic layer (based on Recker et. al., 1974). This is probably because FEECON can account for stress redistribution during construction, as well as the non-homogeneous nature of the soils. All methods converge to the one-dimensional case at the top of the clay, as they should. The comparison indicates that the FEECON predicted $\bar{\sigma}_{vf}$ values are reasonable.

Figure 6-6 also shows the initial vertical effective stress, based on FEECON predictions of $\Delta\sigma_v$ and the initial excess pore pressure (Section 6-5). Assuming an undrained loading, there is an initial apparent slight reduction in $\bar{\sigma}_v$ throughout the NC zone. However, this has probably been eliminated by the end of construction due to some consolidation. FEECON stress predictions are tabulated in Tables 6-4 to 6-6. These include vertical and horizontal stresses, principal stresses and octahedral stresses.

6.5 PORE PRESSURES

Figures 6-7 to 6-9 present the maximum "measured" excess pore pressures beneath the embankment, and initial excess pore pressures predicted by three different methods. The maximum "measured" values are the peak values occurring after Stage 2, plus the measured increase in pore pressure due to Stage 3 filling. To determine these values, it was occasionally necessary to use graphic interpolation, as discussed in Chapter 4.

All three methods use various stresses predicted by FEECON. The methods include:

1) $\Delta u = \Delta\sigma_{oct}$

2) $\Delta u = \Delta\sigma_v$

3) $\Delta u = \Delta\sigma_{oct} + a\Delta\tau_{oct}^{k}$ (Henkel, 1960)

FEECON uses Henkel's equation to predict pore pressures. However, Henkel's a and k parameters were both input as zero, so that FEECON pore pressure output was generated as $\Delta\sigma_{oct}$.

For the application of Henkel's method, his a parameter was related to Skempton's A parameter at failure, A_f (D'Appolonia et. al., 1971):

$$a = \frac{3\ A_f - 1}{\sqrt{2}}$$

This relation does not strictly apply outside the yielded zone, but since so much of the foundation is near yielding, it was chosen as a reasonable yet simple approximation.

Figure 6-10 plots both Skempton's and Henkel's parameters as a function of OCR on a log scale for the three stress conditions: PSA, DSS, and PSP. The PSA and PSP A_f parameters are based on plane strain tests on resedimented BBC (Ladd et. al., 1971). These curves were extrapolated to OCR = 8, and the DSS curve was assumed to be an average of the PSA and PSP curves. The equivalent Henkel a parameter was then computed and plotted.

The curves in Figure 6-10 permit taking the stress conditions into effect in a simple way. The foundation was divided into zones where each of the three conditions (PSA, DSS, PSP) might reasonably be expected to predominate. The PSA zone was chosen as that beneath the maximum height of Fill (0 to 45' R.), DSS beneath the embankment slope (45'R. to 140' R.), and PSP outside the toe (+ 140' R.). Pore pressures were then computed within each zone with the appropriate a parameter. Henkel's k parameter was assumed equal to 1.

$$\Delta u = \Delta\sigma_{oct} + a\Delta\tau_{oct}$$

$$\Delta\sigma_{oct} = \frac{\Delta\sigma_1 + \Delta\sigma_2 + \Delta\sigma_3}{3}$$

$$\Delta\sigma_2 = \frac{\Delta\sigma_1 + \Delta\sigma_3}{2}$$

$$\Delta\tau_{oct} = \frac{1}{3}\sqrt{(\Delta\sigma_1 - \Delta\sigma_2) + (\Delta\sigma_1 - \Delta\sigma_3)^2 + (\Delta\sigma_2 - \Delta\sigma_3)^2}$$

Pore pressures predicted with Henkel's method are tabulated in Table 6-7

Study of Figures 6-7 to 6-9 shows that for locations beneath the embankment (0 to 95' R.) the modified Henkel equation , as used in this study, most closely matches the measured maximum pore pressures in the mid-third of the clay (where consolidation effects are least). Beneath the embankment crest the relation $\Delta u = \Delta\sigma_V$ is quite good for the NC region, but significantly high in the upper OC zone. The change in octahedral stress, $\Delta\sigma_{oct}$, gives the lowest values for initial pore pressures beneath the embankment, and apparently underestimates undrained excess pore pressures.

Considering that the Davis and Poulos $\Delta\sigma_V$ distribution is somewhat greater than the FEECON $\Delta\sigma_V$ (Figure 6-6), it may be that the use of their relation for bulk stress, $\Delta\sigma_\theta$ (equal to $\Delta\sigma_{oct}$) might be a fair approximation for excess pore pressure if a linear distribution equal to $\Delta\sigma_\theta$ at the mid-plane is assumed. It should be noted that the jogs in the predicted pore pressure plots at some locations are apparently due to the use of a finite number of discrete elements in the analysis.

The pore pressures predicted with the modified Henkel relation were used as the initial excess pressures in the consolidation analysis (Chapter 7).

FEECON HORIZONTAL DEFLECTIONS (INS.), LOAD STEPS 9 & 1 (FILL ELS. +40 & +9)

ELEV.	30'R			45'R			66'R			95'R			130'R			160'R			225'R		
	δ_9	δ_1	$\Delta\delta$	δ_9	δ_1	$\Delta\delta$	δ_9	δ_1	$\Delta\delta$	δ_9	δ_1	$\Delta\delta$	δ_9	δ_1	$\Delta\delta$	δ_9	δ_1	$\Delta\delta$	δ_9	δ_1	$\Delta\delta$
-10	1.74	.07	1.67	2.74	.11	2.63	3.60	.16	3.44	3.95	.25	3.70	3.59	.40	3.19	2.80	.30	2.50	1.63	.17	1.46
-20	1.74	.06	1.68	2.68	.10	2.58	3.54	.14	3.40	3.87	.23	3.64	3.32	.32	3.00	2.58	.28	2.30	1.48	.16	1.32
-30	1.86	.06	1.80	2.77	.10	2.67	3.46	.14	3.32	3.74	.20	3.54	3.12	.28	2.84	2.37	.25	2.12	1.35	.16	1.19
-40	1.90	.06	1.84	2.89	.09	2.80	3.42	.13	3.29	3.56	.19	3.37	2.87	.24	2.63	2.17	.23	1.94	1.24	.14	1.10
-50	1.97	.05	1.92	2.75	.08	2.67	3.31	.12	3.19	3.28	.17	3.11	2.57	.22	2.35	1.95	.20	1.75	1.11	.13	.98
-60	1.78	.05	1.73	2.60	.08	2.52	2.90	.11	2.79	2.80	.14	2.66	2.21	.19	2.02	1.69	.18	1.51	.98	.12	.86
-70	1.70	.04	1.66	2.12	.07	2.05	2.36	.10	2.26	2.32	.13	2.19	1.87	.16	1.71	1.48	.16	1.32	.85	.11	.74
-85	1.15	.04	1.11	1.53	.06	1.47	1.72	.08	1.64	1.73	.11	1.62	1.44	.13	1.31	1.16	.12	1.04	.68	.09	.59
-100	.74	.03	.71	.99	.04	.95	1.12	.06	1.06	1.17	.08	1.09	1.04	.09	.95	.85	.09	.76	.50	.07	.43
-115	.41	.02	.39	.55	.03	.52	.67	.04	.63	.73	.05	.68	.70	.06	.64	.56	.06	.50	.34	.05	.29
-130	.17	.01	.16	.23	.01	.22	.34	.02	.32	.35	.03	.32	.34	.03	.31	.29	.03	.26	.17	.02	.15

TABLE 6-1 FEECON PREDICTED HORIZONTAL DEFLECTIONS

ELEV.	℄ ρ_9	℄ ρ_1	℄ $\Delta\rho$	30'R ρ_9	30'R ρ_1	30'R $\Delta\rho$	45'R ρ_9	45'R ρ_1	45'R $\Delta\rho$	60'R ρ_9	60'R ρ_1	60'R $\Delta\rho$	95'R ρ_9	95'R ρ_1	95'R $\Delta\rho$	160'R ρ_9	160'R ρ_1	160'R $\Delta\rho$	225'R ρ_9	225'R ρ_1	225'R $\Delta\rho$
	FEECON INITIAL SETTLEMENTS (FT.), LOAD STEPS 9 & 1 (FILL ELS. +40 & +9)																				
-10	.499	.019	.480	.415	.019	.396	.295	.019	.276	.185	.020	.165	-.028	.019	-.047	-.125	-.008	-.117	-.067	-.007	-.060
-20	.437	.016	.421	.358	.016	.342	.238	.016	.222	.144	.016	.128	-.031	.015	-.046	-.107	-.005	-.102	-.057	-.006	-.051
-30	.381	.013	.368	.307	.013	.294	.192	.013	.179	.112	.013	.099	-.031	.012	-.043	-.089	-.004	-.085	-.048	-.005	-.043
-40	.324	.011	.313	.252	.011	.241	.148	.011	.137	.088	.011	.077	-.027	.009	-.036	-.073	-.003	-.070	-.040	-.004	-.036
-50	.274	.009	.265	.198	.009	.189	.114	.009	.105	.066	.009	.057	-.018	.007	-.025	-.057	-.002	-.055	-.033	-.003	-.030
-60	.218	.007	.211	.143	.007	.136	.090	.007	.083	.048	.007	.041	-.009	.006	-.015	-.043	-.001	-.042	-.025	-.003	-.022
-70	.165	.006	.159	.090	.006	.084	.067	.006	.061	.039	.006	.033	.008	.005	.003	-.033	-.001	-.032	-.019	-.002	-.017
-85	.108	.004	.104	.055	.004	.051	.041	.004	.037	.027	.004	.023	.008	.003	.005	-.019	.000	-.019	-.013	-.001	-.012
-100	.053	.002	.051	.031	.002	.029	.023	.002	.021	.018	.002	.016	.007	.002	.005	-.010	.000	-.010	-.007	-.001	-.006
-115	.020	.001	.019	.015	.001	.014	.011	.001	.010	.010	.001	.009	.005	.010	-.005	-.004	.000	-.004	-.003	.000	-.003
-130	.003	.000	.003	.004	.000	.004	.003	.000	.003	.003	.000	.003	.002	.000	.002	-.001	.000	-.001	-.001	.000	-.001

TABLE 6-2 FEECON PREDICTED INITIAL SETTLEMENTS

ELEV.	℄ CF (I-3)	℄ $\rho_{i\,FT}$ CORR.	30'R CF (I-3)	30'R $\rho_{i\,FT}$ CORR.	45'R CF (I-3)	45'R $\rho_{i\,FT}$ CORR.	60'R CF (I-3)	60'R $\rho_{i\,FT}$ CORR.	95'R CF (I-4)	95'R $\rho_{i\,FT}$ CORR.	160'R CF (I-5)	160'R $\rho_{i\,FT}$ CORR.	225'R CF (I-6)	225'R $\rho_{i\,FT}$ CORR.
-10	.42	.202	.42	.174	.42	.124	.42	.077	.85	-.024	.83	-.104	.27	-.018
-20	.38	.166	.38	.136	.38	.090	.38	.055	.84	-.026	.86	-.092	.28	-.016
-30	.32	.122	.32	.098	.32	.061	.32	.036	.82	-.025	.89	-.079	.29	-.014
-40	.28	.091	.28	.071	.28	.041	.28	.025	.79	-.021	.92	-.067	.29	-.012
-50	.23	.061	.23	.046	.23	.026	.23	.015	.80	-.014	.95	-.054	.28	-.009
-60	.16	.033	.16	.023	.16	.014	.16	.008	.81	-.007	.97	-.042	.27	-.007
-70	.10	.016	.10	.009	.10	.007	.10	.004	.80	-.003	.99	-.032	.26	-.005
-85	.06	.006	.06	.003	.06	.002	.06	.002	.80	.002	1.02	-.020	.23	-.003
-100	.05	.002	.05	.002	.05	.001	.05	.001	.97	.003	1.10	-.011	.23	-.002
-115	.03	.001	.03	0	.03	0	.03	0	1.34	.003	1.25	-.005	.22	-.001
-130	0	0	0	0	0	0	0	0	1.84	.002	1.40	-.001	.07	0

TABLE 6-3 FEECON SETTLEMENT CORRECTION FACTORS AND CORRECTED INITIAL SETTLEMENTS

ELEV	INITIAL		LOCATION & CHANGE IN FEECON TOTAL VERTICAL & HORIZ. STRESS (PSF), END OF LOADING: ℄		30'R		45'R		60'R		95'R		160'R		225'R	
	$\bar{\sigma}_{VO}$	$\bar{\sigma}_{HO}$	$\Delta\sigma_V$	$\Delta\sigma_H$	$\Delta\sigma_V$	$\Delta\sigma_H$	$\Delta\sigma_V$	$\Delta\sigma_H$	$\Delta\sigma_V$	$\Delta\sigma_H$	$\Delta\sigma_V$	$\Delta\sigma_H$	$\Delta\sigma_V$	$\Delta\sigma_H$	$\Delta\sigma_V$	$\Delta\sigma_H$
-15	1015	1269	4046	2653	3923	2599	3878	2587	3286	2281	1666	1592	16	590	12	2811
-25	1570	1570	3891	1840	3778	1860	3636	1820	3332	1871	1890	1794	59	1022	22	2468
-35	2090	1797	3854	1613	3671	1601	3875	1959	3658	2248	1897	1878	137	1249	69	2014
-45	2610	1931	3781	1768	3799	1909	2545	869	2427	1095	1495	1584	179	1332	35	1497
-55	3130	1909	3662	2156	3375	1984	4341	3082	3963	2950	1917	2019	179	1341	68	1274
-65	3650	1898	3547	2628	3619	2679	3513	2614	3141	2427	1717	1788	266	1407	22	890
-77.5	4300	2150	3386	2626	3375	2465	3237	2277	2640	1892	1625	1705	330	1414	192	677
-92.5	5080	2540	3361	2476	3312	2267	2918	1816	2620	1823	2087	2052	364	1375	107	217
-107.5	5860	2930	2963	1984	2947	1808	3237	2123	2564	1721	1300	1142	542	1307	216	-318
-122.5	6640	3320	2883	1862	2771	1697	2207	1269	2389	1560	1825	1649	712	1172	259	-1103
-137.5	7420	3710	2403	1681	2775	2117	2660	2156	2391	1955	1584	1440	656	813	203	-2090

TABLE 6-4 CHANGE IN FEECON VERTICAL & HORIZONTAL STRESSES

ELEV.	LOCATION & CHANGE IN FEECON PRINCIPLE TOTAL STRESSES (PSF), END OF LOADING																				
	℄			30'R			45'R			60'R			95'R			160'R			225'R		
	$\Delta\sigma_1$	$\Delta\sigma_2$	$\Delta\sigma_3$	$\Delta\sigma_1$	$\Delta\sigma_2$	$\Delta\sigma_3$	$\Delta\sigma_1$	$\Delta\sigma_2$	$\Delta\sigma_3$	$\Delta\sigma_1$	$\Delta\sigma_2$	$\Delta\sigma_3$	$\Delta\sigma_1$	$\Delta\sigma_2$	$\Delta\sigma_3$	$\Delta\sigma_1$	$\Delta\sigma_2$	$\Delta\sigma_3$	$\Delta\sigma_1$	$\Delta\sigma_2$	$\Delta\sigma_3$
-15	3792	3477	2907	3750	3388	2771	3758	3359	2706	3234	2911	2333	1849	1756	1409	598	430	8	355	308	7
-25	3891	2866	1840	3840	2819	1798	3742	2728	1714	3486	2602	1717	2372	1843	1313	1046	541	35	659	335	11
-35	3854	2911	1674	3719	2783	1553	3952	3063	1881	3789	3100	2117	2357	2034	1418	1022	839	364	553	588	331
-45	3782	3115	1768	3831	3194	1877	2619	2047	796	2532	2101	990	1910	1879	1169	817	1095	694	291	770	570
-55	3633	3505	2156	3392	3290	1967	4367	4322	3055	4032	4067	2881	2282	2579	1654	609	1370	911	182	1103	804
-65	3547	3964	2628	3626	4025	2671	3546	3947	2588	3253	3660	2315	2047	2629	1459	555	1712	1117	122	1332	789
-77.5	3386	4081	2626	3389	3995	2451	3292	3832	2222	2775	3341	1757	1959	2740	1371	627	1947	1118	285	1688	941
-92.5	3361	4189	2476	3334	4059	2245	2991	3637	1743	2793	3491	1649	2437	3340	1702	668	2140	1071	224	1767	770
-107.5	2963	3939	1984	2994	3842	1761	3318	4145	1353	2743	3608	1542	1599	2686	843	834	2389	1014	348	2014	750
-122.5	2885	4033	1860	2849	3893	1618	2316	3398	1160	2573	3635	1376	2118	3398	1357	988	2601	895	396	2148	581
-137.5	2410	3898	1675	2865	4301	2026	2800	4264	2017	2610	4030	1740	1895	3367	1128	940	2589	529	341	2141	231

TABLE 6-5 CHANGE IN FEECON PRINCIPLE TOTAL STRESSES

ELEV.	LOCATION & CHANGE IN FEECON OCTAHEDRAL TOTAL STRESSES (PSF), END OF LOADING													
	℄		30'R		45'R		60'R.		95'R		160'R		225'R	
	$\Delta\sigma_{oct}$	$\Delta\tau_{oct}$	$\Delta\sigma_{oct}$	$\Delta\tau_{oct}$	$\Delta\sigma_{oct}$	$\Delta\tau_{oct}$	$\Delta\sigma_{oct}$	$\Delta\tau_{oct}$	$\Delta\sigma_{oct}$	$\Delta\tau_{oct}$	$\Delta\sigma_{oct}$	$\Delta\tau_{oct}$	$\Delta\sigma_{oct}$	$\Delta\tau_{oct}$
-15	3320	368	2427	406	437	3210	2758	374	1622	187	730	250	181	156
-25	2852	836	2221	836	828	2710	2583	724	1828	431	936	412	331	262
-35	2752	892	2365	886	848	2900	2939	686	1878	387	917	275	437	112
-45	2758	836	2783	811	761	1700	1747	649	1529	343	861	168	424	193
-55	2883	668	2914	649	608	3700	3438	549	1959	387	867	312	487	381
-65	3083	555	3139	568	570	3050	2771	562	1741	480	830	474	456	493
-77.5	3001	593	2664	636	669	2750	2259	655	1660	562	755	543	605	574
-92.5	2908	699	2839	743	786	2360	2209	761	2059	668	749	624	493	636
-107.5	2459	799	2627	855	1171	2670	2128	849	1211	755	686	693	543	711
-122.5	2359	886	2802	930	914	1730	1959	924	1728	842	537	786	487	786
-137.5	2028	924	2427	942	931	2390	2159	942	1498	930	300	892	281	874

TABLE 6-6 CHANGE IN FEECON OCTAHEDRAL TOTAL STRESSES

		PSA ZONE			DSS ZONE			PSP ZONE		
EL	OCR	HENKEL'S a	u_o, FT.		HENKEL'S a	u_o, FT.		HENKEL'S a	u_o, FT.	
			℄	30'R		60'R	95'R		160'R	225'R
-15	7.8	-.69	49.1	34.4	-.58	40.7	24.3	-.45	9.9	1.8
-25	4.4	-.47	39.4	29.3	-.13	39.9	28.4	.23	16.5	6.3
-35	2.9	-.24	40.7	34.5	.21	49.4	31.4	.69	17.7	8.2
-45	2.0	.01	44.3	44.7	.52	33.4	27.4	1.03	16.6	10.0
-55	1.4	.46	51.1	51.5	.86	62.7	36.7	1.29	20.4	15.7
-65	1.1	.84	56.9	57.9	1.10	54.3	36.4	1.39	23.9	18.3
-77.5	1.0	.99	57.5	52.8	1.20	48.8	37.4	1.46	24.8	23.1
-92.5	↓	↓	57.7	57.3	↓	50.0	45.8	↓	26.6	22.8
-107.5	↓	↓	52.1	55.7	↓	50.4	33.9	↓	27.2	25.3
-122.5	↓	↓	51.9	59.7	↓	49.2	43.9	↓	27.0	26.2
-137.5	↓	↓	47.2	53.9	↓	52.7	41.9	↓	25.7	24.9

$u_o = \Delta\sigma_{oct} + a\,\Delta\tau_{oct}$ (HENKEL)

TABLE 6-7 FEECON PREDICTED INITIAL EXCESS HEAD.

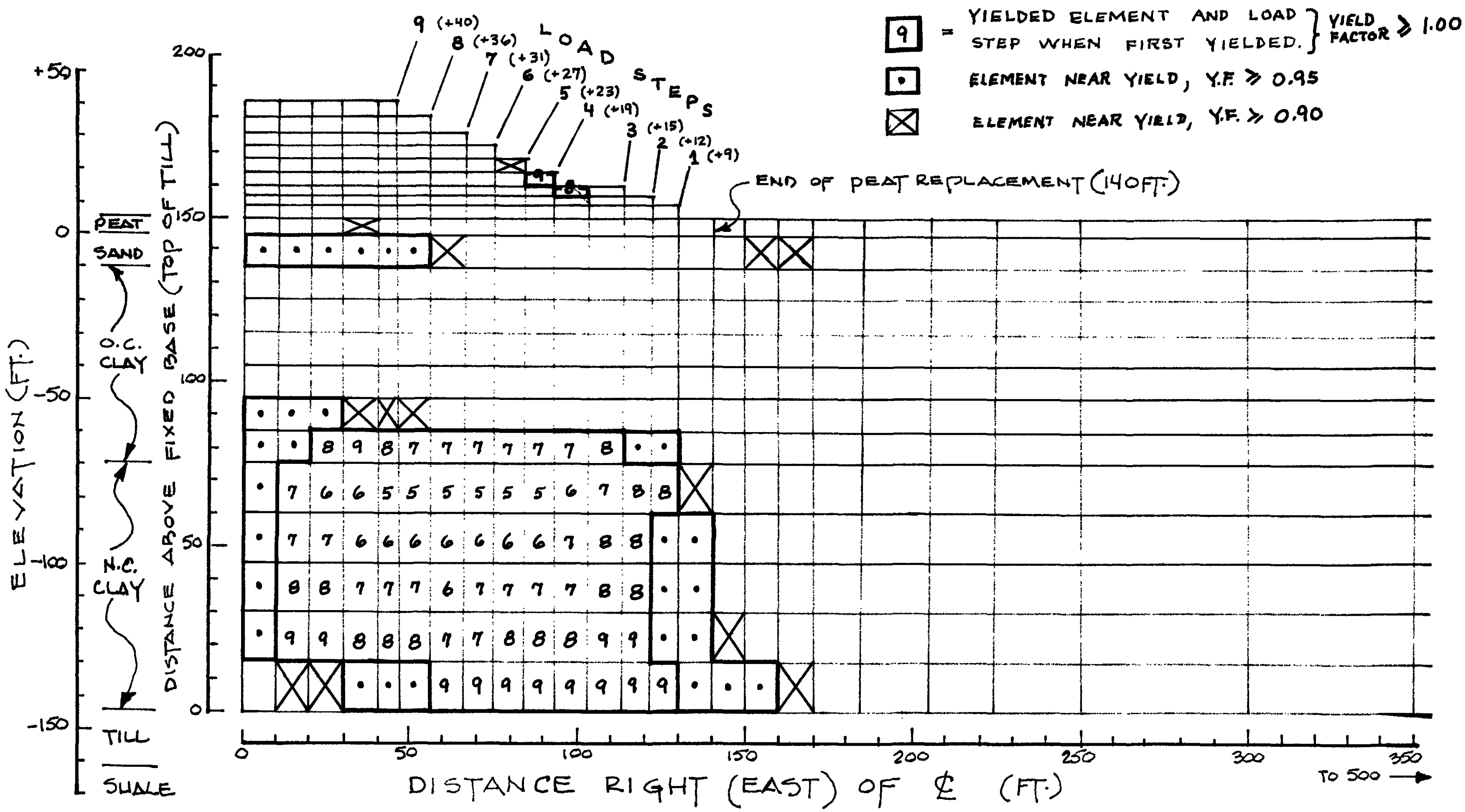

FIGURE 6-1 FINITE ELEMENT YIELDING

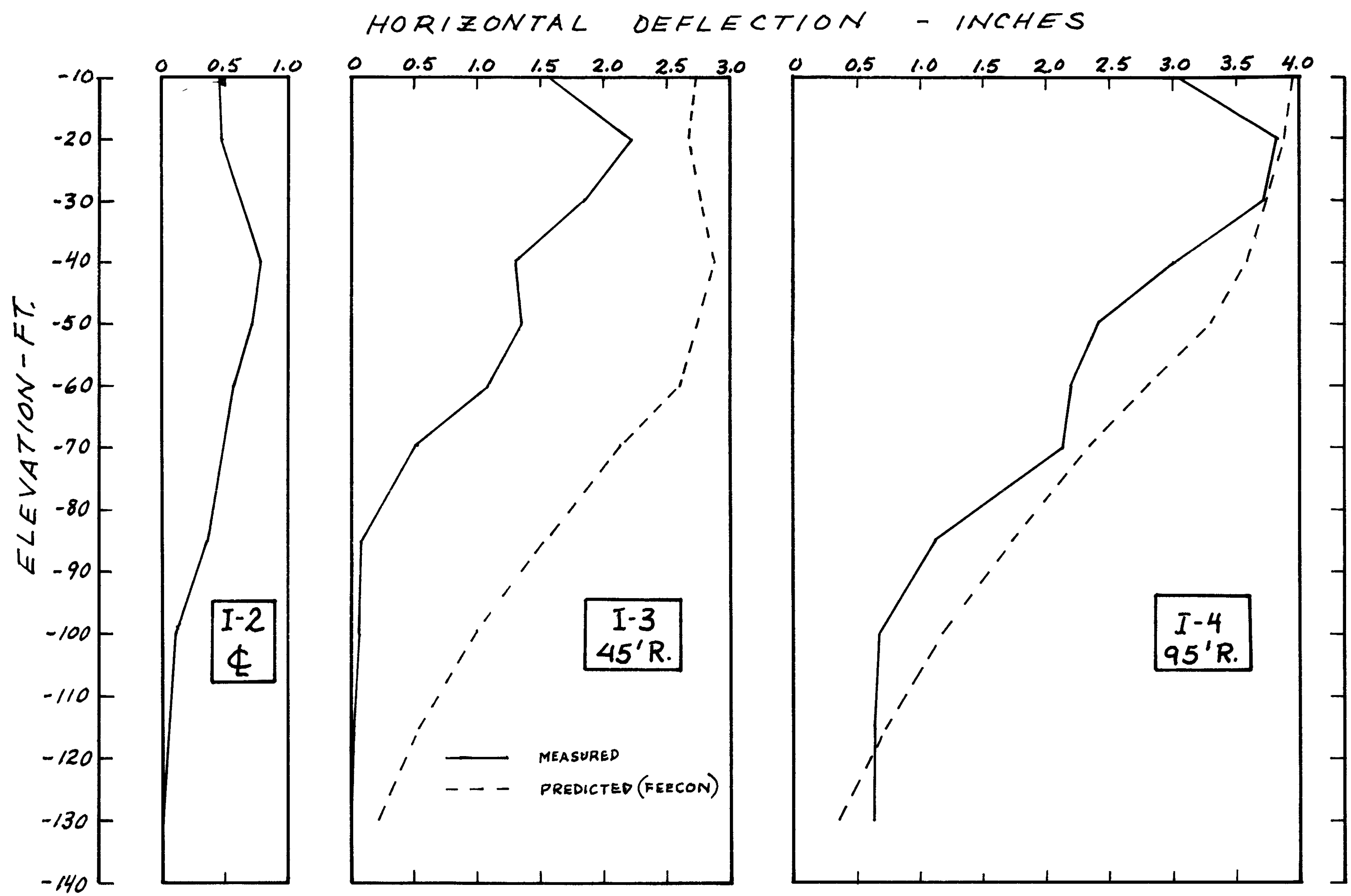

FIGURE 6-2 PREDICTED & MEASURED HORIZONTAL DEFLECTION (END OF CONSTRUCTION) STA. 246

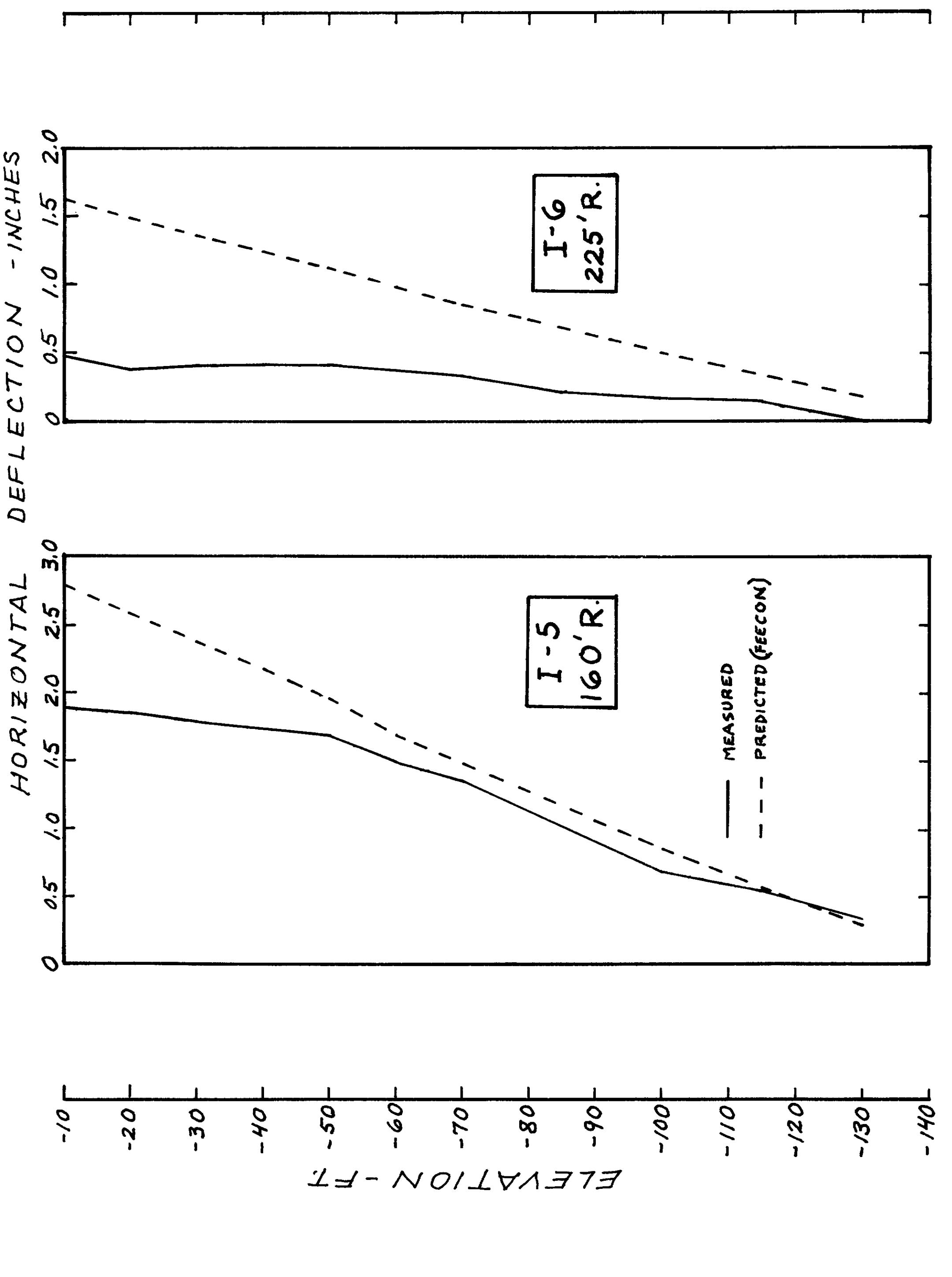

FIGURE 6-2 CONT'D.

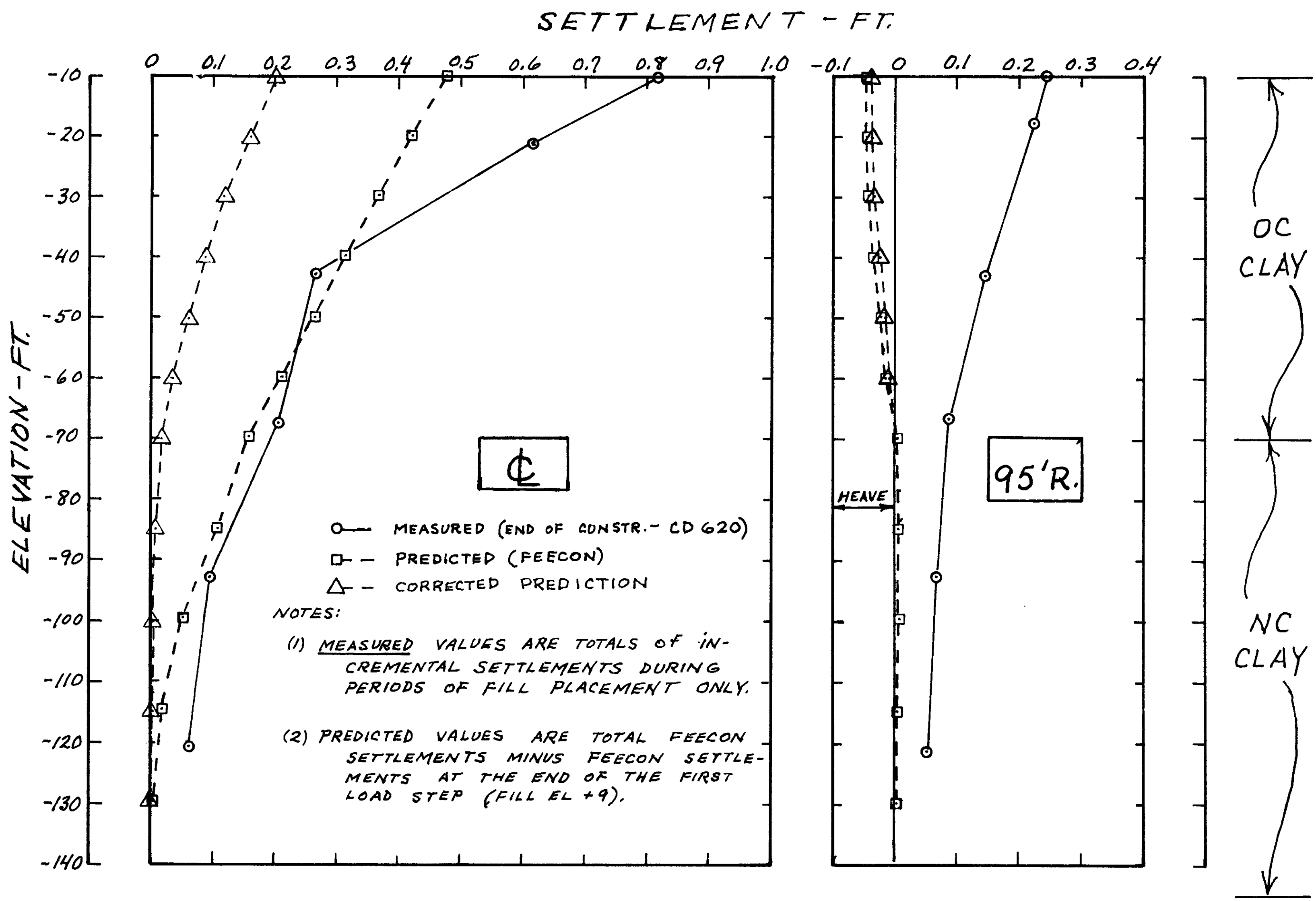

FIGURE 6-3 PREDICTED AND MEASURED INITIAL SETTLEMENT (CD 620) STA. 246

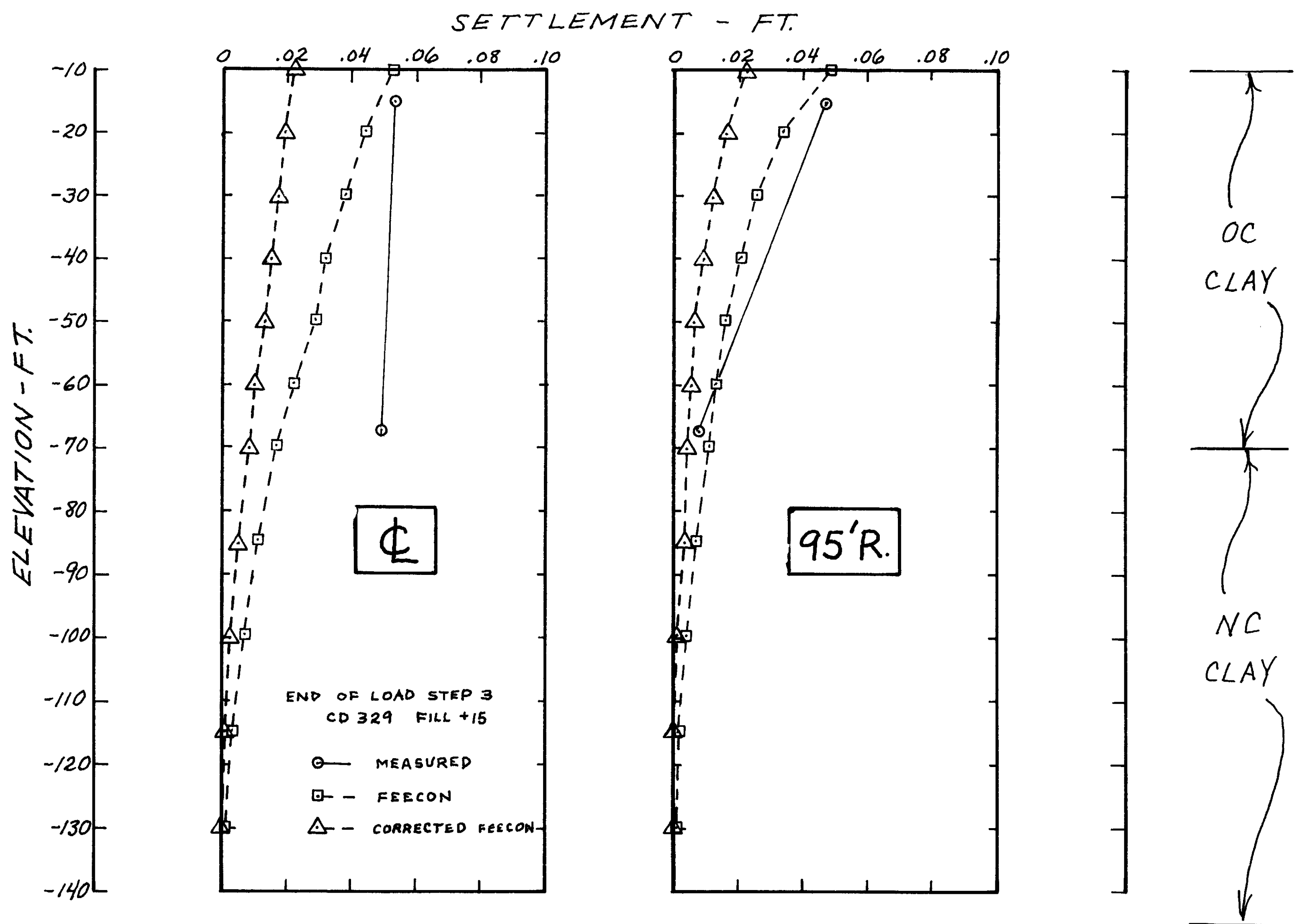

FIGURE 6-4 PREDICTED AND MEASURED INITIAL SETTLEMENT (CD 329) STA. 245

DEFLECTION VS. DEPTH

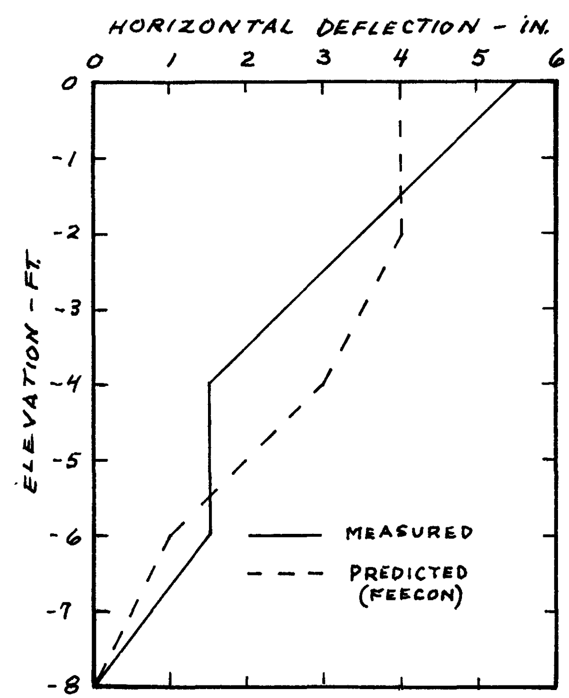

CORRECTION FACTOR

C.F. = A_M / A_F

EL.	A MEAS. IN.-FT.	A FEECON IN.-FT.	C.F. A_M/A_F
0	18.5	20.0	0.93
-2	9.5	12.0	0.79
-4	4.5	5.0	0.90
-6	1.5	1.0	1.50

CORRECTED SETTLEMENT PREDICTION

$\rho_{CORR.} = \rho_{PRED.} \times C.F.$

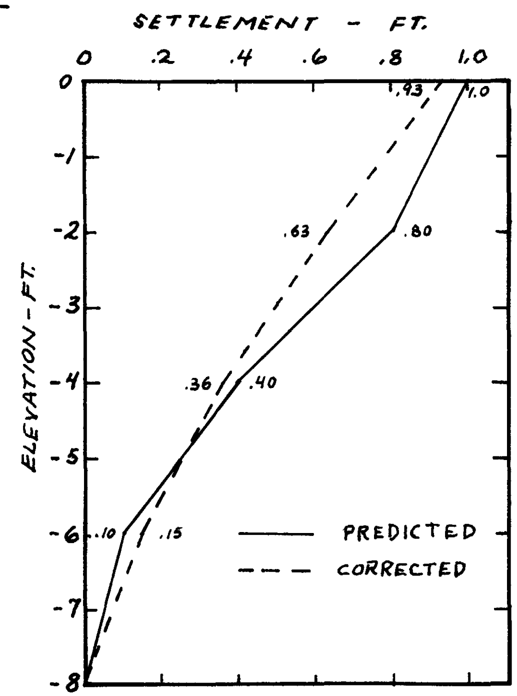

FIGURE 6-5 METHOD OF CORRECTING SETTLEMENT PREDICTIONS

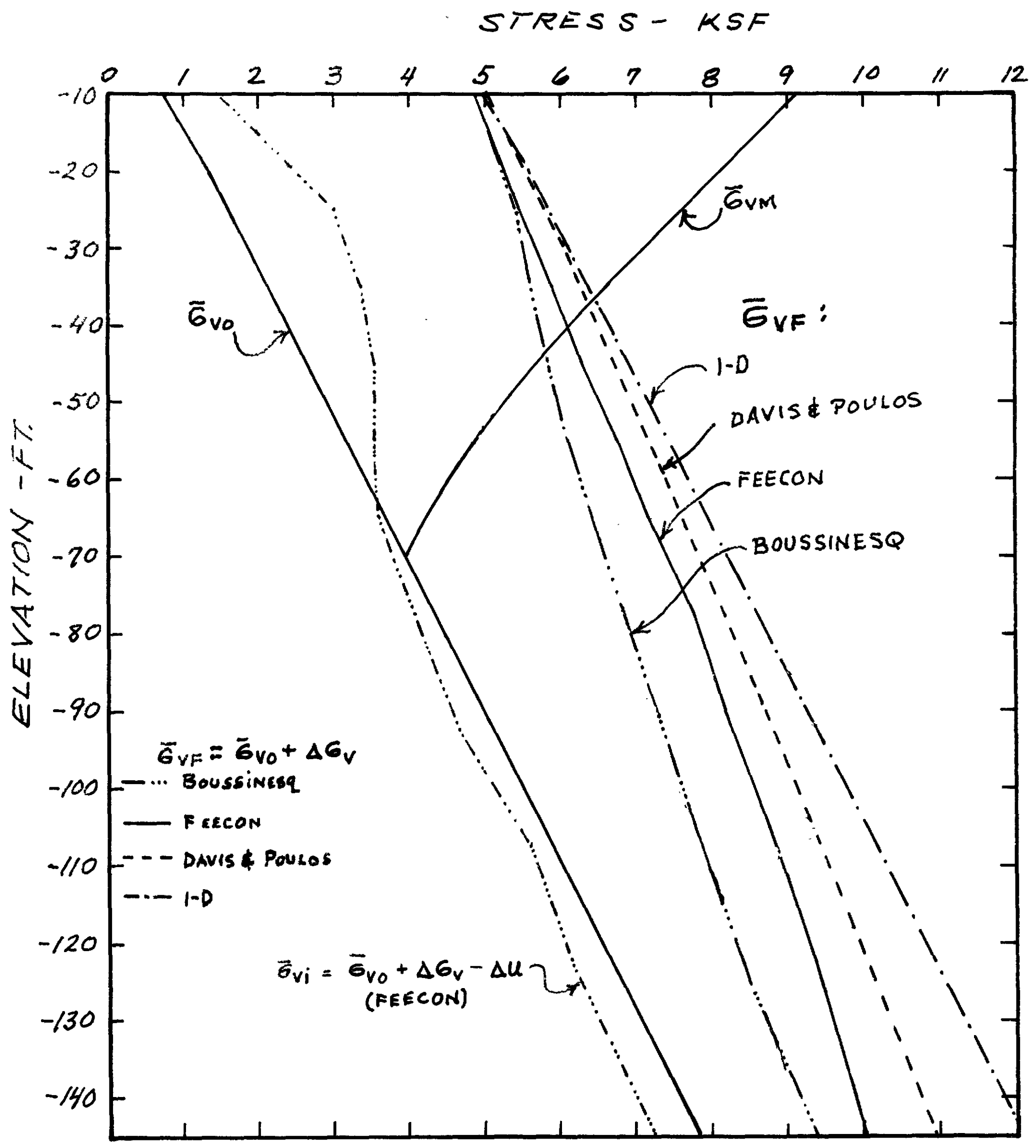

FIGURE 6-6 DRAINED VERTICAL STRESSES IN CLAY
STA. 246, ℄

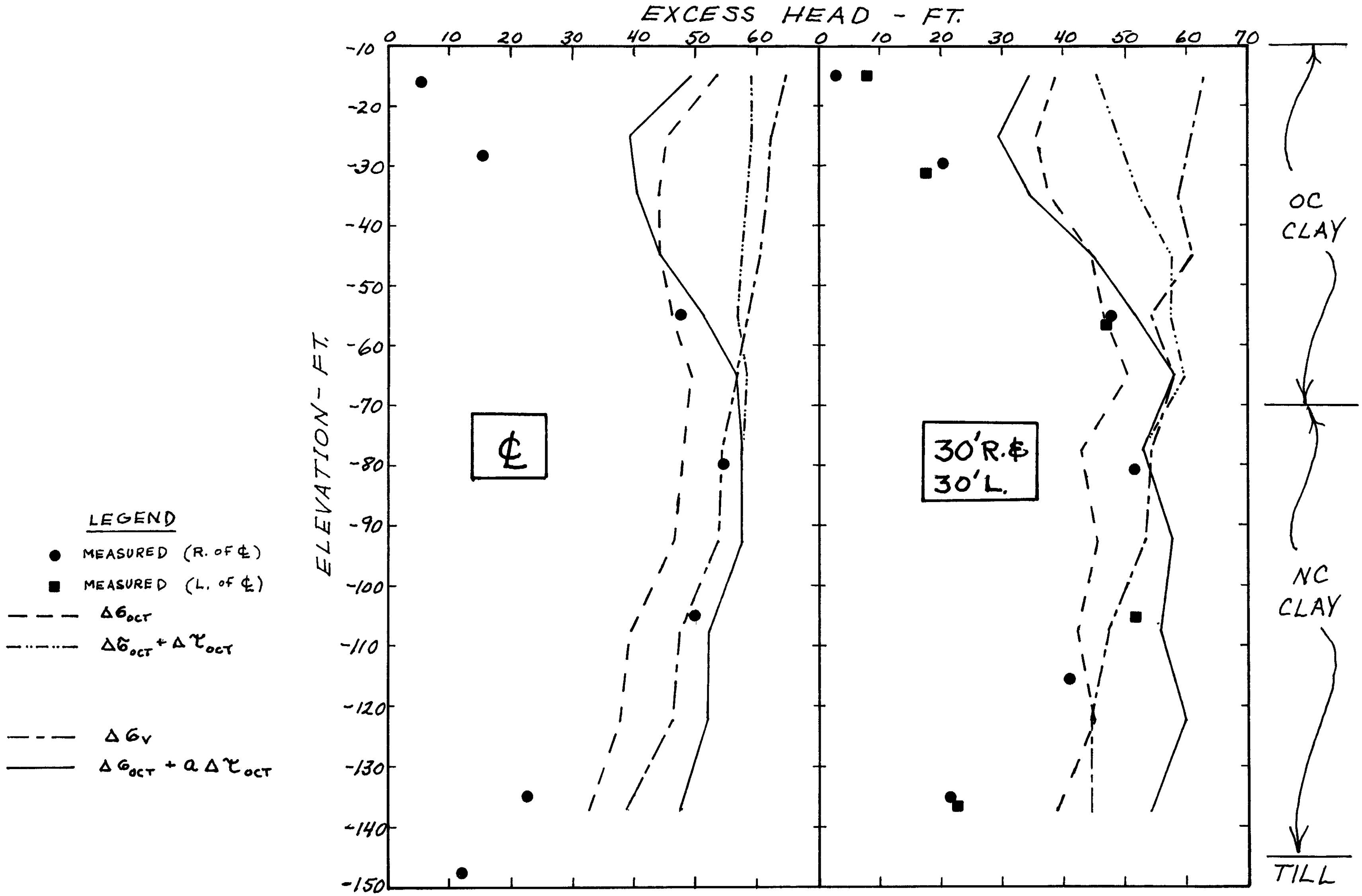

FIGURE 6-7 INITIAL EXCESS PORE PRESSURES UNDER EMBANKMENT TOP, ℄ & 30'R.

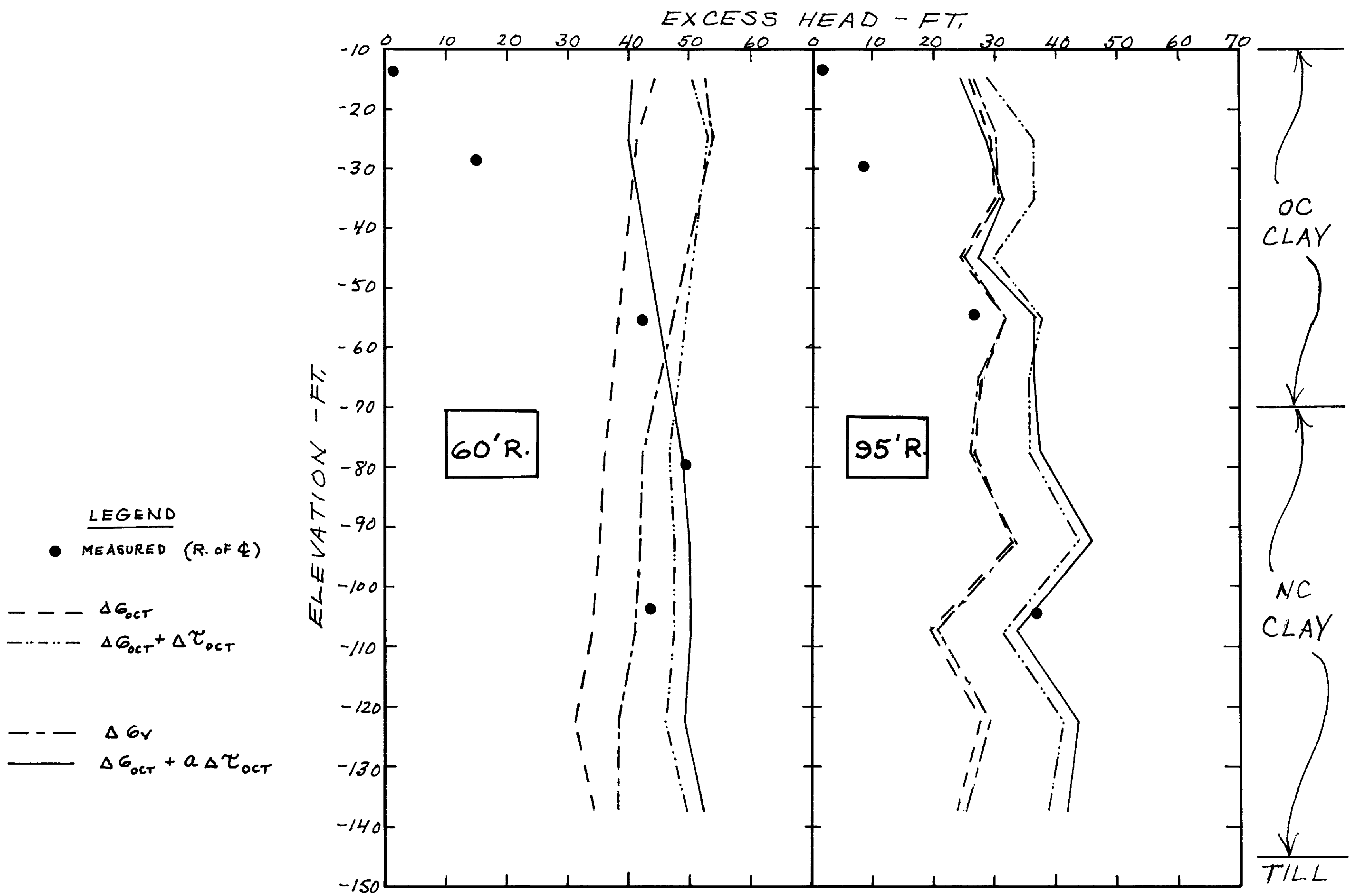

FIGURE 6-8 INITIAL EXCESS PORE PRESSURES UNDER EMBANKMENT SLOPE, 60'R. & 95'R.

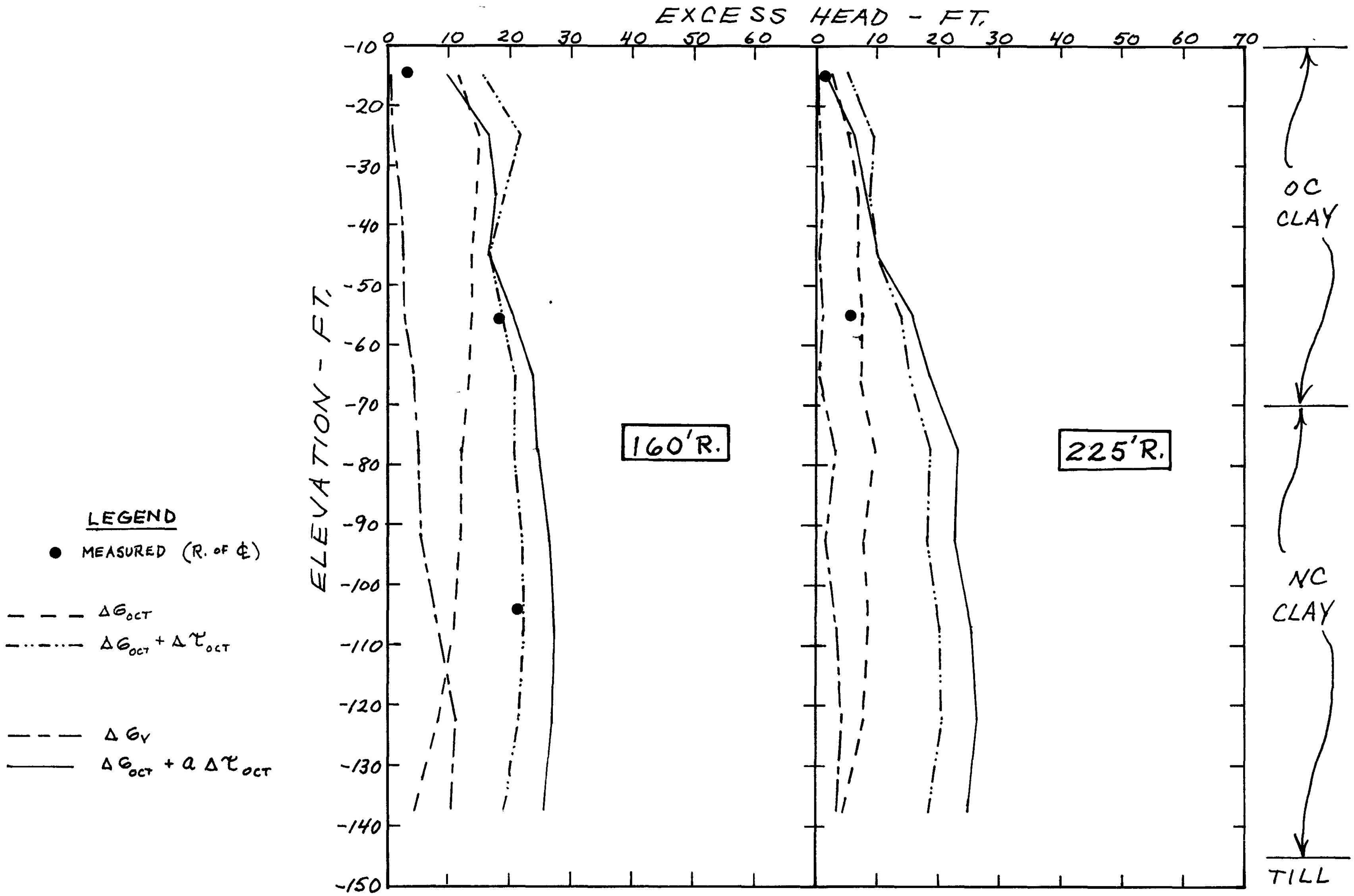

FIGURE 6-9 INITIAL EXCESS PORE PRESSURES OUTSIDE EMBANKMENT TOE 160'R. & 225'R.

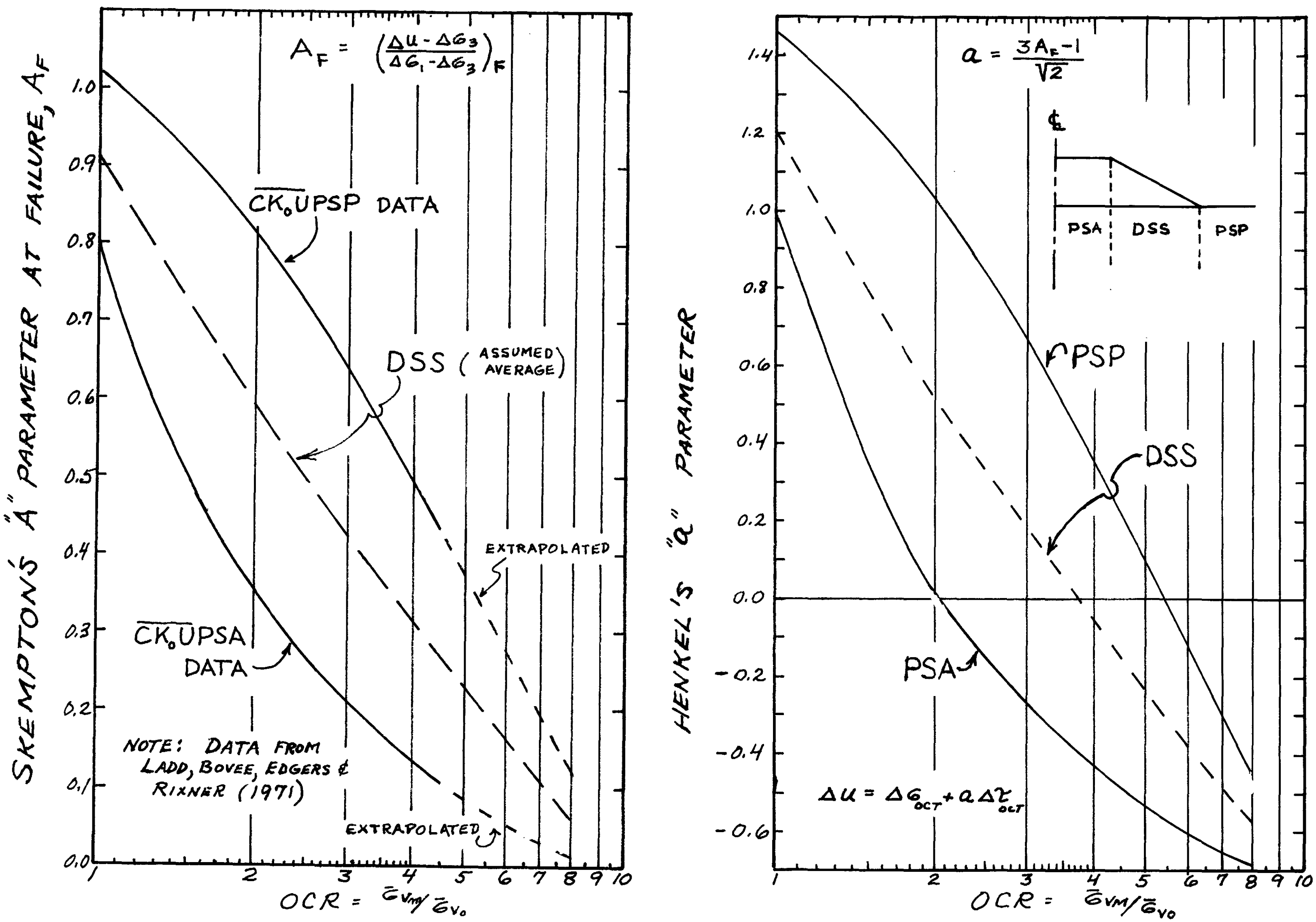

FIGURE 6-10 SKEMPTON'S AND HENKEL'S PARAMETERS

7. ANALYSIS OF CONSOLIDATION BEHAVIOR

7.1 PORE PRESSURE

Figure 7-1 shows the vertical distribution of excess pore pressure beneath the embankment centerline at different items. The predicted initial excess pore pressures and the artesian pore pressure are also shown. Table 7-1 tabulates the pore pressure dissipation with time. It is apparent there was significant dissipation by the end of loading (CD 620), even at the center of the clay.

In order to determine how the rate of consolidation varied within the clay, the dissipation of pore pressure was computed at varying times. This was done both for the entire thickness and for several layers within the clay. The excess pore pressure was assumed to be linearly distributed between the piezometers. Additionally, the artesian head was assumed to be linearly distributed through the full thickness of clay. The average degree of consolidation, $\bar{U}$, was computed from the total areas to the left of the appropriate curves:

$$\bar{U} = 1 - \frac{A_m - Aa}{Ai - Aa}$$

where Am is the area left of the measured pore pressure curve at some time (computed by summing the trapezoids), Ai is the area left of the initial curve (a constant, Ai = 6810 ft.- ft. water), and Aa is the area left of the artesian curve (also a constant, Aa = 338 ft. - ft. water). This method is depicted and the computations tabulated in Table 7-2.

In addition, in a similar manner, the degree of consolidation was computed for several layers within the clay. These layers were chosen to coincide with layers for which valid differential settlement data exist:

Layer A	El. -10 to -21.5
B	-21.5 to -43.0
C	-43.0 to -93.1
D & E	-93.1 to -145
D	-93.1 to 120.7
E	-120.7 to -145

Layer D & E was subdivided into D and E in order to take into account rapid consolidation just above the till drainage surface.

Figure 7-2 indicates the average and incremental pore pressure dissipation with respect to time in days (log scale) after an instantaneous loading. The time of instantaneous loading, t_o, was taken as CD 357. This is the average of the times at the beginning and end of construction, since there was no dissipation at the centerline between Stage 1 and piezometer installation (Chapter 4). The equivalent loading ramp is shown in Figure 3-1.

The incremental degree of consolidation was computed identically to $\overline{U}$, except that only the areas within the layer boundaries were considered.

From Figure 7-2, the average degree of consolidation at the end of loading was already 40%, and it reached 60% about 4.7 years after the middle of the loading period (22 August, 1968). The two uppermost layers (A and B), where the OCR is greater than 2.5, consolidated most rapidly. Pore pressure in the bottom layer (E) above the till also dissipated fairly quickly. Layers C and D in the interior of the clay, however, are consolidating much more slowly and at about the same rate. Incremental consolidation data are tabulated in Table 7.3.

7.2 CONSOLIDATION SETTLEMENT

7.2.1 General

In order to determine the degree of consolidation from settlement data, it is necessary to either know the final consolidation settlement, ρ_{cf}, from field data or have an accurate prediction of it. Fortunately there are valid settlement data for the top 33 feet of clay, which has essentially reached ρ_{cf}. These data allow the computation of a field recompression ratio (RR). There are also valid data which permit the computation of a field virgin compression ratio (CR), but it is not as good due to the great thickness of clay involved (52 feet, from El. -93 to -145).

There are essentially two methods of predicting ρ_{cf}

beneath an embankment. Both approximate the field consolidation curve by two straight lines. RR is the slope of the recompression curve from some initial stress ($\bar{\sigma}_{vo}$ or $\bar{\sigma}_{vi}$) to the maximum stress ($\bar{\sigma}_{vm}$), and CR is the slope of the virgin compression curve from $\bar{\sigma}_{vm}$ to the final stress ($\bar{\sigma}_{vf}$).

The first method, called a one-dimensional (1-D) prediction, assumes that the change in vertical effective stress ($\Delta\bar{\sigma}_v$) equals the change in the vertical total stress ($\Delta\bar{\sigma}_v$) This method uses a two-dimensional estimate of $\bar{\sigma}_{vf}$ in conjunction with the one-dimensional parameters CR and RR. The formula is:

$$\rho_{cf} = \Sigma H[\ RR \log \frac{\bar{\sigma}_{vm}}{\bar{\sigma}_{vo}} + CR \log \frac{\bar{\sigma}_{vf}}{\bar{\sigma}_{vm}}\ ]$$

where $\bar{\sigma}_{vo}$ is the in-situ vertical effective stress.

The second method, called a modified Skempton-Bjerrum (MSB) prediction, is based on the Skempton-Bjerrum (1957) concept as modified by Ladd (1971). This method also utilizes a two-dimensional $\bar{\sigma}_{vf}$ with CR and RR. However, it accounts for non-one-dimensional conditions by assuming that $\Delta\bar{\sigma}_v$ equals the change in pore pressure (Δu). The initial vertical effective stress ($\bar{\sigma}_{vi}$) is estimated by:

$$\bar{\sigma}_{vi} = \bar{\sigma}_{vo} + \Delta\sigma_v - \Delta u$$

and 1-D compression from $\bar{\sigma}_{vi}$ to $\bar{\sigma}_{vf}$ (instead of from $\bar{\sigma}_{vo}$ to $\bar{\sigma}_{vf}$) is assumed. The formula is identical to the 1-D method except that $\bar{\sigma}_{vo}$ is replaced by $\bar{\sigma}_{vi}$:

$$\rho_{cf} = \Sigma H \left[RR \log \frac{\bar{\sigma}_{vm}}{\bar{\sigma}_{vi}} + CR \log \frac{\bar{\sigma}_{vf}}{\bar{\sigma}_{vm}} \right]$$

All measured consolidation settlements were derived by subtracting the corrected FEECON initial settlements from total measured settlements. Initial stresses ($\bar{\sigma}_{vi}$) are those predicted from FEECON analyses for final stresses and pore pressures:

$$\bar{\sigma}_{vi} = \bar{\sigma}_{vo} + \Delta\sigma_v - \Delta u = \bar{\sigma}_{vf} - \Delta u$$

7.2.2 Laboratory Compression Parameters and Predicted ρ_{cf}

Initial predictions of ρ_{cf} were performed by both 1-D and MSB methods using corrected laboratory CR values. The average laboratory value of 0.024 was used for RR throughout the clay. To compensate for sample disturbance, the laboratory CR values were increased by 15% (Ladd, 1971). The resulting values for CR were: El. -10 to -40, CR = 0.173; El. -40 to -70 , CR = 0.219; El. -70 to -145, CR = 0.242. The computations and results of both analyses are shown in Tables 7-4 and 7-5, and depicted in Figure 7-5. The 1-D method predicted a settlement of the clay of 4,26 feet, and the MSB method a value of 4.59 feet.

7.2.3 Field Compression Parameters

Firgures 7-3 and 7-4 show the valid measured differential consolidation settlements at the centerline and 90'R. The upper 33 feet of clay (Layers A and B) has reached ρ_{cf}. This is slightly at odds with the pore pressure data, which indicates that layer B is at 89% of ρ_{cf}. Final consolidation of layer A is given by SR 1-2 = 0.26 feet and layer B ρ_{cf} (SR 2-3) = 0.43 feet. Since only recompression occurs in both these layers (Figure 6-6), the field RR values can be easily computed by the ratio of measured to initial predicted ρ_{cf} within these layers. This procedure and the results are tabulated in Table 7-6.

For the 1-D case, field RR's are 0.034 (El. -10 to -21.5) and 0.039 (El. -21.5 to -43). These values are 50% greater than the laboratory value. The MSB field RR's are 0.061 (-10 to -21.5) and 0.066 (-21.5 to -43). These are greater than the 1-D values because a much smaller change in stress ($\bar{\sigma}_{vi}$ to $\bar{\sigma}_{vf}$ instead of $\bar{\sigma}_{vo}$ to $\bar{\sigma}_{vf}$) must cause the same measured ρ_{cf}. For analysis the field RR's for El. -21.5 to -43 were also assumed to be the RR's below -43.

Table 7-7 presents the calculations and results for field CR values. The analysis is restricted to the layer subjected only to virgin compression, layer D & E, El. -93.1 to -145. CR's were computed from the changes in consolidation settlement ($\Delta\rho_{cf}$) and vertical effective stress ($\Delta\bar{\sigma}_v$) for three time increments after the end of loading from the formula:

$$CR = \frac{\Delta\rho_c}{\Sigma\ H\ \Delta\log\ \bar{\sigma}_v}$$

Layer D & E was divided into three layers, and for each the term ($H\ \Delta\log\ \bar{\sigma}_v$) was evaluated. The $\bar{\sigma}_v$ was computed by subtracting excess pore pressures at each time from $\bar{\sigma}_{vf}$. The ($H\ \Delta\log\bar{\sigma}_v$) terms were then summed for layer D & E, and with $\Delta\rho_c$ (SR5) over a time increment, CR for that increment was computed.

The field CR for layer D & E is increasing with time because the increase in $\bar{\sigma}_v$ is due to pore pressure dissipation, which is occurring more and more slowly (Figures 4-8 and 7-2). However, the average of field CR values for the three time increments was chosen between El. -93.1 and -145 (CR = 0.391). This is 86% greater than the laboratory value of 0.21. It was assumed that field CR values vary with depth in the same way as laboratory values. This results in the following field CR values (which were used in further analyses): El. -10 to -40, CR = 0.279; El. -40 to -70, CR = 0.354; El. -70 to -145, CR = 0.391.

7.2.4 Predicted Final Consolidation Settlement

Figure 7-5 indicates the predicted ρ_{cf} at the embankment centerline. Both 1-D and MSB predictions were performed with the appropriate field RR and CR values. Comparison of the new predicted ρ_{cf} with the measured values in layers A and B indicated better agreement with the 1-D method. Therefore, a composite prediction of 1-D above El. -70 and MSB below El. -70 was chosen as the best estimate and used in consolidation analysis. With the field RR and CR values, the ρ_{cf} predicted at the top of the clay are: 1-D, 7.66 feet; MSB, 7.82 feet; composite, 7.82 feet. These predictions are tabulated in Table 7-8 to 7-10.

It is apparent that the ρ_{cf} values predicted with field RR's and CR's are much greater than the predictions based on laboratory RR's and CR's. This is chiefly due to the very large field CR computed for layer D & E. The increase of 86% over laboratory values seems very large to be entirely explained by disturbance (Ladd, 1971). It may be that increased compressibility due to artesian leaching of the marine clay is a factor, especially in this bottom layer.

7.2.4 Consolidation

Based on the composite prediction of ρ_{cf}, the average and incremental degrees of consolidation for the clay were computed. These values are tabulated in Tables 7-2 and 7-11, and plotted in Figure 7-6 versus time in days since an instantaneous loading. A different t_o was chosen for settlement than for pore pressure. This was necessary since settlement due only to Stages 2 and 3 was measured. The t_o was chosen as CD390. The average consolidation of the entire clay stratum was given by SR1 at the top of the clay. Incremental consolidation of the layers within the clay was computed from differential settlements of the layers.

There were sufficient valid data to compute consolidation of layers D and E up to CD 958. Based on the ratios of consolidation in layers D and E to that in the whole layer D & E for these early times, consolidation values were extrapolated for these two seperate layers.

Figure 7-6 indicates the same general relative rates of consolidation for the average and different layers as the pore pressure data. The two uppermost layers (A and B) and the lowest (E) consolidate more quickly than the other layers or the average of the whole thickness. In the two upper layers, A and B, settlement apparently proceeds more quickly than the rate of pore pressure dissipation. On the other hand, at any given time, all other layers and the average indicate significantly less settlement than pore pressure dissipation. However, the amount of change in consolidation for these other layers is about the same for settlement and pore pressure:

	$\bar{U}$%	CD2053	$\Delta\bar{U}$%	CD 620-2053
Layer	u	ρ	u	ρ
Average	60.0	28.4	19.1	15.6
C	43.9	21.7	21.9	17.0
D + E	58.3	20.4	17.9	14.3

7.3 FIELD COEFFICIENTS OF CONSOLIDATION

7.3.1 General

Coefficients of consolidation, c_v, were backfigured from both the pore pressure and settlement data. In order to account for the markedly different laboratory values of c_v for the OC (c_{v1}) and NC (c_{v2}) clay, the two layer system was transformed to a single equivalent layer with $c_v = c_{v2}$. This method was first proposed by Gray and later expanded by Leonards (1962)

For an upper layer H_1 and c_{v1} and a lower layer H_2 and c_{v2}, the single equivalent layer is:

$$He = H_2 + H_1 \sqrt{\frac{c_{v2}}{c_{v1}}}$$

and has one $c_v = c_{v2}$. For all analyses the ratio of c_{v2}/c_{v1} was taken equal to the ratio of the average lab c_{v2} and c_{v1} values at $\bar{\sigma}_{vo}$ and $\bar{\sigma}_{vf}$ (i.e. $c_{v2}/c_{v1} = 1/3$) as discussed in Chapter 2. Analyses were performed for both the full clay thickness and a reduced thickness in an attempt to remove the affect of the very rapid consolidation of Layer A. In addition, for both thicknesses, varying elevations were used for the break between c_{v1} and c_{v2} in the transformation to a single equivalent layer

7.3.2 Full Clay Thickness

For analyses on the full thickness, the break between

c_{v1} and c_{v2} was located at El. -70, -43 and -21.5. This resulted in three different single equivalent layer thicknesses: 110, 121, and 130 ft., respectively. Field values of c_{v2} were then computed from the relation:

$$c_{v2} = \frac{TvHd^2}{t}$$

The Davis and Poulos (1972) graph for two-dimensional consolidation, with permeable top and base, was used to determine Tv. This value must be multiplied by 4, since their Tv is related to full height rather than drainage height. This graph and one for an impermeable base are reproduced in Figures 7-7 and 7-8. These graphs account for lateral drainage to some degree, since they assume isotropic permeability. A value of H/b = 2 was used, and $\overline{U}$ was taken from the pore pressures over the full depth, and the consolidation settlement of SR-1.

For all analyses, both the total time (t) and incremental time (Δt) methods were used. In the Δt method, ΔTv and Δt are substituted in the basic equation. Table 7-12 summarizes the computed field c_{v2}'s, and Table 7-13 and 7-14 present the actual computations.

Table 7-12 indicates theat there is better agreement between t and Δt values for the settlement data than for the pore pressure data. For both t and Δt methods there is relatively poor agreement between pore pressure and settlement

c_{v2}'s, with pore pressure values being significantly greater. For the t method, pore pressure values exceed settlement values by a factor of 5.5. The Δt method gives much better agreement, with pore pressure c_v's greater by a factor of 2.5. The settlement data gives good agreement with laboratory c_{v2} of 0.093 ft^2/day, and for the Δt method with the c_v change at -43 , matches it exactly.

7.3.3 Reduced Clay Thickness

In an attempt to minimize the effect of the extremely rapid consolidation of layer A (110 to -21.5), analyses were performed only on the clay below El. -21.5. It was necessary to compute $\overline{U}$ values considering only the consolidation in the clay below El. -21.5. With the change in c_v at El. -70 and -43, the single equivalent layers were 103.5 and 114.5 feet respectively.

Field c_{v2} values were then computed in the same way as for the full thickness analyses. However, new values of $\overline{U}$ were computed, based on the pore pressures only below El. -21.5, and on the ρ_c of SR-2 (El. -21.5). Table 7-15 summarizes the resultant values, and the computations are presented in Tables 7-16 and 7-17.

In this instance, the settlement data give excellent agreement between the t and Δt methods and with the laboratory c_{v2} values. The pore pressure data do not give as good agreement between the t and Δt methods, although it is much better than for the full thickness analyses. Pore pressure c_v values are much higher than settlement values. For the t method, they are higher by a factor of 5.1, and for the Δt method higher by a factor of 3.1.

7.3.4 Predicted Consolidation Settlements

Several field c_{v2} values were used to predict consolidation settlment versus time. The value which gave the prediction closest to measured ρ_c at the end of loading was c_{v2} = 0.236 ft^2/day. This value was derived from pore pressure data with a full thickness analysis using Δt and the c_v change at El. -43. The predicted and measured ρ_c for four times are shown in Figure 7-9.

The laboratory and settlement values were too low,but the chosen value gives an excellent prediction at the end of loading (CD 620). For the laboratory measured (Guertin, 1967) ratio of horizontal to vertical permeability (k_H/k_V) of 1.67, the initial effects of lateral drainage are slight (Ladd and Wissa, 1970). These effects are somewhat accounted for by the use of the Davis and Poulos charts ($k_H/k_V = 1$). However, with increasing time the discrepancy in the k_H/k_V ratio becomes more important, and the predicted ρ_c lags slightly behind measured values.

Consolidation settlements are predicted by entering the appropriate $\overline{U}$ - Tv graph with Tv from the relation,

$$Tv = \frac{c_v t}{Hd^2} .$$

The $\overline{U}$ thus derived is applied to the predicted ρ_{cf} to determine the settlement at time t.

Rather than determining a single $\overline{U}$ for the full layer by using c_{v2} and the transformed drainage height (Lacasse and Ladd, 1973), a different approach was used. Based on the lab ratio $c_{v1}/c_{v2} = 3$, field c_{v1} values were computed from the field c_{v2} values. T_{v1} and T_{v2} values were computed as discussed above, and Davis and Poulos' chart for an impermeable base was used to determine $\overline{U}_1$ and $\overline{U}_2$ values. These were applied to the predicted differential ρ_{cf} in the c_{v1} and c_{v2} zones and the resultant values summed vertically. This method more closely relates to the layered consolidation behavior.

As a result of the above considerations, it appears that the best prediction is given by $c_{v1} = 0.71$ ft^2/day above El. -43, where OCR > 2.5, and $c_{v2} = 0.24$ ft^2/day below El. -43. These values are more than 2.5 times as great as the laboratory values ($c_{v1} = 0.27$, $c_{v2} = 0.09$).

INSTRU.	ELEV.	TIME (CONSTRUCTION DAY) AND EXCESS HEAD (FT.)										
		CD 620	CD 792	CD 958	CD 1104	CD 1268	CD 1412	CD 1568	CD 1727	CD 1877	CD 2053	
P5	-15.9	2.0	0.7	0	0	0	0	0	0	0	0	
P6	-28.6	10.0	5.7	3.4	2.2	1.7	1.4	1.4	1.3	1.3	1.3	
P7	-55.0	39.2	35.5	32.2	30.5	28.8	27.5	26.5	25.7	25.0	24.4	
P8	-80.2	50.0	47.8	46.0	45.0	44.0	43.4	42.8	41.9	41.7	41.2	
P9	-105.2	45.0	42.6	41.0	40.0	39.1	38.4	37.9	37.5	37.0	36.5	
P10	-135.0	21.0	18.0	15.7	14.4	13.0	12.2	11.6	11.1	10.9	10.5	
P11	-147.4	5.0	5.0	5.0	5.0	5.0	5.0	5.0	5.0	5.0	5.0	

NOTE: NOT CORRECTED FOR ARTESIAN PRESSURE

TABLE 7-1 PORE PRESSURE DISSIPATION AT ℄, STA. 246

CONSTR. DAY	SETTLEMENT (SR-1) ρ_{CF}(SR1) = 7.804 FT. t_o = CD390					PORE PRESSURE t_o = CD357		
	TIME DAYS	$\rho_{MEAS.}$ FT.	$\rho_{INITIAL}$ (FEECON) FT.	ρ_{CONSOL} FT.	$\overline{U}_\rho$ %	TIME DAYS	$A_{MEAS.}$ FT.-FT.(H_2O)	$\overline{U}_u$ %
620	230	1.202	0.202	1.000	12.8	263	4162.26	40.9
792	402	1.519		1.317	16.9	435	3786.13	46.7
958	568	1.697		1.495	19.2	601	3512.66	50.9
1104	714	1.817		1.615	20.7	747	3366.97	53.2
1268	878	1.953		1.751	22.4	911	3235.72	55.2
1412	1022	2.046		1.844	23.6	1055	3146.15	56.6
1568	1178	2.148		1.946	24.9	1211	3079.65	57.6
1727	1337	2.239		2.037	26.1	1370	3013.56	58.7
1877	1487	2.324		2.122	27.2	1520	2972.80	59.3
2053	1663	2.421		2.219	28.4	1696	2926.89	60.0

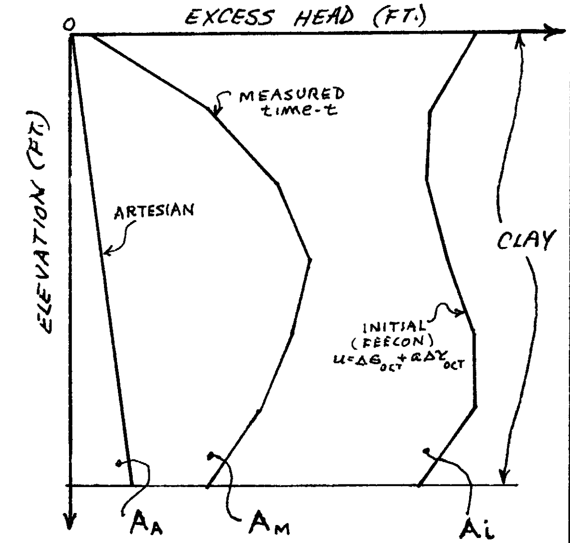

$$\overline{U}_u = 1 - \frac{A_M - A_A}{A_i - A_A}$$

$A_i = 6810$ FT. - FT.(H_2O)

$A_A = 338$ FT. - FT.(H_2O)

$$\overline{U}_u = 1 - \frac{A_M - A_A}{6472.}$$

TABLE 7-2 AVERAGE DEGREE OF CONSOLIDATION ON ℄

$U = 1 - \frac{A_M - A_A}{A_i - A_A}$

t_o = CD 357

		LAYER AND DEGREE OF CONSOLIDATION											
		A (-10.0 / -21.5)		B (-21.5 / -43.0)		C (-43.0 / -93.1)		D (-93.1 / -120.7)		E (-120.7 / -145.0)		D+E (-93.1 / -145.0)	
		A_{INIT} = 544.18, $A_{ART.}$ = 2.45		A_{INIT} = 881.54, A_{ART} = 17.74		A_{INIT} = 2712.70, A_{ART} = 107.72		A_{INIT} = 1485.56, A_{ART} = 94.61		A_{INIT} = 1186.44, A_{ART} = 115.07		A_{INIT} = 2672.00, A_{ART} = 209.68	
CONSTR DAY	ELAPSED TIME DAYS	A_M FT-FT	U %	A_M FT-FT	U %	A_M FT-FT	U %	A_M FT-FT	U %	A_M FT-FT	U %	A_M FT-FT	U %
620	263	32.88	94.4	313.83	65.7	2138.32	22.0	1087.92	28.6	589.82	55.7	1677.28	40.4
792	435	14.21	97.8	229.61	75.5	1989.10	27.8	1025.59	33.1	527.51	61.5	1553.15	45.4
958	601	4.20	99.7	179.47	81.3	1865.60	32.5	982.36	36.2	481.15	65.8	1463.41	49.1
1104	747	2.72	100	154.10	84.2	1799.76	35.0	956.04	38.1	454.40	68.3	1410.44	51.2
1268	911	2.10	"	139.59	85.9	1736.10	37.5	931.42	39.8	426.48	70.9	1357.89	53.4
1412	1055	1.74	"	129.86	87.0	1691.32	39.2	913.62	41.1	409.62	72.5	1323.30	54.8
1568	1211	1.74	"	125.90	87.5	1654.50	40.6	903.91	41.8	397.16	73.7	1297.51	55.8
1727	1370	1.60	"	121.62	88.0	1615.90	42.1	888.46	42.9	386.85	74.6	1275.26	56.7
1877	1520	1.60	"	118.45	88.3	1594.14	42.9	877.47	43.7	381.12	75.2	1258.58	57.4
2053	1696	1.60	"	116.08	88.6	1568.30	43.9	865.04	44.6	371.98	76.0	1237.07	58.3

TABLE 7-3 INCREMENTAL CONSOLIDATION (PORE PRESSURE)

LAYERS (ELS) FT.	LAYER ₵ EL FT.	$\bar{\sigma}_{vo}$ PSF	$\bar{\sigma}_{vm}$ PSF	(FEECON) $\bar{\sigma}_{vF}$ PSF	$\log \frac{\bar{\sigma}_{vm}}{\bar{\sigma}_{vo}}$	$\log \frac{\bar{\sigma}_{vF}}{\bar{\sigma}_{vm}}$	H FT.	$\Delta \rho_{cF}$ FT.	ρ_{cF} FT.
-10									4.764
	-15	1015	8610	5050	.6968		10	.1672	
-20									4.596
	-25	1570	7600	5460	.5413		10	.1299	
-30									4.466
	-35	2090	6610	5900	.4507		10	.1082	
-40									4.358
	-45	2610	5700	6300	.3392	.0435	10	.1767	
-50									4.182
	-55	3130	4850	6750	.1902	.1436	10	.3601	
-60									3.821
	-65	3650	4200	7150	.0610	.2311	10	.5207	
-70									3.301
	-77.5	4300	4300	7650		.2502	15	.9082	
-85									2.393
	-92.5	5080		8250		.2106	15	.7645	
-100									1.628
	-107.5	5860		8840		.1786	15	.6483	
-115									0.980
	-122.5	6640		9360		.1491	15	.5412	
-130									0.439
	-137.5	7420		9800		.1208	15	.4385	
-145									

SENSOR LOCATION (EL-FT.)	ρ_{cF} FT.	$\Delta \rho_{cF}$ FT.
SR1-10.5	4.756	0.179
SR2-21.5	4.577	0.272
SR3-43.0	4.305	
SR4-67.6		
SR5-93.1		
SR6-120.7		

NOTES: CORRECTED LAB RR & CR: RR = .024 CR = .173 (-10/-40), .219 (-40/-70), .242 (-70/-145)

$$\rho_{cF} = \Sigma H \left(RR \log \frac{\bar{\sigma}_{vm}}{\bar{\sigma}_{vo}} + CR \log \frac{\bar{\sigma}_{vF}}{\bar{\sigma}_{vm}} \right)$$

TABLE 7-4 FINAL CONSOLIDATION SETTLEMENT (1-D) WITH CORRECTED LAB RR & CR. ₵

LAYERS ELS-FT.	LAYER ℄ EL FT.	$\bar{\sigma}_{vo}$ PSF	$\bar{\sigma}_{vi}$ PSF	$\bar{\sigma}_{vm}$ PSF	$\bar{\sigma}_{vf}$ PSF	$\log \frac{\bar{\sigma}_{vm}}{\bar{\sigma}_{vi}}$	$\log \frac{\bar{\sigma}_{vf}}{\bar{\sigma}_{vm}}$	H FT.	$\Delta\rho_{cf}$ FT.	ρ_{cf} FT.	SENSOR LOCATION	ρ_{cf} FT	$\Delta\rho_{cf}$ FT.
-10										4.589	SR1 -10.5	4.584	
	-15	1015	1986	8610	5050	.4053		10	.0973				0.101
-20										4.492	SR2 -21.5	4.483	
	-25	1570	3001	7600	5460	.2599		10	.0624				
-30										4.429			0.156
	-35	2090	3360	6610	5900	.2445		10	.0587				
-40										4.370	SR3-43.0	4.327	
	-45	2610	3536	5700	6300	.2074	.0435	10	.1450				
-50										4.225			
	-55	3130	3536	4850	6750	.1372	.1436	10	.3474				
-60										3.878			
	-65	3650	3599	4200	7150	.0671	.2311	10	.5222		SR4 -67.5		
-70										3.356			
	-77.5	4300	4062	4300	7650	.0247	.2502	15	.9171				
-85										2.439			
	-92.5	5080	4650		8250	.0384	.2106	15	.7783		SR5-93.1		
-100										1.660			
	-107.5	5860	5589		8840	.0206	.1786	15	.6557				
-115										1.005			
	-122.5	6640	6121		9360	.0353	.1491	15	.5539		SR6 -120.7		
-130										0.451			
	-137.5	7420	6855		9800	.0344	.1208	15	.4509				
-145													

NOTES: CORRECTED LAB RR & CR: RR = .024 (-10/-145), CR = .173 (-10/-40), .219 (-40/-70), .242 (-70/-145)

$$\rho_{CF} = \sum H \left(RR \log \frac{\bar{\sigma}_{vm}}{\bar{\sigma}_{vi}} + CR \log \frac{\bar{\sigma}_{vf}}{\bar{\sigma}_{vm}} \right)$$

(when $\bar{\sigma}_{vi} < \bar{\sigma}_{vo}$, used RR from $\bar{\sigma}_{vi}$ to $\bar{\sigma}_{vo}$, CR from $\bar{\sigma}_{vo}$ to $\bar{\sigma}_{vf}$)

TABLE 7-5 FINAL CONSOLIDATION SETTLEMENT (MODIFIED SKEMPTON-BJERRUM) WITH CORRECTED LAB RR & CR

				ONE-DIMENSIONAL			MODIFIED SKEMPTON-BJERRUM		
LAYER	SETTLEMENT DATA	MEASURED $\Delta\rho_{CF}$ FT.	CORRECTED LAB RR	PREDICTED $\Delta\rho_{CF}$ FT.	$\Delta\rho_{CF}$ RATIO $\frac{MEASURED}{PREDICTED}$	FIELD RR $\left(\frac{MEAS}{PRED} \times Lab\right)$	PREDICTED $\Delta\rho_{CF}$ FT.	$\Delta\rho_{CF}$ RATIO $\frac{MEASURED}{PREDICTED}$	FIELD RR $\left(\frac{MEAS}{PRED} \times Lab\right)$
A (-10.5 to -21.5)	SR1-2	0.256	0.024	0.179	1.430	0.034	0.101	2.535	0.061
B (-21.5 to -43.0)	SR2-3	0.428	0.024	0.272	1.574	0.039	0.156	2.744	0.066

TABLE 7-6 FIELD RR VALUES

SR-5 LAYER D+E (−93.1 to −145) $CR = \frac{\Delta \rho_c}{\Sigma H \Delta \log \bar{\sigma}_v}$ $\bar{\sigma}_v = \bar{\sigma}_{vF} - u_e$

Elev.	H Ft.	CD620 $\rho_c = 0.202$ AVG $\bar{\sigma}_v$ psf	CD 1104 $\rho_c = 0.414$ $\Delta\rho_c = 0.212$ AVG $\bar{\sigma}_v$ psf	CD 1104 $H \Delta \log \bar{\sigma}_v$	CD 1568 $\rho_c = 0.544$ $\Delta\rho_c = 0.130$ AVG $\bar{\sigma}_v$ psf	CD 1568 $H \Delta \log \bar{\sigma}_v$	CD 2053 $\rho_c = 0.674$ $\Delta\rho_c = 0.130$ AVG $\bar{\sigma}_v$ psf	CD 2053 $H \Delta \log \bar{\sigma}_v$
−93.1 to −122.5	29.4	6521	6855	0.638	6997	0.262	7082	0.155
−122.5 to −137.5	15.0	8357	8695	0.259	8839	0.107	8904	0.047
−137.5 to −145	7.5	9527	9681	0.052	9746	0.022	9772	0.009
			$\Sigma = 0.949$	$CR = \frac{0.212}{0.949} = 0.223$	$\Sigma = 0.391$	$CR = \frac{0.130}{0.391} = 0.333$	$\Sigma = 0.211$	$CR = \frac{0.130}{0.211} = 0.616$

EL. −70 to −145, AVG. FIELD CR = 0.391
AVG. LAB CR = 0.210
RATIO, $\frac{\text{FIELD CR}}{\text{LAB CR}} = 1.862$

ELEVATION	LAB CR	FIELD CR (= 1.862 × LAB CR)
−10 to −40	0.150	0.279
−40 to −70	0.190	0.354
−70 to −145	0.210	0.391

TABLE 7-7 FIELD CR VALUES

LAYERS ELS-FT.	LAYER ℄ EL FT.	$\bar{\sigma}_{vo}$ PSF	$\bar{\sigma}_{vM}$ PSF	$\bar{\sigma}_{vF}$ PSF	$\log \frac{\bar{\sigma}_{vm}}{\bar{\sigma}_{vo}}$	$\log \frac{\bar{\sigma}_{vF}}{\bar{\sigma}_{vM}}$	H FT.	$\Delta\rho_{cF}$ FT.	ρ_{cF} FT.	SENSOR LOCATION	ρ_{cF} FT.	$\Delta\rho_{cF}$ FT.
-10									7.664	SR1 -10.5	7.652	
	-15	1015	8610	5050	.6968		10	.2369				
-20									7.427			0.255
	-20.75	1334	8029	5286	.5980		1.5	.0305				
-21.5									7.397	SR2 -21.5	7.397	
	-25.75	1609	7526	5493	.5333		8.5	.1768				
-30									7.220			0.439
	-35	2090	6610	5900	.4507		10	.1758				
-40									7.044			
	-45	2610	5700	6300	.3392	.0435	10	.2863		SR3 -43.0	6.958	
-50									6.758			
	-55	3130	4850	6750	.1902	.1436	10	.5825				
-60									6.175			
	-65	3650	4200	7150	.0610	.2311	10	.8419		SR4 -67.6	5.535	
-70									5.333			
	-77.5	4300	4300	7650		.2502	15	1.4674				
-85									3.866			
	-92.5	5080		8250		.2106	15	1.2352		SR5 -93.1	3.199	
-100									2.631			
	-107.5	5860		8840		.1786	15	1.0475				
-115									1.583			
	-122.5	6640		9360		.1491	15	.8745		SR6 -120.7	1.251	
-130									0.709			
	-137.5	7420		9800		.1208	15	.7085				
-145												

NOTES: FIELD RR & CR: RR = .034 (-10/-21.5), .039 (-21.5/-145)
CR = .279 (-10/-40), .354 (-40/-70), .391 (-70/-145)

$$\rho_{cF} = \Sigma H \left(RR \log \frac{\bar{\sigma}_{vm}}{\bar{\sigma}_{vo}} + CR \log \frac{\bar{\sigma}_{vF}}{\bar{\sigma}_{vm}} \right)$$

TABLE 7-8 FINAL CONSOLIDATION SETTLEMENT (1-D) WITH FIELD RR & CR

LAYERS ELS.-FT.	LAYER ℄ EL. FT.	$\bar{\sigma}_{vo}$ PSF	$\bar{\sigma}_{vi}$ PSF	$\bar{\sigma}_{vm}$ PSF	$\bar{\sigma}_{vf}$ PSF	$\log \frac{\bar{\sigma}_{vm}}{\bar{\sigma}_{vi}}$	$\log \frac{\bar{\sigma}_{vf}}{\bar{\sigma}_{vm}}$	H FT.	$\Delta \rho_{cf}$ FT.	ρ_{cf} FT.
-10										7.820
	-15	1015	1986	8610	5050	.4053		10	.2472	
-20										7.572
	-20.75	1334	2570	8029	5286	.3132		1.5	.0287	
-21.5										7.544
	-25.75	1609	3028	7526	5493	.2587		8.5	.1451	
-30										7.399
	-35	2090	3360	6610	5900	.2445		10	.1614	
-40										7.237
	-45	2610	3536	5700	6300	.2074	.0435	10	.2909	
-50										6.946
	-55	3130	3536	4850	6750	.1372	.1436	10	.5989	
-60										6.347
	-65	3650	3599	4200	7150	.0671	.2311	10	.8624	
-70										5.485
	-77.5	4300	4062	4300	7650	.0247	.2502	15	1.4919	
-85										3.993
	-92.5	5080	4650		8250	.0384	.2106	15	1.2732	
-100										2.720
	-107.5	5860	5589		8840	.0206	.1786	15	1.0679	
-115										1.652
	-122.5	6640	6121		9360	.0353	.1491	15	.9094	
-130										0.743
	-137.5	7420	6855		9800	.0344	.1208	15	.7425	
-145										

SENSOR LOCATION	ρ_{cf} FT.	$\Delta \rho_{cf}$ FT.
SR1-10.5	7.808	
		.264
SR2-21.5	7.544	
		.394
SR3-43.0	7.150	
SR4-67.5	5.701	
SR5-93.1	3.306	
SR6-120.7	1.307	

NOTES: FIELD RR & CR: RR: .061 (-10/-21.5), .066 (-21.5/-145) CR = .279 (-10/-40), .354 (-40/-70), .391 (-70/-145)

$$\rho_{cf} = \Sigma H \left(RR \log \frac{\bar{\sigma}_{vm}}{\bar{\sigma}_{vi}} + CR \log \frac{\bar{\sigma}_{vf}}{\bar{\sigma}_{vm}} \right)$$

TABLE 7-9 FINAL CONSOLIDATION SETTLEMENT (MODIFIED SKEMPTON-BJERRUM) WITH FIELD RR & CR

Layer ℄ Els. Ft.	$\bar{\sigma}_{vo}$ PSF	$\bar{\sigma}_{vi}$ PSF	$\bar{\sigma}_{vm}$ PSF	$\bar{\sigma}_{vf}$ PSF	$\Delta\rho_{cf}$ Ft.
-15	1015		8610	5050	.2369
-20.75	1334		8029	5281	.0305
-25.75	1609		7526	5493	.1768
-35	2090		6610	5900	.1758
-45	2610		5700	6300	.2863
-55	3130		4850	6750	.5825
-65	3650		4200	7150	.8419
-77.5		4062	4300	7650	1.4919
-92.5		4650	5080	8250	1.2732
-107.5		5589	5860	8840	1.0679
-122.5		6121	6640	9360	.9094
-137.5		6855	6788	9800	.7425

1-D (layers -15 to -65)

RR = .034 (-10/-21.5)
.039 (-21.5/-145)

CR = .279 (-10/-40)
.354 (-40/-70)
.391 (-70/-145)

$\rho_{cf} = \Sigma H\left(RR \log \frac{\bar{\sigma}_{vm}}{\bar{\sigma}_{vo}} + CR \log \frac{\bar{\sigma}_{vf}}{\bar{\sigma}_{vm}}\right)$

MODIFIED SKEMPTON-BJERRUM (layers -77.5 to -137.5)

RR = .061 (-10/-21.5)
.066 (-21.5/-145)

CR = .279 (-10/-40)
.354 (-40/-70)
.391 (-70/-145)

$\rho_{cf} = \Sigma H\left(RR \log \frac{\bar{\sigma}_{vm}}{\bar{\sigma}_{vi}} + CR \log \frac{\bar{\sigma}_{vf}}{\bar{\sigma}_{vm}}\right)$

Layers Els.-Ft.	ρ_{cf} Ft.
-10	7.816
-20	7.579
-21.5	7.548
-30	7.371
-40	7.196
-50	6.909
-60	6.327
-70	5.486
-85	3.993
-100	2.720
-115	1.652
-130	0.743
-145	

NOTE: THESE VALUES USED IN ANALYSIS

Sensor Location	ρ_{cf} Ft.	$\Delta\rho_{cf}$ Ft.
SR1 -10.5	7.804	0.256
SR2 -21.5	7.548	0.438
SR3 -43.0	7.110	
SR4 -67.5	5.696	3.804
SR5 -93.1	3.306	
SR6 -120.7	1.307	3.306

TABLE 7-10 COMPOSITE FINAL CONSOLIDATION SETTLEMENT WITH FIELD RR & CR.

$U = \frac{\rho_{c_M}}{\rho_{c_F}}$

t_o = CD 390

		LAYER AND DEGREE OF CONSOLIDATION											
		A (-10.5 / -21.5)		B (-21.5 / -43.0)		C (-43.0 / -93.1)		D (-93.1 / -120.7)		E (-120.7 / -145.0)		D+E (-93.1 / -145.0)	
		ρ_{c_F} = 0.256*		ρ_{c_F} = 0.428*		ρ_{c_F} = 3.804		ρ_{c_F} = 1.999		ρ_{c_F} = 1.307		ρ_{c_F} = 3.306	
CONSTR DAY	ELAPSED TIME (DAYS)	ρ_{c_M} FT.	U %	ρ_{c_M} FT.	U %	ρ_{c_M} FT.	U %	ρ_{c_M} FT.	U %	ρ_{c_M} FT.	U %	ρ_{c_M} FT.	U %
620	230	.209	81.6	.412	96.3	.177	4.7	.065	3.3	.137	10.5	.202	6.1
792	402	.260	100.0	.429	100.0	.330	8.7	.089	4.5	.209	16.0	.298	9.0
958	568					.433	11.4	.115	5.8	.255	19.5	.370	11.2
1104	714					.503	13.2		(6.5)		(21.8)	.414	12.5
1268	878					.577	15.2		(7.4)		(24.8)	.468	14.2
1412	1022					.631	16.6		(8.0)		(26.7)	.505	15.3
1568	1178					.688	18.1		(8.6)		(28.8)	.544	16.5
1727	1337					.746	19.6		(9.1)		(30.6)	.577	17.5
1877	1487					.783	20.6		(9.7)		(32.7)	.618	18.7
2053	1663					.827	21.7		(10.6)		(35.6)	.674	20.4

NOTES:

* = ρ_{c_F} FROM FIELD DATA

( ) = U % OF D+E LAYERS EXTRAPOLATED FROM AVERAGE RATIOS $\frac{U(D)}{U(D+E)}$ AND $\frac{U(E)}{U(D+E)}$ BETWEEN CD 620 AND CD 958:

$\frac{U(D)}{U(D+E)} \cong 0.520$

$\frac{U(E)}{U(D+E)} \cong 1.747$

TABLE 7-11 INCREMENTAL CONSOLIDATION (SETTLEMENT)

Lab C_{V2} = 0.093

	C_{V2} (FT²/DAY) PORE PRESSURES $C_{V1}/C_{V2} = 3$						C_{V2} (FT²/DAY) SETTLEMENTS $C_{V1}/C_{V2} = 3$					
	C_{V1}/C_{V2} AT -21.5		C_{V1}/C_{V2} AT -43.0		C_{V1}/C_{V2} AT -70.0		C_{V1}/C_{V2} AT -21.5		C_{V1}/C_{V2} AT -43.0		C_{V1}/C_{V2} AT -70.0	
	H_1 = 11.5, H_2 = 123.5, He = 130.14		H_1 = 33, H_2 = 102, He = 121.05		H_1 = 60, H_2 = 75, He = 109.64		H_1 = 11.5, H_2 = 123.5, He = 130.14		H_1 = 33, H_2 = 102, He = 121.05		H_1 = 60, H_2 = 75, He = 109.64	
CONSTR. DAY	t	Δt	t	Δt	t	Δt	t	Δt	t	Δt	t	Δt
620	1.706*	—	1.476*	—	1.211*	—	.185*	—	.160*	—	.131*	—
792	1.372*	.862*	1.187*	.746*	.974*	.612*	.190*	.197*	.165*	.171*	.135*	.140*
958	1.240*	.893*	1.073*	.773*	.880*	.634*	.172	.128	.149	.111	.122	.091
1104	1.065	.348	.922	.301	.756	.247	.161	.116	.139	.100	.114	.082
1268	.938	.362	.812	.313	.666	.257	.155	.130	.134	.112	.110	.092
1412	.859	.352	.744	.305	.610	.250	.145	.089	.126	.077	.103	.063
1568	.779	.244	.674	.211	.553	.173	.144	.135	.124	.117	.102	.096
1727	.720	.266	.623	.230	.511	.189	.137	.080	.118	.069	.097	.057
1877	.669	.197	.579	.171	.475	.140	.134	.113	.116	.098	.095	.080
2053	.614	.144	.531	.124	.436	.102	.127	.072	.110	.062	.090	.051
SELECTED VALUES:	.806	.273	.698	.236	.572	.194	.147	.108	.127	.093	.104	.077

* = APPARENT ANOMALOUS VALUES, IGNORED

TABLE 7-12 COMPUTED FIELD Cv'S - FULL THICKNESS

$C_V = \frac{T_V H d^2}{t}$

$C_V = \frac{\Delta T_V H d^2}{\Delta t}$

			C_{V_2} (FT²/DAY) by PORE PRESSURES - FULL THICKNESS									
			C_{V_1}/C_{V_2} AT -70						C_{V_1}/C_{V_2} AT -43		C_{V_1}/C_{V_2} AT -21.5	
			LAB: C_{V_1} = .27, C_{V_2} = .09; $He = H_2 + H_1 \sqrt{\frac{C_{V_2}}{C_{V_1}}}$			H_1 = 60, H_2 = 75, He = 109.64			H_1 = 33, H_2 = 102, He = 121.05		H_1 = 11.5, H_2 = 123.5, He = 130.14	
CONSTR DAY	$\bar{U}$	T_{VP} (DAVIS & POULOS)	T_V	t	C_{V_2}	ΔT_V	Δt	C_{V_2}	$\frac{t}{C_{V_2}}$	$\frac{\Delta t}{C_{V_2}}$	$\frac{t}{C_{V_2}}$	$\frac{\Delta t}{C_{V_2}}$
620	.409	.0265	.106	263	1.211	—	—	—	1.476	—	1.706	—
792	.467	.0352	.141	435	.974	.035	172	.612	1.187	.746	1.372	.862
958	.509	.0441	.176	601	.880	.035	166	.634	1.073	.773	1.240	.893
1104	.532	.0470	.188	747	.756	.012	146	.247	.922	.301	1.065	.348
1268	.552	.0505	.202	911	.666	.014	164	.257	.812	.313	.938	.362
1412	.566	.0535	.214	1055	.610	.012	144	.250	.744	.305	.859	.352
1568	.576	.0557	.223	1211	.553	.009	156	.173	.674	.211	.779	.244
1727	.587	.0582	.233	1370	.511	.010	159	.189	.623	.230	.720	.266
1877	.593	.0600	.240	1520	.475	.007	150	.140	.579	.171	.669	.197
2053	.600	.0615	.246	1696	.436	.006	176	.102	.531	.124	.614	.144

TABLE 7-13 CALCULATION OF FIELD C_{V_2} FROM PORE PRESSURE, FULL CLAY THICKNESS

$$C_v = \frac{T'_v H_d^2}{t}$$

$$C_v = \frac{\Delta T'_v H_d^2}{\Delta t}$$

			C_{v_2} (FT^2/DAY) by SETTLEMENT (SR1) FULL THICKNESS									
			C_{v_1}/C_{v_2} AT -70						C_{v_1}/C_{v_2} AT -43		C_{v_1}/C_{v_2} AT -21.5	
			LAB: C_{v_1} = .27, C_{v_2} = .09; $H_e = H_2 + H_1 \sqrt{\frac{C_{v_2}}{C_{v_1}}}$			H_1 = 60, H_2 = 75, H_e = 109.64			H_1 = 33, H_2 = 102, H_e = 121.05		H_1 = 11.5, H_2 = 123.5, H_e = 130.14	
CONSTR DAY	$\bar{U}$	T_v (DAVIS & POULOS)	T'_v	t	C_{v_2}	$\Delta T'_v$	Δt	C_{v_2}	t C_{v_2}	Δt C_{v_2}	t C_{v_2}	Δt C_{v_2}
620	.128	.0026	.010	230	.131	—	—	—	.160	—	.185	—
792	.169	.0044	.018	402	.135	.008	172	.140	.165	.171	.190	.197
958	.192	.0057	.023	568	.122	.005	166	.091	.149	.111	.172	.128
1104	.207	.0067	.027	711	.114	.004	146	.082	.139	.100	.161	.116
1268	.224	.0079	.032	878	.110	.005	164	.092	.134	.112	.155	.130
1412	.236	.0087	.035	1022	.103	.003	144	.063	.126	.077	.145	.089
1568	.249	.0099	.040	1178	.102	.005	156	.096	.124	.117	.144	.135
1727	.261	.0108	.043	1337	.097	.003	159	.057	.118	.069	.137	.080
1877	.272	.0117	.047	1487	.095	.004	150	.080	.116	.098	.134	.113
2053	.284	.0126	.050	1663	.090	.003	176	.051	.110	.062	.127	.072

TABLE 7-14 CALCULATION OF FIELD C_{v_2} FROM SETTLEMENT, FULL CLAY THICKNESS

LAB C_{V2} = 0.093

CONSTR. DAY	C_{V_2} (FT²/DAY) PORE PRESSURE C_{V_1}/C_{V_2} = 3				C_{V_2} (FT²/DAY) SETTLEMENT C_{V_1}/C_{V_2} = 3			
	C_{V_1}/C_{V_2} AT −43.0		C_{V_1}/C_{V_2} AT −70.0		C_{V_1}/C_{V_2} AT −43.0		C_{V_1}/C_{V_2} AT −70.0	
	H_1 = 21.5, H_2 = 102, H_e = 114.41		H_1 = 49.5, H_2 = 75, H_e = 103.58		H_1 = 21.5, H_2 = 102, H_e = 114.41		H_1 = 49.5, H_2 = 102, H_e = 1	
	t	Δt	t	Δt	t	Δt	t	Δt
620	.721*	—	.591*	—	.100	—	.082	—
792	.632	.494	.518	.405	.098	.095	.080	.078
958	.577	.433	.473	.355	.093	.079	.076	.065
1104	.530	.337	.434	.276	.092	.089	.075	.073
1268	.482	.260	.395	.213	.089	.079	.073	.065
1412	.447	.227	.366	.186	.087	.068	.071	.056
1568	.405	.126	.332	.103	.087	.084	.071	.069
1787	.375	.144	.307	.118	.083	.062	.068	.051
1877	.351	.131	.288	.107	.084	.088	.069	.072
2053	.325	.093	.266	.076	.083	.074	.068	.061
SELECTED VALUES:	.458	.249	.375	.204	.090	.080	.073	.066

* APPARENT ANOMALOUS VALUES, IGNORED

TABLE 7-15 COMPUTED FIELD C_V'S - REDUCED THICKNESS

			C_{V_2} (FT^2/DAY) by Pore Pressures – Reduced Thickness							
			C_{V_1}/C_{V_2} at −70						C_{V_1}/C_{V_2} at −43	
			Lab: $C_{V_1} = .27$, $C_{V_2} = .09$; $H_e = H_2 + H_1\sqrt{\frac{C_{V_2}}{C_{V_1}}}$			$H_1 = 49.5$; $H_2 = 75$; $H_e = 103.58$			$H_1 = 21.5$; $H_2 = 102$; $H_e = 114.41$	
CONSTR DAY	$\bar{U}$	T_{VP} DAVIS & POULOS	T_v	t DAYS	C_{V_2} FT^2/DAY	ΔT_v	Δt DAYS	C_{V_2} FT^2/DAY	t C_{V_2} FT^2/DAY	Δt C_{V_2} FT^2/DAY
620	.304	.0145	.058	263	.591	—	—	—	.721	—
792	.364	.0210	.084	435	.518	.026	172	.405	.632	.494
958	.408	.0265	.106	601	.473	.022	166	.355	.577	.433
1104	.433	.0303	.121	747	.434	.015	146	.276	.530	.337
1268	.455	.0335	.134	911	.395	.013	164	.213	.482	.260
1412	.470	.0360	.144	1055	.366	.010	144	.186	.447	.227
1568	.481	.0374	.150	1211	.332	.006	156	.103	.405	.126
1727	.492	.0392	.157	1370	.307	.007	159	.118	.375	.144
1877	.499	.0408	.163	1520	.288	.006	150	.107	.351	.131
2053	.507	.0421	.168	1696	.266	.005	176	.076	.325	.093

TABLE 7-16 CALCULATION OF FIELD C_{V_2} (PORE PRESSURE) REDUCED CLAY THICKNESS

			C_{v_2} (FT^2/DAY) by SETTLEMENT (SR2) REDUCED THICKNESS							
			C_{v_1}/C_{v_2} AT -70						C_{v_1}/C_{v_2} AT -4/3	
			LAB: C_{v_1} = .27 C_{v_2} = .09; $H_e = H_2 + H_1\sqrt{\frac{C_{v_2}}{C_{v_1}}}$			H_1 = 49.5, H_2 = 75, H_e = 103.58			H_1 = 21.5, H_2 = 102, H_e = 114.41	
CONSTR DAY	$\bar{U}$	T_{v_P} DAVIS & POULOS	T_v	t	C_{v_2} FT^2/DAY	ΔT_v	Δt	C_{v_2} FT^2/DAY	t C_{v_2} FT^2/DAY	Δt C_{v_2} FT^2/DAY
620	.105	.0018	.007	230	.082	—	—	—	.100	—
792	.140	.0031	.012	402	.080	.005	172	.078	.098	.095
958	.163	.0041	.016	568	.076	.004	166	.065	.093	.079
1104	.179	.0050	.020	711	.075	.004	146	.073	.092	.089
1268	.195	.0059	.024	878	.073	.004	164	.065	.089	.079
1412	.208	.0067	.027	1022	.071	.003	144	.056	.087	.068
1568	.220	.0077	.031	1178	.071	.004	156	.069	.087	.084
1727	.233	.0085	.034	1337	.068	.003	159	.051	.083	.062
1877	.243	.0094	.038	1487	.069	.004	150	.072	.084	.088
2053	.256	.0105	.042	1663	.068	.004	176	.061	.083	.074

TABLE 7-17. CALCULATION OF FIELD C_{v_2} (SETTLEMENT) REDUCED CLAY THICKNESS

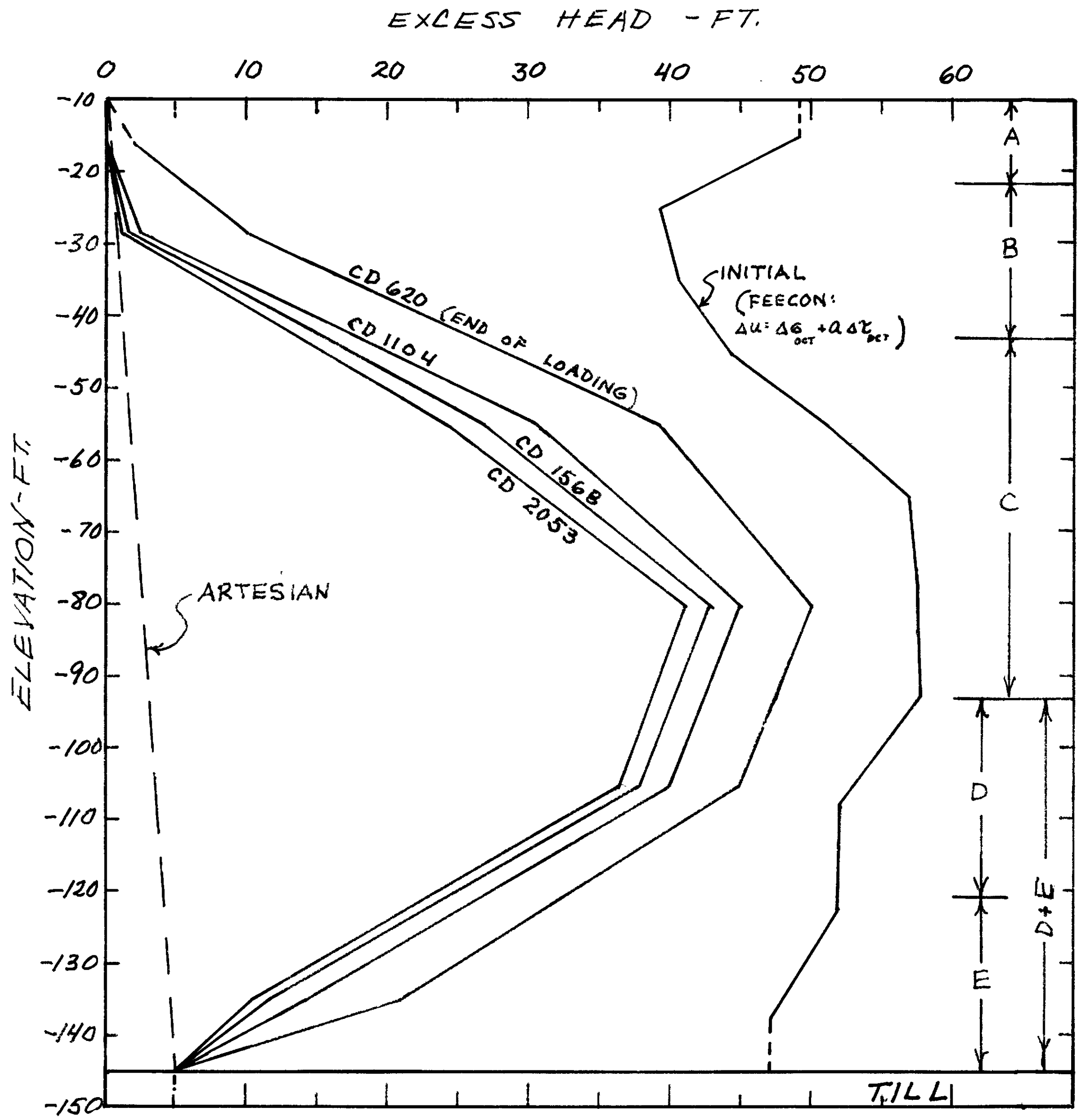

FIGURE 7-1 PORE PRESSURE DISSIPATION BENEATH CENTERLINE

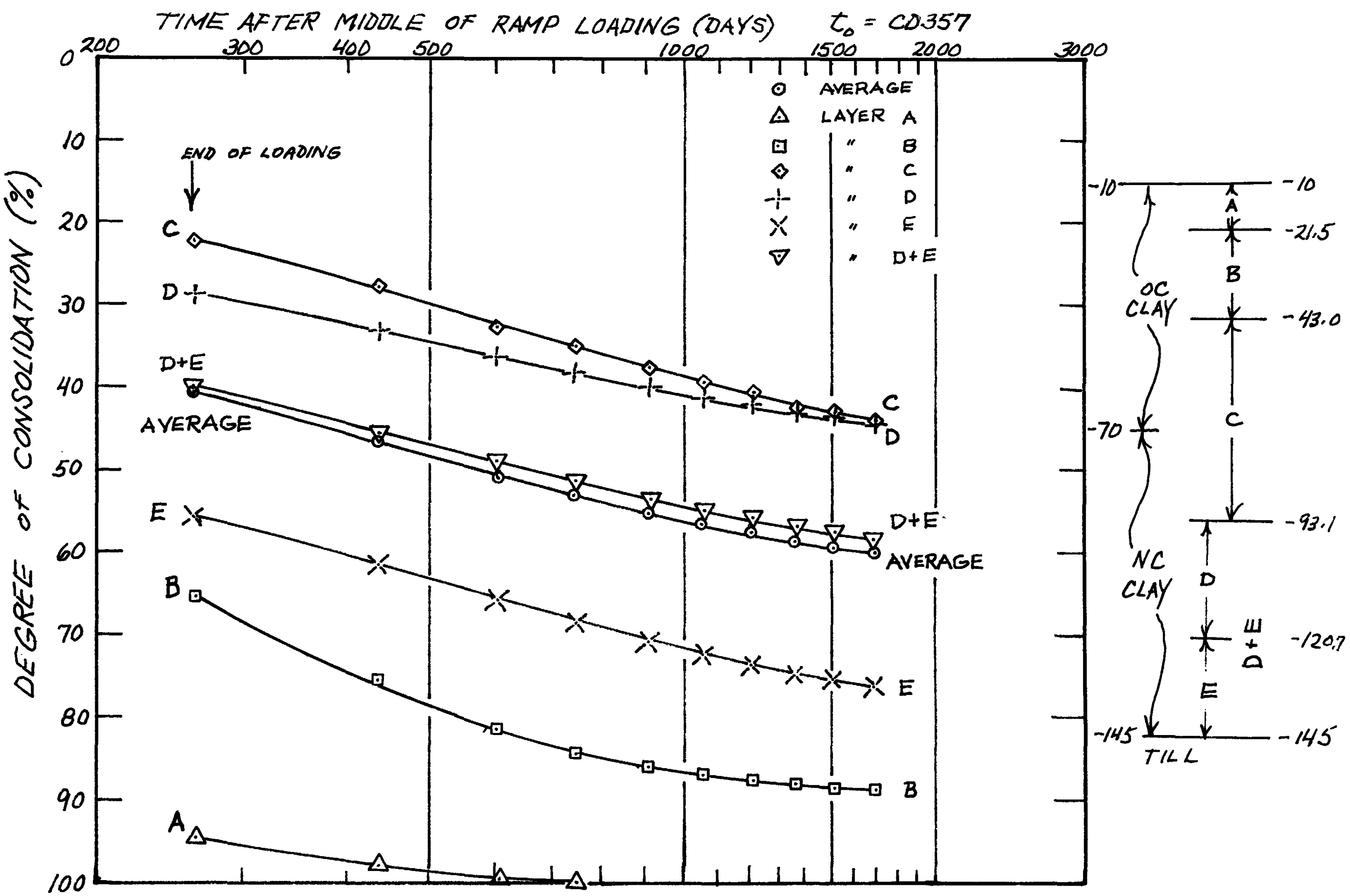

FIGURE 7-2 CENTERLINE CONSOLIDATION (PORE PRESSURE)

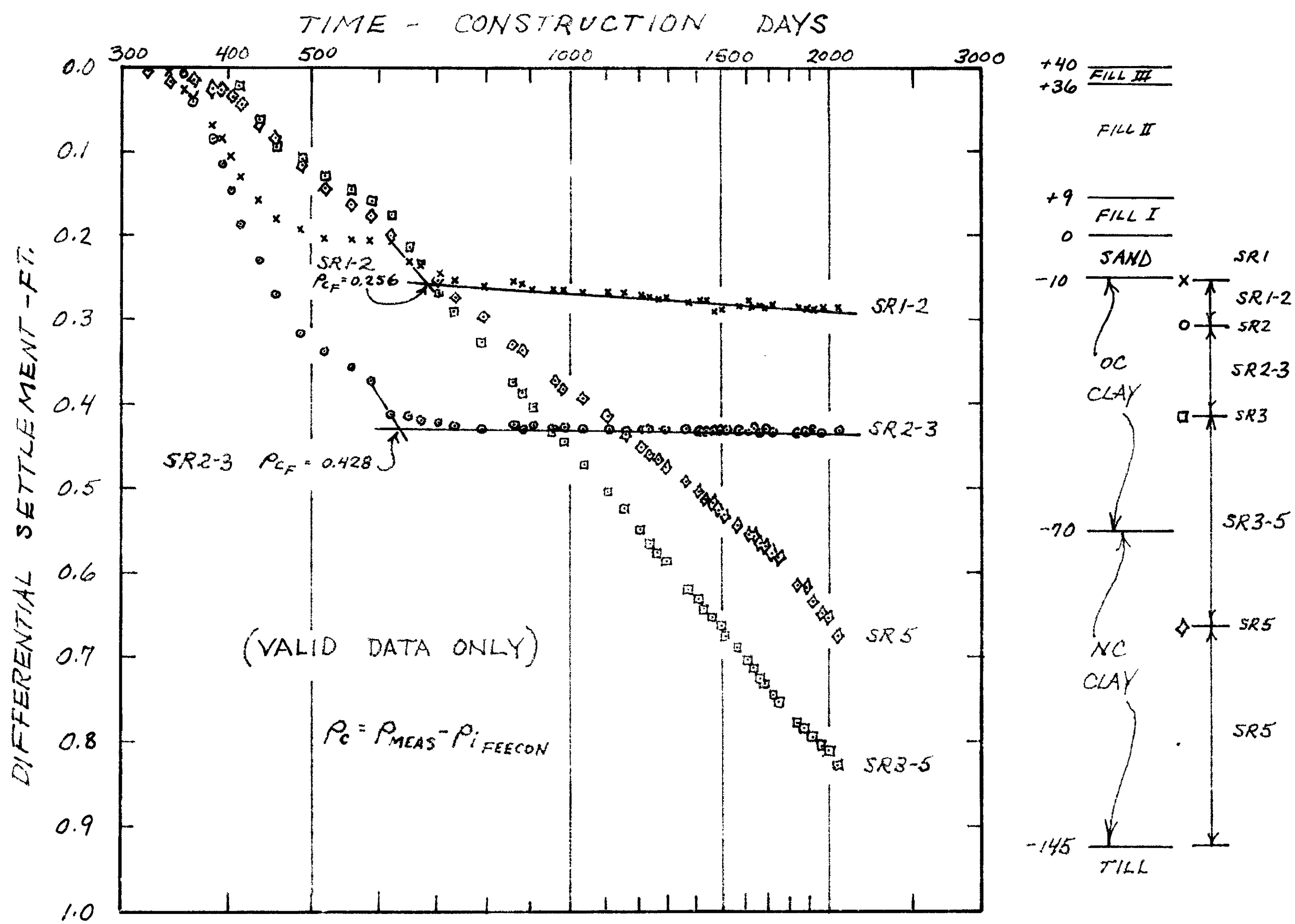

FIGURE 7-3 DIFFERENTIAL CONSOLIDATION SETTLEMENT, STA. 246, ℄

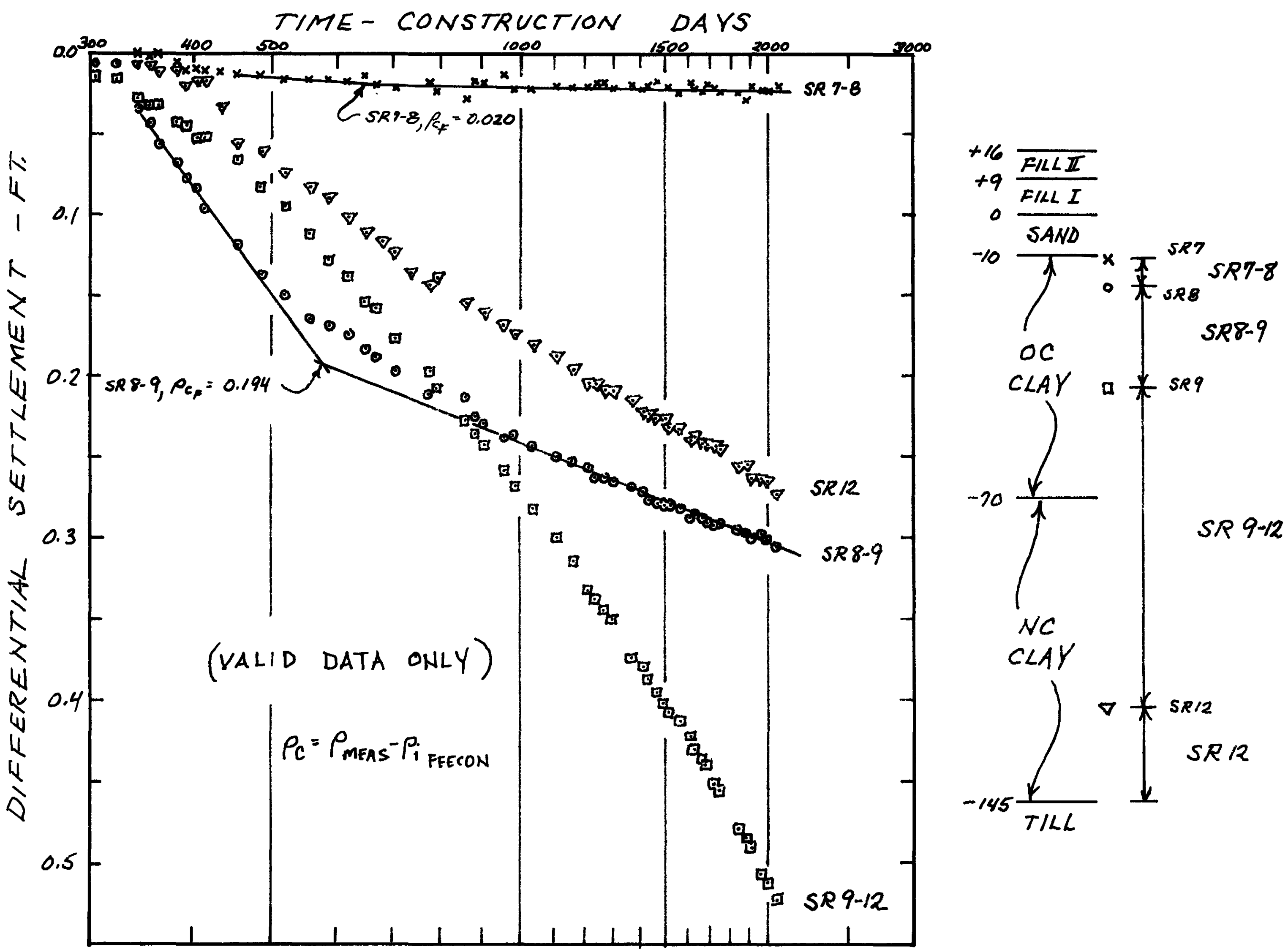

FIGURE 7-4 DIFFERENTIAL CONSOLIDATION SETTLEMENT, STA. 246, 90'R.

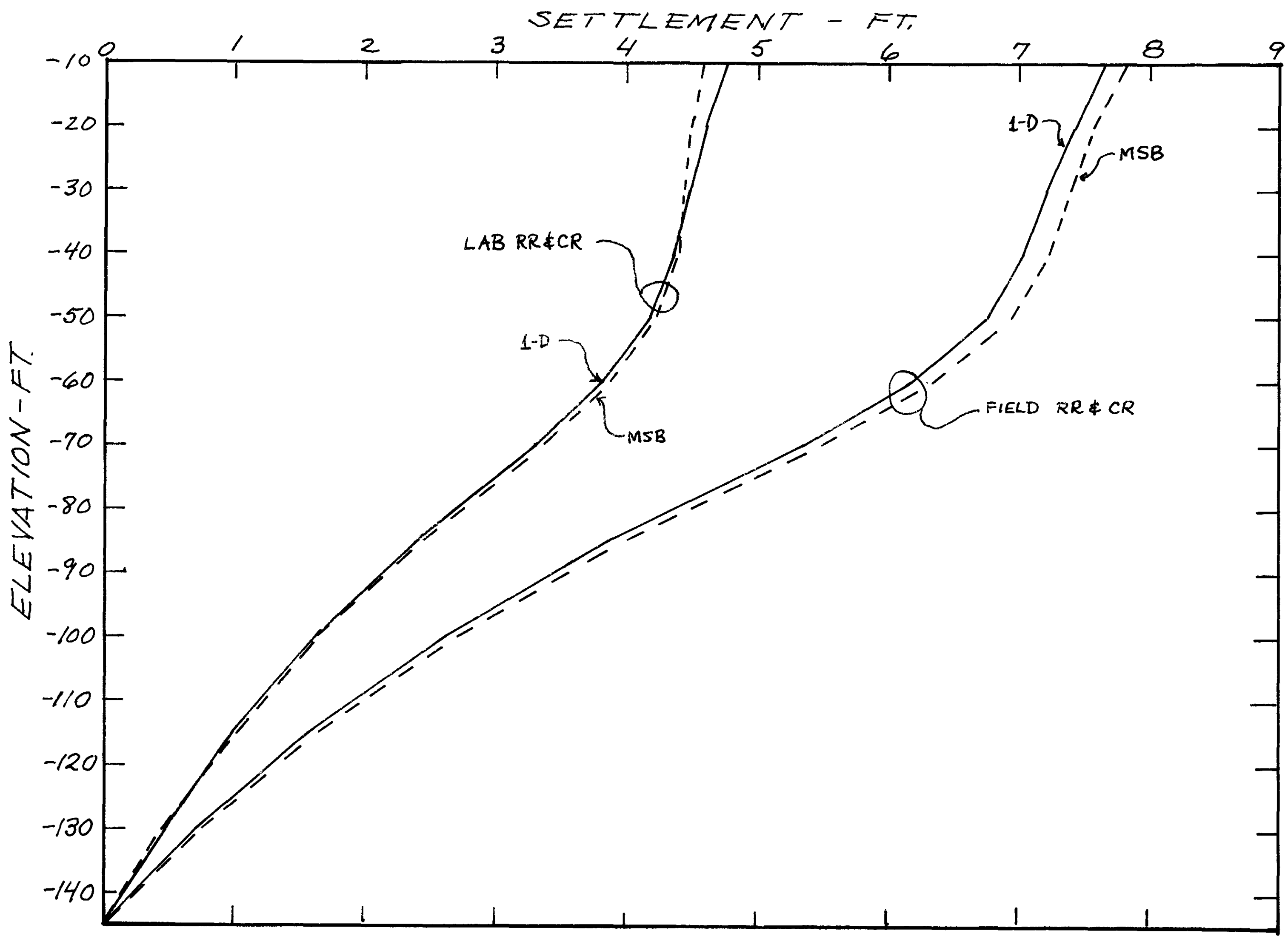

FIGURE 7-5 PREDICTED FINAL CONSOLIDATION SETTLEMENT

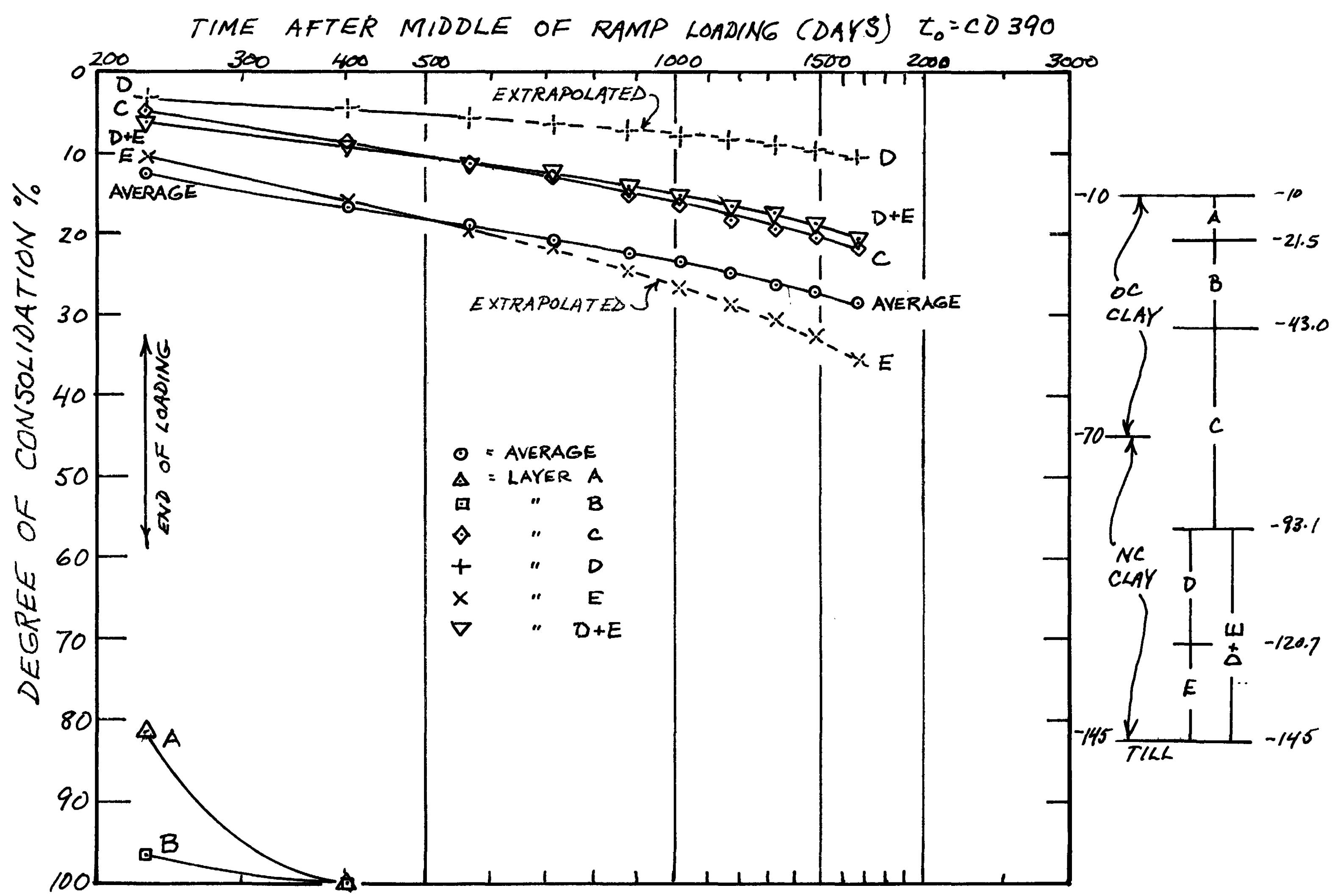

FIGURE 7-6 CENTERLINE CONSOLIDATION (SETTLEMENT)

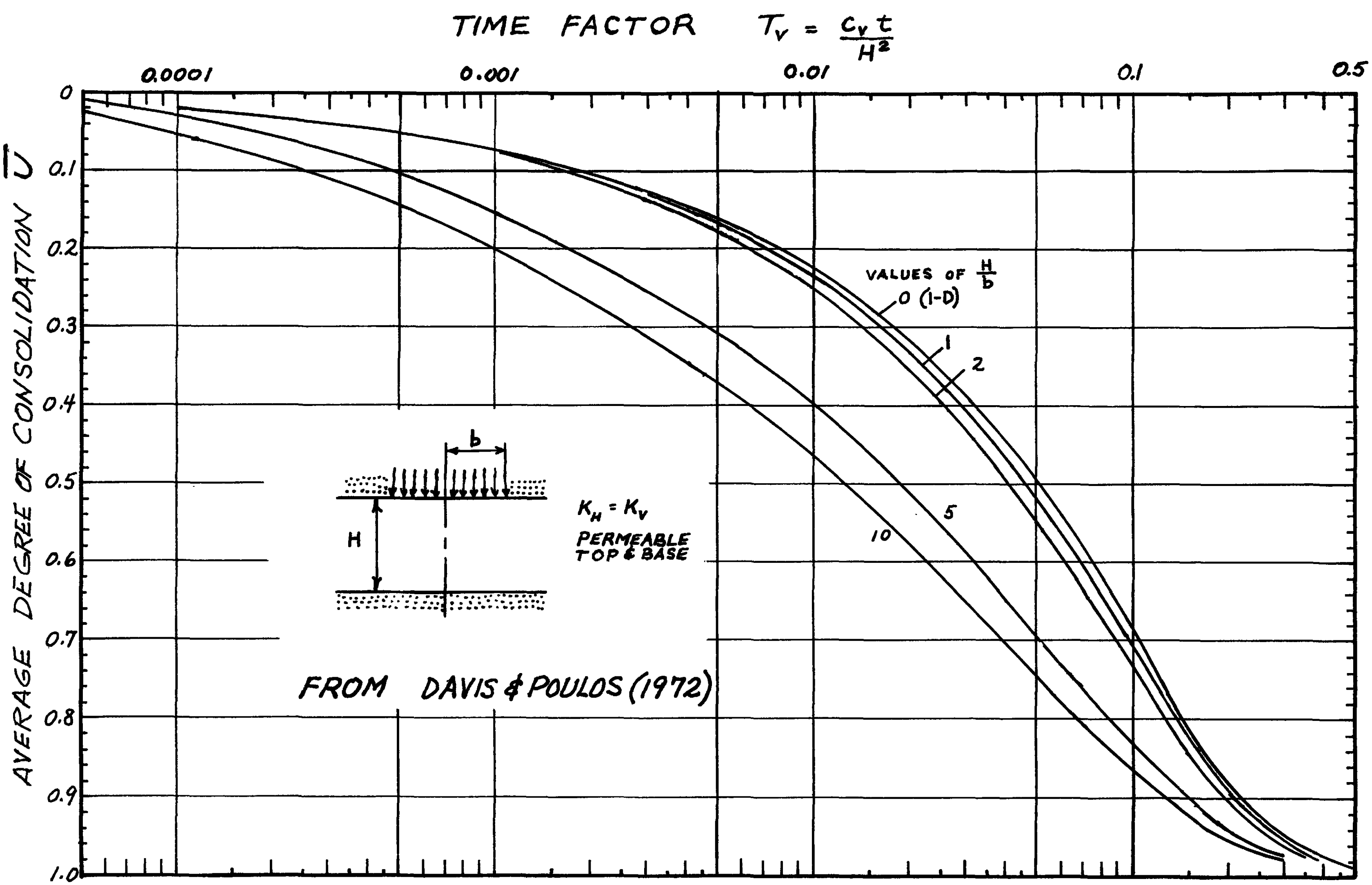

FIGURE 7-7 2-D CONSOLIDATION, PERMEABLE TOP AND BASE

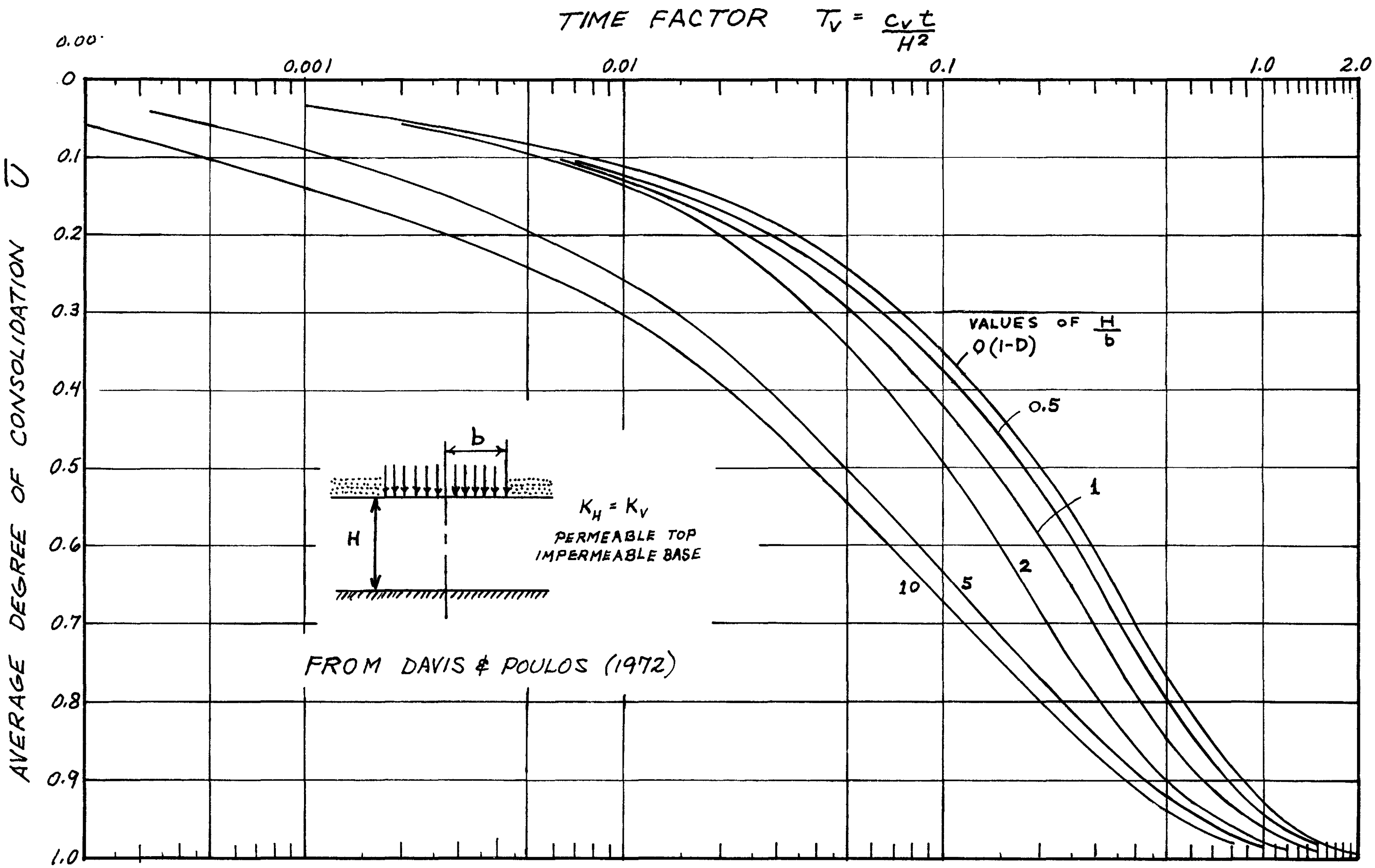

FIGURE 7-8 2-D CONSOLIDATION, PERMEABLE TOP AND IMPERMEABLE BASE

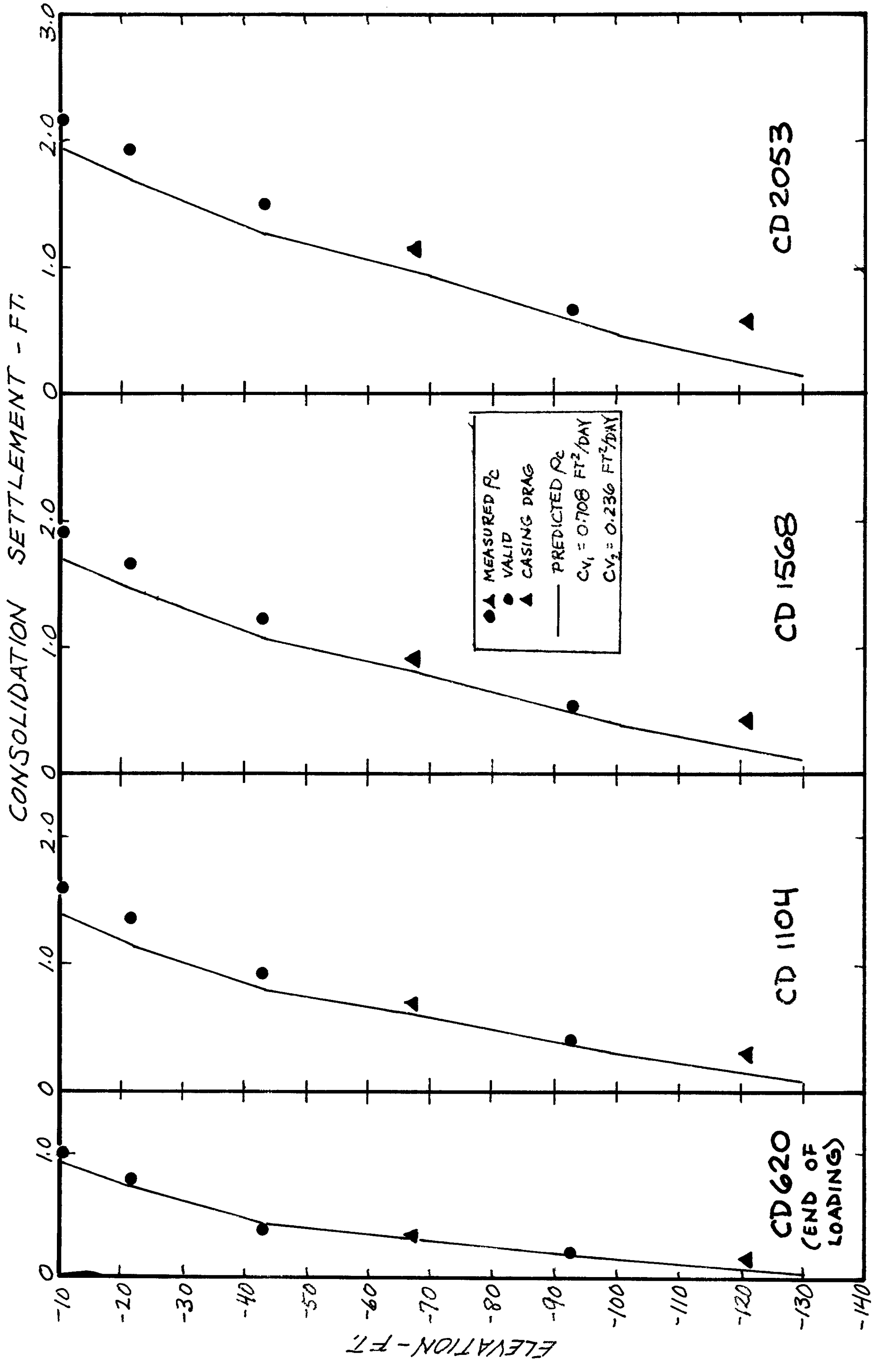

FIGURE 7-9 PREDICTED CONSOLIDATION SETTLEMENT, STA. 246, ℄

8. CONCLUSIONS AND RECOMMENDATIONS

It is apparent from this study that the details of a field instrumentation program are extremely important. Improper installation of a few settlement rods and failure to monitor casing settlements resulted in the loss of critical data, making a detailed analysis much more difficult.

When there is any possiblilty that casing settlement can interfere with a sensor, the casing must be monitored periodically. In addition, the interchangeable use of several instruments to monitor horizontal deflection must be avoided, since this can result in very erratic data. In this respect, the M.I.T. Beaver system appears to produce very high quality deflection data.

In order to maximize the usable data in this expensive instrumentation program, it is essential to repair or replace certain critical instruments. This should be accomplished at least two months prior to the removal of the surcharge at the test section.

Of greatest priority is the repair of settlement rods affected by casing drag (SR-4, 6, 10 and 11). It is recommended that these casings be jacked out at least one foot. It may be necessary to electro-osmotically release the casings from the clay. The procedure might provide valuable electro-osmotic data for Boston Blue Clay as a bonus.

In addition, at least some of the inoperative piezometers must be replaced To reduce the expense, simple single tube Geonor M206 devices can be used. As a minimum, the following piezometers should be replaced: P7, P17, P18, P22, P24, P27, and P28.

Based on comparisons of predicted and measured performance, the use of $\overline{CK_oU}DSS$ hyperbolic parameters in conjunction with the finite element program FEECON is highly effective. However, it is recommended that additional FEECON analyses be performed for the model footing tests to investigate the effect of $\bar{\sigma}_{vc}$ on shear modulus for normally consolidated clay. It is also recommended that FEECON predicted and measured internal embankment stresses be studied.

Excess pore pressures beneath the embankment were equal to the modified Henkel relation $\Delta u = \Delta\sigma_{oct} + a\Delta\tau_{oct}$ where the a parameter is related to Skempton's A parameter at failure: $a = \frac{3A_f - 1}{\sqrt{2}}$. The choice of a is also dependent on the stress system, whether PSA, DSS, or PSP. Good results were obtained by assuming PSA conditions beneath the embankment crest, DSS conditions beneath the slope, and PSP conditions outside the toe.

In the region where DSS conditions are likely (beneath the slope) FEECON horizontal deflections agree well with measured values. It would be advisable to perform additional analyses with input parameters based on $\overline{CK_oUPSA}$ and PSP data in the appropriate locations.

At the top of the clay below the centerline, the predicted initial settlement is 0.2 feet. The predicted final consolidation settlement is 7.8 feet.

Field values of RR are 1.4 to 2.7 times as great as laboratory values, Field values of CR are 1.8 to 1.9 times as great as laboratory CR and field values of c_v are 2.7 times greater than laboratory c_v's. The pore pressure and settlement data indicate significantly different values for the degree of consolidation in the field. However, both types of data show about the same change in degree of consolidation with time.

In view of the very high field value of CR, it is recommended that soluble salt analyses be performed on samples from the clay stratum. These may indicate leaching due to the artersian pressure, a possible cause of increased compressibility.

9. REFERENCES

1. Bromwell, L.G., Ryan, C.R., and Toth, W.E. (1971) "Recording Inclinometer for Measuring Soil Movement", Porceedings, 4th Pan-American Conference on Soil Mechanics and Foundation Engineering, Puerto Rico, Vol. II, pp. 333-343, 1971.

2. D'Appolonia, D.J., Lambe, T.W., and Poulos, H.G. (1971) Evaluation of Pore Pressures Beneath an Embankment", ASCE, JSMFD, Vol. 97, No. SMG, June, 1971, pp. 881-897.

3. D'Appolonia, D.J., Poulos, H.G., and Ladd, C.C. (1971), "Initial Settlement of Structures on Clay", ASCE, JSMFD, Vol. 97, No. SM10, October, 1971, pp. 1359-1377.

4. Davis, E.H. and Christian, J.T. (1971) "Bearing Capacity of Anisotropic Cohesive Soil", ASCE, JSMFD, Vol. 97, No. SM5, May, 1971, pp. 753-769.

5. Davis, E.H. and Poulos, H.G. (1972) "Rate of Settlement Under Two- and Three-Dimensional Conditions", GEOTECHNIQUE 22, No. 1, 1972, pp. 95-114.

6. Duncan, J.M. and Chang C.Y. (1970), "Non-Linear Analysis of Stress and Strain in Soils", ASCE, JSMFD, Vol. 96, No. SM5, pp. 571-582, 1970.

7. Foott, R. and Ladd, C.C. (1973), "The Behavior of Atchafalaya Test Embankments During Construction", Dept. of Civ. Eng. Research Report R73-27, M.I.T., 1973.

8. Guertin, J.D. Jr., (1967), "Stability and Settlement Analyses of an Embankment Clay", S.M. Thesis. Dept. of Civ. Eng., M.I.T., June, 1967.

9. Kinner, E.B. and Ladd, C.C. (1970), "Load Deformation Behavior of Saturated Clays During Undrained Shear", Dept. of Civ. Eng. Research Report R70-27, M.I.T., May, 1970.

10. Kulhway, F.H., Duncan, J.M. and Seed, H.B. (1969), "Finite Element Analysis of Stresses and Movements in Embankments During Construction", Dept of Civ. Eng. Report TE69-4, Univ. of Calif., Berkeley, 1969.

11. Lacasse, S.M. and Ladd, C.C. (1973), "Behavior of Embankments on New Liskeard Varved Clay", Dept. of Civ. Eng. Research Report R73-44 (unpublished) M.I.T. September, 1973.

12. Ladd, C.C. (1971), "Settlement Analyses for Cohesive Soils", Dept. of Civ. Eng. Research Report R71-2, M.I.T. August, 1971.

13. Ladd, C.C. and Edgers, L. (1972), "Consolidated Undrained Direct Simple Shear Tests on Saturated Clays", Dept. of Civ. Eng. Research Report R72-82, M.I.T., July, 1972.

14. Lambe, T.W. and Whitman, R.V. (1969), <u>SOIL MECHANICS</u>, John Wiley and Sons, New York, 1969, 533 p.

15. Lysmer, J. and Duncan J.M. (1972), "Stresses and Deflections in Foundations and Pavements", Dept of Civ. Eng., Univ. of Calif., Berkeley, 1972.

16. Mitchell, J.K. and Gardner, W.S. (1971), "Analysis of Load-Bearing Fills over Soft Subsoils", ASCE, JSMFD, Vol. 97, SM 11, November, 1971, pp. 1549-1571.

17. Park, Y.K. (1974), "Determination of In-Situ Stress in Soil by Hydraulic Fracturing", S.M. Thesis, Dept. of Civ. Eng., M.I.T., February, 1974

18. Perloff, W.H., Baladi, G.Y. and Harr, M.E. (1967), "Stress Distribution Within and Under Long Elastic Embankments", HRB, HRR, No. 181, pp. 12-29, 1967.

19. Recker, K.L. (1973), "Measured Deformations and Pore Pressures Under an Embankment on Soft Clay", S.M. Thesis, Dept. of Civ. Eng., M.I.T., June, 1973.

20. Recker, K.L., Dowding, C.H. and Lambe, T.W. (1973), "Prediction of the Magnitude and Rate of Movement of the Embankment Upon Removal of the Surcharge at I-95", Dept. of Civ. Eng. Research Report R73-45, M.I.T., August, 1973.

21. Reed, D.E. (1973), "Generalized Subsurface Soil and Rock Descriptions in the Boston Area", Internal Report, Haley and Aldrich, Inc., Cambridge, Mass., 1973, (unpublished).

22. Simon, R.M. (1972), "Analysis of Embankment Construction by Finite Elements", S.M. Thesis, Dept. of Civ. Eng. M.I.T., Spetember, 1972.

23. Simon, R.M., Christian, J.T., and Ladd, C.C. (1974), "Analysis of Undrained Behavior of Loads on Clay", ASCE Specialy Conference on Anlysis and Design in Geotechnical Engineering, Austin, Texas, June, 1974.

24. Simon, R.M., Ladd, C.C. and Cristian, J.T. (1972), "Finite Element Program FEECON for Undrained Deformation Analyses of Granular Embankments on Soft Clay Foundations", Dept. of Civ. Eng. Research Report R72-9, M.I.T., 1972.

25 Storch Engineers (1965) "Soils and Foundations Report for Interstate Route 95, Revere - Saugus, Massachusetts" prepared for Highway Engineers, Inc., Boston, Mass., 1965.

26. Wolfskill, L.A. and Soydemir, C. (1971), "Soil Instumentation for the I-95 MIT-MDPW Test Embankment", Dept. of Civ. Eng. Research Report R71-28, M.I.T., August, 1971.

DATE-DAY CONVERSION CHART

DATE	CONSTR. DAY	DATE	CONSTR. DAY	DATE	CONSTR. DAY
1 SEP 67	1	1 JAN 70	854	1 MAY 72	1705
1 OCT 67	31	1 FEB 70	885	1 JUN 72	1736
1 NOV 67	62	1 MAR 70	913	1 JUL 72	1766
1 DEC 67	92	1 APR 70	944	1 AUG 72	1797
1 JAN 68	123	1 MAY 70	974	1 SEP 72	1828
*1 FEB 68	154	1 JUN 70	1005	1 OCT 72	1858
1 MAR 68	183	1 JUL 70	1035	1 NOV 72	1889
1 APR 68	214	1 AUG 70	1066	1 DEC 72	1919
1 MAY 68	244	1 SEP 70	1097	1 JAN 73	1950
1 JUN 68	275	1 OCT 70	1127	1 FEB 73	1981
1 JUL 68	305	1 NOV 70	1158	1 MAR 73	2009
1 AUG 68	336	1 DEC 70	1188	1 APR 73	2040
1 SEP 68	367	1 JAN 71	1219	1 MAY 73	2070
1 OCT 68	397	1 FEB 71	1250	1 JUN 73	2101
1 NOV 68	428	1 MAR 71	1278	1 JUL 73	2131
1 DEC 68	458	1 APR 71	1309	1 AUG 73	2162
1 JAN 69	489	1 MAY 71	1339	1 SEP 73	2193
1 FEB 69	520	1 JUN 71	1370	1 OCT 73	2223
1 MAR 69	548	1 JUL 71	1400	1 NOV 73	2254
1 APR 69	579	1 AUG 71	1431	1 DEC 73	2284
1 MAY 69	609	1 SEP 71	1462	1 JAN 74	2315
1 JUN 69	640	1 OCT 71	1492	1 FEB 74	2346
1 JUL 69	670	1 NOV 71	1523	1 MAR 74	2374
1 AUG 69	701	1 DEC 71	1553	1 APR 74	2405
1 SEP 69	732	*1 JAN 72	1584	1 MAY 74	2435
1 OCT 69	762	1 FEB 72	1615	1 JUN 74	2466
1 NOV 69	793	1 MAR 72	1644	1 JUL 74	2496
1 DEC 69	823	1 APR 72	1675	1 AUG 74	2527

* LEAP YEAR

TABLE A1 DATE & CONSTRUCTION DAY

TEST-SECTION INSTRUMENTATION

INSTRUMENT	LOCATION: STATION	LOCATION: OFFSET	LOCATION: ELEV.	INSTALLATION: DATE	INSTALLATION: DAY	INITIAL READING: DATE	INITIAL READING: DAY	REMARKS
SA1	245+00	℄	-15.1	8/31/67	0	9/22/67	22	Borros Point
SA2	"	"	-67.5	9/1/67	1	"	"	" "
SA3	"	95'R	-15.5	9/6/67	6	"	"	" "
SA4	"	"	-67.5	9/5/67	5	"	"	" "
SA5	"	160'R	-15.1	9/7/67	7	"	"	" "
SA6	"	"	-150.6	"	"	"	"	" " (TEMP. BENCH)
PCP1	"	℄	-5.0	9/1/67	1	10/17/67	47	M206 PIEZ.
PCP2	"	"	-30.0	"	"	10/20/67	50	" "
PCP3	"	"	-79.9	8/30/67	0	10/17/67	47	" "
PCP4	"	"	-138.8	9/8/67	8	"	"	" "
PCP6	"	160'R	-3.9	11/28/67	99	11/28/67	99	NGI Bronze Pt.
PCP5	"	"	-30.0	9/7/67	7	10/17/67	47	M206 PIEZ.
SP1	246+00	4'L	+0.6	2/14/68	167	4/2/68	215	PLATFORM
SR1	"	2'R	-10.5	2/6/68	159	"	"	CASED ROD
SR2	"	4'R	-21.5	2/7/68	160	"	"	" "
SR3	"	6'R	-43.0	2/6/68	159	"	"	" "
SR4	"	8'R	-67.6	"	"	"	"	" "
SR5	"	10'R	-93.1	2/7/68	160	"	"	" "
SR6	"	12'R	-120.7	2/2/68	155	"	"	" "
SP2	"	37.5'R	+1.0	2/15/68	168	5/7/68	250	PLATFORM
SP3	"	99'R	+0.4	"	"	4/23/68	236	PLATFORM
SR7	"	93'R	-10.7	2/12/68	165	4/23/68	236	CASED ROD
SR8	"	91'R	-17.8	2/16/68	169	4/2/68	215	" "
SR9	"	89'R	-43.0	"	"	"	"	" "
SR10	"	87'R	-66.9	2/9/68	162	"	"	" "
SR11	"	85'R	-92.7	2/20/68	173	4/23/68	236	" "
SR12	"	83'R	-121.5	2/28/68	181	4/2/68	215	" "
SP4	245+95	130'R	-1.4	7/16/68	320	7/16/68	320	PLATFORM
SP5	246+00	125'L	0.0	7/17/68	321	11/6/68	433	PLATFORM (STATE)
WP1	246+00	7'L	-7.5	2/15/68	168	3/13/68	195	WELL POINT
P5	246+25	℄	-15.9	4/25/68	238	7/22/68	326	2 LEAD HYDRAUL.
P6	246+20	"	-28.6			7/16/68	320	" "
P6A		"	-28.3	10/24/70	1150	12/21/70	1208	" "

TABLE A2 INSTRUMENTATION

TEST-SECTION INSTRUMENTATION

INSTRUMENT	LOCATION			INSTALLATION		INITIAL READINGS		REMARKS
	STATION	OFFSET	ELEV.	DATE	DAY	DATE	DAY	
Pe 6A		℄				1/27/71	1245	VIBRAT. WIRE
P7	245+75	"	-55.0	3/6/68	188	7/19/68	323	2 LEAD HYDRAUL.
P8	246+15	"	-80.2	4/25/68	238	7/16/68	320	" "
P8A	"	"	-80.3	10/24/70	1150	1/5/71	1223	" "
Pe 8A	"	"	-75.3	"	"	1/27/71	1245	VIBRAT. WIRE
P9	245+80	"	-105.2	2/29/68	182	7/16/68	320	2 LEAD HYDRAUL.
P10	245+85	"	-135.0	2/28/68	181	"	"	" "
P10A	"	"	-135.0	10/23/70	1149	12/21/70	1208	" "
Pe 10A	"	"				1/27/71	1245	VIBRAT. WIRE
P11	246+10	"	-147.4	4/17/68	230	7/16/68	320	2 LEAD HYDRAUL.
P13	245+88	11'L	-169.6	7/30/68	334	7/22/68	326	" "
WP2	246+00	30'R	-6.9	2/15/68	168	3/13/68	195	WELL POINT
P14	246+20	30'R	-15.0	4/12/68	225	7/30/68	334	2 LEAD HYDRAUL.
P15	245+80	"	-29.7	3/8/68	190	7/15/68	319	" "
P16	245+85	"	-55.1	3/7/68	189	"	"	" "
P17	246+15	"	-80.8	4/12/68	225	7/16/68	320	" "
P18	246+10	"	-115.5	4/9/68	191	7/15/68	319	" "
P19	245+90	"	-135.0	3/6/68	188	"	"	" "
WP3	246+00	60'R	-7.3	2/15/68	168	3/13/68	195	WELL POINT
P20	246+20	"	-13.8	5/24/68	267	7/15/68	319	2 LEAD HYDRAUL.
P21	246+15	"	-28.8	"	"	"	"	" "
P22	245+85	"	-55.8			"	"	" "
P23	245+90	"	-79.9	3/12/68	194	"	"	" "
P24	246+10	"	-104.0	5/23/68	266	"	"	" "
WP4	246+00	95'R	-7.4	2/15/68	168	3/13/68	195	WELL POINT
P25	246+15	"	-13.6	5/29/68	272	7/15/68	319	2 LEAD HYDRAUL.
P26	245+85	"	-29.9	3/29/68	211	"	"	" "
P27	245+90	"	-54.8	4/1/68	214	"	"	" "
P28	246+10	"	-104.7	5/28/68	271	"	"	" "
WP5	246+00	160'R				7/3/68	307	WELL POINT
P29	246+15	"	-14.5	6/21/68	295	7/29/68	333	2 LEAD HYDRAUL.
P30	245+90	"	-55.5	6/25/68	299	7/29/68	333	" "
P31	246+10	"	-104.2	6/21/68	295	7/29/68	333	" "
P33	"	225'R	-14.9	6/28/68	302	8/8/68	343	" "
P32	245+90	"	-55.1	6/17/68	291	"	"	" "
Pe 1	246+19	30'L	-15.0			7/10/68	314	VIBRAT. WIRE
Pe 2	245+87	"	-31.2	7/12/68	316	7/18/68	322	" "
Pe 3	245+90	"	-56.6			7/10/68	314	" "

TABLE A2 CONT'D.

TEST-SECTION INSTRUMENTATION								
INSTRU-MENT	LOCATION			INSTALLATION		INITIAL READINGS		REMARKS
	STATION	OFFSET	ELEV.	DATE	DAY	DATE	DAY	
Pe 4	246+10	30'L	-81.0			7/10/68	314	VIBRAT. WIRE
Pe 5	246+05	"	-105.3			"	"	" "
Pe 6	246+00	"	-136.6			"	"	" (STATE) "
P3	246+05	95'L	-53.3	6/19/68	293	7/29/68	333	2 LEAD HYDRAUL.
P2	246+00	140'L	-15.7	"	"	"	"	" (STATE) "
P1	246+05	"	-28.8	"	"	"	"	" (STATE) "
P12	245+95	145'L	-79.5	6/20/68	294	"	"	" (STATE) "
P4	"	"	-106.6	6/12/68	286	8/13/68	348	" (STATE) "
I2	246+00	℄				7/3/68	307	FLEX. COUPLING INCLIN.
I3	"	45'R				6/30/68	304	" " "
I4	"	95'R				7/9/68	313	" " "
I5	"	160'R				7/2/68	306	" " "
I6	"	225'R				"	"	" " (DESTROYED) "
I1	"	140'L				7/3/68	307	" " (STATE) "
SC-A	246+00	℄	+16.7			8/20/68	355	3 TOTAL STRESS CELLS
SC-B	"	30'R	+17.0			"	"	" " " "
SC-C	"	60'R	+17.1			"	"	" " " "
BM	246+00	20'R						PERM. BENCH

TABLE A2 CONT'D.

CONSTRUCTION HISTORY- STA.246			
DATE	CONSTR. DAY	AVG. EMB'KM'T EL. (FT.)	REMARKS
12/1/67	92		} EXCAV. & REPLACE PEAT
12/7/67	98	+8.0	
12/12/67	103	8.5	
1/1/68	123	9.0	
2/1/68	154	9.5	
2/2/68	155	9.1	RIGHT GR'DED. +9.5 ℄ → +6.0 (TO INST. SR7-12)
3/7/68	189	8.9	EXCAV. SR1-7 LOCAT. TO +9.8 ℄ → +7
5/9/68	252	9.0	GRADE RIGHT TO +8 ℄ → +6 FOR TUNNEL
5/10/68	253	9.0	EXCAV. & REPL PEAT OUTSIDE RT. TOE FOR TUNNEL
5/30/68	273	9.0	
6/7/68	281	9.0	PEAT COVERED OUTSIDE TOES FOR INSTR. INSTALL.
6/24/68	298	9.3	
6/25/68	299	9.5	
6/26/68	300	9.6	
6/27/68	301	9.7	
6/28/68	302	9.8	
7/1/68	305	9.9	
7/3/68	307	10.2	
7/8/68	312	10.6	
7/10/68	314	11.0	
7/11/68	315	11.0	EXCAV. 2 DITCHES 10'W.×8'D. 230' R&L
7/13/68	317	11.0	OUTSIDE TOES, EXCAV. FILL & PEAT, REPL. W. FILL
7/15/68	319	11.3	
7/16/68	320	11.3	
7/18/68	322	11.4	
7/19/68	323	11.8	
7/22/68	326	13.2	
7/23/68	327	14.3	
7/24/68	328	14.6	
7/25/68	329	16.0	
7/26/68	330	16.5	
7/29/68	333	17.0	STA. 245 HISTORY NOW SAME AS STA. 246
7/30/68	334	17.5	↓
7/31/68	335	17.6	
8/1/68	336	18.0	
8/2/68	337	18.2	
8/5/68	340	18.7	
8/6/68	341	18.7	

TABLE A3 CONSTRUCTION HISTORY

CONSTRUCTION HISTORY - STA. 246					
DATE	CONSTR. DAY	AVG. EMB'KM'T EL. (FT.)	DATE	CONSTR. DAY	AVG. EMB'KM'T EL. (FT.)
8/7/68	342	+19.7	10/10/68	406	+31.2
8/10/68	345	19.7	10/11/68	407	32.0
8/12/68	347	20.0	10/14/68	410	32.0
8/13/68	348	20.3	10/16/68	412	32.2
8/14/68	349	20.5	10/17/68	413	32.2
8/16/68	351	21.0	10/18/68	414	32.6
8/19/68	354	21.5	10/21/68	417	32.6
8/20/68	355	21.9	10/22/68	418	32.9
8/21/68	356	22.5	10/23/68	419	33.3
8/22/68	357	22.5	10/24/68	420	33.7
8/23/68	358	22.5	10/29/68	425	33.7
8/26/68	361	23.0	10/30/68	426	33.8
8/27/68	362	23.6	10/31/68	427	33.8
8/28/68	363	23.7	11/1/68	428	34.3
8/29/68	364	24.0	11/8/68	435	35.3
8/30/68	365	24.0	11/11/68	438	35.6
9/3/68	369	24.3	11/14/68	441	35.6
9/5/68	371	24.5	11/15/68	442	35.9
9/9/68	375	24.5	11/22/68	449	36.2
9/10/68	376	24.7	12/4/68	461	36.2
9/12/68	378	25.7	4/15/69	593	35.8
9/13/68	379	26.7	4/16/69	594	36.0
9/14/68	380	26.7	4/20/69	598	36.4
9/16/68	382	26.8	4/23/69	601	36.8
9/19/68	385	27.0	4/24/69	602	37.2
9/20/68	386	26.9	4/25/69	603	37.2
9/23/68	389	27.5	4/28/69	606	37.2
9/25/68	391	27.9	4/29/69	607	37.3
9/26/68	392	28.1	4/30/69	608	37.5
9/27/68	393	28.3	5/1/69	609	37.7
9/30/68	396	29.4	5/2/69	610	38.1
10/1/68	397	29.5	5/5/69	613	38.3
10/2/68	398	29.7	5/6/69	614	38.6
10/3/68	399	29.8	5/7/69	615	39.0
10/4/68	400	30.1	5/8/69	616	39.0
10/7/68	403	30.9	5/9/69	617	39.4
10/8/68	404	30.8	5/12/69	620	39.8
10/9/68	405	30.9	5/14/69	622	40.1

TABLE A3 CONT'D.

CONSTRUCTION HISTORY - STA. 245			
DATE	CONSTR. DAY	AVG. EMB'KM'T EL. (FT.)	REMARKS
12/1/67	92	+8.0	EXCAV. & REPL. PEAT EXCEPT AT INSTRUM.
12/7/67	98		
12/9/67	100	8.0	EXCAV. & REPL. PEAT AT INSTRUMENTS
12/12/67	103	8.5	
1/1/68	123	9.0	
2/2/68	155	9.5	
6/23/68	297	9.5	
6/24/68	298	10.0	
6/25/68	299	10.5	
6/26/68	300	10.8	
6/27/68	301	11.5	
6/28/68	302	11.7	
7/1/68	305	12.1	
7/3/68	307	14.0	
7/8/68	312	14.5	
7/14/68	318	14.5	
7/15/68	319	15.0	
7/18/68	322	15.2	
7/20/68	324	15.5	
7/21/68	325	15.8	
7/23/68	327	16.5	
7/24/68	328	17.0	
7/29/68	333	17.0	STA. 245 HISTORY SAME AS STA. 246
7/30/68	334	17.5	

TABLE A3 CONT'D.

		INSTRUMENT, LOCATION, & SETTLEMENT (FT.)					
DATE	CONSTR DAY	SA 1 ℄, -15.1	SA 2 ℄, -67.5	SA 3 95'R, -15.5	SA 4 95'R, -67.5	SA 5 160'R, -15.1	SA 6 160'R, -150.6
9/22/67	22	0	0	0	0	0	0
10/3/67	64	0	0	0	-.002	0	0
12/4/67	95	-.002	0	.003	-.002	0	
12/7/67	98	-.003	.001	.019	.006	-.003	
12/8/67	99	.003	-.011	.005	-.004	-.012	
12/13/67	104	.049	.047	.005	-.004		
12/14/67	105	.046	.043	.008	.005	-.007	(USED AS TEMPORARY BENCHMARK)
12/18/67	107	.049	.045	.005	.005	-.001	
12/20/67	109	.049	.045	.006	.004		
1/3/68	125	.060	.055	.015	.007	.006	
1/18/68	140	.057	.049	.013	.003	.005	
2/8/68	161	.049	.037	.006	-.005	-.013	
2/29/68	182	.062	.056	.020	.005	0	
3/14/68	196	.068	.057	.023	.013	0	
4/23/68	236	.070	.059	.025	.007	-.002	
5/7/68	250	.068	.055	.024	.007	-.003	
5/31/68	274	.073	.063	.031	.010	-.001	
6/25/68	299	.079	.064	.035	.017	0	
7/22/68	326	.089	.072	.044	.018		

TABLE A4-1 SETTLEMENT DATA; STA. 245; ℄, 95'R., 160'R.

DATE	CONSTR. DAY	INSTRUMENT, LOCATION, & SETTLEMENT (FT.)						
		SP1 4'L., +0.6	SR 1 2'R., -10.5	SR 2 4'R., -21.5	SR 3 6'R., -43.0	SR 4 8'R., -67.6	SR 5 10'R., -93.1	SR 6 12'R., -120.7
4/23/68	236	.021	.007	.004	.004	.004	.004	.004
5/7/68	250	.021	.006	.004	.005	.003	.003	.005
7/1/68	305	.026	.015	.011	.006	.007	.003	.003
7/19/68	323	.048	.027	.019	.014	.013	.009	.007
8/8/68	343	.179	.131	.092	.038	.026	.017	.015
8/21/68	356	.263	.195	.133	.051	.031	.015	.010
8/29/68	364	.327	.256	.180	.063	.041	.022	.015
9/16/68	382	.431	.350	.243	.083	.053	.030	.017
9/26/68	392	.496	.408	.287	.096	.060	.032	.017
10/7/68	403	.580	.486	.342	.120	.078	.038	.022
10/18/68	414	.695	.585	.417	.157	.110	.049	.028
11/6/68	433	.837	.715	.520	.216	.164	.068	.045
11/27/68	454	.967	.831	.615	.270	.206	.088	.062
12/30/68	487	1.073	.933	.705	.315	.241	.118	.076
1/31/69	519	1.147	1.008	.770	.357	.274	.143	.093
3/10/69	557	1.212	1.071	.831	.399	.307	.167	.111
4/9/69	587	1.257	1.116	.874	.427	.328	.180	.121
5/12/69	620	1.353	1.202	.957	.470	.366	.206	.137
6/11/69	650	1.446	1.288	1.018	.527	.396	.226	.154
7/1/69	670	1.489	1.328	1.053	.558	.411	.236	.161
8/6/69	706	1.553	1.389	1.109	.612	.443	.257	.174
9/4/69	735	1.599	1.440	1.153	.654	.471	.277	.213
10/16/69	777	2.753	1.992	1.106	.727	.403	.300	.504
10/31/69	792	1.676	1.519	1.223	.719	.512	.302	.209
1/7/70	860	1.757	1.587	1.296	.795	.560	.332	.227
1/28/70	881	1.781	1.613	1.320	.815	.573	.341	.235
2/23/70	907	1.807	1.643	1.344	.843	.591	.353	.240
4/15/70	958	1.868	1.697	1.396	.894	.626	.374	.255
5/13/70	986	1.896	1.720	1.421	.918	.643	.385	.262
7/3/70	1037	1.939	1.765	1.462	.958	.671	.399	.269
9/8/70	1104	1.988	1.817	1.514	1.008	.711	.418	.285
10/28/70	1154	2.031	1.859	1.556	1.049	.740	.438	.298
12/21/70	1208	2.080	1.903	1.596	1.090	.774	.455	.316
1/22/71	1240	2.103	1.930	1.619	1.115	.789	.464	.326
2/19/71	1268	2.126	1.953	1.640	1.136	.804	.472	.333
3/18/71	1295	2.145	1.968	1.658	1.153	.819	.479	.339
6/4/71	1373	2.194	2.023	1.707	1.204	.859	.497	.360
7/13/71	1412	2.224	2.046	1.734	1.227	.880	.509	.371

TABLE A4-2 SETTLEMENT DATA, STA. 246, ℄

		INSTRUMENT, LOCATION, & SETTLEMENT (FT.)						
DATE	CONSTR. DAY	SP 1 4'L., +0.6	SR 1 2'R., -10.5	SR 2 4'R., -21.5	SR 3 6'R., -43.0	SR 4 8'R., -67.6	SR 5 10'R., -93.1	SR 6 12'R., -120.7
8/10/71	1440	2.224	2.067	1.755	1.246	.894	.517	.380
9/9/71	1470	2.264	2.095	1.770	1.262	.906	.522	.387
10/7/71	1498	2.279	2.111	1.786	1.279	.920	.529	.394
11/8/71	1510	2.300	2.120	1.804	1.298	.938	.536	.404
12/16/71	1568	2.328	2.148	1.829	1.323	.956	.548	.415
1/28/72	1611	2.353	2.172	1.858	1.351	.977	.561	.431
2/16/72	1630	2.362	2.187	1.867	1.362	.987	.562	.434
3/22/72	1665	2.388	2.208	1.890	1.382	1.004	.570	.447
4/11/72	1685	2.394	2.219	1.899	1.392	1.011	.573	.449
5/23/72	1727	2.416	2.239	1.922	1.414	1.031	.581	.460
6/15/72	1750	2.438	2.253	1.937	1.429	1.040	.589	.466
9/20/72	1847	2.488	2.312	1.990	1.482	1.087	.617	.503
10/20/72	1877	2.499	2.324	2.000	1.492	1.096	.622	.508
11/28/72	1916	2.524	2.347	2.023	1.520	1.119	.638	.520
1/19/73	1968	2.552	2.376	2.054	1.544	1.138	.651	.538
2/15/73	1995	2.564	2.387	2.063	1.556	1.149	.658	.547
4/12/73	2053	2.599	2.421	2.099	1.592	1.178	.678	.573
11/8/73	2261	2.698	2.520	2.196	1.687	1.258	.738	.637

TABLE A4-2 CONT'D.

		INSTRUMENT, LOCATION, & SETTLEMENT (FT.)						
DATE	CONSTR. DAY	SP3 99'R., +0.4	SR7 93'R., -10.7	SR8 91'R., -17.8	SR9 89'R., -43.0	SR 10 87'R., -66.9	SR 11 85'R., -92.7	SR 12 83'R., -121.5
4/23/68	236			.006	.006	.006		.014
5/7/68	250	.005	-.007	.004	.006	.006	-.006	.009
7/1/68	305	.004	-.011	-.003	-.005	-.006	-.013	-.003
7/19/68	323	.080		.004	.002	.010	-.003	.001
8/8/68	343	.098	.050	.048	.018	.013	-.005	.005
8/21/68	356	.112	.068	.064	.024	.009	-.002	.006
8/29/68	364	.130	.085	.083	.030	.016	.008	.010
9/16/68	382	.151	.111	.103	.038	.018	.005	.008
9/26/68	392	.166	.135	.123	.050	.030	.016	.018
10/7/68	403	.178	.147	.135	.055	.033		.016
10/18/68	414	.185	.161	.148	.055	.044	.020	.017
11/6/68	433	.216	.196	.182	.119	.057	.037	.031
11/27/68	454	.249	.236	.222	.107	.081	.058	.054
12/30/68	487	.288	.278	.262	.128	.106	.067	.059
1/31/69	519	.329	.318	.300	.154	.128	.083	.073
3/10/69	557	.360	.357	.339	.178	.145	.093	.080
4/9/69	587	.382	.380	.362	.197	.163	.103	.088
5/12/69	620	.418	.408	.388	.217	.182	.116	.099
6/11/69	650	.434	.438	.422	.243	.208	.126	.109
7/1/69	670	.452	.461	.439	.254	.218	.129	.115
8/6/69	706	.480	.495	.472	.278	.237	.143	.121
9/4/69	735	.504	.519		.301		.155	.134
10/16/69	777	.673	.547	.526	.319	.271	.162	.142
10/31/69	792	.540	.555	.529	.325	.279	.165	.137
1/7/70	860	.581	.601	.570	.361	.309	.183	.153
1/28/70	881	.593	.614	.594	.372	.320	.189	.156
2/23/70	907	.608	.630	.609	.383	.328	.194	.159
4/15/70	958	.635	.657	.641	.406	.347	.205	.167
5/13/70	986	.649	.678	.654	.421	.360	.212	.172
7/3/70	1037	.673	.703	.679	.440	.373	.223	.178
9/8/70	1104	.705	.735	.713	.467	.399	.240	.187
10/28/70	1154	.728	.760	.737	.489	.416	.254	.194
12/21/70	1208	.757	.790	.767	.514	.436	.270	.202
1/22/71	1240	.764	.800	.779	.520	.442	.280	.202
2/19/71	1268	.776	.812	.791	.532	.453	.279	.207
3/18/71	1295	.789	.822	.799	.538	.458	.283	.207
6/4/71	1373	.812	.855	.833	.568	.482	.319	.213
7/13/71	1412	.832	.872	.848	.580	.493	.311	.220

TABLE A4-3 SETTLEMENT DATA, STA. 246, 90'R.

		INSTRUMENT, LOCATION, & SETTLEMENT (FT.)						
DATE	CONSTR. DAY	SP3	SR7	SR8	SR9	SR 10	SR 11	SR 12
8/10/71	1440	.841	.885	.863	.590	.503	.316	.222
9/9/71	1470	.853	.894	.874	.599	.511	.324	.224
10/7/71	1498	.860	.904	.882	.606	.516	.329	.224
11/8/71	1510	.875	.917	.894	.618	.528	.339	.230
12/16/71	1568	.887	.930	.902	.624	.532	.345	.231
1/28/72	1611	.906	.944	.924	.640	.545	.355	.237
2/16/72	1630	.907	.954	.930	.647	.552	.360	.236
3/22/72	1665	.919	.968	.942	.658	.561	.366	.240
4/11/72	1685	.927	.969	.947	.660	.566	.369	.240
5/23/72	1727	.935	.984	.960	.672	.575	.377	.241
6/15/72	1750	.943	.994	.967	.679	.582	.385	.243
9/20/72	1847	.980	1.034	1.007	.715	.610	.411	.255
10/20/72	1877	.984	1.042	1.011	.718	.613	.409	.253
11/28/72	1916	.999	1.052	1.029	.733	.626	.424	.262
1/19/73	1968	1.013	1.068	1.043	.749	.637	.433	.262
2/15/73	1995		1.076	1.051	.754	.645	.438	.263
4/12/73	2053	1.042	1.099	1.076	.775	.664	.456	.272
11/8/73	2261	1.098	1.159	1.135	.829	.711	.495	.282

TABLE A4-3 SETTLEMENT DATA, STA. 246, 90'R.

DATE	CONSTR. DAY	INSTRUMENT, LOCATION & SETTLEMENT (FT.) SP 2 37.5'R +1.0	SP 4 130'R -1.4
7/1/68	305	0.008	
8/8/68	343	0.154	
8/21/68	356	0.219	
8/28/68	363		0.278
8/29/68	364	0.281	
9/16/68	382	0.378	
9/25/68	391		0.276
9/26/68	392	0.451	
10/7/68	403	0.570	
10/18/68	414	0.617	0.237
11/6/68	433	0.739	0.274
11/27/68	454	0.854	
12/2/68	459		0.273
12/30/68	487	0.953	
1/9/69	497		0.280
1/31/69	519	1.030	
3/10/69	557	1.091	
4/7/69	585		0.283
4/9/69	587	1.136	
5/5/69	613		0.277
5/12/69	620	1.215	
6/3/69	642		0.309
6/11/69	650	1.301	
7/1/69	670	1.339	
7/14/69	683		0.322
8/6/69	706	1.401	
8/29/69	729		0.346
9/4/69	735	1.446	
10/16/69	777	1.504	
10/31/69	792	1.519	0.355
12/12/69	834		0.348
1/7/70	860	1.599	
1/28/70	881	1.623	
2/23/70	907	1.648	
3/16/70	928		0.375
4/15/70	958	1.700	
5/13/70	986	1.725	

TABLE A4-4 SETTLEMENT DATA, INTERMEDIATE PLATFORMS, STA. 246, 38'¢/130'R.

DATE	CONSTR. DAY	INSTRUMENT, LOCATION & SETTLEMENT (FT.) SP2 37.5'R +1.0	SP4 130'R -1.4
7/3/70	1037	1.768	
8/13/70	1078		0.398
9/8/70	1104	1.820	
10/28/70	1154	1.861	0.452
12/21/70	1208	1.908	
1/22/71	1240	1.926	
2/19/71	1268	1.948	
3/18/71	1295	1.966	
6/4/71	1373	2.012	
7/13/71	1412	2.044	
8/10/71	1440	2.060	
9/9/71	1470	2.076	
10/7/71	1498	2.093	
11/8/71	1530	2.114	
12/16/71	1568	2.136	
1/28/72	1611	2.164	
2/16/72	1630	2.174	
3/22/72	1665	2.193	
4/11/72	1685	2.202	
5/23/72	1727	2.226	
6/15/72	1750	2.243	
9/20/72	1847	2.293	
10/20/72	1877	2.305	
11/28/72	1916	2.329	
1/19/73	1968	2.357	
2/15/73	1995	2.368	
4/12/73	2051	2.402	
11/8/73	2261	2.498	

TABLE A4-4 CONT'D.

		INSTRUMENT, LOCATION, & ELEVATION (FT.)							
DATE	CONSTR. DAY		PCP 1 -5.0	PCP 2 -30.0	PCP 3 -79.9	PCP 4 -138.8		PCP 6 -3.9	PCP 5 -30.0
9/1/67	1		℄					160'R.	
10/17/67	47		+3.24		+4.87	+3.49			+3.48
10/24/67	54		4.12	+4.17	3.77	3.42			3.29
11/1/67	62		5.15	7.11	4.00	4.87			
11/9/67	70		4.78		3.88	3.23			3.94
11/20/67	81		4.99	5.73	4.01	3.85			4.04
11/27/67	88		3.94	3.89	4.00	5.73			3.88
11/29/67	90		5.87	3.77	4.12	6.62		+3.48	3.46
12/4/67	95		5.76	5.18	4.13	5.77		3.64	4.64
12/8/67	99		4.59	5.32	7.92	5.89		3.20	4.84
12/14/67	105		3.48	4.21	8.00	4.07		3.48	4.44
12/15/67	106		3.28	5.18	8.50	4.22		3.48	4.34
12/20/67	111		3.16	4.60		3.57		3.02	4.10
12/28/67	119		3.42	4.27		4.35		3.50	3.66
1/4/68	126		4.60	4.38	9.37	3.58		3.18	4.12
1/15/68	137				10.94	3.46		2.65	
2/1/68	154				8.50	2.97		3.35	
2/8/68	161				7.89	2.90		3.19	
3/7/68	189				11.20	3.20			
3/25/68	207					4.81			
4/12/68	225		4.35	5.10	10.35	3.68		3.74	4.51
4/23/68	236		5.17	4.94		3.67		3.95	4.53
5/3/68	246		6.51	5.04	10.89	3.18		3.72	4.49
5/24/68	267		6.10	4.53	9.74	3.25		3.47	4.13
6/7/68	281		7.02		9.28			3.05	4.00
6/14/68	288		6.59	5.94	10.44				
6/21/68	295		6.01						
6/25/68	299								
7/1/68	305		7.20		11.82			2.60	
7/12/68	316		6.56	4.95					
7/17/68	321		6.25	5.05	13.90			1.60	
7/22/68	326		5.86	5.17	14.13				
7/23/68	327		5.91	5.64	16.43				
7/24/68	328		6.03	5.90	15.28	4.45			
7/25/68	329		5.99	6.19	15.97	4.95			
7/26/68	330		5.95	5.99	17.35	4.19			
7/31/68	335		5.30	5.71	20.81				
8/1/68	336	(END)	5.45	5.75	20.81				

TABLE A5-1 WELL & PIEZOMETER DATA, STA. 245, ℄ & 160'R.

		INSTRUMENT, LOCATION, & ELEVATION (FT.)							
DATE	CONSTR DAY	WP1 (4'L)	P5 -15.9	P6 -28.6	P7 -55.0	P8 -80.2	P9 -105.2	P10 -135.0	P11 -147.4
9/1/67	1								
7/15/68	319	+2.86							
7/19/68	323	3.26			+9.52	+13.41	+12.50	+5.10	+13.41
7/24/68	328	3.07	+7.58	+4.98	15.50	18.25	17.57	10.65	15.49
7/25/68	329	3.07	8.37	4.98	17.34	19.41	18.26	10.65	15.02
7/29/68	333	3.14	6.11	4.41	18.03	19.87	19.42	10.08	
8/1/68	336	2.26	5.54	4.98	18.26	20.10	19.42	9.52	
8/5/68	340	2.26			20.80	21.72	21.03	9.74	
8/7/68	342	2.35			21.26	22.18	21.72	10.08	8.37
8/8/68	343	2.39	6.11	5.54	21.49	22.18	21.72	9.74	7.81
8/12/68	347	2.61	6.11	6.11	21.72	22.18	21.95	9.74	
8/16/68	351	2.47	4.98	6.67	22.18	23.10	22.45	9.74	
8/21/68	356	2.27	4.42	8.94	25.42	25.64	24.49	10.65	
8/26/68	361	2.52	4.60	8.60	26.30	26.10	25.00	10.70	
8/29/68	364	2.61	3.30	9.70	27.00	27.30	26.30	10.70	
9/6/68	372	2.49	3.40	9.50	28.00	27.90	26.30	10.65	
9/11/68	377	2.46		10.07	29.11	29.10	26.80	11.81	
9/16/68	382	2.21	3.96	10.64	31.42	31.20	27.03	11.81	
9/19/68	385	2.07	3.96	10.64	31.42	31.41	26.80	10.65	
9/26/68	392	2.73	3.96	11.80	34.19	34.41	29.11	12.50	
9/30/68	396	2.81	5.55	12.72	35.57	36.26	30.04	12.50	
10/4/68	400	2.85	4.99	12.95	36.50	38.33	32.57	12.73	
10/7/68	403	2.58	4.31	12.50	36.51	39.50	32.82	12.05	
10/8/68	404	2.19	4.31	12.50	36.97	39.73	33.28	12.28	
10/18/68	414	1.89	3.74	14.11	40.20	40.42	40.20	13.43	
10/28/68	424	2.42	4.54	14.34	42.05	36.50	42.97	14.80	14.11
11/6/68	433	2.53	4.87	14.11	41.82	35.35	45.97	16.89	13.88
11/15/68	442	2.95	5.19	13.86	44.85	41.12	45.49	18.26	8.58
11/20/68	447	3.23	5.19	12.67		38.81	47.10	18.95	8.58
11/27/68	454	3.03	4.62	13.43	43.41	39.73	45.49	18.95	8.58
12/4/68	461	2.84		13.86	44.62	44.58	46.64	19.64	7.45
12/9/68	466	2.70	4.87	14.11	43.43	44.33	46.64	19.64	7.06
12/20/68	477	3.23	5.19	13.86	42.26	44.10	46.18	20.34	7.45
12/30/68	487	2.48	4.74	13.86	41.57	42.48	45.72	20.11	6.88
1/10/69	498	2.07	4.30	13.61	41.32	42.96	44.78	19.86	7.20
1/20/69	508	2.17	4.04	13.61	40.16	42.23	44.55	20.55	7.20
1/31/69	519	2.27	4.37	13.61	39.73	41.08	43.89	20.55	7.20
2/7/69	526	2.17	4.04	13.61	39.04	41.31	43.66	20.42	7.20

TABLE A5-2 WELL & PIEZOMETER DATA, STA. 246, ℄

DATE	CONSTR DAY	INSTRUMENT, LOCATION & ELEVATION (FT.) WP1 (4'L)	P5 -15.9	P6 -28.6	P7 -55.0	P8 -80.2	P9 -105.2	P10 -135.0	P11 -147.4
2/19/69	538	+2.47	+4.94	+13.61	+39.04	+41.31	+43.43	+20.55	+7.20
3/10/69	557	2.43	4.74	13.61	38.11	41.31	42.24	20.55	7.20
3/22/69	569	2.91	4.94	13.84	37.39	41.08	42.01	20.32	7.76
3/29/69	576	3.04	4.94	13.61	36.93	40.62	40.76	20.55	7.09
4/9/69	587	2.68	4.58	13.38	36.93	39.67	41.30	19.84	6.84
4/16/69	594	2.57	4.49	12.67	36.22	39.67	41.53	20.07	6.73
4/23/69	601	2.76	4.49	13.13	37.84	41.52	43.61	20.99	6.73
4/30/69	608	2.58	4.35	12.90	38.96	41.98	43.84	21.22	6.50
5/6/69	614	2.71	4.58	12.44	39.22	43.60	45.22	22.38	6.51
5/12/69	620	2.58	4.25	12.67	40.78	44.68	46.32	23.01	6.28
5/14/69	622	2.44	4.25	12.57	41.47	45.38	47.24	23.24	6.28
6/11/69	650	2.30	3.12	12.93	41.14		42.29	23.79	6.06
7/2/69	671	2.51	3.23	12.70			36.29	23.56	6.18
8/6/69	706	2.51	2.89	12.58		43.08	35.96	22.97	6.28
9/4/69	735	2.01	2.66	12.58		42.97	40.35	22.51	6.06
10/16/69	777	2.25					44.50	22.05	
10/31/69	792	1.99	2.77	12.58		42.62	44.27	21.36	6.06
1/7/70	860	2.92	4.36	13.04		43.54	45.43	22.28	6.06
1/28/70	881	2.20	5.49	13.04		41.46	44.50	21.36	6.06
2/23/70	907	2.41	7.53	13.04		43.08	43.81	20.66	6.06
4/15/70	958	1.90	7.76	13.04	8.92	43.08	43.58	20.43	6.06
5/7/70	980	2.40	7.76	13.04	8.92	41.23	42.99	20.43	6.06
7/3/70	1037	2.36	5.49			34.30	38.96	19.28	7.98
9/18/70	1114	1.96	6.62	8.89		35.46	41.73	18.59	7.87
10/30/70	1156	1.64	6.06	12.35		34.76	41.73	18.36	7.76
12/21/70	1208	1.87	7.76	3.44		43.02	37.57		7.76
1/22/71	1240	1.63	7.64	3.21		43.26	41.96	14.61	7.87
2/11/71	1260	2.12	7.53	3.26		44.52	41.96	14.74	7.64
3/18/71	1295	2.25	7.76	3.38		46.38	41.50	14.60	7.98
6/4/71	1373	2.07	7.19				41.27		7.98
7/13/71	1412	2.91	6.28	3.47		47.20	40.81	14.40	7.98
8/10/71	1440	1.98	6.62	3.38		46.37	39.88	14.20	8.44
9/9/71	1470	2.28	6.40	3.49		46.07	39.42	13.25	8.32
10/7/71	1498	2.33	6.62				39.88		8.32
11/8/71	1510	2.17	6.62	3.79		45.78	39.88	13.10	8.32
12/16/71	1568	1.94	6.62	3.25		45.25	40.81	13.50	7.98
1/24/72	1607	2.11	6.62	3.41		45.42	40.81	13.47	7.98
2/11/72	1625	1.51	6.62	2.85		45.44	40.35	13.35	7.98

TABLE A5-2 CONT'D.

		INSTRUMENT, LOCATION & ELEVATION (FT.)							
DATE	CONSTR DAY	WP1 (4'L)	P5 -15.9	P6 -28.6	P7 -55.0	P8 -80.2	P9 -105.2	P10 -135.0	P11 -147.4
3/22/72	1665	2.83	6.74	3.88		45.50	40.81	13.86	7.98
4/5/72	1679	2.38	6.62	3.46		45.33	40.58	13.60	7.98
5/23/72	1727	2.49	6.28	3.68		45.25	40.12	13.46	8.32
6/15/72	1750	3.15	6.06	4.15		45.31	39.88	13.65	8.10
9/20/72	1847	1.99	4.92	3.42		44.79	38.96	12.70	8.32
10/20/72	1877	1.94	5.26	3.53		44.62	38.96	12.80	8.32
11/28/72	1916	1.84	5.49	4.04		45.05	39.42	13.34	8.32
1/19/73	1968	2.39	6.51	3.92		44.07	39.42	13.13	8.44
2/15/73	1995	2.26	6.62	3.96		44.28	39.42	13.23	8.32
4/12/73	2053	2.75	7.19	4.89		43.90	39.42	13.18	8.32
7/18/73	2148	2.20	5.73	3.65		43.86	39.19	12.65	8.44
1/3/74	2317	2.40	5.50	4.48			36.65	12.37	7.99

TABLE A5-2 CONT'D

		INSTRUMENT, LOCATION, & ELEVATION (FT.)						
DATE	CONSTR DAY	WP2 (30'R)	P 14 -15.0	P 15 -29.7	P 16 -55.1	P 17 -80.8	P 18 -115.5	P 19 -135.0
9/1/67	1							
7/15/68	319	+2.85	+3.40	+5.45	+6.35	+9.97	+8.38	+6.01
7/19/68	323	2.30		6.01	8.28	11.82	9.18	7.37
7/24/68	328	2.25	3.17	8.85	16.21	17.35	14.82	14.13
7/25/68	329	2.35	3.17	8.28	16.90	18.74	15.74	13.67
7/29/68	333	2.49	3.17	7.71	18.05	19.66	16.66	14.59
8/1/68	336	2.02		7.71	18.28	20.58	16.89	9.41
8/5/68	340	2.30		8.28	19.67	21.73	18.04	9.98
8/7/68	342	2.34	3.17	8.28	20.36	22.20	18.27	9.98
8/8/68	343	2.37	3.17	8.28	20.36	22.66	18.27	9.98
8/12/68	347	2.60	3.74	8.28	20.36	23.35	18.27	9.41
8/16/68	351	2.45	3.17	9.07	21.75	24.05	19.20	9.98
8/21/68	356	2.31	3.40	11.14	24.29	26.35	20.35	11.14
8/26/68	361	2.49	3.70	11.80	25.70	27.00	21.00	11.14
8/29/68	364	2.57	3.40	12.50	26.60	28.40	21.50	12.10
9/6/68	372	2.39	3.20	12.98	27.74	29.13	21.51	11.84
9/11/68	377	2.41	3.52	13.67	28.44	30.28	21.51	11.84
9/16/68	382	2.26	3.19	14.60	30.52	32.36	21.51	12.07
9/19/68	385	2.10	3.19	14.14	30.52	32.59	21.97	11.84
9/26/68	392	2.72	3.75	16.90	33.06	35.36	23.36	12.30
9/30/68	396	2.75	3.75	16.67	34.21	36.28	23.82	12.30
10/4/68	400	2.90	3.99	17.36	36.52	37.89	23.82	12.76
10/7/68	403	2.55	2.77	16.72	36.79	38.63	23.17	12.33
10/8/68	404	2.48	3.10	16.95	37.02	38.86	23.40	12.79
10/18/68	414	2.00	3.10	18.79	41.64		25.70	16.25
10/28/68	424	2.34	3.67	19.02	42.33	44.42	28.47	18.46
11/6/68	433	2.50	3.10	19.25	43.02	45.78	27.62	20.41
11/15/68	442	3.00	3.67	19.94	43.71		28.31	21.33
11/20/68	447	3.20	3.67	19.71	43.94		31.24	22.02
11/27/68	454	2.95	3.33	19.36	43.48		31.82	21.67
12/4/68	461	2.90	3.33	20.05	42.21		32.05	20.98
12/9/68	466	2.65	3.33	18.21	42.44		32.28	20.98
12/20/68	477	3.30	3.56	16.37	41.43		33.90	20.98
12/30/68	487	2.52	3.33	17.03	41.98		34.36	20.75
1/10/69	498	1.97	3.33	15.44			34.82	20.75
1/20/69	508	2.17	3.10	14.06	41.98		34.82	20.52
1/31/69	519	2.32	3.33	14.29	39.33	42.35	35.14	20.20
2/7/69	526	2.22	3.33	13.83	38.55	41.89	35.55	19.89

TABLE A5-3 WELL & PIEZOMETER DATA, STA. 246, 30'R

DATE	CONSTR DAY	INSTRUMENT, LOCATION, & ELEVATION (FT.) WP2 (30'R.)	P14 -15.0	P15 -29.7	P16 -55.1	P17 -80.8	P18 -115.5	P19 -135.0
2/19/69	538	+2.52	+3.56	+14.06	+38.55	+37.04	+36.70	+20.20
3/10/69	557	2.45	3.61	14.02	36.89	39.12	37.59	20.25
3/22/69	569	3.02	6.01	13.33	36.63	42.78	36.63	19.10
3/29/69	576	3.15	4.42	11.94	36.40	42.78	37.79	20.02
4/9/69	587	2.72	3.29	11.91	35.94	37.01	37.33	19.79
4/16/69	594	2.56	3.18	11.71	35.94	38.17	36.63	19.33
4/23/69	601	2.72	3.18	12.40	37.56	36.87	37.33	20.48
4/30/69	608	2.56	3.18	12.63	38.71	39.89	36.87	20.93
5/6/69	614	2.74		13.33	39.87	41.25		21.87
5/12/69	620	2.64		13.68	41.14	43.20		22.68
5/14/69	622	2.51		13.45	42.29	44.58		22.91
6/11/69	650	2.30		14.51	42.70	45.91	36.44	22.81
7/2/69	671	2.52		13.12	41.77		36.44	22.36
8/6/69	706	2.50		12.31	39.81		36.09	21.54
9/4/69	735	2.29		11.62	39.11		35.63	19.23
10/16/69	777	2.32					35.40	
10/31/69	792	2.04		11.16	38.42		35.40	14.62
1/7/70	860	2.91		10.70	38.88		35.63	15.08
1/28/70	881	2.23		10.70	38.88		35.63	15.08
2/23/70	907	1.99		10.24	38.88		34.94	15.03
4/15/70	958	1.88		10.24	37.34		33.78	15.03
5/7/70	980	2.33	2.70	10.24	37.27		33.78	15.08
7/3/70	1037	2.14		8.39	31.72		31.24	24.77
9/18/70	1114	2.11		7.26	32.65	10.68	30.55	19.92
10/30/70	1156	1.67		6.69	32.65	10.45	31.47	19.69
12/21/70	1208	1.94		7.26	33.68	12.75	31.47	19.92
1/22/71	1240	1.68		6.80	33.34	10.68	31.47	19.23
2/11/71	1260	2.15		7.37	32.65	9.29	31.47	15.31
3/18/71	1295	2.12		7.14	32.41	9.29	31.47	15.03
6/4/71	1373	1.91		7.82	33.80	8.83	31.47	13.47
7/13/71	1412	2.03		6.69	34.72	10.68	31.47	18.08
8/10/71	1440	2.01		6.12	34.49	10.68	30.78	17.39
9/9/71	1470	2.59		5.56	35.65	10.22	30.32	15.31
10/7/71	1498	2.38		5.56	36.11	10.22	31.01	17.16
11/8/71	1510	2.26			35.65	10.22	33.32	17.62
12/16/71	1568	2.43			35.19	10.45	34.70	18.08
1/24/72	1607	1.76			32.65	10.22	36.09	18.08
2/11/72	1625	1.38			32.41	10.22	36.32	17.39

TABLE A5-3 CONT'D.

DATE	CONSTR DAY	INSTRUMENT, LOCATION, & ELEVATION (FT.) WP2 (30'R)	P14 -15.0	P15 -29.7	P16 -55.1	P17 -80.8	P18 -115.5	P19 -135.0
3/22/72	1665	+2.62			+32.18	+ 9.52	+38.40	+17.39
4/5/72	1679	2.10			31.49	9.52	38.40	18.08
5/23/72	1727	2.50			30.80	9.99	38.40	17.85
6/15/72	1750	2.84			30.80	9.52	37.94	17.16
9/20/72	1847	2.01			28.49	12.98	36.09	15.03
10/20/72	1877	2.05			28.49	12.52	36.32	15.03
11/28/72	1916	2.35			28.49	12.75	36.78	15.03
1/19/73	1968	2.74			28.49	20.83	38.40	15.54
2/15/73	1995	2.80			28.95	16.21	39.09	16.23
4/12/73	2053	2.89			28.95	12.75	39.56	17.62
7/18/73	2148	1.96	4.40	6.36	26.41	12.75	36.09	15.32
1/3/74	2317	2.50	4.96	6.13	26.41	11.37	35.86	13.93

TABLE A5-3 CONT'D.

		INSTRUMENT, LOCATION, & ELEVATION (FT.)						
DATE	CONSTR DAY	WP-1 (4'L.)	Pe 1 -15.0	Pe 2 -31.2	Pe 3 -56.6	Pe 4 -81.0	Pe 5 -105.3	Pe 6 -136.6
7/10/68	314	+2.86	+1.00		+0.60	+10.60	+15.10	+5.40
7/15/68	319	2.86	0.80		2.10	10.60	15.10	5.90
7/19/68	323	3.26	1.00	2.80	2.10	12.50	16.30	6.40
7/24/68	328	3.07	1.20	2.80	4.30	12.50	18.50	7.40
7/25/68	329	3.07	1.00	5.20	6.80	16.00	22.30	10.20
7/29/68	333	3.14	1.80		7.70	17.30	22.00	11.00
8/1/68	336	2.26						
8/6/68	340	2.26	1.80	4.80	8.60	20.20	24.20	9.20
8/7/68	342	2.35	1.20	5.20	8.60	20.20	25.00	9.20
8/8/68	343	2.39	1.20	5.20	8.90	20.50	25.80	9.20
8/12/68	347	2.61	1.80	5.80	9.80	21.40	26.20	9.20
8/16/68	351	2.47						
8/21/68	356	2.27	-0.20	8.00	12.00	24.60	28.50	10.40
8/26/68	361	2.52	+0.20	7.20	12.50	25.20	29.30	9.20
8/29/68	364	2.61	-0.20	8.00	13.60	25.80	30.10	10.20
9/6/68	372	2.49	+1.80	7.20	14.60	27.60	31.30	10.20
9/10/68	377	2.46	1.80	8.00	14.60	28.40	33.30	10.20
9/16/68	382	2.21	1.80	9.60	17.40	31.70	32.10	10.20
9/18/68	385	2.07	2.30	9.20	17.40	31.70	32.70	10.20
9/26/68	392	2.73	2.30	10.40	20.40	34.80	33.90	10.80
9/30/68	396	2.81	2.80	10.40	20.40	36.00	34.50	10.80
10/4/68	400	2.85	2.40	11.10	22.60	38.00	34.50	10.20
10/7/68	403	2.58	3.80	11.10	23.60	39.10	34.70	10.60
10/8/68	404	2.19	3.80	12.40	24.10	39.40	34.90	12.60
10/18/68	414	1.89	3.10	12.40	27.40	43.40	40.10	13.80
10/28/68	424	2.42	4.00	13.20	29.40	44.80	41.10	18.70
11/6/68	433	2.53	5.30	12.40		47.60	44.70	20.10
11/15/68	442	2.95	6.00	12.40		49.30	47.00	22.00
11/20/68	447	3.23	6.00	12.40		49.60	48.00	22.30
11/27/68	454	3.03	3.80	10.80		49.60	47.30	21.70
12/4/68	461	2.84	7.70	10.40		50.20	48.00	21.40
12/9/68	466	2.70	5.30	9.60		50.20	48.30	21.40
12/20/68	477	3.23		8.80		49.60	49.10	21.00
12/30/68	487	2.48	5.40	8.00		49.60	49.80	20.70
1/8/69	498	2.07	4.30	7.20		49.00		20.70
1/20/69	508	2.17						
1/27/69	515	2.27	3.80	6.50		48.40		19.70
2/7/69	526	2.17	8.00	5.80		47.60		20.00

TABLE A5-4 WELL & PIEZOMETER DATA, STA. 246, 30'L.

		INSTRUMENT, LOCATION, & ELEVATION (FT.)						
DATE	CONSTR DAY	WP 1 (4'L)	Pe 1 -15.0	Pe 2 -31.2	Pe 3 -56.6	Pe 4 -81.0	Pe 5 -105.3	Pe 6 -136.6
2/19/69	538	+2.47	+7.40	+5.80		+47.00		+19.70
3/10/69	557	2.43	6.80	5.10		46.20		19.70
3/22/69	569	2.91						
3/25/69	572	3.04	10.00	5.10		45.90		18.90
4/9/69	587	2.68	14.50	2.80		45.60		18.60
4/16/69	594	2.57						
4/23/69	601	2.76	16.50	3.00		46.60		19.20
4/30/69	608	2.58	16.50	3.60		47.30		19.80
5/6/69	614	2.71	19.70	4.40		48.70		20.00
5/12/69	620	2.58	21.20	5.90		49.60		21.10
5/14/69	622	2.44	19.10	5.50		50.20		21.70
6/11/69	650	2.30	23.00	4.70		51.00		22.10
7/2/69	671	2.51		5.10		49.60		21.10
8/6/69	706	2.51		2.80				20.80
9/4/69	735	2.01						
10/16/69	777	2.25						
10/31/69	792	1.99						18.20
1/7/70	860	2.92						18.60
1/28/70	881	2.20						18.00
2/23/70	907	2.41						17.80
4/15/70	958	1.90						17.00
5/7/70	980	2.40						17.40
7/3/70	1037	2.36				41.40		16.00
9/18/70	1114	1.96						
10/30/70	1156	1.64				40.02		15.25
12/21/70	1208	1.84						
1/22/71	1240	1.63				40.02		
2/11/71	1260	2.12						
3/18/71	1295	2.25						
6/4/71	1373	2.07		0.0				
7/13/71	1412	2.91		0.80				13.25
8/10/71	1440	1.98		1.20				13.45
9/9/71	1470	2.28		1.20				13.25
10/7/71	1498	2.33		3.60				13.25
11/8/71	1510	2.17		1.20				13.25
12/16/71	1568	1.94						
1/24/72	1607	2.11						
2/11/72	1625	1.51						10.85

TABLE A5-4 CONT'D.

		INSTRUMENT, LOCATION, & ELEVATION (FT.)						
DATE	CONSTR DAY	WP1 (4'L.)	Pe 1 -15.0	Pe 2 -31.2	Pe 3 -56.6	Pe 4 -81.0	Pe 5 -105.3	Pe 6 -136.6
3/22/72	1665	2.83		2.04				12.65
4/5/72	1679	2.38		2.04				11.85
5/23/72	1727	2.49		2.86				11.85
6/15/72	1750	3.15		3.64				11.85
9/20/72	1847	1.99		2.86				9.25
10/20/72	1877	1.94		2.86				9.25
11/28/72	1916	1.84		4.44				11.45
1/19/73	1968	2.39						
2/15/73	1995	2.26		5.04				11.85
4/12/73	2053	2.75		5.04				11.45
7/18/73	2148	2.20						
1/3/74	2317	2.40						

TABLE A5-4 CONT'D.

DATE	CONSTR. DAY	INSTRUMENT, LOCATION, & ELEVATION (FT.)					
		WP3 (60'R)	P20 -13.8	P21 -28.8	P22 -55.8	P23 -79.9	P24 -104.0
9/1/67	1						
7/15/68	319	+2.74	+3.25	+3.35	+9.05	+9.05	+9.47
7/19/68	323	2.24	2.68	3.81	8.15	9.62	10.85
7/24/68	328	2.24	2.68	5.50	14.93	16.08	15.93
7/25/68	329	2.24	2.68	4.94	15.39	16.54	16.39
7/29/68	333	2.03	2.68	4.37	16.77	17.69	16.85
8/1/68	336	2.04	2.68	4.37	17.00	18.39	17.08
8/5/68	340	2.37			18.39	19.08	18.70
8/7/68	342	2.35			18.39	20.00	18.83
8/8/68	343	2.39	3.25	4.94	18.39	20.00	18.93
8/12/68	347	2.42	3.25	4.94	18.39	20.23	19.39
8/16/68	351	2.23	2.68	5.72	19.08	21.15	20.78
8/21/68	356	2.17	3.26	6.64	21.16	23.01	21.70
8/26/68	361	2.28	3.30	7.20	22.50	23.50	22.60
8/29/68	364	2.46	3.50	7.80	23.50	24.90	23.30
9/6/68	372	2.10	3.26	8.34	23.93	25.54	23.55
9/11/68	377	2.18	3.26	8.45	24.85	26.47	23.78
9/16/68	382	2.07	3.26	9.47	26.24	28.31	25.16
9/19/68	385	1.91	3.26	9.47	26.47	29.24	25.16
9/26/68	392	2.49	3.26	11.32	28.54	31.54	26.52
9/30/68	396	2.56		11.78	29.93	33.16	27.01
10/4/68	400	2.81	3.83	12.47	31.08	35.47	27.93
10/7/68	403	2.14	2.43	11.98	30.82	36.49	27.44
10/8/68	404	2.03	2.76	11.98	30.59	36.82	27.67
10/18/68	414	1.88	2.20	14.06	34.75	41.44	
10/28/68	424	2.10	3.33	14.29	37.05	43.98	
11/6/68	433	2.27	3.00	14.75	36.59	45.36	
11/15/68	442	2.73	3.00	15.44	39.13	46.75	
11/20/68	447	2.99	3.33	15.90	39.36	47.90	
11/27/68	454	2.69	3.33	14.75	39.36	48.13	
12/4/68	461	2.77	3.33	15.44	39.36	48.36	
12/9/68	466	2.39	3.33	15.67	39.13	51.59	
12/20/68	477	3.09	3.59	12.84	38.80	48.03	
12/30/68	487	2.41	3.48	13.07	38.37	49.88	
1/10/69	498	1.86	3.03	11.45	37.68		
1/20/69	508	2.06	3.03	10.99	36.98		
1/31/69	519	2.21	3.03	10.99	36.29	46.45	
2/7/69	526	2.46	3.03	9.83	35.65	46.22	

TABLE A5-5 WELL & PIEZOMETER DATA, STA. 246, 60'R.

		INSTRUMENT, LOCATION, & ELEVATION (FT.)					
DATE	CONSTR. DAY	WP3 (60'R)	P20 -13.8	P21 -28.8	P22 -55.8	P23 -79.9	P24 -104.0
2/19/69	538	+2.86	+3.24	+11.22	+35.37	+45.30	
3/10/69	557	2.36	3.03	12.84	34.67	44.37	
3/22/69	569	2.92	4.16	10.53	34.29	43.45	
3/29/69	576	2.99	4.16	8.98	33.72	43.88	
4/9/69	587	2.55	3.03	9.37	33.03	43.65	
4/16/69	594	2.41	3.03	8.91	32.57	44.34	
4/23/69	601	2.55	3.03	9.14	34.42	45.96	
4/30/69	608	2.39	2.81	9.37	34.65	47.11	
5/6/69	614	2.58	3.03	9.84	36.03	48.03	
5/12/69	620	2.57	2.75	10.48	36.89	49.81	
5/14/69	622	2.45	2.75	10.71	37.58	50.04	
6/11/69	650	2.23	2.68	10.41	37.98	51.04	38.33
7/2/69	671	2.40	2.68	9.95	37.29	50.33	38.57
8/6/69	706	2.48	2.66	9.39	36.25	49.22	38.53
9/14/69	735	1.94	2.32	8.93	35.33	48.29	38.07
10/16/69	777	2.14	2.77				37.84
10/31/69	792	1.95	2.32	8.13	34.63	46.68	37.61
1/7/70	860	2.81	3.11	8.48	34.87	46.80	11.50
1/28/70	881	2.21	2.55	8.70	33.71	45.76	9.42
2/23/70	907	2.40	2.55	9.39	33.25	45.53	35.76
4/15/70	958	3.06	2.77	7.22	32.56	44.84	19.34
5/7/70	980	2.26	2.55	7.22	31.40	44.15	10.58
7/3/70	1037	2.81	1.53	10.32	31.17	42.53	31.60
9/18/70	1114	1.99	1.53	5.97	29.09	41.14	10.58
10/30/70	1156	1.62	1.41	5.75	28.63	40.91	17.96
12/21/70	1208	1.85	1.98	6.45	28.40	40.68	27.65
1/22/71	1240	1.60	1.75	6.54	28.86	40.22	23.73
2/11/71	1260	2.10	2.21	6.77	30.01	40.22	28.37
3/18/71	1295	2.59	2.21	7.11	28.86	39.76	33.22
6/4/71	1373	1.90	1.98	5.41	28.63	39.53	8.73
7/13/71	1412	2.00	2.55	5.41	26.76	38.83	31.37
8/10/71	1440	1.98	1.98	4.95	27.45	38.37	32.53
9/9/71	1470	2.49	6.51	5.41	27.72	38.37	31.83
10/7/71	1498	2.39	7.64		27.22	38.14	32.29
11/8/71	1510	2.34	7.08	5.97	27.22	38.14	32.53
12/16/71	1568	2.10	4.92	5.75	27.22	38.37	32.76
1/24/72	1607	1.69	4.24	5.97	26.52	38.14	31.14
2/11/72	1625	1.35	3.68	6.20	27.45	38.14	31.14

TABLE A5.5 CONT'D.

		INSTRUMENT, LOCATION, & ELEVATION (FT.)					
DATE	CONSTR. DAY	WP3 (60'R)	P20 -13.8	P21 -28.8	P22 -55.8	P23 -79.9	P24 -104.0
3/22/72	1665	+2.59	+3.90	+6.88	+28.17	+38.37	+31.14
4/5/72	1679	2.04	3.79	6.88	28.40	38.37	31.83
5/23/72	1727	2.47	4.58	6.43	26.76	37.91	31.83
6/15/72	1750	1.83	5.38	6.31	26.76	37.91	31.83
9/20/72	1847	2.09	4.92	4.73	21.68	36.98	29.52
10/20/72	1877	2.15	4.36	4.84	22.14	36.98	25.11
11/28/72	1916	2.32	4.81	5.07	22.83	37.22	19.80
1/19/73	1968	2.69	8.44	6.20	26.76	36.98	26.57
2/15/73	1995	2.88	9.36	7.11	30.71	37.45	31.60
4/12/73	2053	2.91	6.51	7.11	31.63	36.52	28.83
7/18/73	2148	2.03	6.29	5.19	23.32	36.06	5.22
1/3/74	2317	2.50	6.51	5.91	22.14	36.06	19.82

TABLE A5-5 CONT'D.

		INSTRUMENT, LOCATION, & ELEVATION (FT.)				
DATE	CONSTR. DAY	WP4 (95'R.)	P25 -13.8	P26 -29.9	P27 -54.8	P28 -104.7
9/1/67	1					
7/15/68	319	+2.53	+4.12	+3.22	+4.12	+11.19
7/19/68	323	2.45	3.78	3.44	5.48	13.26
7/24/68	328	2.33		4.91	11.19	16.49
7/25/68	329	2.27		4.35	11.19	17.18
7/29/68	333	1.93	0.74	4.35		17.88
8/1/68	336	1.93		3.78	11.19	18.11
8/5/68	340	2.54			11.42	18.57
8/7/68	342	2.11			11.42	18.57
8/8/68	343	2.37	7.75	4.35	11.42	18.80
8/12/68	347	2.32		3.78	11.19	19.26
8/16/68	351	2.15		4.35	11.42	20.19
8/21/68	356	2.23		4.35	13.04	20.65
8/26/68	361	2.10		4.90	13.50	21.60
8/29/68	364	2.50		4.90	13.50	22.00
9/6/68	372	1.93	3.23	4.92	13.83	22.27
9/11/68	377	2.02	3.23	5.16	14.06	22.50
9/16/68	382	2.03	3.23	5.49	15.34	22.96
9/19/68	385	1.88	3.23	5.49	15.57	22.96
9/26/68	392	2.30	3.23	6.18	16.95	24.57
9/30/68	396	2.32	3.79	6.62	17.19	24.80
10/4/68	400	2.78	3.79	7.18	18.11	25.26
10/7/68	403	2.02	3.07	6.45	18.63	25.33
10/8/68	404	2.01	3.07	6.67	18.40	25.79
10/18/68	414	1.95	3.70	7.58	22.10	28.79
10/28/68	424	2.01	3.62	8.14	22.79	30.40
11/6/68	433	2.28	3.62	8.14		32.71
11/15/68	442	2.78	4.19	8.71	24.86	34.33
11/20/68	447	2.89	4.19	8.71	25.32	35.25
11/27/68	454	2.54	3.62	8.71	25.55	35.25
12/4/68	461	2.83	4.75	8.71	25.09	35.94
12/9/68	466	2.16	3.62	8.71		35.71
12/20/68	477	2.91	4.29	8.14	25.32	35.94
12/30/68	487	2.48	4.19	8.14	25.09	35.94
1/10/69	498	1.75	1.93	7.58	24.86	30.66
1/20/69	508	2.20	1.93	7.58	24.40	34.35
1/31/69	519	2.40	2.59	7.24	24.17	34.03
2/7/69	526	2.30	1.93	7.01		34.35

TABLE A5-6 WELL & PIEZOMETER DATA, STA. 246, 95'R.

		INSTRUMENT, LOCATION, & ELEVATION (FT.)				
DATE	CONSTR. DAY	WP4 (95'R.)	P25 -13.8	P26 -29.9	P27 -54.8	P28 -104.7
2/19/69	538	+3.10	+2.14			+34.35
3/10/69	557	2.80	2.49	+7.35	+23.47	34.12
3/22/69	569	3.05	3.05	7.01		34.12
3/29/69	576	3.18	3.05	6.67		33.87
4/9/69	587	2.44	2.84	6.45	22.33	32.94
4/16/69	594	2.22	2.73	6.34	21.87	32.71
4/23/69	601	2.36	2.73	6.90		33.63
4/30/69	608	2.22	2.49	6.67	23.02	33.87
5/6/69	614	2.39	2.73	7.12	23.71	34.10
5/12/69	620	2.63	2.45	7.32	24.61	34.28
5/14/69	622	2.51	2.21	7.43	24.61	34.97
6/11/69	650	2.33	2.06	7.29	25.73	36.09
7/2/69	671	2.32	1.96	6.95		36.09
8/6/69	706	2.82	2.01			36.08
9/4/69	735	2.60	1.55	6.55	24.33	35.42
10/16/69	777	2.40		6.43	23.87	35.19
10/31/69	792	1.98	1.44	6.21	23.17	34.72
1/7/70	860	2.79	2.69	6.09	23.17	34.72
1/28/70	881	2.10	2.12	6.09	22.48	34.03
2/23/70	907	1.64	2.46	6.09	22.02	34.03
4/15/70	958	2.77	2.69	5.53	22.02	33.34
5/7/70	980	3.04	2.80			32.41
7/3/70	1037	2.47	2.69	4.96	20.87	24.08
9/18/70	1114	3.76	1.78	4.96		27.66
10/30/70	1156	1.82	1.55	4.39		27.31
12/21/70	1208	2.14	1.61	4.90	20.64	15.77
1/22/71	1240	2.06	3.82	4.73	22.02	24.54
2/11/71	1260	2.14	2.12	5.07		28.00
3/18/71	1295	2.76	2.57	4.79	19.71	27.31
6/4/71	1373	1.96		4.39	19.71	
7/13/71	1412	2.04	3.59	4.39	19.71	26.85
8/10/71	1440	2.04	7.22	4.51	19.25	26.38
9/9/71	1470	2.29	7.22	4.96	19.71	26.38
10/7/71	1498	2.79		4.39	19.48	26.38
11/8/71	1510	2.67	6.31	4.96	19.48	26.38
12/16/71	1568	1.80	6.99	4.62	18.79	26.38
1/24/72	1607	2.02	6.08	4.39		26.15
2/11/72	1625	1.51	6.88	4.39		26.85

TABLE A5-6 CONT'D.

		INSTRUMENT, LOCATION, & ELEVATION (FT.)				
DATE	CONSTR. DAY	WP4 (95'R.)	P25 -13.8	P26 -29.9	P27 -54.8	P28 -104.7
3/22/72	1665	+2.70	+6.08	+ 4.96	+24.56	+28.26
4/5/72	1679	2.24	6.08	4.96		27.54
5/23/72	1727	2.41	6.99	4.96	17.41	24.77
6/15/72	1750	2.98	7.44	4.96	13.04	22.92
9/20/72	1847	1.92	7.78	4.39	8.64	19.92
10/20/72	1877	1.81	7.78	4.62	12.79	21.31
11/28/72	1916	2.75	7.90	4.96	15.79	22.69
1/19/73	1968	2.20	8.35	4.96	20.17	25.46
2/15/73	1995	2.32	8.35	5.53	24.10	27.54
4/12/73	2053	3.39	8.35	4.96	22.71	27.31
7/18/73	2148	2.41	8.35	4.40	8.41	21.79
1/3/74	2317		7.45	3.95	18.11	26.87

TABLE A5-6 CONT'D.

		INSTRUMENT, LOCATION, & ELEVATION (FT.)							
DATE	CONSTR. DAY	WP5 (160'R.)		P29 -14.5	P30 -55.5	P31 -104.2		P33 -14.9	P32 -55.1
9/1/67	1			160'R.				225'R.	
7/15/68	319	+1.90							
7/19/68	323								
7/24/68	328								
7/25/68	329								
7/29/68	333			+3.25	+9.46	+11.32			
8/1/68	336			3.25	9.46	11.78			
8/5/68	340								
8/7/68	342								
8/8/68	343					11.32		+3.42	
8/12/68	347			2.12	8.34	11.78		6.82	+5.65
8/16/68	351				9.46	13.39		5.12	5.65
8/21/68	356				9.46	12.24		6.26	5.65
8/26/68	361				9.50	13.20		5.70	5.70
8/29/68	364			4.40	9.50	13.60		5.70	5.70
9/6/68	372			4.38	8.34	13.62		2.87	5.10
9/11/68	377								
9/16/68	382			4.38	8.45	13.39			
9/19/68	385			5.51	8.56	13.62		1.90	5.23
9/26/68	392			5.51	9.13	14.31		1.99	5.47
9/30/68	396			5.51	9.46	14.54			5.47
10/4/68	400			6.08	11.55	14.77			
10/7/68	403								
10/8/68	404	1.78		5.51	11.08	15.23			
10/18/68	414	1.90		5.51	12.23	16.95		2.08	6.70
10/28/68	424	1.45		4.38	12.92	18.24		0.81	6.62
11/6/68	433	2.05						1.92	6.77
11/15/68	442	1.56		3.82	15.23			2.51	6.77
11/20/68	447	1.49		3.82	16.15				
11/27/68	454	1.81		2.12	15.92			1.09	7.34
12/4/68	461	2.49							
12/9/68	466	2.20		3.71	13.85			2.94	
12/20/68	477	2.85		4.95	13.62	20.09		2.34	7.37
12/30/68	487	3.10		4.95	12.69	21.01		2.77	
1/10/69	498	1.50		3.71	12.69	20.55			
1/20/69	508	2.70		4.84	12.46	20.55			
1/31/69	519	2.90		4.95	12.23	20.55			6.47
2/7/69	526	3.00						2.99	6.55

TABLE A5-7 WELL & PIEZOMETER DATA, STA. 246, 160' & 225' R.

DATE	CONSTR. DAY	INSTRUMENT, LOCATION, & ELEVATION (FT.) WP5 (160'R.)		P29 -14.5	P30 -55.5	P31 -104.2		P33 -14.9	P32 -55.1
				160'R.				225'R.	
2/19/69	538	+2.90						+2.69	+6.47
3/10/69	557	2.62						2.29	6.37
3/22/69	569	2.97		+3.25	+11.77			2.78	6.11
3/29/69	576	2.79		2.69	12.00			2.31	6.02
4/9/69	587	2.24		2.12	12.00	+14.54		1.73	5.93
4/16/69	594	2.41		2.69	11.77	14.54		2.32	5.94
4/23/69	601	1.91		2.35	11.77	14.54		1.36	6.11
4/30/69	608	2.45		2.23	12.00	14.54		1.37	6.20
5/6/69	614	2.65		2.80	12.92	15.01		1.41	6.44
5/12/69	620	3.28		3.71	13.62	15.24		2.31	6.80
5/14/69	622	3.87		4.05	13.85	15.24		3.17	7.05
6/11/69	650	3.05		2.79	15.92	16.85		2.20	7.13
7/2/69	671	2.81		2.69	14.07	17.08		1.34	6.83
8/6/69	706	2.72		3.81	13.84	17.08		2.80	6.91
9/4/69	735	2.69		2.79	15.00	16.85		1.34	6.40
10/16/69	777	2.54			14.54	16.85		4.02	6.52
10/31/69	792	2.49		3.24	13.38	16.39		1.34	6.17
1/7/70	860	4.62			14.30	16.85			
1/28/70	881	3.09			15.23				
2/23/70	907	3.56		7.09	9.46	14.78			5.72
4/15/70	958	2.38		9.47	9.46	16.11			
5/7/70	980	3.14		9.47	11.77	15.01			
7/3/70	1037	3.94		1.31	8.44	16.16		1.66	5.87
9/18/70	1114	2.58		2.79	13.84	16.16			6.57
10/30/70	1156	1.50		3.35	12.46	14.12		3.06	3.99
12/21/70	1208	0.97		1.02	11.31	14.12			
1/22/71	1240	1.12		0.74	11.31	14.81			6.66
2/11/71	1260	2.04		2.21	10.85	15.04			6.73
3/18/71	1295	1.60		1.99	11.31	14.35			
6/4/71	1373	0.99		3.35	11.08	13.89			
7/13/71	1412	1.95		6.52	10.85	14.12		0.35	5.65
8/10/71	1440	2.10		15.24	10.38	14.12		-1.03	5.10
9/9/71	1470	1.47		21.01	11.31	13.65		-0.90	4.79
10/7/71	1498	3.37			11.31	14.12			
11/8/71	1510	2.30		21.70	10.85	13.65			4.75
12/16/71	1568	3.12		22.39	10.85	13.65		+2.38	4.78
1/24/72	1607	1.02		20.08	10.15	13.65		1.12	4.73

TABLE A5-7 CONT'D.

		INSTRUMENT, LOCATION, & ELEVATION (FT.)							
DATE	CONSTR. DAY	WP5 (160'R.)		P 29 -14.5	P 30 -55.5	P31 -104.2		P 33 -14.9	P32 -55.1
				160'R.				225'R.	
2/11/72	1625	+0.87		+20.54	+10.15	+13.65		-1.40	
3/22/72	1665	1.61		18.01	10.85	13.89		-0.55	+4.68
4/5/72	1679	0.97		16.85	10.15	13.65		-1.16	4.48
5/23/72	1727	2.17		14.55	11.54	13.19		-0.08	4.81
6/15/72	1750	2.30		13.62	10.15	13.65		+1.09	4.91
9/20/72	1847	2.27		9.93	9.00	13.42			5.25
10/20/72	1877	2.61		9.01	9.46	13.42		+0.77	4.91
11/28/72	1916	1.45		8.22	11.31	13.19		-0.85	4.84
1/19/73	1968	3.00		1.85	11.08	13.42		+0.57	5.55
2/15/73	1995	3.29		22.39	11.31	13.65		1.62	5.48
4/12/73	2053	2.43		22.16	10.15	12.27		0.10	4.92
7/18/73	2148	1.77		13.63	21.24	12.27		-0.41	
1/9/74	2323			7.99	31.64	8.02			

TABLE A5-7 CONT'D.

		ELEVATION (FT.) AND HORIZONTAL DEFLECTION (INCHES)												
DATE	CONSTR. DAY	+5	0	-10	-20	-30	-40	-50	-60	-70	-85	-100	-115	-130
7/24/68	328	+.324	+.269	+.192	+.132	+.154	+.126	+.080	+.071	+.066	-.022	-.022	+.035	+.027
8/29/68	364	.588	.605	.456	.451	.495	.423	.343	.297	.253	+.198	+.154	.107	.038
9/24/68	390	.088	.077	.055	.093	.016	.011	.002	-.033	-.038	-.137	-.055	-.019	-.027
10/3/68	399	.357	.390	.275	.275	.352	.412	.451	+.434	+.357	+.280	+.242	+.247	+.115
11/5/68	432	.511	.495	.324	.324	.500	.665	.649	.610	.511	.379	.275	.330	.170
12/7/68	464	.517	.534	.358	.358	.515	.677	.610	.457	.369	.226	.132	.259	.084
3/13/69	560	.424	.424	.281	.297	.462	.699	.662	.513	.396	.286	.072	.292	.012
4/19/69	597	.462	.462	.275	.292	.449	.688	.655	.501	.380	.292	.121	.270	-.010
6/13/69	652	.671	.666	.451	.457	.622	.787	.714	.561	.479	.358	.105	.303	-.033
7/7/69	676	.715	.726	.545	.545	.702	.841	.776	.663	.345	.517	.363	.567	+.092
8/8/69	708	.390	.289	.226	.238	.313	.430	.181	.157	-.011	.152	.022	.206	-.026
9/4/69	735	.021	-.061	-.085	-.004	.240	.462	.466	.518	+.341	.414	.318	.504	-.011
10/7/69	768	-.362	-.426	-.425	-.366	-.107	.162	.100	.139	.044	.193	.141	.407	+.108
12/1/69	823	+.451	+.336	+.268	+.304	+.471	.603	.400	.364	.212	.283	.120	.366	.037
1/28/70	881	.691	.570	.523	.570	.691	.867	.820	.832	.588	.637	.538	.711	.104
2/13/70	897	.749	.657	.600	.619	.736	.885	.844	.759	.553	.587	.423	.709	.142
5/13/70	986	.860	.720	.630	.680	.874	1.082	.980	.954	.705	.666	.494	.750	
7/22/70	1056	.981	.728	.725	.835	.887	1.018	.816	.814	.515	.630	.461	.713	.221
9/22/70	1118	.444	.327	.288	.324	.531	.755	.678	.593	.481	.462	.371	.625	.160
1/6/71	1224		.170	.121	.003	.209	.434	.453	.502	.324	.248	.058	.532	.079
4/5/71	1313	.352	.459	.368	.167	.439	.550	.619	.450	.203	.296	.004	.510	.053
6/15/71	1384		.383	.275	.090	.360	.570	.659	.474	.229	.289	.009	.502	.065
7/13/71	1412		.495	.403	.180	.523	.733	.737	.548	.289	.313	.030	.546	.083
8/17/71	1447		.413	.339	.168	.463	.691	.696	.514	.278	.288	-.009	.532	.066
9/23/71	1484		.516	.437	.211	.520	.720	.806	.604	.323	.387	+.047	.520	.049
10/22/71	1513		.263	.176	.028	.223	.484	.571	.423	.201	.313	.004	.538	.057

TABLE A6-1 I-2 INCLINOMETER DATA, STA. 246, ℄

		ELEVATION (FT.) AND HORIZONTAL DEFLECTION (INCHES)												
DATE	CONSTR. DAY	+5	0	-10	-20	-30	-40	-50	-60	-70	-85	-100	-115	-130
4/13/72	1687	+.671	+.547	+.486	+.481	+.654	+.809	+.735	+.728	+.398	+.334	+.351	+.805	+.163
12/26/72	1944	.798	.656	.642	.672	.864	1.094	1.092	1.048	.903	.784	.527	.917	.160

TABLE A6-1 CONT'D.

DATE	CONSTR. DAY	ELEVATION (FT.) AND HORIZONTAL DEFLECTION (INCHES)												
		+5	0	-10	-20	-30	-40	-50	-60	-70	-85	-100	-115	-130
7/24/68	328	+.022	+.110	+.073	+.126	+.077	+.110	+.132	+.088	+.115	+.093	+.060	+.033	-.005
8/29/68	364	-.154	-.022	.093	.247	.187	.121	.148	.077	.099	.071	.005	-.027	-.022
11/5/68	432	+.434	+.775	1.144	1.562	1.353	.935	1.006	.803	.698	.456	.203	+.126	+.027
12/11/68	468	.325	.710	1.243	1.793	1.546	1.111	1.133	.858	.655	.303	.149	.127	.033
3/13/69	560	.479	.946	1.573	2.156	1.914	1.326	1.353	1.045	.726	.352	.149	.143	.083
4/19/69	597	-.044	.429	1.062	1.672	1.397	.946	.979	.726	.330	-.050	-.055	.011	.006
5/1/69	609	+.083	.572	1.210	1.810	1.496	1.084	1.117	.842	.424	+.083	-.039	.022	.022
6/2/69	652	.429	.902	1.573	2.206	1.848	1.298	1.353	1.089	.501	.072	-.066	-.022	0.000
7/7/69	676	.727	1.017	1.797	2.265	1.977	1.371	1.460	1.152	.432	-.050	-.138	-.059	.013
8/8/69	708		.301	1.161	1.694	1.443	.926	1.070	.728	-.231	-.232	-.233	-.119	-.055
9/30/69	761	.094	.405	1.336	1.750	1.423	1.018	1.167	.831	+.112	+.211	-.172	+.037	-.006
12/1/69	823	.999	1.275	2.115	2.442	2.107	1.420	1.614	1.127	.406	-.027	-.072	.099	+.053
12/19/69	841	1.023	1.301	2.072	2.471	2.132	1.614	1.697	1.337	.497	-.127	-.399	.141	.044
1/28/70	881	1.318	1.613	2.494	2.897	2.570	2.032	2.068	1.502	.675	-.020	-.134	.161	.079
2/13/70	897	.965	1.258	2.146	2.519	2.140	1.595	1.678	1.117	.325	-.044	-.126	.127	.046
5/13/70	986	.979	1.393	2.256	2.730	2.341	1.711	1.983	1.250	.468	+.008	-.009	.158	.065
7/22/70	1056	.962	1.276	2.257	2.796	2.456	1.734	2.014	1.161	.364	-.065	-.015	.154	.039
9/22/70	1118	.857	1.270	2.205	2.714	2.408	1.738	2.028	1.249	.474	+.076	+.001	.242	.167
1/6/71	1224		1.604	2.486	3.045	2.757	2.206	2.278	1.706	1.161	.340	.116	.379	.406
4/5/71	1313		1.844	2.739	3.256	2.991	2.481	2.645	1.838	1.240	.389	.127	.419	.437
6/15/71	1384		1.643	2.551	3.127	2.873	2.379	2.546	1.866	1.357	.466	.180	.483	.470
7/13/71	1412		1.990	2.924	3.533	3.194	2.697	2.515	1.884	1.399	.486	.168	.464	.472
8/17/71	1447		1.689	2.609	3.195	2.913	2.411	2.562	2.042	1.477	.543	.240	.516	.682
9/23/71	1484		1.818	2.716	3.286	2.976	2.482	2.631	1.966	1.513	.610	.295	.571	.516
10/22/71	1513		2.054	3.033	3.632	3.335	2.823	3.002	2.084	1.515	.567	.235	.541	.509
4/13/72	1687	1.648	2.135	3.170	3.741	3.501	2.841	3.210	2.193	1.357	.804	.450	.741	.512

TABLE A6-2 I-3 INCLINOMETER DATA, STA. 246, 45'R.

		ELEVATION (FT.) AND HORIZONTAL DEFLECTION (INCHES)												
DATE	CONSTR DAY	+5	0	-10	-20	-30	-40	-50	-60	-70	-85	-100	-115	-130
12/26/72	1944	1.476	1.868	2.886	3.574	3.403	2.806	3.072	2.234	1.455	.666	.449	.783	.567

TABLE A6-2 CONT'D.

DATE	CONSTR DAY.	ELEVATION (FT.) AND HORIZONTAL DEFLECTION (INCHES)												
		+5	0	-10	-20	-30	-40	-50	-60	-70	-85	-100	-115	-130
7/24/68	328	+.440	+.379	+.280	+.363	+.379	+.308	+.231	+.192	+.115	+.143	+.077	+.055	+.005
8/29/68	364	.621	.577	.528	.610	.572	.445	.291	.247	.170	.220	.137	.099	.016
10/31/68	427	1.727	1.952	2.178	2.524	2.343	1.799	1.534	1.353	1.210	.863	.566	.396	.187
12/5/68	462	1.678	2.013	2.387	2.849	2.679	1.991	1.656	1.452	1.353	.886	.605	.512	.396
3/12/69	559	2.063	2.453	3.047	3.702	3.531	2.882	2.255	1.997	1.892	1.144	.803	.682	.616
4/19/69	597	2.266	2.662	3.322	4.026	3.883	3.146	2.503	2.255	2.167	1.293	.886	.754	.655
5/17/69	625	1.804	2.239	3.025	3.806	3.707	2.998	2.398	2.184	2.118	1.095	.655	.644	.638
6/2/69	641	2.068	2.530	3.355	4.131	4.021	3.328	2.684	2.459	2.387	1.238	.781	.710	.704
7/7/69	676	2.750	3.251	3.608	4.499	4.362	3.597	2.899	2.728	2.723	1.474	1.007	1.018	.930
9/30/69	735	2.528	2.820	3.859	4.509	4.199	3.321	2.796	2.650	2.467	1.378	.925	.932	.744
12/1/69	823	3.091	3.373	4.426	5.204	4.921	3.773	3.350	3.138	3.044	1.962	.987	.949	.934
12/19/69	841	3.528	3.807	4.948	5.679	5.449	4.576	3.987	3.754	3.549	2.132	1.489	1.552	1.335
1/28/70	881	2.789	3.106	4.371	5.195	4.954	4.004	3.407	3.168	2.958	1.597	.977	.967	.885
2/13/70	897	4.039	4.340	5.563	6.281	6.027	4.977	4.331	4.072	3.885	2.442	1.704	1.890	1.385
5/13/70	986	2.696	2.851	4.344	5.252	5.058	3.936	3.494	3.315	2.980	1.572	1.006	1.035	.991
7/22/70	1056	3.364	3.522	5.059	6.017	5.776	4.673	4.110	3.919	3.632	2.038	1.364	1.347	1.160
9/22/70	1118	3.222	3.351	4.955	5.898	5.721	4.719	4.091	3.921	3.622	1.984	1.342	1.342	1.188
1/6/71	1224		2.698	4.813	6.063	5.891	4.937	4.322	4.189	4.018	2.170	1.415	1.402	1.198
4/5/71	1313	2.895	3.084	4.235	5.653	5.586	4.613	4.027	3.886	3.710	1.851	1.116	1.377	1.199
6/15/71	1384	2.983	3.200	4.367	5.652	5.596	4.749	4.146	4.049	3.947	2.050	1.264	1.430	1.229
7/14/71	1413	3.040	3.188	4.958	6.130	5.989	4.824	4.368	4.216	3.940	2.016	1.361	1.395	1.218
8/17/71	1447	3.040	3.181	4.977	6.054	5.943	4.823	4.340	4.184	3.966	2.039	1.398	1.408	1.220
9/23/71	1484	2.900	3.026	4.859	6.031	5.934	4.826	4.405	4.262	4.019	2.004	1.326	1.364	1.208
10/22/71	1513	3.065	3.194	4.993	6.201	6.038	5.016	4.600	4.475	4.253	2.247	1.521	1.584	1.295
4/13/72	1687	2.875	3.000	4.931	6.125	6.128	5.140	4.676	4.546	4.332	2.207	1.424	1.416	1.271
12/26/72	1944	3.853	3.981	6.058	7.460	7.417	6.295	5.930	5.755	5.550	3.179	2.019	1.904	1.557

TABLE A6-3 I-4 INCLINOMETER DATA, STA. 246, 95'R.

DATE	CONSTR. DAY	ELEVATION (FT.) AND HORIZONTAL DEFLECTION (INCHES)												
		+5	0	-10	-20	-30	-40	-50	-60	-70	-85	-100	-115	-130
8/7/68	342	+1.507	+.896	+.330	+.159	+.082	+.099	+.071	+.038	+.104	+.082	+.077	+.159	+.110
8/28/68	363	.440	.561	.561	.555	.484	.445	.385	.319	.302	.209	.143	.049	-.005
10/31/68	427	1.270	1.276	1.215	1.160	1.094	.990	.907	.814	.753	.561	.357	.247	+.132
12/5/68	462	.836	.990	.985	.990	.963	.952	.897	.869	.842	.660	.512	.402	.215
2/17/69	536	1.205	1.298	1.359	1.370	1.320	1.298	1.293	1.271	1.199	.968	.748	.605	.341
5/3/69	611	1.590	1.733	1.716	1.722	1.700	1.656	1.634	1.518	1.397	1.078	.754	.616	.402
5/24/69	632	1.733	1.881	1.887	1.854	1.777	1.727	1.683	1.491	1.353	1.012	.693	.550	.336
7/7/69	676	2.279	1.728	1.598	1.646	1.742	1.745	1.826	1.692	1.462	1.163	.797	.701	.489
8/11/69	711	2.356	1.798	1.611	1.631	1.655	1.602	1.599	1.522	1.452	1.014	.804	.681	.404
9/29/69	760	1.971	1.416	1.254	1.301	1.245	1.235	1.243	1.176	1.091	.765	.492	.392	.101
12/1/69	823	2.045	1.475	1.316	1.375	1.380	1.331	1.387	1.349	1.261	.826	.498	.430	.146
12/19/69	841	2.566	1.980	1.816	1.866	1.767	1.748	1.767	1.675	1.589	1.200	.889	.831	.654
1/16/70	869	3.341	2.847	2.689	2.740	2.741	2.775	2.797	2.705	2.578	2.086	1.735	1.582	1.433
2/13/70	897	3.176	2.682	2.471	2.562	2.503	2.472	2.499	2.429	2.349	1.867	1.639	1.444	1.310
5/13/70	986	2.336	1.766	1.717	1.733	1.717	1.801	1.818	1.655	1.538	1.073	.983	.896	.590
7/22/70	1056	2.865	2.273	2.147	2.294	2.339	2.371	2.413	2.367	2.254	1.625	1.229	1.019	.662
10/10/70	1136	4.086	3.515	3.513	3.538	3.503	3.558	3.587	3.454	3.321	2.847	2.403	2.329	1.999
1/6/71	1224	2.703	2.156	2.066	2.251	2.271	2.332	2.421	2.383	2.320	1.742	1.348	1.270	.753
4/5/71	1313	2.980	2.461	2.478	2.555	2.556	2.644	2.663	2.505	2.380	1.728	1.221	1.112	.755
6/15/71	1384	2.917	2.435	2.473	2.569	2.538	2.574	2.615	2.493	2.347	1.746	1.223	1.125	.743
7/14/71	1413	2.862	2.427	2.446	2.546	2.534	2.614	2.705	2.592	2.432	1.734	1.202	1.147	.780
8/17/71	1447	2.726	2.288	2.350	2.451	2.538	2.655	2.727	2.606	2.461	1.866	1.340	1.216	.821
9/23/71	1484	2.824	2.383	2.418	2.510	2.503	2.614	2.712	2.547	2.412	1.765	1.219	1.143	.751
10/22/71	1513	2.786	2.233	2.269	2.409	2.384	2.473	2.491	2.393	2.273	1.676	1.140	1.045	.745
4/13/72	1687	2.586	2.080	2.187	2.336	2.423	2.566	2.692	2.621	2.520	1.794	1.327	1.254	.781
12/27/72	1945	2.392	2.018	2.182	2.484	2.527	2.757	2.854	2.778	2.593	1.821	1.168	1.125	.697

TABLE A6-4 I-5 INCLINOMETER DATA, STA. 246, 160'R.

DATE	CONSTR. DAY	ELEVATION (FT.) AND HORIZONTAL DEFLECTION (INCHES) +5	0	-10	-20	-30	-40	-50	-60	-70	-85	-100	-115	-130
8/7/68	342			+.429	+.451	+.407	+.512	+.539	+.473	+.374	+.253	+.143	+.089	+.011
8/28/68	363			.045	.088	.078	.093	.095	.088	.045	.017	-.039	-.022	-.033
10/1/68	397			-.275	-.115	-.165	-.149	.017	.011	.039	-.011	+.028	-.033	-.011
10/31/68	427			+.314	+.336	+.287	+.259	.264	.231	.248	+.105	.033	-.017	-.022
12/14/68	471			.237	.281	.275	.253	.270	.264	.253	.220	.077	+.033	-.011
5/17/69	625			-.171	-.138	-.116	-.072	-.022	.006	.033	.017	-.011	.011	-.011
7/7/69	676	+7.968	+.504	+.321	+.353	+.375	+.364	+.340	.323	.281	.194	+.076	.122	+.012
8/11/69	711	7.794	.487	.364	.326	.382	.417	.414	.370	.343	.296	.216	.194	.148
			— DESTROYED BY VANDALS —											

TABLE A6-5 I-6 INCLINOMETER DATA, STA. 246, 225'R.

LIST OF SYMBOLS

w_l	=	liquid limit
w_n	=	natural water content
w_p	=	plastic limit
N	=	standard penetration test, blows/ft.
γ_b	=	bouyant unit weight
γ_t	=	total unit weight
σ	=	total normal stress
$\bar{\sigma}$	=	effective normal stress
τ	=	shear stress
$\bar{\sigma}_{vo}$	=	initial vertical effective stress
σ_{ho}	=	initial horizontal effective stress
$\bar{\sigma}_{vm}$	=	maximum vertical effective stress
σ_1	=	major principle total stress
σ_2	=	intermediate principle total stress
σ_3	=	minor principle total stress
σ_{oct}	=	octahedral total normal stress
τ_{oct}	=	octahedral shear stress
RR	=	recompression ratio
CR	=	virgin compression ratio
NC	=	normally consolidated (OCR = 1)
OC	=	overconsolidated (OCR > 1)
OCR	=	overconsolidation ratio
C_α	=	ratio of secondary compression

C_v	=	coefficient of consolidation
S_u	=	undrained shear strength
$S_u/\bar{\sigma}_{vc}$	=	normalized undrained shear strength
$\overline{\text{CIU}}\text{C}$	=	isotropically consolidated undrained triaxial compression test
$\overline{\text{CK}_o\text{U}}\text{C}$	=	K_o - consolidated undrained triaxial compression test
$\overline{\text{CK}_o\text{U}}\text{PSA}$	=	K_o - consolidated undrained plane strain active test
$\overline{\text{CK}_o\text{U}}\text{PSP}$	=	K_o - consolidated undrained plain strain passive test
$\overline{\text{CK}_o\text{U}}\text{DSS}$	=	K_o - consolidated undrained direct simple shear test
U, UU	=	unconfined and unconsolidated undrained triaxial compression test
K_s	=	ratio $S_u(H)/S_u(V)$
K_o	=	coefficient of lateral stress at rest
a/b	=	ratio of major to minor half-axis in anisotropic strength ellipse
A	=	Skempton's pore pressure parameter
a, b	=	Henkle's pore pressure parameters
q_o	=	initial shear stress
ρ	=	settlement
ρ_c	=	consolidation settlement
ρ_i	=	initial settlement
ρ_{cf}	=	final consolidation settlement
u	=	pore pressure
u_e	=	excess pore pressure
$\bar{U}$	=	average degree of consolidation

ε_v = vertical strain

γ = shear strain

E = Young's modulus

G = Shear modulus, also Poisson's ratio in granular relationship

R_f = ultimate stress factor

K = Bulk modulus

F = stress dependency factor for Poisson's ratio

d = strain dependency factor for Poisson's ratio

S_uH = undrained shear strength for max. compressive stress horizontal

S_uV = undrained shear strength for max. compressive stress vertical